2

AD-A278 579

NAVAL POSTGRADUATE SCHOOL

Monterey, California

DTIC
ELECTE
APR 26 1994
S B D

THESIS

VARIABILITY OF THE CALIFORNIA CURRENT SYSTEM OFF POINT SUR, CALIFORNIA FROM APRIL 1988 TO DECEMBER 1990

by
Frederick William Rischmiller
December 1993

Thesis Advisor:	Newell Garfield
Co-Advisor	Curtis A. Collins

Approved for public release; distribution is unlimited.

94-12648

168P

DTIC QUALITY INSPECTED 3

94 4 25 060

REPORT DOCUMENTATION PAGE

Form Approved OMB No. 0704-0188

Public reporting burden for this collection of information is estimated to average 1 hour per response, including the time for reviewing instructions, searching existing data sources, gathering and maintaining the data needed, and completing and reviewing the collection of information. Send comments regarding this burden estimate or any other aspect of this collection of information, including suggestions for reducing this burden, to Washington Headquarters Services, Directorate for Information Operations and Reports, 1215 Jefferson Davis Highway, Suite 1204, Arlington, VA 22202-4302, and to the Office of Management and Budget, Paperwork Reduction Project (0704-0188), Washington, DC 20503.

1. AGENCY USE ONLY *(Leave blank)*

2. REPORT DATE December 1993

3. REPORT TYPE AND DATES COVERED Master's Thesis

4. TITLE AND SUBTITLE
Variability of the California Current System off Point Sur, CA. from April 1988 to December 1990.

5. FUNDING NUMBERS

6. AUTHOR(S)
Rischmiller, Frederick William

7. PERFORMING ORGANIZATION NAME(S) AND ADDRESS(ES)
Naval Postgraduate School
Monterey, CA 93943-5000

8. PERFORMING ORGANIZATION REPORT NUMBER

9. SPONSORING/MONITORING AGENCY NAME(S) AND ADDRESS(ES)
Naval Postgraduate School
Monterey, CA 93943-5000

10. SPONSORING/MONITORING AGENCY REPORT NUMBER

11. SUPPLEMENTARY NOTES
The views expressed in this thesis are those of the author and do not reflect the official policy or position of the Department of Defense or the U.S. Government.

12a. DISTRIBUTION/AVAILABILITY STATEMENT
Approved for public release; distribution is unlimited.

12b. DISTRIBUTION CODE

13. ABSTRACT *(Maximum 200 words)*
The Point Sur Transect was established in 1987 by the Department of Oceanography at the Naval Postgraduate School in order to further understand the nature of poleward flows in the California Current System (CCS). The POST extends offshore, perpendicular to bottom topography along 36°20'N to 123°01.7W where it meets and coincides with the California Cooperative Fisheries Investigation (CalCOFI) line 67. The sampling scheme along the transect consists of 22 CTD stations and is approximately 215 km in length. POST was occupied 19 times from April 1988 to April 1991. Data from 15 of the 19 cruises were selected in order to determine the temporal and spatial variability of the CCS off Point Sur. PEGASUS data as well as hydrographic data and NOAA 11 AVHRR satellite imagery were utilized for comparison. The CUC was observed with speeds in excess of 20 cm/s throughout the year. Mean speed and depth of the CUC was 10 cm/s and 100 m respectively, 33 km offshore. The CC was found to have a

14. SUBJECT TERMS
California Current, California Undercurrent, mesoscale features, PEGASUS

15. NUMBER OF PAGES 168

16. PRICE CODE

17. SECURITY CLASSIFICATION OF REPORT	18. SECURITY CLASSIFICATION OF THIS PAGE	19. SECURITY CLASSIFICATION OF ABSTRACT	20. LIMITATION OF ABSTRACT
Unclassified	Unclassified	Unclassified	

NSN 7540-01-280-5500

Standard Form 298 (Rev. 2-89)
Prescribed by ANSI Std. Z39-18
298-102

DTIC QUALITY INSPECTED

semi-permanent onshore meander located 150 km offshore. Maximum speeds of this meander were in excess of 20 cm/s. Mesoscale variability was a dominant feature along POST. Meanders of the CC and the CUC, anticyclonic eddies and cyclonic eddies were all present during this study. Anomalously deep poleward flow was observed along POST. This flow appeared during all seasons with speeds in excess of 10 cm/s to depths of up to 2000 m. Geostrophic velocity calculations agreed favorably with PEGASUS derived absolute velocities except during the upwelling season. Reasons for the disparity include the selection of 1000 m asthe level of no motion and surface wind stress. The variability of the CCS was determined to be interannual rather than seasonal. The short duration of this data set, when compared to earlier geostrophic studies, and the absence of upper slope and shelf velocity data may account for the absence of a significant seasonal signal.

Approved for public release; distribution is unlimited.

Variability of the California Current System off Point Sur, California from April 1988 to December 1990.

by

Frederick William Rischmiller
Lieutenant , United States Navy
B.S., University of Rochester, 1986

Submitted in partial fulfillment of the requirements for the degree of

MASTER OF SCIENCE IN PHYSICAL OCEANOGRAPHY

from the

NAVAL POSTGRADUATE SCHOOL
December 1993

Author: ______________________________
Frederick William Rischmiller

Approved by: ______________________________
Newell Garfield, Thesis Advisor

____
Curtis A. Collins, Second Reader

____
Curtis A. Collins, Chairman, Department of Oceanography

Accession For
NTIS GRA&I ☑
DTIC TAB ☐
Unannounced ☐
Justification

By
Distribution/
Availability Codes
Dist | Avail and/or Special
A-1

ABSTRACT

The Point Sur Transect was established in 1987 by the Department of Oceanography at the Naval Postgraduate School in order to further understand the nature of poleward flows in the California Current System (CCS). The POST extends offshore, perpendicular to bottom topography along 36°20'N to 123°01.7'W where it meets and coincides with the California Cooperative Fisheries Investigation (CalCOFI) line 67. The sampling scheme along the transect consists of 22 CTD stations and 9 PEGASUS stations and is approximately 215 km in length. POST was occupied 19 times from April 1988 to April 1991.

Data from 15 of the 19 cruises were selected in order to determine the temporal and spatial variability of the CCS off Point Sur. PEGASUS data as well as hydrographic data and NOAA 11 AVHRR satellite imagery were utilized for comparison. The CUC was observed with speeds in excess of 20 cm s^{-1} throughout the year. Mean speed and depth of the CUC was 10 cm s^{-1} and 100 m respectively, 33 km offshore. The CC was found to have a semi-permanent onshore meander located 150 km offshore. Maximum speeds of this meander were in excess of 20 cm s^{-1}.

Mesoscale variability was a dominant feature along POST. Meanders of the CC and the CUC, anticyclonic eddies and cyclonic eddies were all present during this study. Anomalously deep poleward flow was observed along POST. This flow appeared during all seasons with speeds in excess of 10 cm s^{-1} to depths of up to 2000 m. Geostrophic velocity calculations agreed favorably with PEGASUS derived absolute velocities except during the upwelling season.

Reasons for the disparity include; the selection of 1000 m as the level of no motion and surface wind stress.

The variability of the CCS was determined to be interannual rather than seasonal. The short duration of this data set, when compared to earlier geostrophic studies, and the absence of upper slope and shelf velocity data may account for the absence of a significant seasonal signal.

TABLE OF CONTENTS

ACKNOWLEDGMENTS

This study would not have been possible without the support and guidance of my advisors, Prof. Toby Garfield and Prof. Curt Collins. In addition, I would like to thank Robin Tokmakian for her assistance with the Empirical Orthogonal Analysis of this data set and Prof. Jeff Paduan for providing surface drifter data. Last but certainly not least, I would like to thank QM1 Ben Martin for his tireless efforts in providing the satellite imagery for this study.

I. INTRODUCTION

The North Pacific anticyclonic gyre consists of the North Equatorial Current to the south, the Kuroshio to the west, the North Pacific Current to the north and the California Current (CC) which forms the eastern limb. The CC extends from Washington to Baja California and is characterized as a broad (~500 km), shallow (0-300 m), weak (< 25 cm s^{-1}) equatorward flowing current (Reid and Schwartzlose 1962; Wooster and Reid 1963; Lynn and Simpson 1987). The core of the CC lies 200-300 km off the California coast. The western boundary, marked by a continuation of the subarctic frontal zone, lies approximately 900 km offshore (Chelton 1984) and separates the CC and the eastern North Pacific water mass (Lynn 1986).

Inshore of the CC there is a seasonal reversal of the equatorward surface flow called the California Countercurrent (CCC, Simpson et al. 1986). During the fall and winter months, the CCC is often poleward but does not show temporal or spatial continuity along the west coast of North America. The CCC is often referred to by regional names such as the Inshore Countercurrent (IC, Lynn and Simpson 1987) off southern California and the Davidson Current (DC) north of Pt. Conception. Hereinafter it will be referred to as the DC.

The final component of the California Current System (CCS) is called the California Undercurrent (CUC). The CUC flows poleward throughout the year, originates in the Equatorial Pacific and flows over the continental slope. The CUC has been observed locally from Baja California (Wooster and Jones 1970) to Vancouver Island (Hickey 1979). However, it's continuity has not been observed.

The position, depth and strength of the CUC is highly variable and can be related to seasonal changes in wind stress and wind stress curl (Hickey 1979).

Four water masses are found in the CCS. Pacific Subarctic water, which is transported south by the CC, is characterized by relatively low temperature, low salinity, high dissolved oxygen and high nutrients (Reid et al. 1958). Equatorial Pacific water is formed in the eastern tropical Pacific and is defined by relatively high temperature, high salinity, high nutrients and low dissolved oxygen (Sverdrup et al. 1942). Equatorial Pacific water is transported north by the CUC and is sometimes termed southern water (Wickham 1975). Eastern North Pacific Central water borders the CCS on the west and is characterized by relatively high temperature, high salinity, low dissolved oxygen and low nutrients (Reid et al. 1958; Lynn and Simpson 1987). Finally, upwelling along the coast brings relatively cold, saline, nutrient rich and oxygen deficient water to the surface (Sverdrup 1938; Reid et al. 1958).

The CUC has been the subject of numerous studies which include calculations of geostrophic velocity derived from hydrographic data to direct current measurements. Tibby (1941) found indirect evidence of the CUC by studying hydrographic sections along the west coast of North America. Intrusion of warm salty Equatorial Pacific water was observed as far north as Cape Blanco, Oregon. Direct measurements of the CUC were made by Reid (1962) off Central California by tracking parachute drogues. The core of the undercurrent was found at 250 m with a speed of 20 cm s^{-1}. Wooster and Jones (1970) used Richardson type current meters and found a narrow (20 km) undercurrent with an average speed of 30 cm s^{-1} over the continental slope off Punta Colnett, B.C., Mexico. Wickham (1975) utilized STD surveys and parachute drogues off Point

Sur to characterize the CUC. The undercurrent was found near the shelf edge with maximum speeds in excess of 40 cm s^{-1}. The geostrophically derived speeds agreed only roughly with the magnitude of the drogue measurements. Halpern et al. (1978) compared hydrographic data with direct current measurements off Oregon and found a poleward current at intermediate depths over the continental slope extending 600 km in the long shore direction.

Chelton (1984) and Lynn and Simpson (1987) studied 23 years of California Cooperative Oceanic Fisheries Investigation (CalCOFI) hydrographic data collected between 1950 and 1978. Chelton focused on two sections of the CalCOFI data, one off Point Sur and the other off Point Conception. The geostrophic flow in the upper 100m, referenced to 500 m, for both locations reversed annually with equatorial flow from February to September and poleward flow from October to January. Below 100m, the flow at Point Conception was poleward throughout the year with two maximum flows occurring in June and December. The nearshore deep flow off Point Sur, however, reversed annually with maximum poleward flow in December and weak equatorward flow from March to May. Lynn and Simpson examined the seasonal variability of the CCS using harmonic analysis of the entire CalCOFI data set. Strong semiannual variability was prevalent for the CUC off Central California, Point Conception and within the Southern California Bight. The CUC became weaker from January through March as it's core was found at increasingly greater depths. The CUC remained weak or vanished from March through May. The maximum velocity was found in late fall to early winter. The minimum CUC velocity was associated with surface equatorward flow.

Based upon two years of current meter array measurements off Cape San Martin, Wickham et al. (1987) described the mean flow of the CUC as a jet limited to the upper 300 m of the water column. The undercurrent was found within 30 km of the coast with core speeds in excess of 15 cm s^{-1}. In 1984, the Central California Coastal Circulation Study (CCCCS) was instituted to obtain a better understanding of the circulation on the continental shelf and upper continental slope between Point Conception and San Francisco. Chelton et al. (1988) focused on the first six months of near surface (70 m) measurements. The mean flow from Point Conception to Point Sur was generally poleward while the mean flow north of Point Sur was equatorward. Variability in alongshore currents was highly correlated with local wind forcing events, except off Point Conception. In July 1984, after a period of calm winds, surface poleward flow was observed to 300 km off the Central California coast. Poleward surface currents had not been previously observed over the continental slope after February.

The Coastal Transition Zone program (CTZ) was initiated in 1987 off Northern California in order to understand the region offshore of the continental shelf which contains numerous cold filaments (Brink and Cowles 1991). As part of the CTZ program, Huyer et al. (1991) utilized hydrographic and ADCP data to describe the structure and characteristics of the CTZ extending offshore from Point Arena to Point Reyes. During the six week survey period in the summer of 1988, the CUC was located adjacent to the continental slope with core speeds of 20 cm s^{-1} located between 150 - 250 m and penetrating to a depth of 440m.

The Northern California Coastal Circulation Study (NCCCS) focused on the continental shelf and slope from San Francisco to the Oregon border (Largier et al. 1993; Bray and Greengrove 1993). Data for the study were collected using moored current meters, pressure recorders, CTD casts and Lagrangian drifters during the periods from March to August 1987 and March 1988 to October 1989. The variability of shelf and slope currents was divided into three seasonal regimes. The upwelling season from April to July is characterized by strong equatorward flow at the surface and a poleward undercurrent inshore of the 90 m isobath. Alongshore differences in nearshore currents are significant during this season. Towards the end of the upwelling season, the strong equatorward surface flow diminishes as a result of a strong northward pressure gradient. The relaxation season from August to November is characterized by maximum deep poleward flow. The increase precedes the minimum equatorward wind stress, indicating that a threshold level of alongshore pressure overcomes the weakened equatorward wind stress. The surface flow tends to be weak as a result of continued equatorward wind stress. The storm season from December through March is a period of winds associated with the passage of weather fronts. The poleward undercurrent is very weak or non-existent north of Cape Mendocino and slightly weaker south of the cape. Major findings of this study include the importance of spatial variations of the wind field, coastal topography and mesoscale oceanic forcing to variations in alongshore and seasonal coastal upwelling cycles. The seasonal variation in alongshore pressure gradient results in a temporal variation in the response of currents to winds. Seasonal variations in the poleward undercurrent occur as a result of the annual strengthening and relaxation of this poleward alongshore pressure gradient.

The Point Sur Transect (POST) was established in 1987 by the Department of Oceanography at the Naval Postgraduate School in order to study the nature of poleward flows in the CCS. Tisch et al. (1992) selected seven cruises along the

POST in order to determine seasonal variations of alongshore geostrophic velocities and water mass characteristics. The CUC occupied a position 12 to 42 km from shore with core speeds between 10 and 35 cm s^{-1} at depths of 70 - 460 m over the continental slope. The variability of the CUC appeared to be related to both local and remote wind forcing.

The purpose of this study is to describe, based upon three years of Pegasus current measurements and hydrographic data collected along POST, the variability of currents off Point Sur. Data collection and processing will be discussed in Chapter II. Analyses of the Pegasus and hydrographic data are discussed in Chapter III. The results and a comparison with earlier studies of the CCS are discussed in Chapter IV. Chapter V contains a summary of conclusions and recommendations for future work.

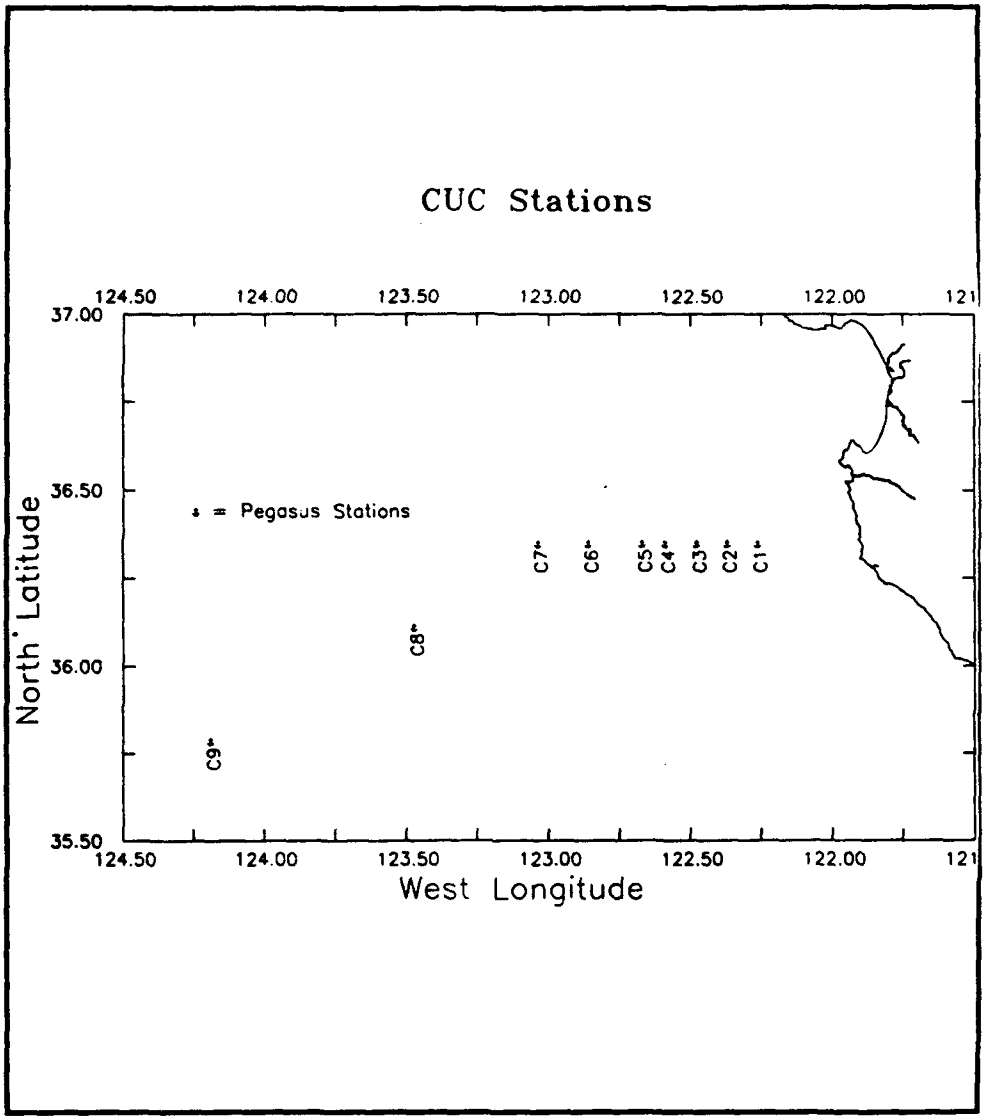

Figure 1. The Point Sur Transect.

II. DATA COLLECTION AND PROCESSING

The POST extends offshore, perpendicular to bottom topography along 36°20'N to 123°01.7'W where it meets and coincides with the California Cooperative Oceanic Fisheries Investigation (CalCOFI) line 67. The sampling scheme along POST consists of 22 CTD stations and 9 PEGASUS stations and is approximately 215 km in length (Figure 1). PEGASUS observations along POST occurred approximately bimonthly during a three year period from April 1988 to April 1991. Data from 15 of the 19 cruises were selected for this study.

A. DATA COLLECTION

PEGASUS is a free falling, acoustically tracked dropsonde that measures pressure, temperature, conductivity and two way acoustic travel times between PEGASUS and bottom mounted transponders. PEGASUS can send and receive different operational frequency signals to and from up to six transponders. The transponder positions are established with a baseline survey after initial deployment. PEGASUS provides a brief snapshot of the currents throughout the water column. The vertical profile of the horizontal velocity, accurate to 1 cm s^{-1} (Spain et al. 1981), is obtained by differentiating with respect to time the trajectory of PEGASUS as it descends and ascends the water column at a rate of approximately 63 cm s^{-1}. PEGASUS transmits a pulse every 16 seconds which allows for a vertical resolution of approximately 10 meters. Two different PEGASUS instruments were used during the three year survey. PEGASUS 8, which could only receive two frequencies and hence utilized a two transponder network per station, was deployed between April 1988 and March 1989. PEGASUS 15, able to receive up to six return frequencies utilized a three transponder network per station and was deployed between May 1989 and February 1992. A total of nine PEGASUS stations were occupied along POST, from 33 km offshore to 225 km offshore (Figure 1). An up cast and downcast were collected at each station and at least two deployments were conducted at each station. The drops were spaced approximately 10 hours apart to partially eliminate inertial effects. The inertial period at this latitude is about 20 hours.

Hydrographic data were collected with a Neil Brown Mark III-B CTD. The Neil Brown Mark III-B CTD has a resolution of ± 0.001 PSU ± 0.005°C and ± 1.75 dbar and has an accuracy of ± .005 PSU, ± .005°C and ± 3.2 dbar. Water samples were collected on the up cast with a General Oceanics Rosette Sampler. The water samples were utilized for biology and chemistry observations and post cruise salinity calibration.

Wind data from NOAA weather buoys located off Monterey Bay (B46042) and Cape San Martin (B46028) were provided by Pacific Fisheries Environmental Group (PFEG).

The satellite data were processed at NPS using the University of Miami DSP software. Level Ib data were ingested and the engineering values converted to radiances. The passes were navigated and then remapped to produce a central California scene having one kilometer resolution at nadir. Multi-channel algorithms were used to obtain sea surface temperature estimates, corrected for atmospheric path-length contamination. The final step was adding geographical and geophysical information to the scenes.

B. DATA PROCESSING

The raw PEGASUS travel times were processed using programs adapted at NPS (Garfield and Rago 1993) from University of Hawaii routines provided by

Eric Firing. The University of Hawaii routines were, in turn, based upon routines developed at Woods Hole Oceanographic Institute (Hunt et al. 1974; Luyten et al. 1982). The general data processing steps to obtain horizontal velocity are: conversion from hex to decimal engineering units for travel time, pressure, temperature (and conductivity on PEGASUS 15); machine editing and hand editing to flag bad points; and conversion of travel times to slant ranges, pressure, temperature (and conductivity) engineering units into decibars, °C, (and in situ conductivity), respectively. For PEGASUS 8, instrument location within the transponder array is obtained from the two slant ranges and the pressure. The solution requires a priori knowledge of where the dropsonde was deployed and recovered relative to the line defined by the two transponders. A unique three slant range solution, independent of the pressure value, can also be determined for PEGASUS 15 data. This allows for an error estimate of the location determination from the two methods. The horizontal velocity is then computed by time differencing successive horizontal positions. The velocity profiles were then vertically filtered to remove noise using a five point weighted filter and visually inspected to remove bad data points. Missing and bad data points were then estimated with linear interpolation.

Raw CTD data were averaged in 2 meter bins utilizing programs written by Paul Jessen, NPS Oceanography Department. Calibration procedures, as described by Tisch et al. (1992), were conducted. Vertical gradients in excess of 0.2°Cm^{-1} and 1.0 PSU m^{-1} were inspected for bad data points and linear interpolation filled in any resulting gaps.

The NOAA wind data were transformed into alongshore and cross shore components. The drag coefficient, C_D was determined using (Large and Pond 1981)

$$C_D = 1.14 \times 10^{-3}, \quad |V| \leq 10 \text{ m s}^{-1}$$

$$C_D = 0.49 \times 10^{-3} + (0.065 \times 10^{-3})(|V|), \ |V| > 10 \text{ m s}^{-1}$$

The alongshore wind stress was then computed as

$$T = P_a C_D |V| V_a$$

where P_a is the density of air, $|V|$ is the magnitude of the wind velocity, and V_a is the alongshore component of the wind velocity.

III. ANALYSIS

A. DESCRIPTION OF MONTHLY PEGASUS AND HYDROGRAPHIC DATA

1. April 1988

For the month preceding this cruise, the alongshore component of equatorward wind stress was strong with values exceeding 2 dynes cm^{-2}. A three day relaxation of wind stress began on April 10 and by the beginning of the cruise, the winds were again equatorward. Inspection of temperature and salinity fields reveal deepening isohalines and doming isotherms in the vicinity of C8, indicative of cooler fresher waters of Pacific Subarctic origin carried south by the CC. The CC is a narrow, slightly equatorward onshore jet centered at C8. Maximum surface speed is 35 cm s^{-1}. The flow of this jet is limited to the upper 200 m of the water column. Existence of a narrow equatorward jet in the coastal transition zone has been identified by Huyer et al. (1991) and Bray and Greengrove (1993) for the coastal region off northern California. The CTZ jet generally appears during the upwelling season and is strongly influenced by local promontories and capes. The currents at C9 and C7 are also onshore with maximum surface speeds of 10 cm s^{-1}. The CUC is evident offshore to C4 with a maximum speed of 10 cm s^{-1} at 300 m in depth. The location of the core of the CUC cannot be determined, since velocity data are not available for C1 or C2 during this cruise. The currents between C4 and C6 were generally weak poleward flows with speeds less than 5 cm s^{-1}.

2. August 1988

The wind data for this cruise show two weeks of calm winds with only a brief upwelling favorable wind event four days prior to the cruise. The winds became equatorward during the last two days of the cruise period with alongshore wind stress less than 1 dyne cm^{-2}. The temperatures along the transect reveal a slight deepening of isotherms inshore of C2. Shallowing isohalines also inshore of C2 are characteristic of the warmer more saline waters of the CUC. A subsurface salinity minimum of 32.7 at C8, 50 m below the surface, is indicative of the fresher waters of the CC.

The CC is a southeasterly flowing surface jet with maximum surface speeds of 25 cm s^{-1} near C7. The CC extends from 100 km to 225 km offshore and is restricted to 200 m in depth. Poleward surface flow inshore of C3 reaches speeds of 10 cm s^{-1}. Tisch et al. (1992) found geostrophic poleward velocities inshore of C1 in excess of 60 cm s^{-1} during the same cruise period. The CUC, with a core speed of 25 cm s^{-1} at 200 m remains strong with velocities greater than 10 cm s^{-1} to 450 m. The undercurrent extends offshore to 75 km where the maximum speed is less than 10 cm s^{-1}.

3. September 1988

The September cruise was preceded by a period of weak equatorward wind stress. Values were generally less than 1 dyne cm^{-2}. During the cruise there were two short relaxation events followed by a brief equatorward wind burst on September 27. There is a salinity minimum of 32.9 at C6 approximately 100 m below the surface. Isohalines slope upwards and isotherms deepen inshore of C3 as a result the transport of Equatorial Pacific water by the CUC.

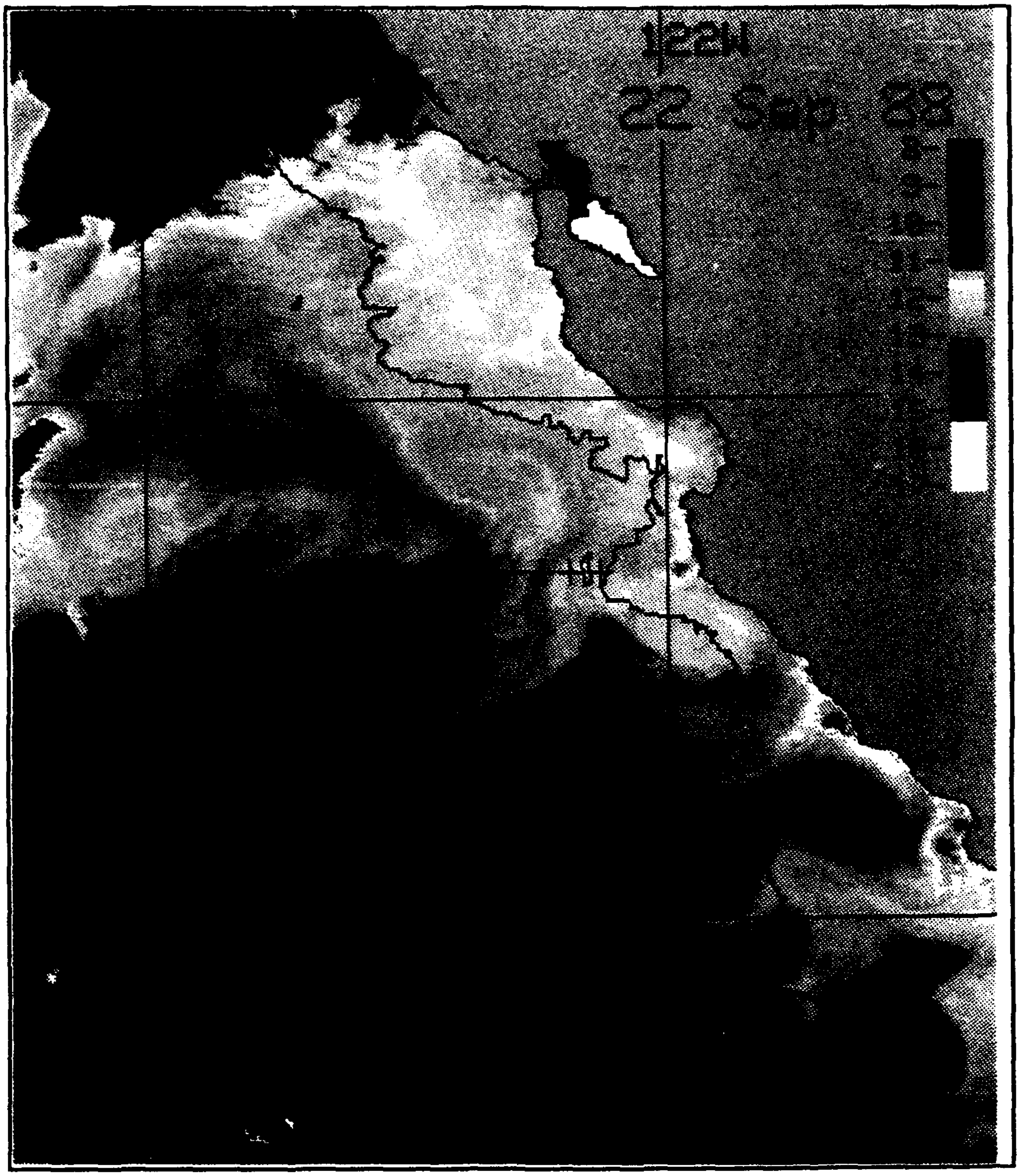

Figure 2. NOAA 11 Satellite SST Imagery from September 22 1988: Clouds contaminate the image west of 124 W.

Poleward surface flow is observed inshore of C3 with speeds typically less than 10 cm s^{-1} (Figure 3). The surface flow along the western portion of the transect is equatorward. An equatorward jet with a speed of 25 cm s^{-1} is present, centered at C3 and restricted to the upper 50 m. NOAA 11 AVHRR satellite imagery on September 22 (Figure 2) shows a cool plume of recently upwelled water extending offshore and then turning to the south in the vicinity of C3. Velocity data are not available for C8 or C9 during this cruise. The CUC has a core depth and speed of 180 m and 25 cm s^{-1} respectively at C2, 43 km offshore.

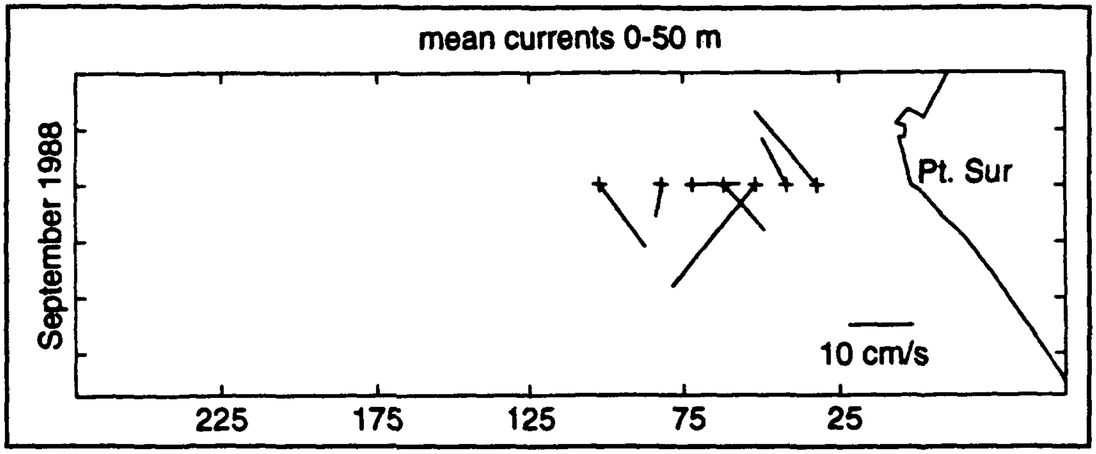

Figure 3. Mean Surface (0-50 m) PEGASUS Velocities for September 1988.

4. November 1988

Winds were weak prior to the November cruise with a short equatorward wind event during the last two days of the cruise. The mean velocity field seems to indicate an anticyclonic feature at the surface east of C7. The surface flow west of C1 is predominantly poleward with speeds in excess of 10 cm s^{-1}. Strong equatorward surface flow (> 30 cm s^{-1}) is present at C1. The eddy is limited to the upper 300 m of the water column. Tisch et al. (1992) also described this mesoscale feature off Pt. Sur in the geostrophic velocity field for November 1988 and found the CUC was restricted to within 10 km of the slope. This agrees with the PEGASUS data, as there is no indication of the CUC along the POST for this cruise. A comparison between PEGASUS data, geostrophic velocities and ADCP data for this cruise was completed by King (1989) and Reece (1989).

5. February 1989

Two equatorward wind events occurred during the week before this cruise with weak equatorward winds shifting to poleward towards the end of the cruise. The salinity field shows no clear indication of CC water since salinity is greater than 33.3 along the entire transect. Temperatures within the upper 100 m are almost isothermal with values between 10.5°C and 11°C.

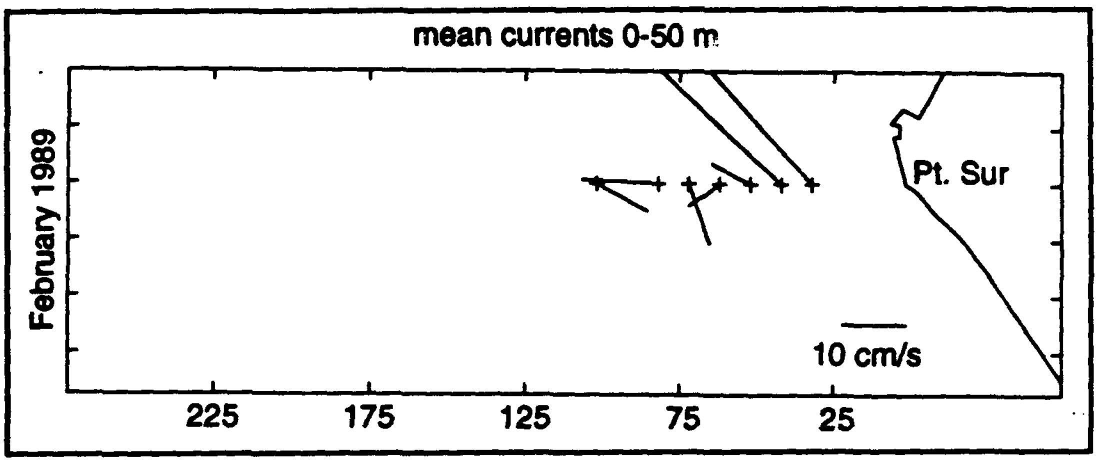

Figure 4. Mean Surface (0-50 m) PEGASUS Velocities for February 1989.

The most prominent feature of the mean February velocity data is strong poleward surface flow within 50 km of the coast (Figure 4). The maximum surface velocity recorded at C2 was 34 cm s^{-1}. Poleward flow remained greater than 10 cm s^{-1} to a depth of 600 m. NOAA 11 AVHRR satellite imagery for February 22 (Figure 5) suggests northward transport of warm surface water beyond San

Francisco. Surface flow along the western side of POST is generally equatorward with velocities less than 10 cm s^{-1}. A comparison between PEGASUS data, geostrophic velocities and ADCP data was completed by Berryman (1989).

Figure 5. NOAA 11 AVHRR Satellite SST Imagery from 13 February 1989: Clouds contaminate the image west of 123 W.

6. March 1989

Two strong upwelling favorable wind events with equatorward wind stress values of 1.5 dynes cm^{-2} occurred in the ten days prior to the cruise. The winds were slightly poleward on March 25, becoming equatorward again the next day. The temperature field for the March cruise is similar to that of February except for warmer surface values west of C8. A surface salinity minimum of 33 at C8 and deepening isohalines in the upper 200 m offshore from C8 are representative of Pacific Subarctic water of the CC.

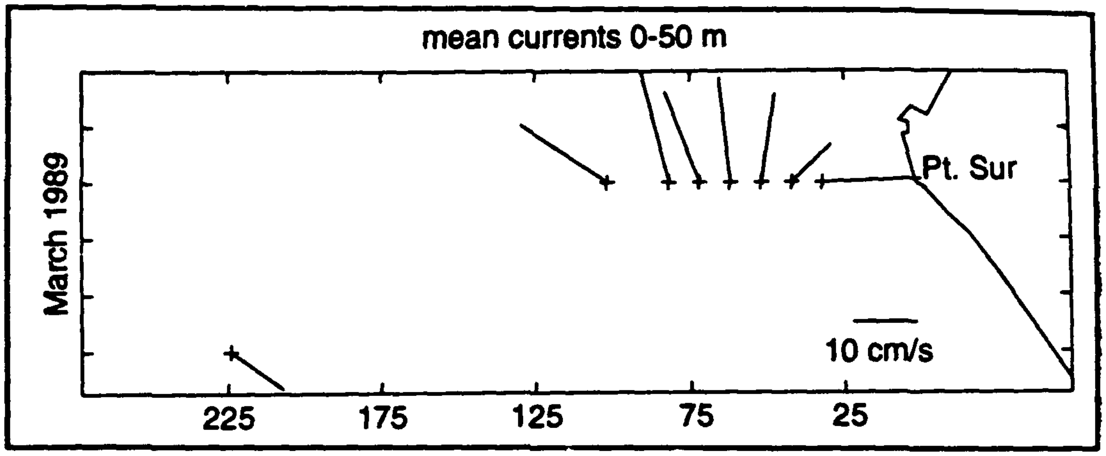

Figure 6. Mean Surface (0-50 m) PEGASUS Velocities for March 1989.

Poleward surface flow extends from C2 to C7 with maximum values greater than 25 cm s^{-1} at C4 and C6 (Figure 6). NOAA 11 AVHRR satellite imagery for March 27 (Figure 7) indicates the transport of warm water northward along POST inshore of C7 and transport of relatively cool water southward centered at C8. The surface flow at C1 is onshore with speeds in excess of 20 cm s^{-1}. The current at C9 is equatorward with a speed of 5 cm s^{-1}. Velocity data are unavailable for C8 during this cruise. The CUC has a core depth of 420 m and a core speed of 20 cm s^{-1} at C2. The poleward flow is unusually strong to the bottom at C2 with a secondary subsurface maximum of 18 cm s^{-1} at a depth of 1200 m. A comparison of PEGASUS data and geostrophic velocities was conducted by Negron (1989) for this cruise period.

Figure 7. NOAA 11 AVHRR Satellite SST Imagery from 27 March 1989: Dark areas along 1000 m isobath are due to cloud contamination

7. May 1989

The wind field during this cruise was characterized by periods of strong equatorward wind stress that exceeded 1.5 dynes cm^{-2}. Poleward surface flow with velocities of 5 cm s^{-1} occurs inshore of C3. The surface flow from C3 to C7 is predominantly offshore with velocities less than 10 cm s^{-1}. At C8, the flow is to the southeast and limited to the upper 200 m. This southeastward flow has a maximum speed of 30 cm s^{-1}. Deepening isohalines in the vicinity of this station indicate waters of subarctic origin.

The CUC is clearly present offshore to C5. Maximum speeds exceed 20 cm s^{-1} at C1. The core of the CUC is difficult to ascertain due to the unusually strong poleward flow throughout the entire water column at C1. Each of four PEGASUS casts show multiple subsurface maxima at C1 with speeds exceeding 10 cm s^{-1} to 850 m. A comparison between PEGASUS data and geostrophic velocities was conducted for this cruise by Robson (1989).

8. July 1989

Winds were strongly equatorward for the two weeks leading up to this cruise, with alongshore wind stress values greater than 2.5 dynes cm^{-2}. Two days prior to the cruise a three day relaxation event occurred with winds becoming equatorward during the cruise. The flow on the surface is predominantly poleward with southeastward flow at C1 and C2. The salinity field is unusual in that salinities are much higher along the entire transect with minimum values of only 33.6. Deepening isotherms between C2 and C4 indicate the presence of warmer water. The higher salinities and warmer temperatures are the result of lateral entrainment of Pacific Equatorial water (CUC). The flow in the upper 500 m reveals an onshore meander of the CUC (Figure 9). Maximum poleward flow is located at C4 with a core speed and depth of 28 cm s^{-1} and 180 m respectively.

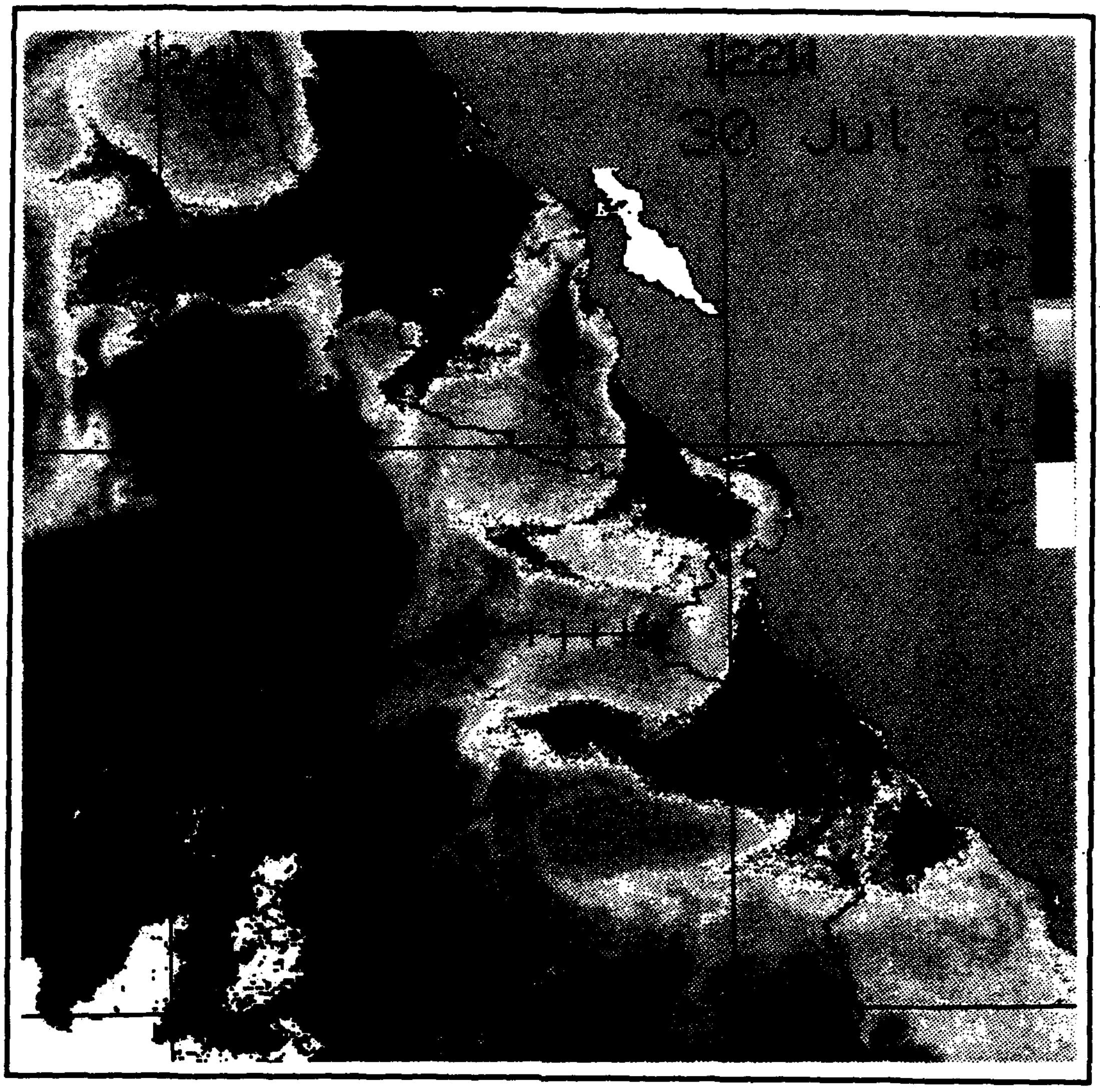

Figure 8. NOAA 11 AVHRR Satellite SST Imagery from July 30 1989.

NOAA 11 AVHRR satellite imagery for July 30 (Figure 8) shows an anticyclonically rotating meander of warmer water between the cool upwelled waters at Point Año Nuevo and Point Sur. Meanders in the undercurrent have been developed with modeling studies by Ikeda et al. (1984). Utilizing a nonlinear numerical model, CUC meanders with a 75 km wavelength were developed. Alongshore topography variations and baroclinic instability appear to be important forcing mechanisms. The unusually strong poleward flow near the surface is most likely the result of a significant wind relaxation event which occurred prior to this cruise. There was an even longer relaxation event farther south recorded at the Cape San Martin buoy. A residual alongshore pressure gradient can cause northward acceleration of surface currents.

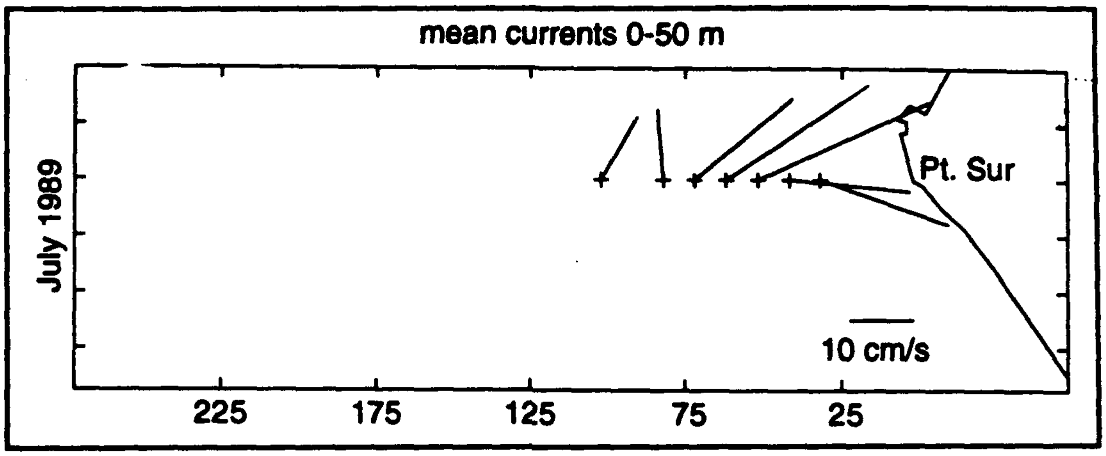

Figure 9. Mean Surface (0-50 m) PEGASUS Velocities for July 1989.

9. September 1989

A strong frontal feature is present in the temperature and salinity fields 100 km offshore to 700 m in depth. This sharp frontal feature separates warm saline water inshore from cooler fresher water offshore. The warm and saline water inshore is Equatorial Pacific water carried by the CUC. In contrast to the onshore flowing CUC meander observed in July 1989, the velocity field for the September cruise shows an offshore flowing meander (Figure 11). This meander, although weaker than the currents below, is also manifested on the surface. The core depth and speed of the meander are 35 cm s^{-1} and 500 m respectively. A NOAA 11 AVHRR satellite image for September 26 (Figure 10) reveals this offshore meander. The cool upwelled water from Point Sur is advected westward to C4 where it turns to the south. Hydrographic data show this cool fresh upwelled water inshore of C5. At C7, the flow is onshore with a maximum speed at the surface of 20 cm s^{-1}. The low salinity values (< 33.2) indicate that this flow is part of the CC.

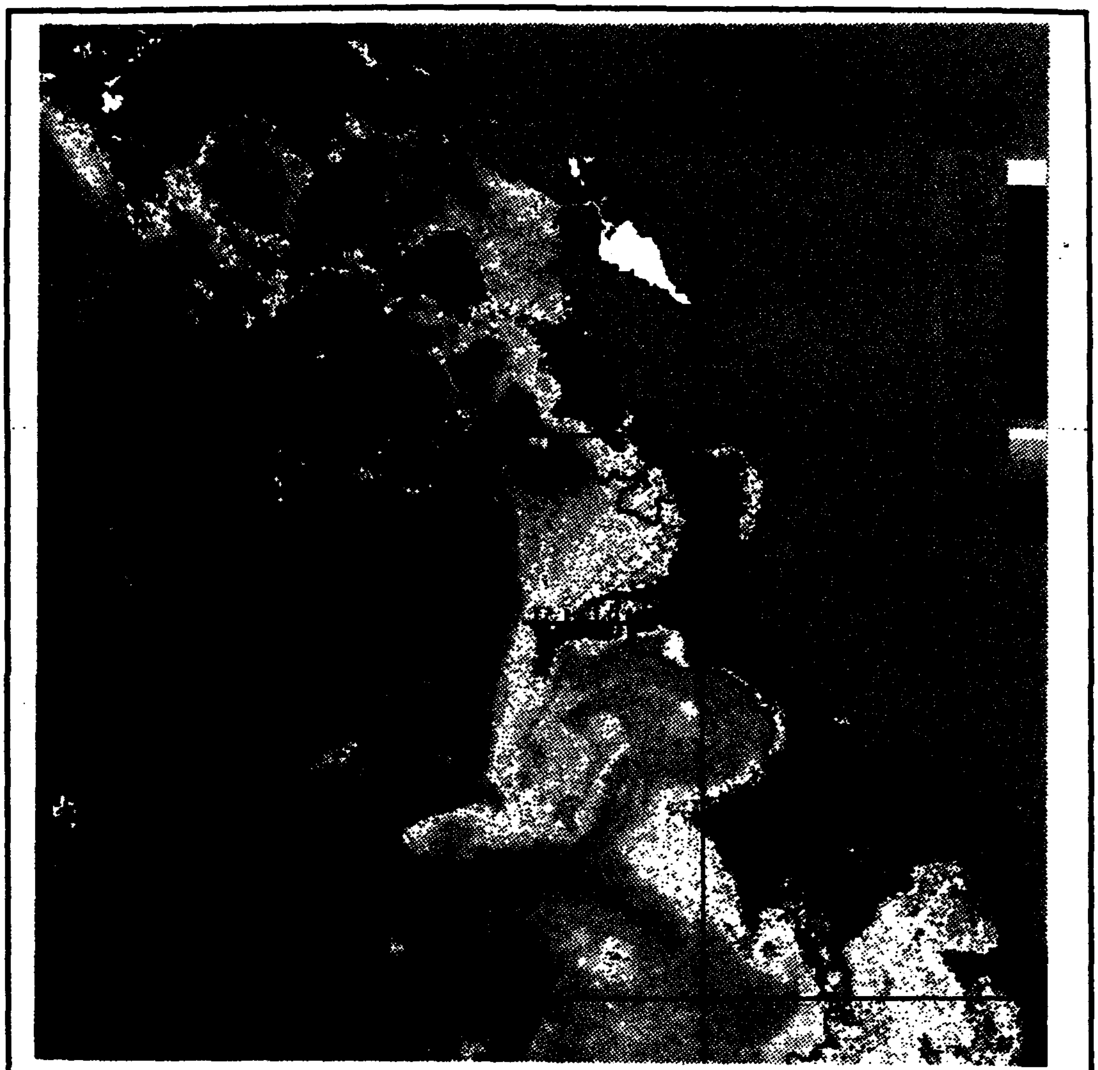

Figure 10. NOAA 11 AVHRR Satellite SST Imagery from 26 September 1989.

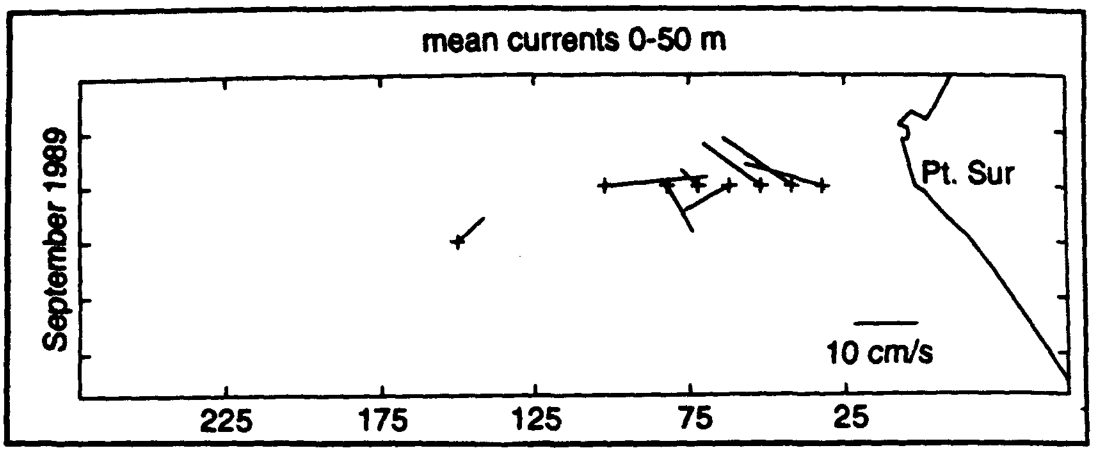

Figure 11. Mean Surface (0-50 m) PEGASUS Velocities for September 1989.

10. November 1989

The salinity and temperature fields for November are similar to those for September, except that the sharp frontal feature has moved farther offshore to 150 km from the coast. This suggests lateral entrainment of CUC water farther offshore. The current pattern again suggests an offshore flowing meander of the CUC (Figure 13). Surface flows are poleward at C1, C2, C3 and C7 and equatorward at C5, C6 and C8. PEGASUS data are unavailable for C4 and C9. Maximum poleward surface flow is 10 cm s^{-1} at C1, while maximum surface equatorward flow at C8 is 20 cm s^{-1}.

The poleward surface flow at C7 appears to consist of CC water since the hydrographic data show a subsurface salinity minimum of 33 and slight doming of isotherms. The flow here is poleward as a result of the interaction between the surface manifestation of the CUC flowing offshore and the southeastward meander of the CC. The core of the CUC is relatively shallow at 180 m with a maximum speed of 30 cm s^{-1} at C1. NOAA 11 AVHRR satellite imagery taken on November 18 (Figure 12) shows a warm pool of water, offshore from C7 north to 37° N, where it then continues westward. A relatively cool water mass intersects POST offshore from C8, where it continues to the south. This cool water is most likely an onshore meander of the CC.

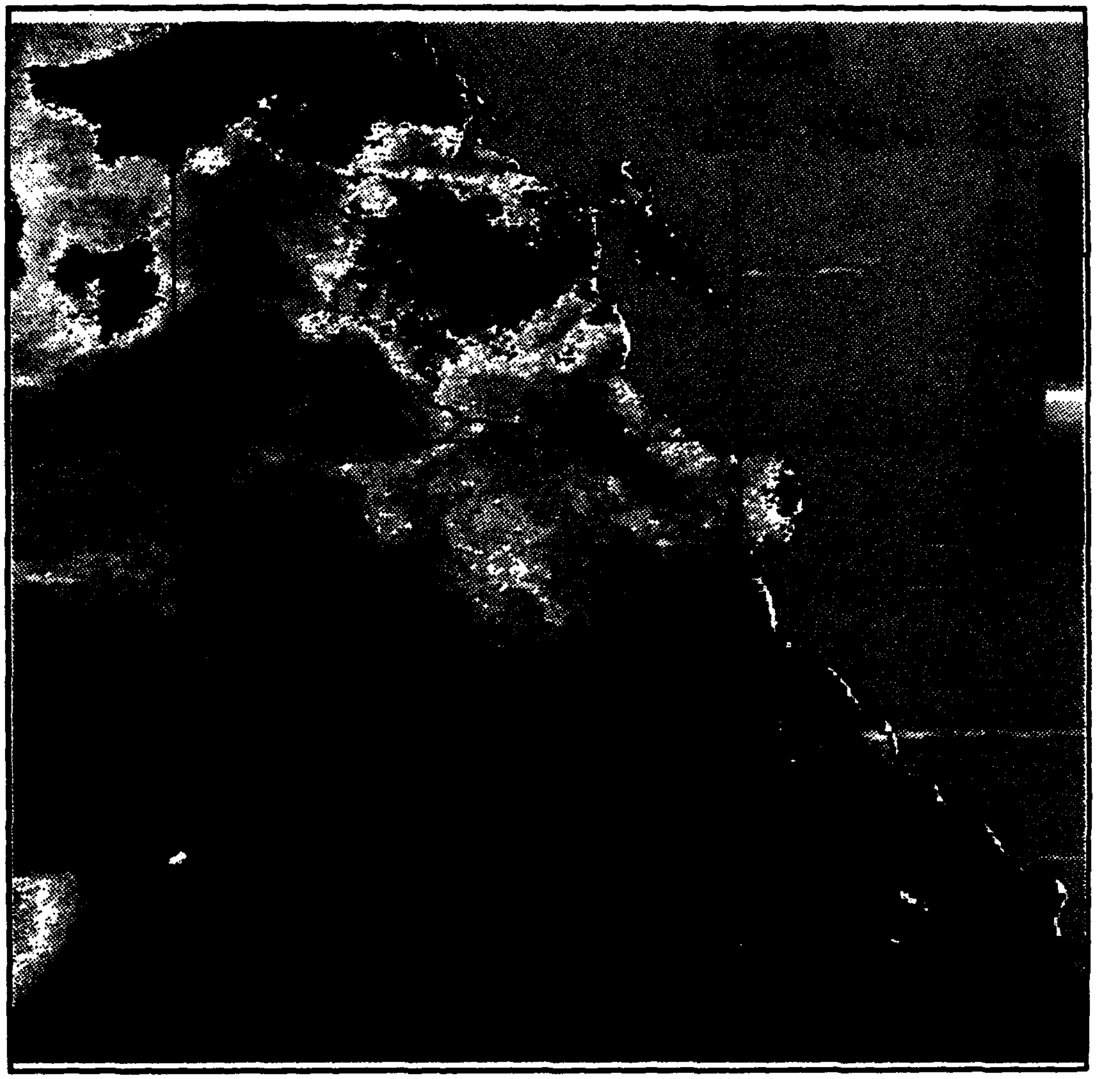

Figure 12. NOAA 11 AVHRR Satellite SST Imagery from November 18 1989.

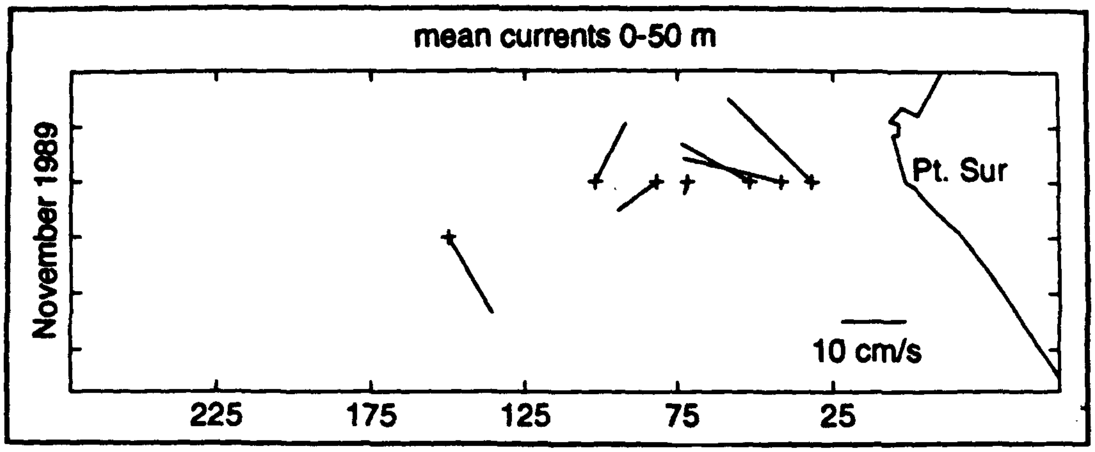

Figure 13. Mean Surface (0-50 m) PEGASUS Velocities for November 1989.

11. January 1990

The January 1990 cruise was preceded by a brief poleward wind event that became equatorward as the transect was occupied. The surface flow to 75 km offshore is poleward, with a maximum speed of 15 cm s^{-1} at C1 (Figure 15). Inshore of C6, upward sloping isohalines and downward sloping isotherms indicate that the broad subsurface poleward flow is the CUC. The CUC has a core speed of 28 cm s^{-1} and an unusually shallow core depth of 50 m at C1. The CUC remains strong (> 10 cm s^{-1}) to a depth of 550m. The current at C8 is southeastward with a maximum velocity of 10 cm s^{-1} at 100 m. Velocity data are unavailable for C8 above 100 m. The subsurface salinity minimum at C8 indicate that this flow is associated with the CC. This agrees favorably with a NOAA 11 AVHRR satellite image taken on January 20 (Figure 14). Cooler water is observed intersecting POST between C7 and C8, where it extends to the southeast. A comparison of PEGASUS data, geostrophic velocities and ADCP data was completed by Buckley (1990).

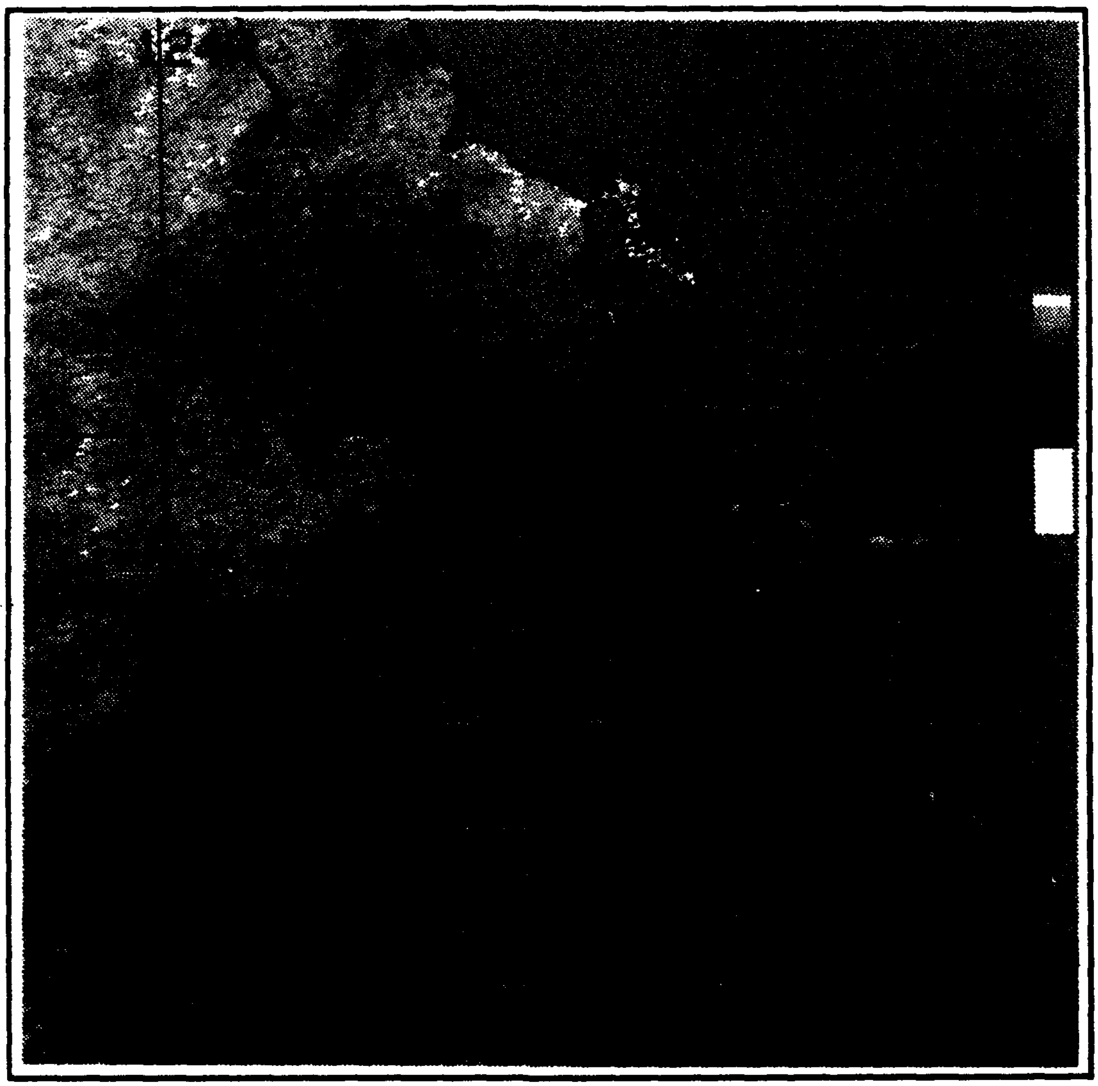

Figure 14. NOAA 11 AVHRR Satellite SST Imagery from January 20 1990.

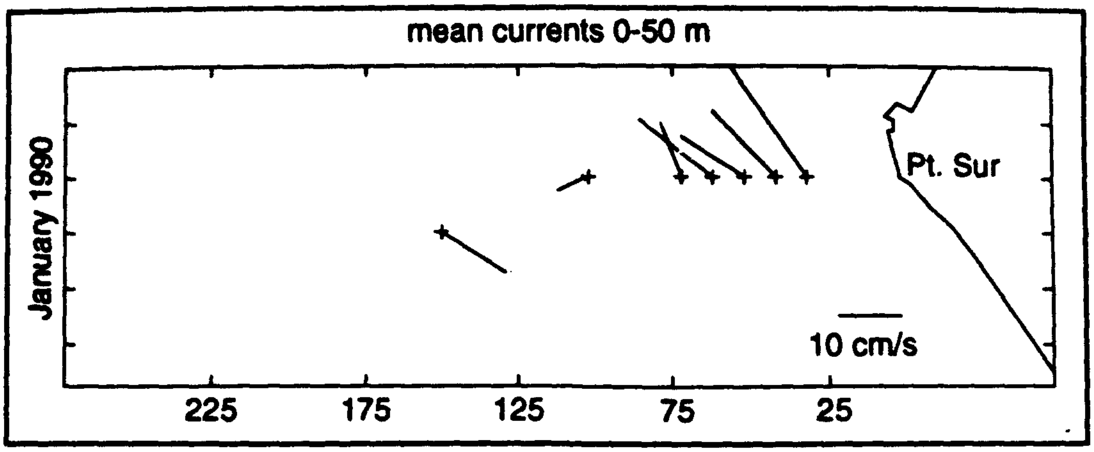

Figure 15. Mean Surface (0-50 m) PEGASUS Velocities for January 1990.

12. May 1990

Strong equatorward wind stress (>1 dyne cm^{-2}) preceded this cruise and persisted until May 23, when the winds relaxed. The flow along POST is unusual in that the CUC and the CC are both absent from 33 km to 150 km offshore. The velocity data for the availabe PEGASUS stations show strong equatorward flow. Maximum surface speeds exceed 20 cm s^{-1} between C3 and C8 (Figure 17). The moderate salinity values of this flow (>33.2) imply that the water is not associated with the CC. Comparison of the surface velocities along POST with a NOAA 11 AVHRR satellite image for May 24 (Figure 16) indicates an anticyclonic feature advecting cool upwelled water from Point Año Nuevo southward to POST, where it then turns to the west. This mesoscale feature is limited to the upper 400 m of the water column.

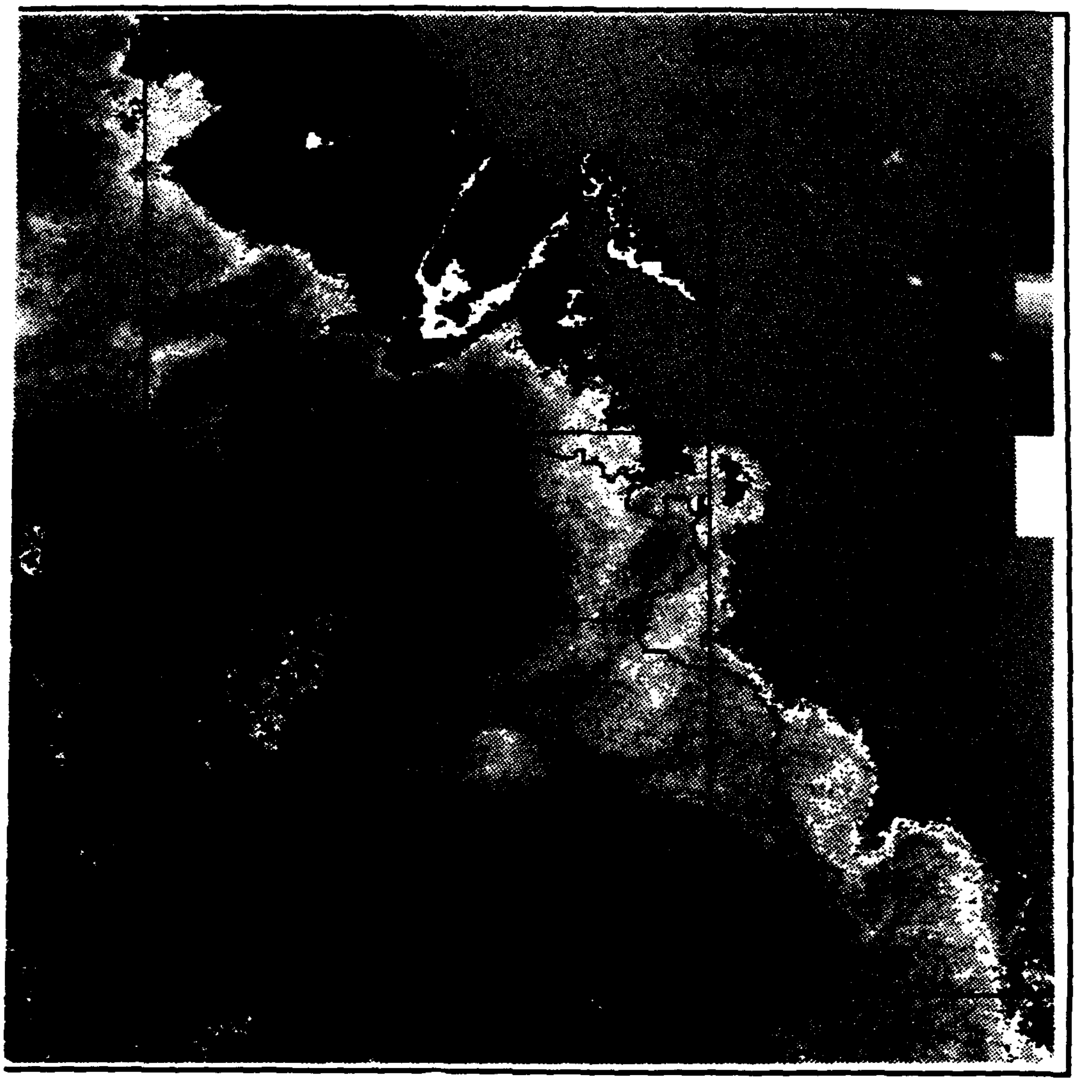

Figure 16. NOAA 11 AVHRR Satellite SST Imagery from May 24 1990: The dark shades north of 37° N are due to cloud contamination.

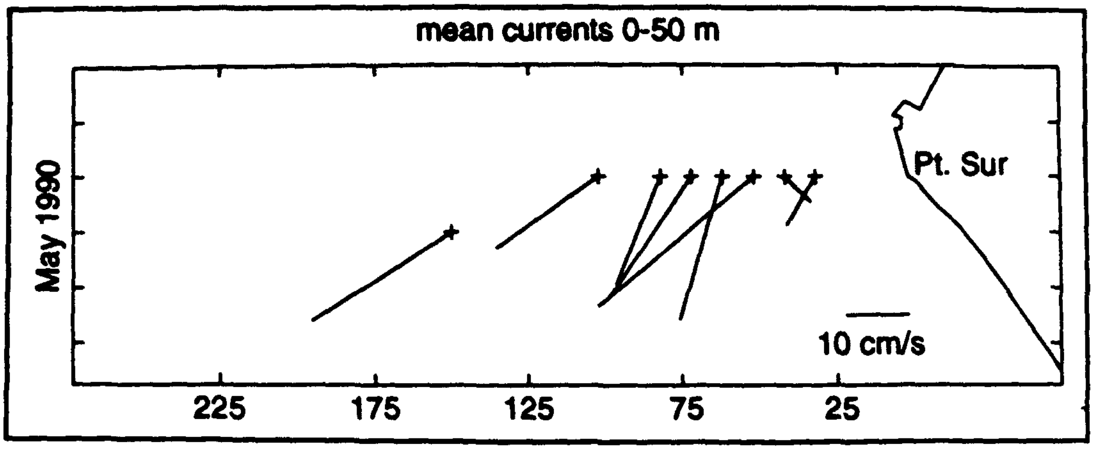

Figure 17. Mean Surface (0-50 m) PEGASUS Velocities for May 1990.

Hicks (1992) studied data from moored current meters off Point Sur at depths of 350 m and 500 m from 17 December 1989 to 4 April 1990. One mooring was located 7 km inshore of C1 and the other was located 3 km inshore of C3. The flow at both depths was predominantly poleward but shifted to equatorward on 8 March remaining equatorward through April. The equatorward flow observed from March to April suggests that the anticyclonic feature present during this cruise, may have persisted from March. The sharp frontal feature present in the salinity field between C8 and C9 suggest that the CC can be found offshore from C8.

13. June 1990

Two strong equatorward wind events with alongshore wind stress values greater than 2 dynes cm^{-2} preceded this cruise along with a two day relaxation period. The PEGASUS data for June show poleward surface flow at C1, C2, C3 and C9 and equatorward flow between C4 and C7. A salinity minimum of 33 at C7 indicates that the strong equatorward flow (>25 cm s^{-1}) is a meander of the CC. The poleward flow at C9 with a higher salinity value of 33.3 most likely consists of Central Pacific water entrained by the high speed CC meander. The CC is located further inshore than usual as is the CUC, which has a core speed of 26 cm s^{-1} at a depth of 100 m 33 km offshore.

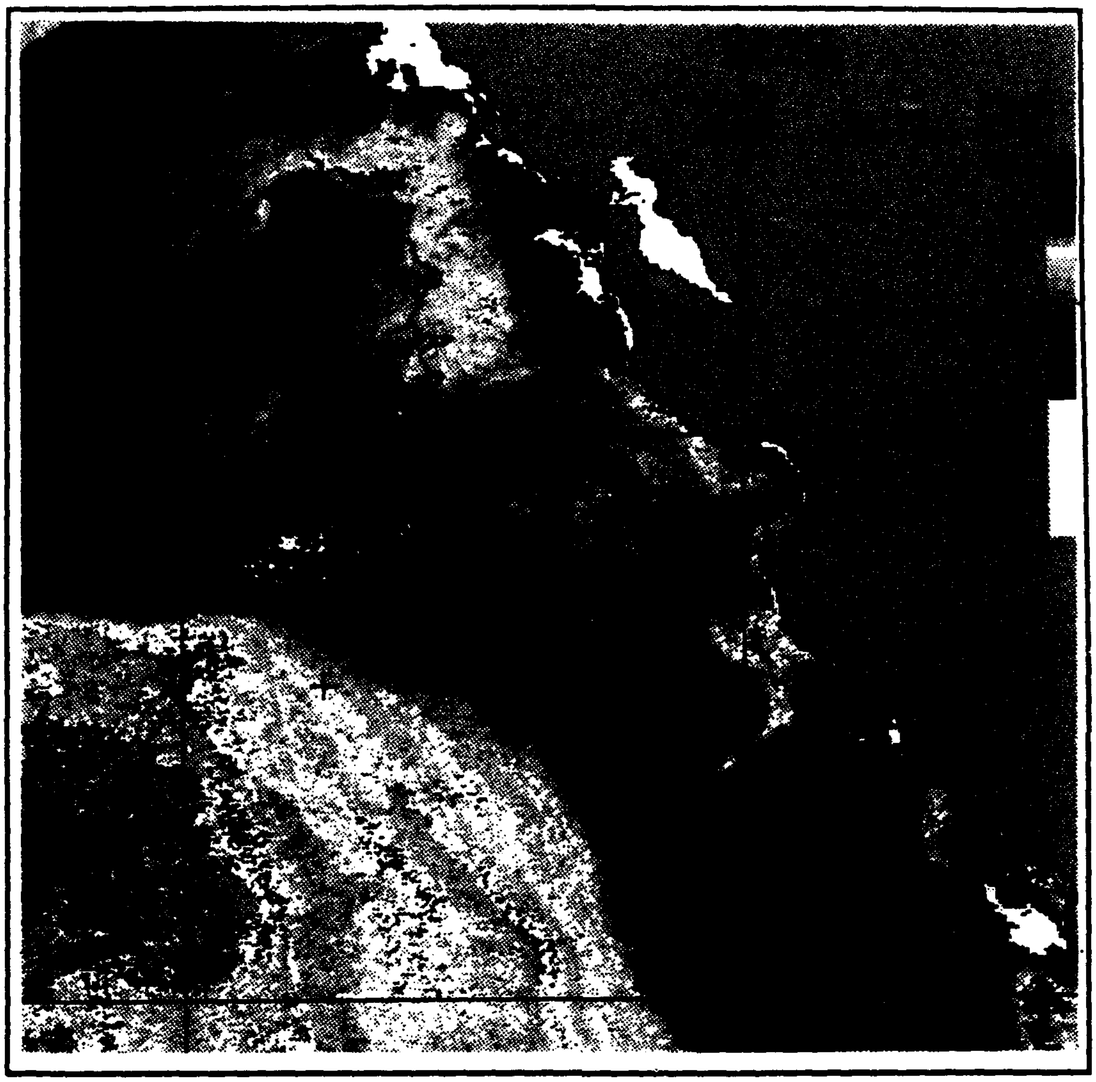

Figure 18. NOAA 11 AVHRR Satellite SST Imagery from June 20 1990: The light shades present in the southwest corner of the image are the result of cloud contamination.

A NOAA 11 AVHRR satellite image for June 20 (Figure 18) reveals a plume of cool upwelled water north just inshore of C1 and a second plume turning to the southwest. This pattern indicates that the poleward surface flow observed inshore of C3 (Figure 19) is not continuous in the alongshore direction.

The satellite image also indicates a southeastward extension of warm water between C7 and C8. A comparison of PEGASUS data, geostrophic velocities and ADCP data for this cruise was completed by Tziagidis (1991).

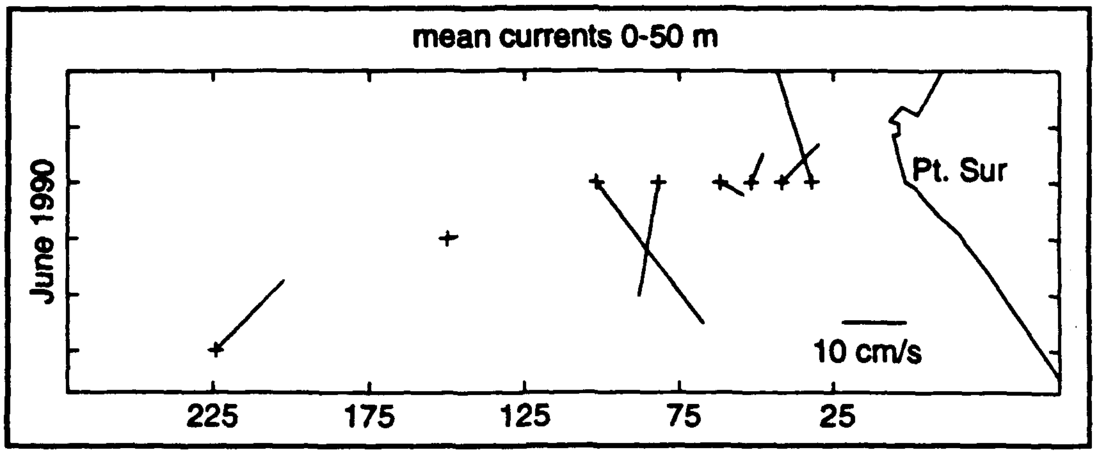

Figure 19. Mean Surface (0-50 m) PEGASUS Velocities for June 1990.

14. August 1990

The August surface velocity profile is dominated by an anticyclonically rotating onshore meander of the CC. Two subsurface salinity minimums at C8 and C4 (32.7 and 32.9 respectively) at 70 m identify fresher waters of the CC. The flow offshore from C6 is to the southeast, with a maximum speed of 26 cm s^{-1} while the flow at C4 is to the northwest, with a maximum speed of 17 cm s^{-1}. Deepening isotherms and shallowing isohalines inshore of C4 suggest water of southern origin. The flow at C2 is northeastward with a surface speed of 5 cm s^{-1} and a maximum speed of 13 cm s^{-1} at 100 m in depth. The poleward flow at C4 below 200 m is also to the northeast and has a core speed of 20 cm s^{-1} at 350 m. This subsurface poleward flow is unrelated to the poleward current observed at the surface, since the subsurface flow has a much higher salinity (+1.2) than the current at the surface. The two poleward currents are separated by a velocity minimum (< 5 cm s^{-1}) at 200 m in depth.

15. December 1990

PEGASUS data are available for C4, C5 and C6 for the December cruise. The flow at these stations is northwestward with a maximum speed of 23 cm s^{-1} at C5. The core depth is located at 60 m. A salinity minimum of 33.1 for this flow indicates that it is not of Pacific Equatorial origin. Low (< 33.2) salinity values along the entire transect above 100 m are most likely the result of recirculation of Pacific Subarctic water. A warm pool of water (> 13.5° C) between C1 and C6 is possibly a result of a cyclonically rotating meander of the CC.

B. DESCRIPTION OF THE VARIABILITY OF PEGASUS DATA

This section focuses on the variability of the currents along POST from 1988 to 1991. A complex or rotary EOF analysis was utilized to determine whether the variability of the slope currents were seasonal or interannual. The details and background of the analysis are described in appendix A. The results of the EOF analysis show the variability at each station along POST is predominantly interannual. The first mode accounts for more than 60 % of the total variance at every station. The spatial patterns indicate that the CUC accounts for most of the variability inshore of C7, while the CC accounts for most of the variability from C7 offshore to C9.

The mean surface currents show equatorward flow from C7 to C8, onshore flow at C9 and poleward flow from C6 inshore to C1 (Figures 20 and 21). The mean currents between C4 and C7 are weak (< 5 cm s^{-1}) at all depths. In order to evaluate the significance of the mean currents for the entire three year period, current vector histograms and variance axes were calculated at each station (Figures 23 through 33). The current direction histograms for C4, C5 and C6 show no clearly dominant current direction in the upper 250 m. Below 250 m there is dominant mode to the northwest for C4 and C5 due to the influence of the CUC. The strongest surface poleward flow is at C2 (8 cm s^{-1}), while the strongest equatorward flow is at C8 (9 cm s^{-1}). The onshore surface flow at C9 has a mean speed of 10 cm s^{-1}. The mean core speed of the CUC is 10 cm s^{-1} at C1, 80 m below the surface. The mean poleward undercurrent is evident offshore to C5 and has a mean speed greater than 5 cm s^{-1} to 500 m in depth.

The current vector histograms for C1, C2 and C3 show a predominant current direction to the northwest down to 500 m in depth. The major axis of variation for C2 is aligned parallel to the coast in the direction of the CUC, while the axis at C1 is oriented from the northwest to the southeast and the axis at C3 is oriented in the southwest to northeast direction. Below 250 m, the major axes of variation are aligned in the cross shore direction for all three stations. This suggests that the current variability at C2 is due to changes in the strength of the CUC in the alongshore direction, while at C1 and C3 the cross shore component of the variability is a result of the lateral translation of the CUC core. The variability for all three stations is greatest in the cross shore direction below 250 m.

The current vector histograms for C7, C8 and C9 show a few dominant current directions in the upper 250 m of the water column. There are two dominant current modes at C7, one to the northeast and the other to the southeast. At C8, one mode is to the southeast and the other is to the southwest. C9 has a dominant mode to the southeast. The major variance axes at C8 and C7 are oriented from the northwest to southeast to 250m. The axis at C9 is oriented perpendicular to the coast in the upper 50 m but becomes aligned northwest to southeast below 50 m. The agreement between the mean current directions, the current direction histograms and major variance axes indicate that the mean currents at these three stations are significant.

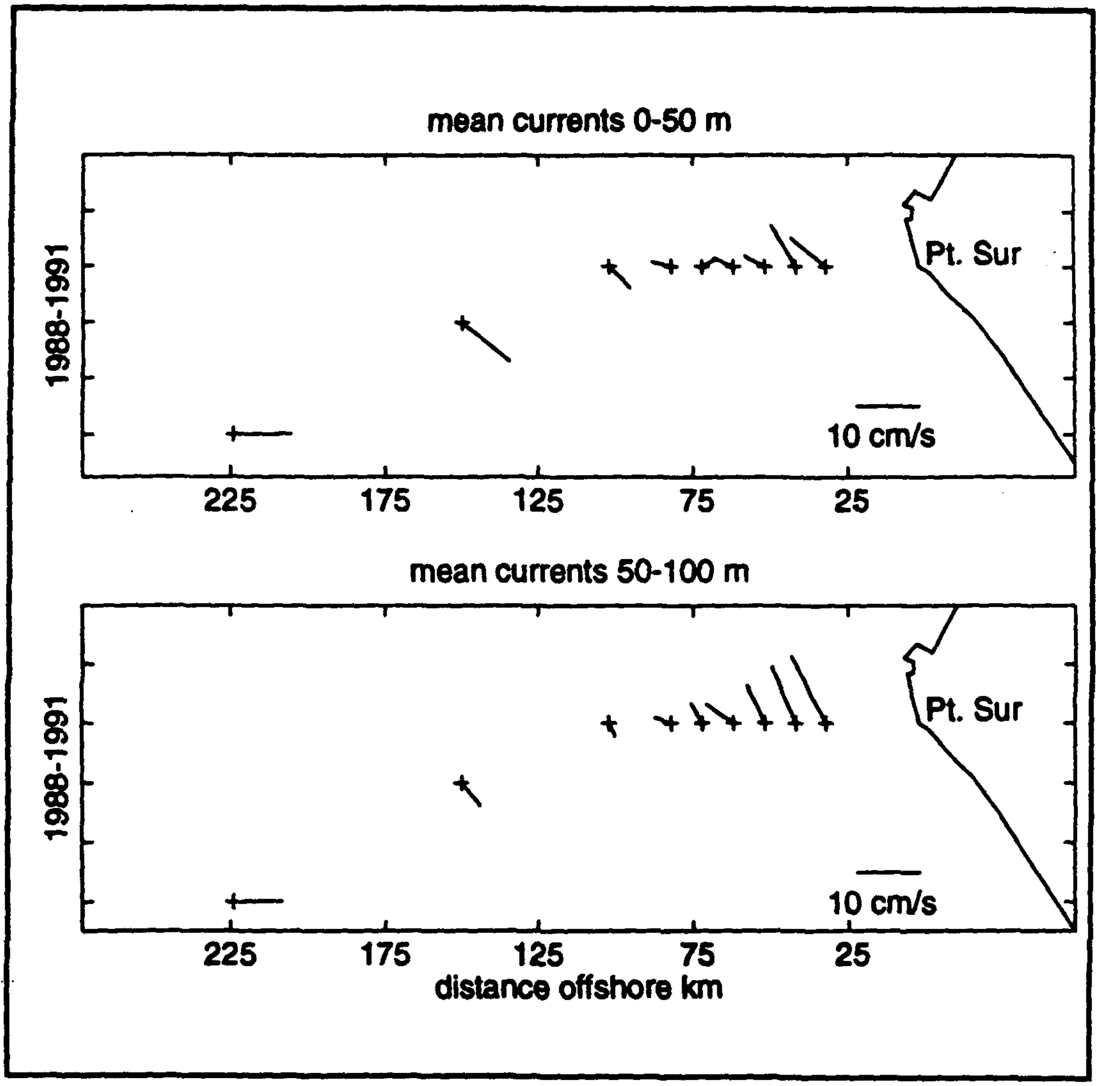

Figure 20. Mean PEGASUS velocities for the period from April 1988 to December 1990.

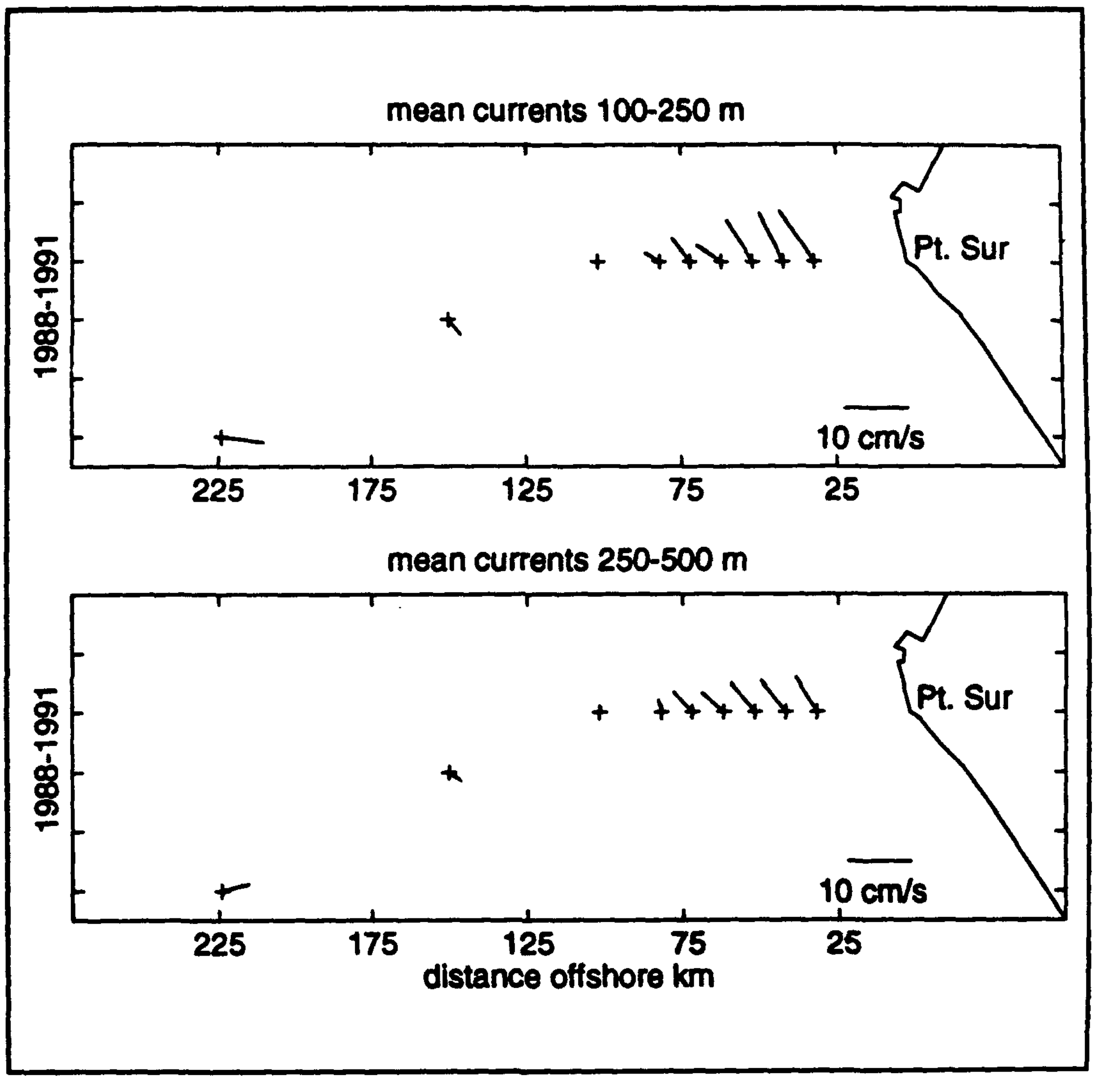

Figure 21. Mean PEGASUS velocities for the period from April 1988 to December 1990.

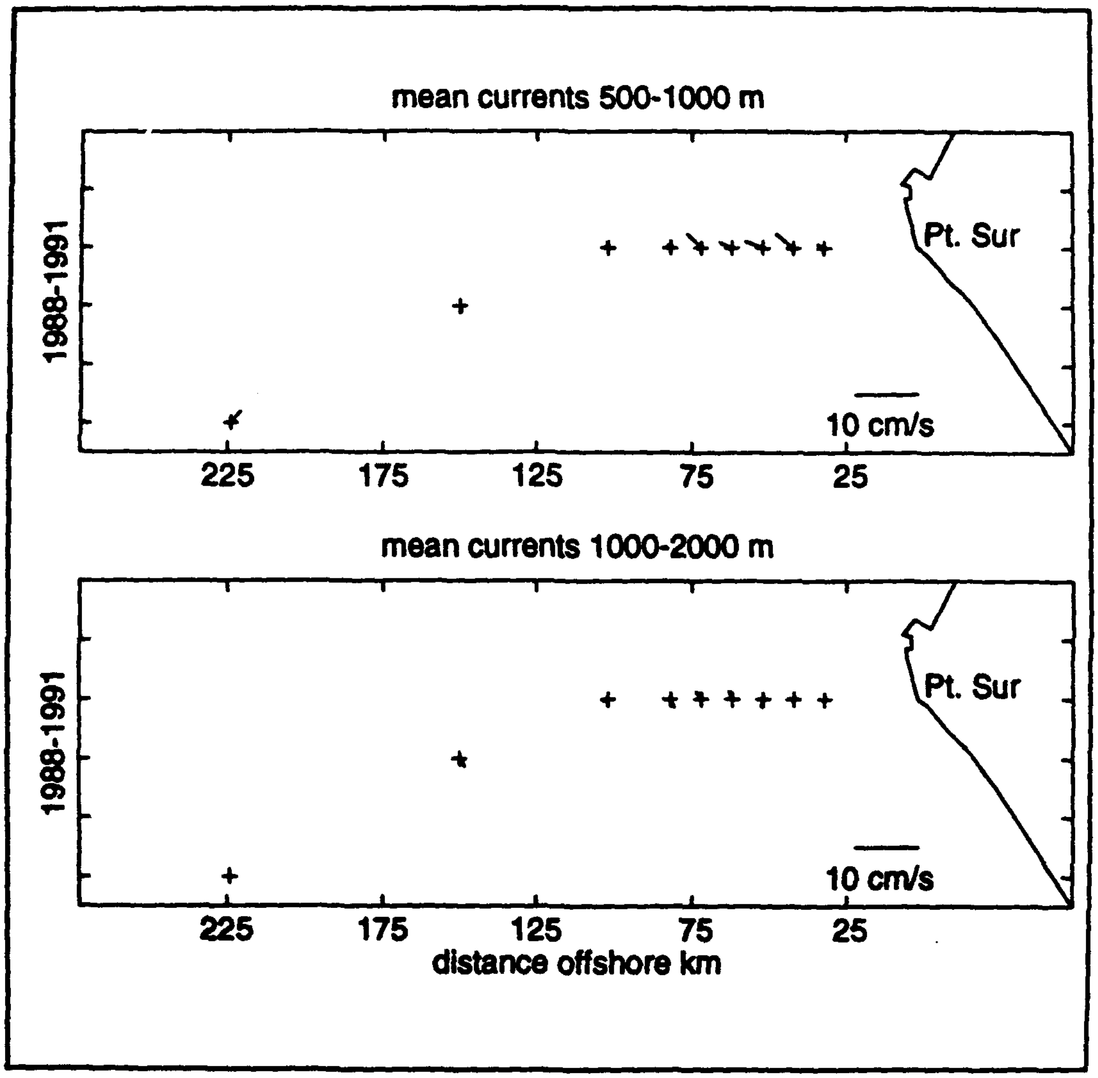

Figure 22. Mean PEGASUS velocities for the period from April 1988 to December 1990.

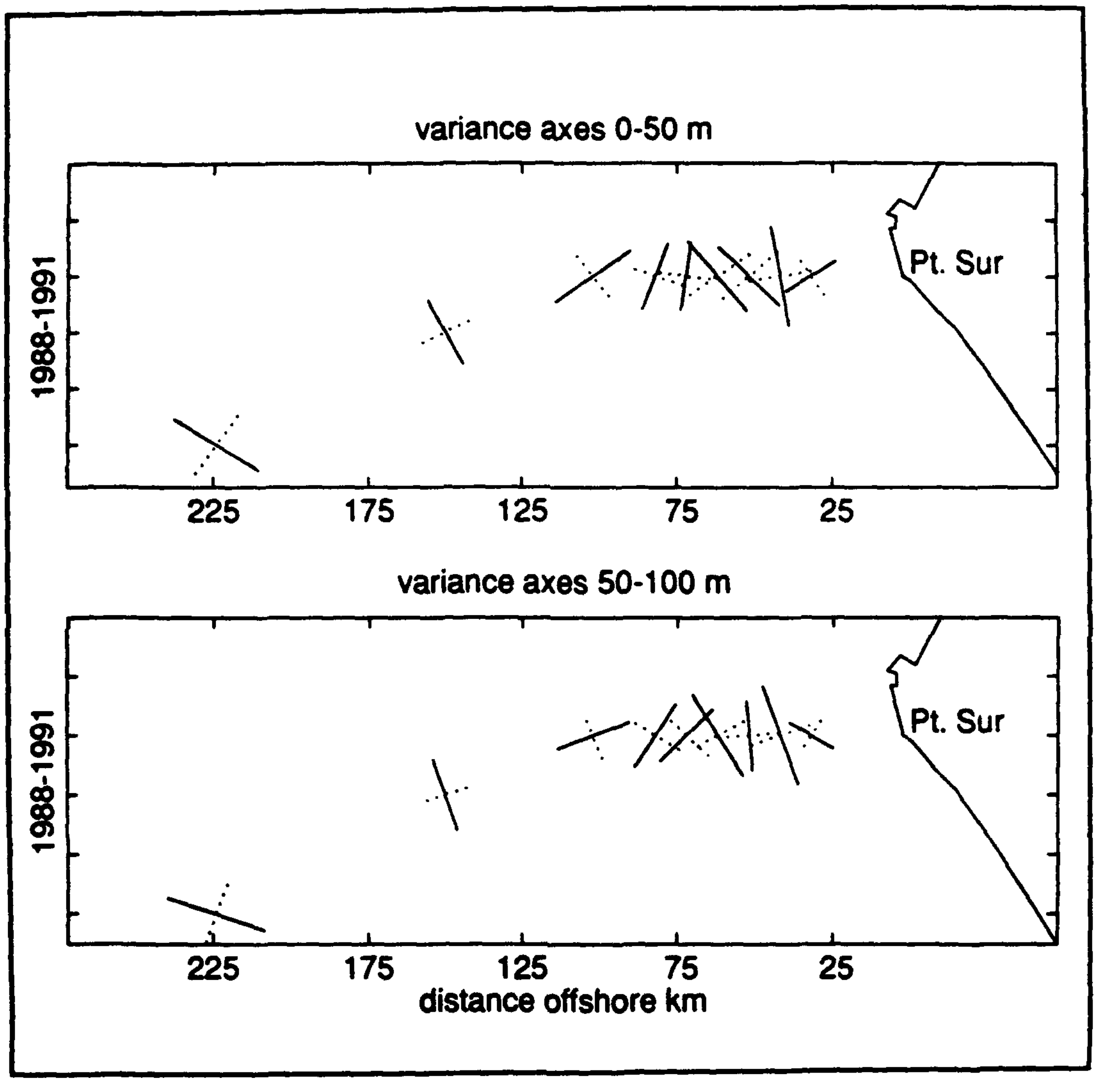

Figure 23. Variance axes for the entire data set: The solid lines represent the major axis of variation and the dotted lines represent the minor axis.

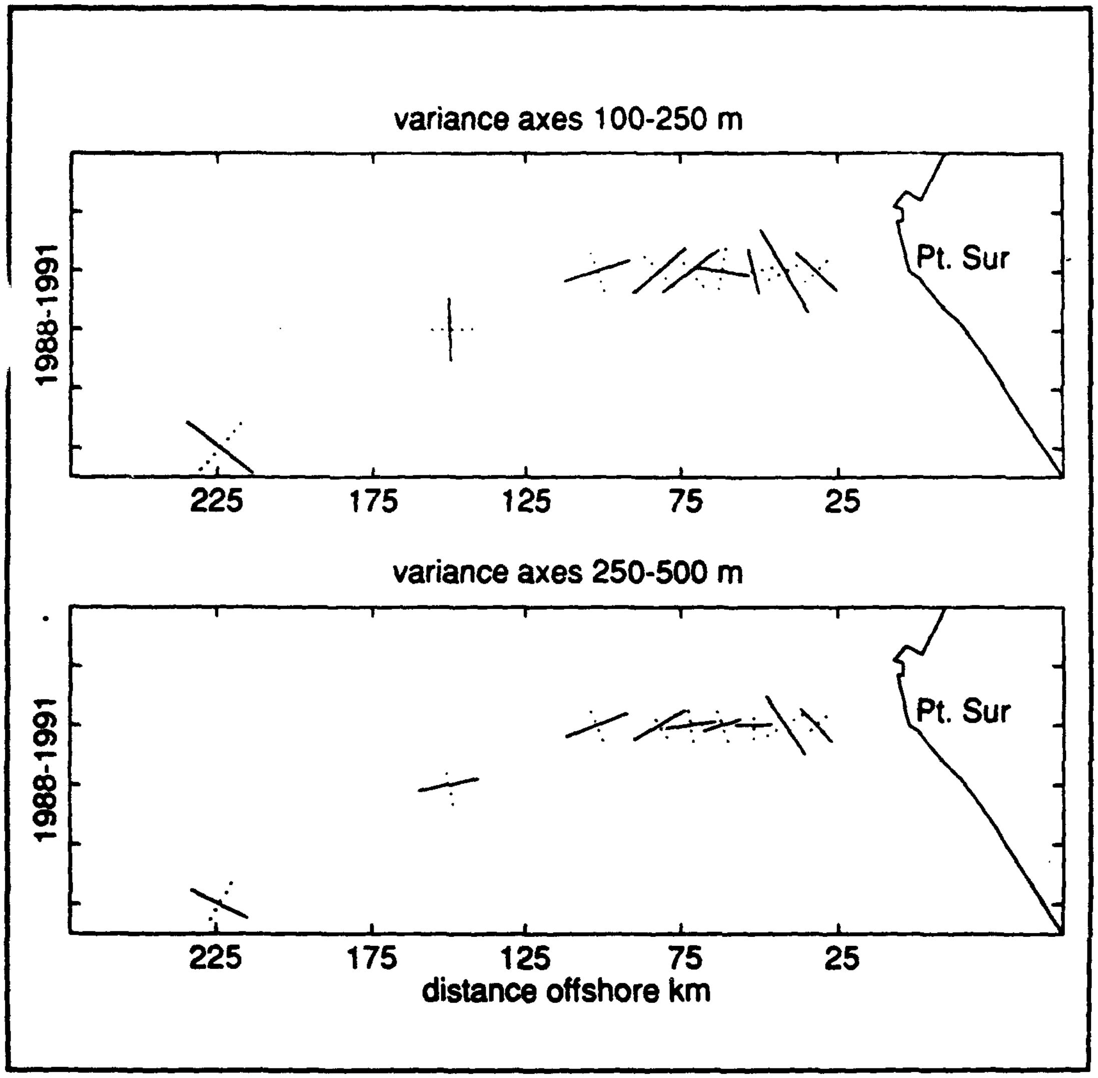

Figure 24. Variance axes for the entire data set: The solid lines represent the major axis of variation and the dotted lines represent the minor axis.

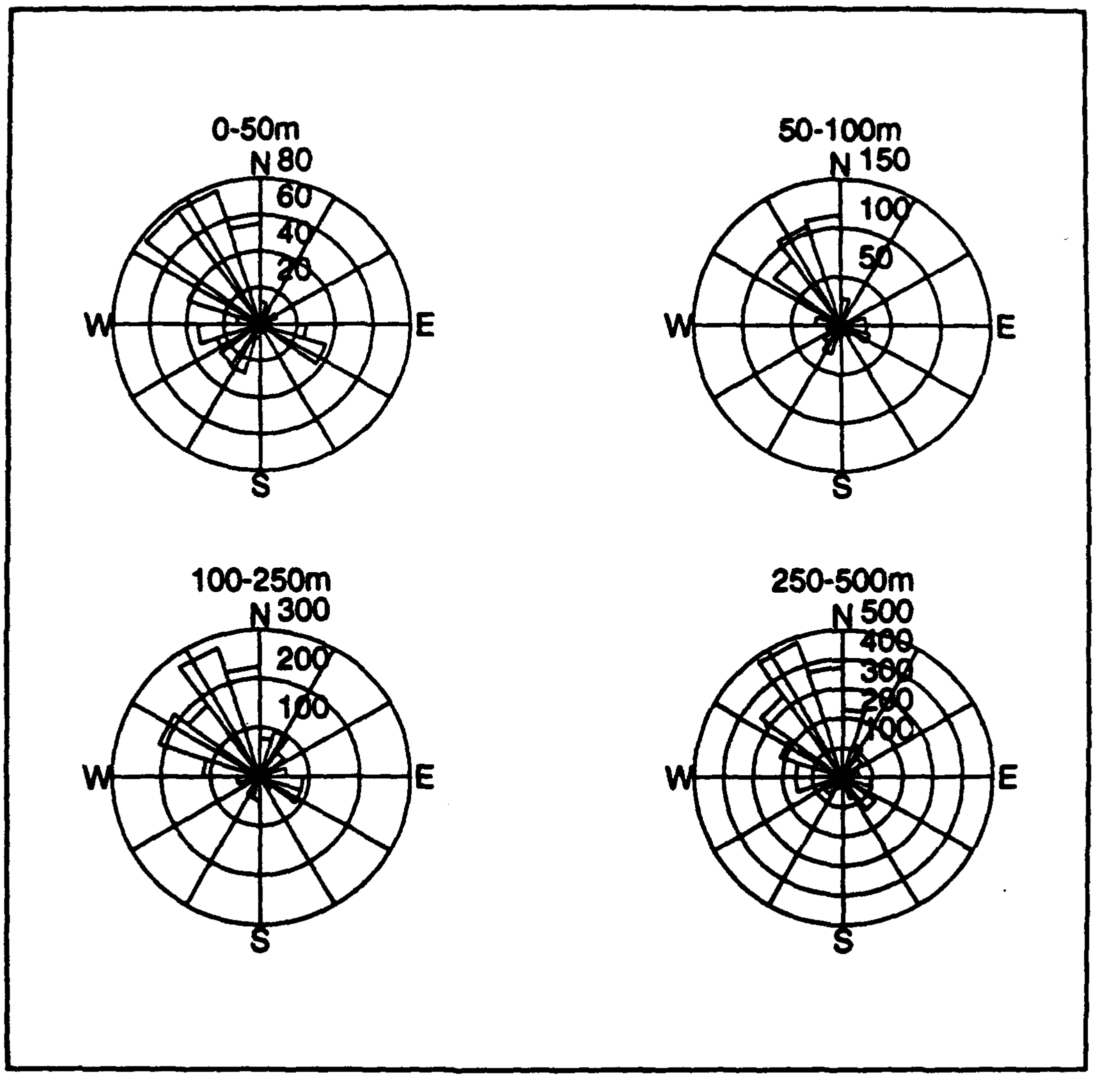

Figure 25. Current direction histograms for C1: Numbers represent observations.

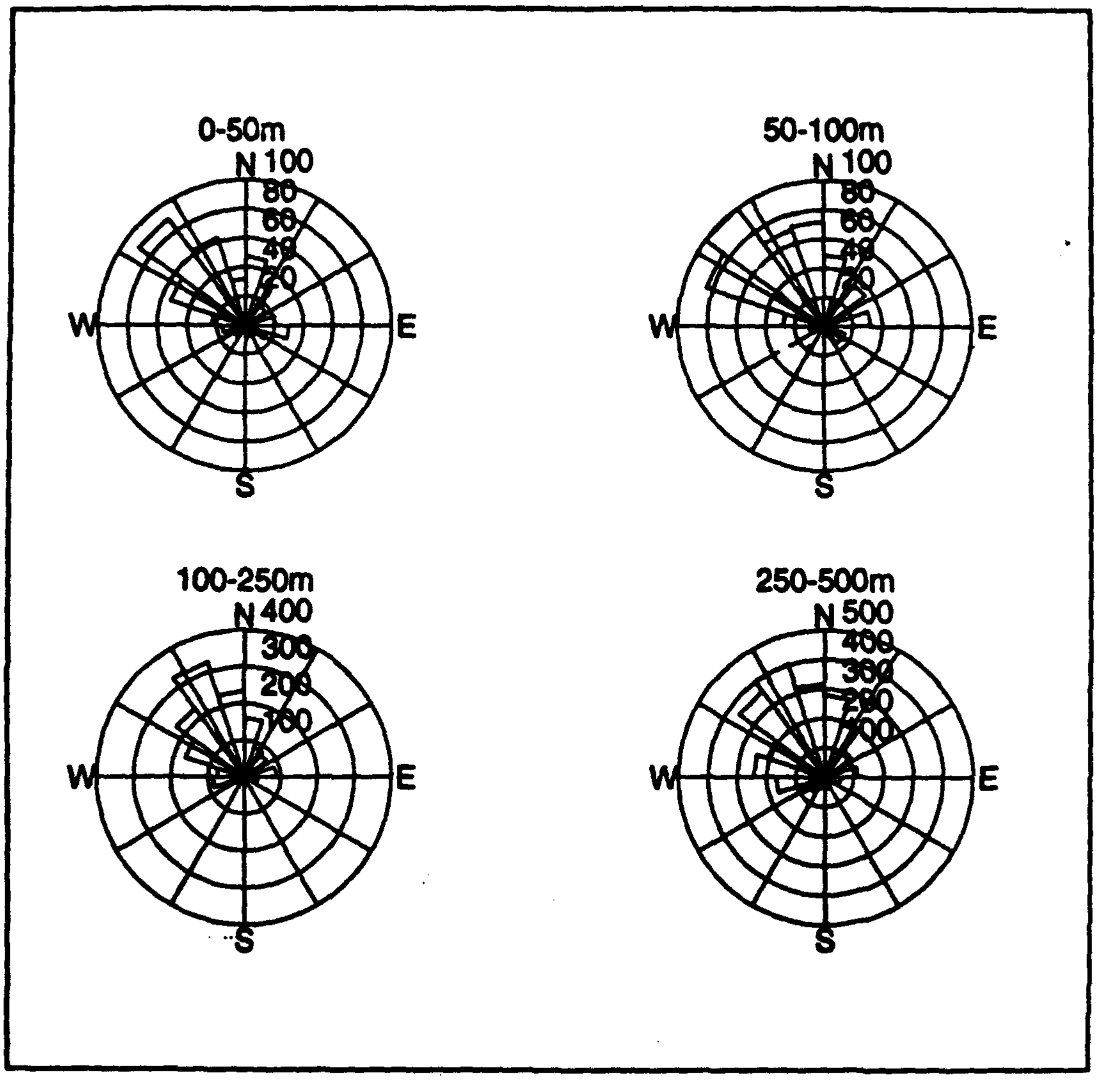

Figure 26. Current direction histograms for C2: Numbers represent observations.

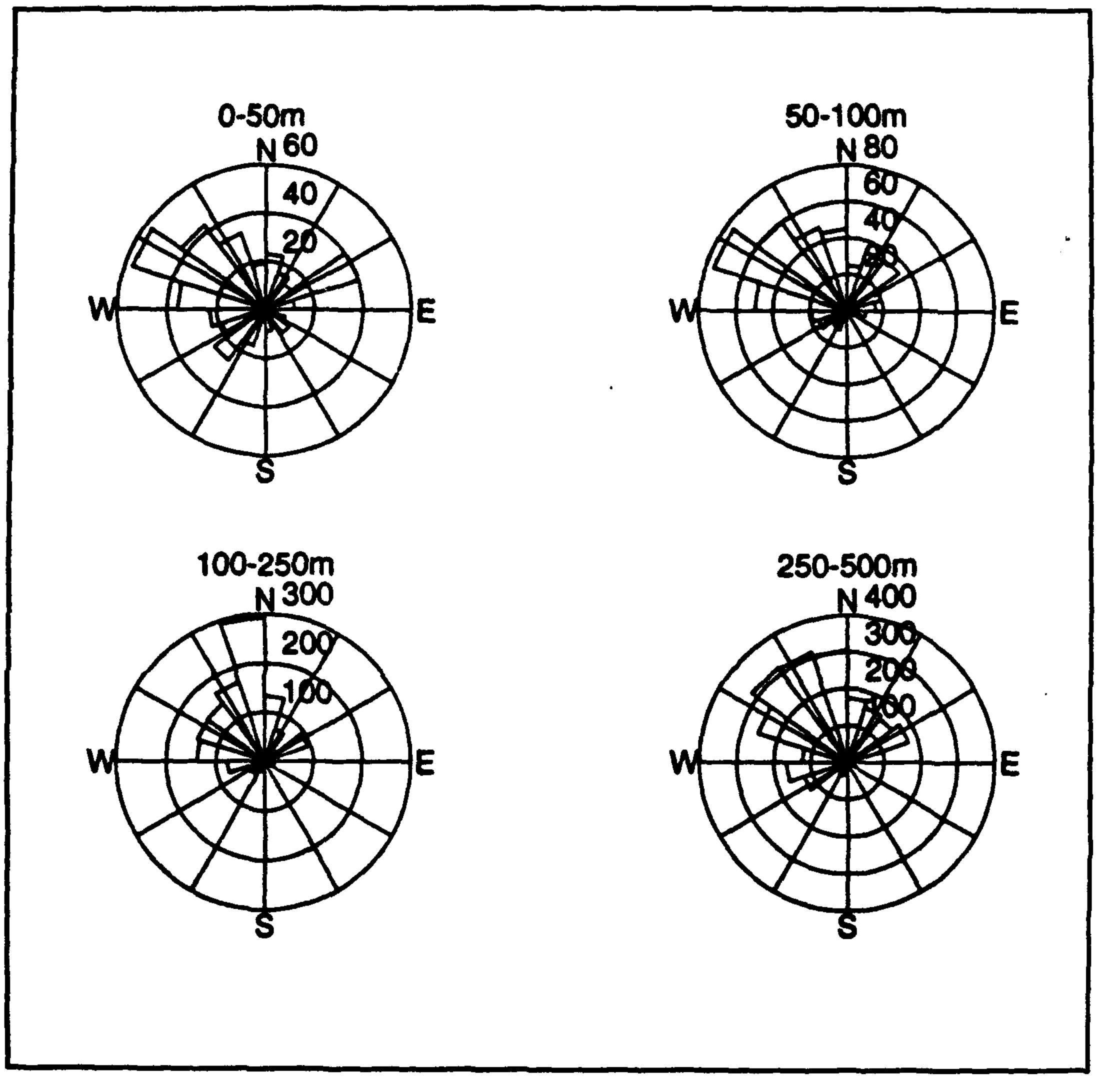

Figure 27. Current direction histograms for C3: Numbers represent observations.

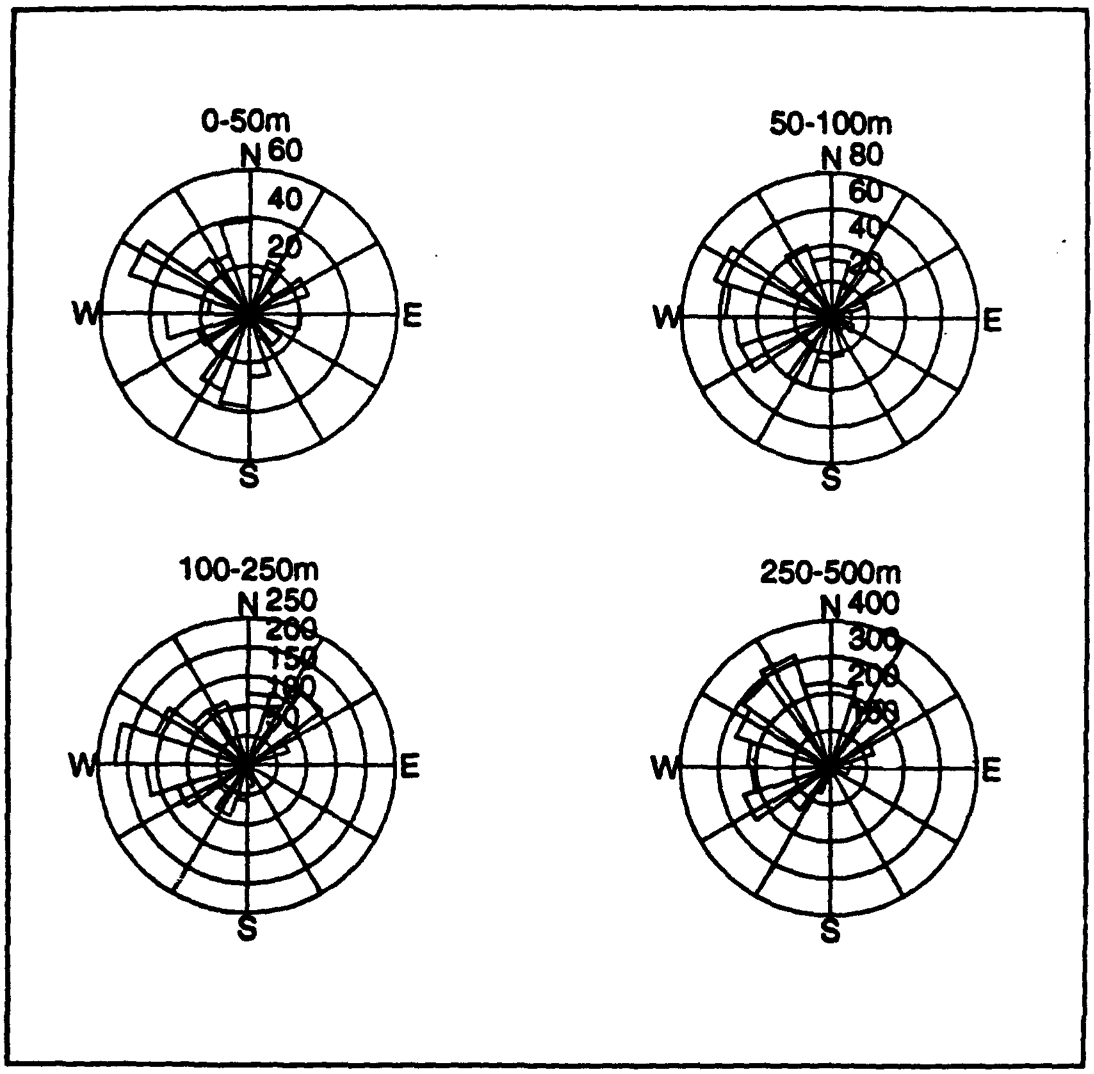

Figure 28. Current direction histograms for C4: Numbers represent observations.

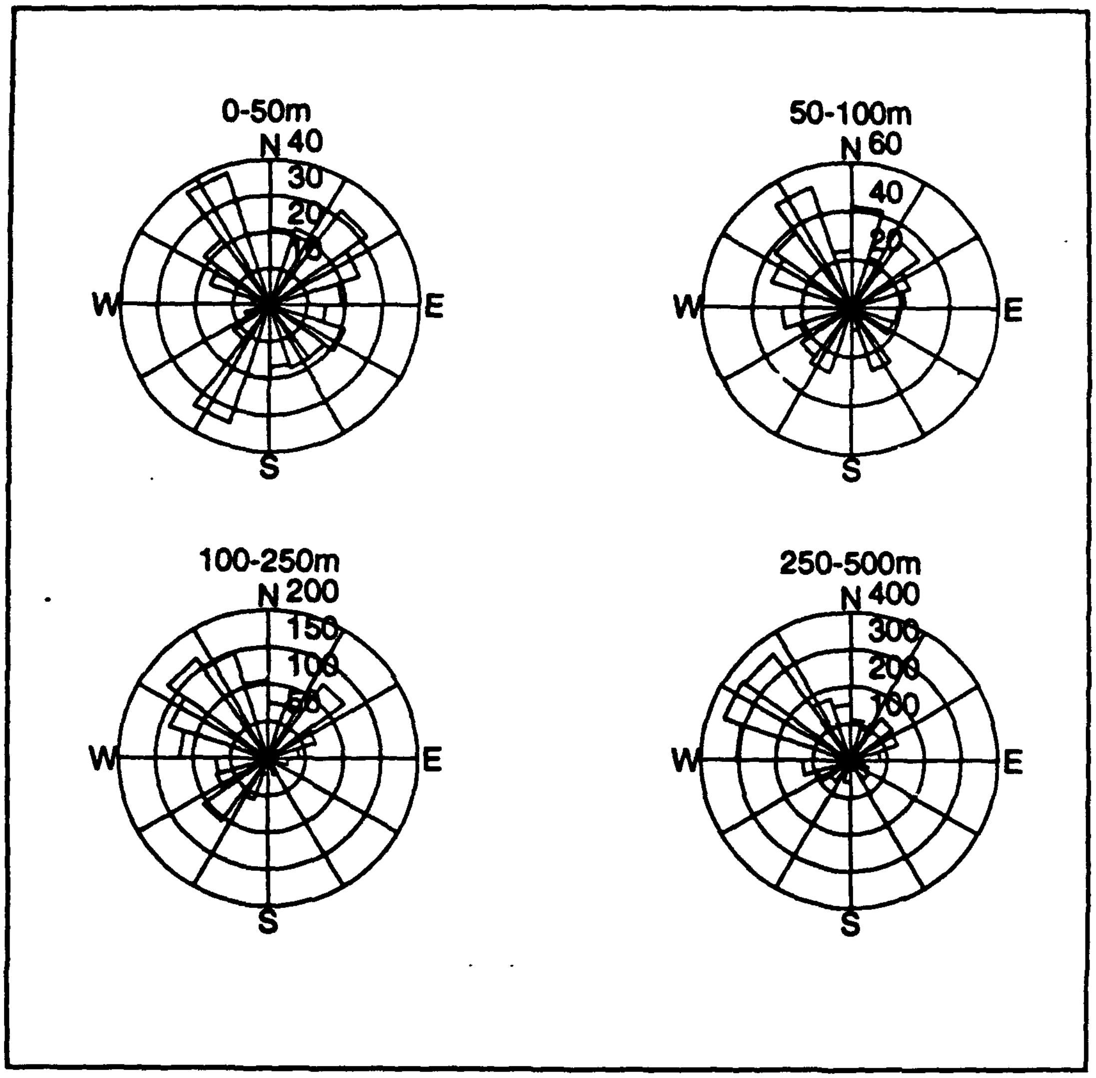

Figure 29. Current direction histograms for C5: Numbers represent observations.

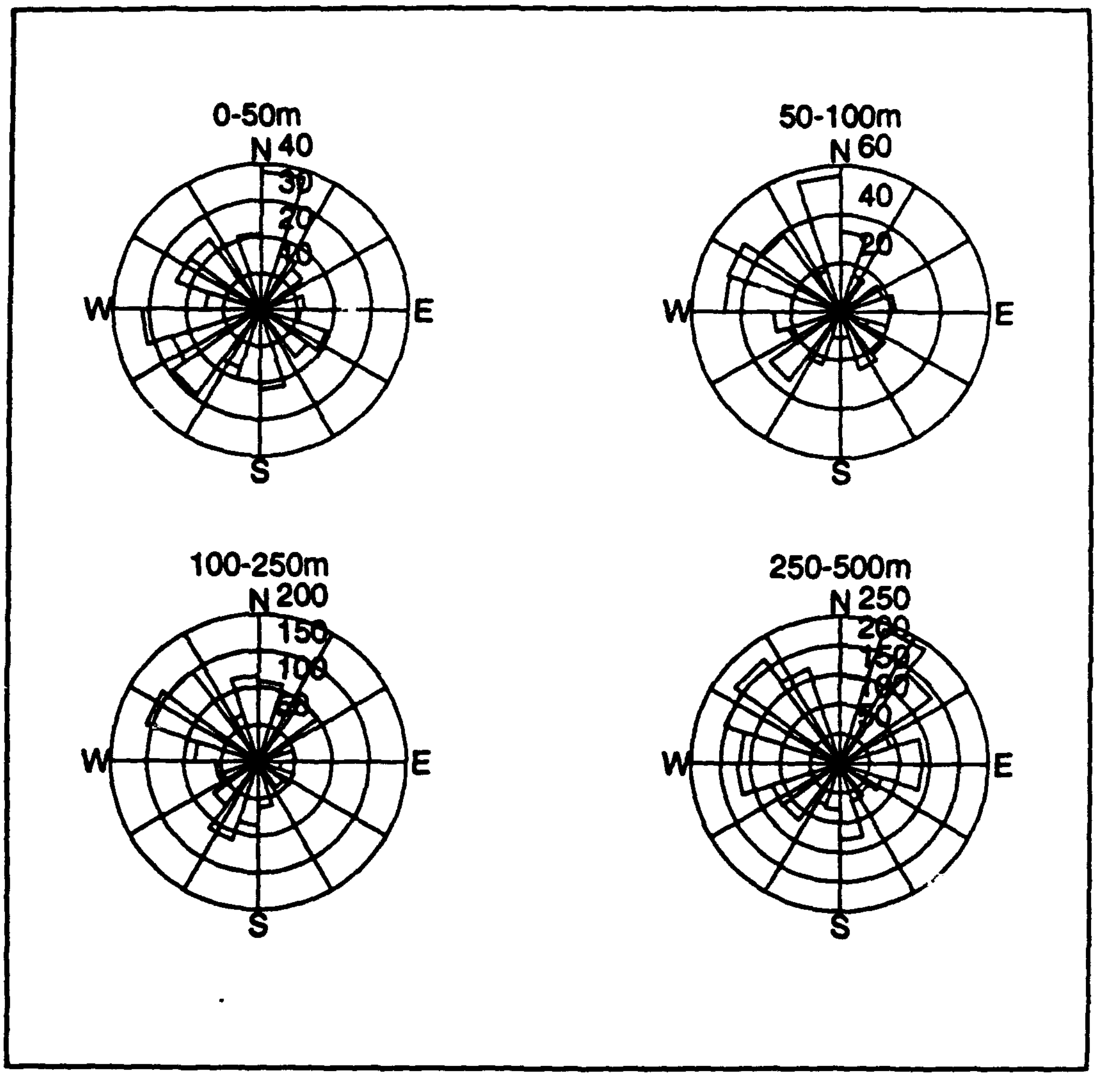

Figure 30. Current direction histograms for C6: Numbers represent observations.

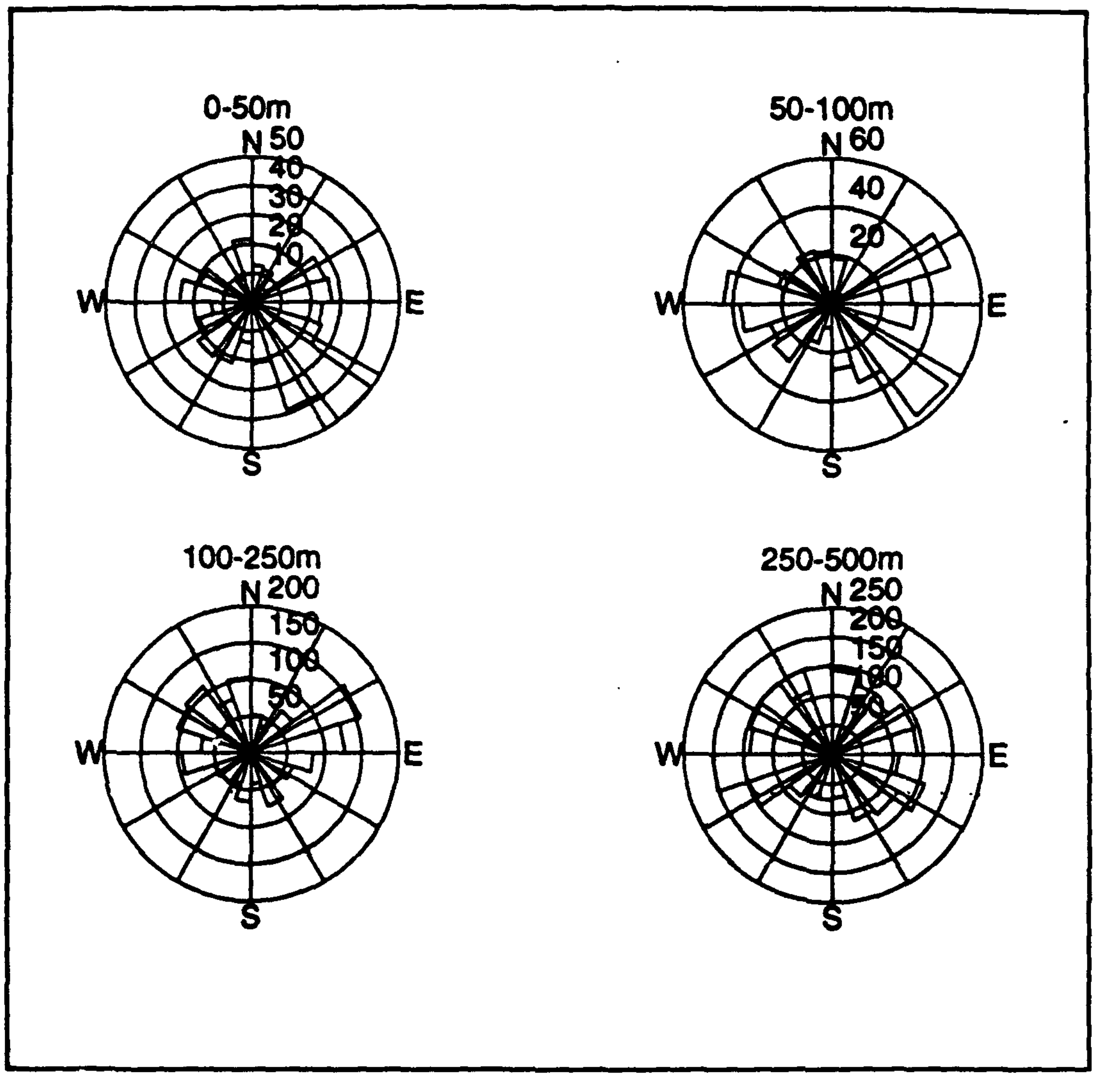

Figure 31. Current direction histograms for C7: Numbers represent observations.

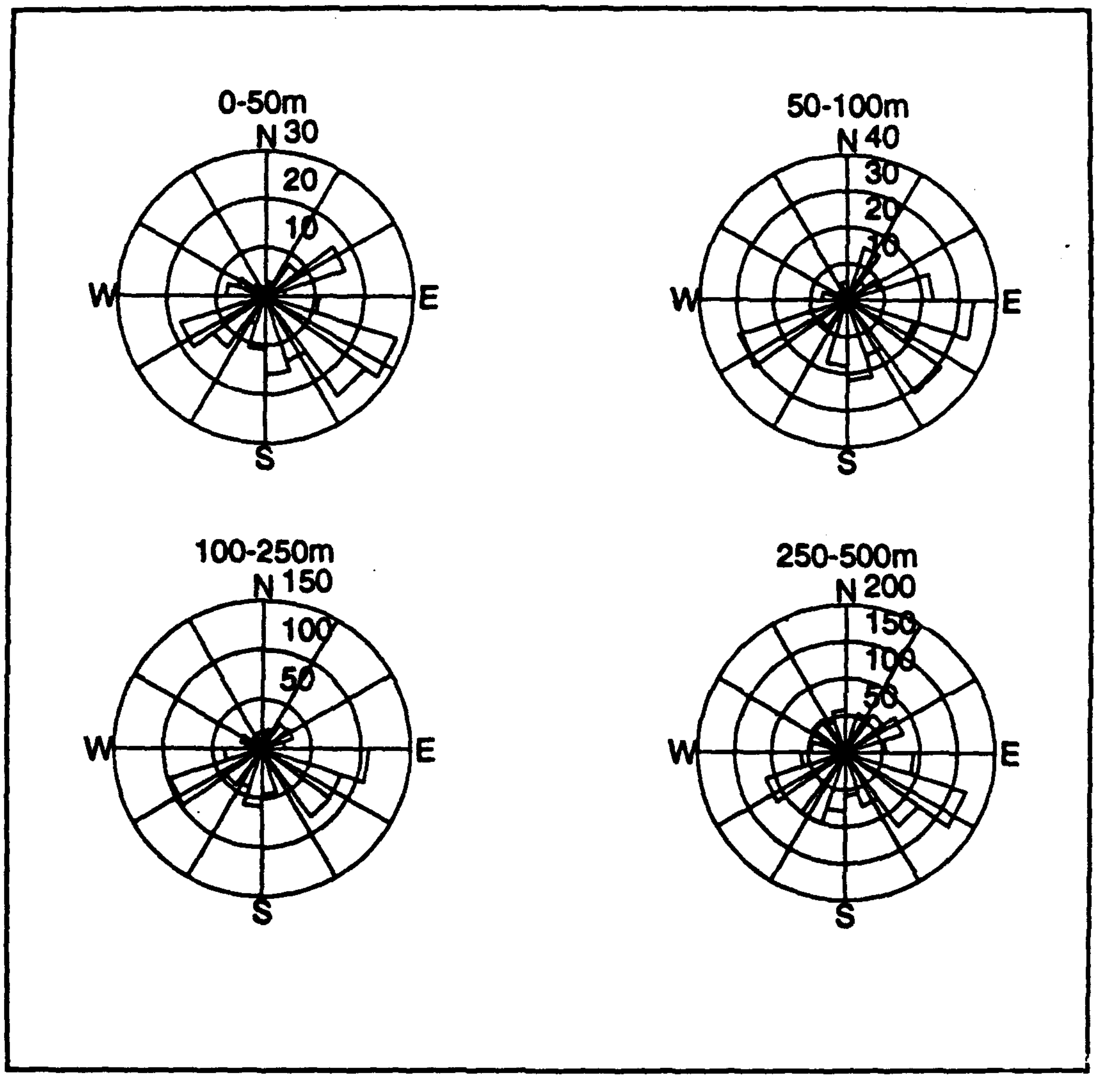

Figure 32. Current direction histograms for C8: Numbers represent observations.

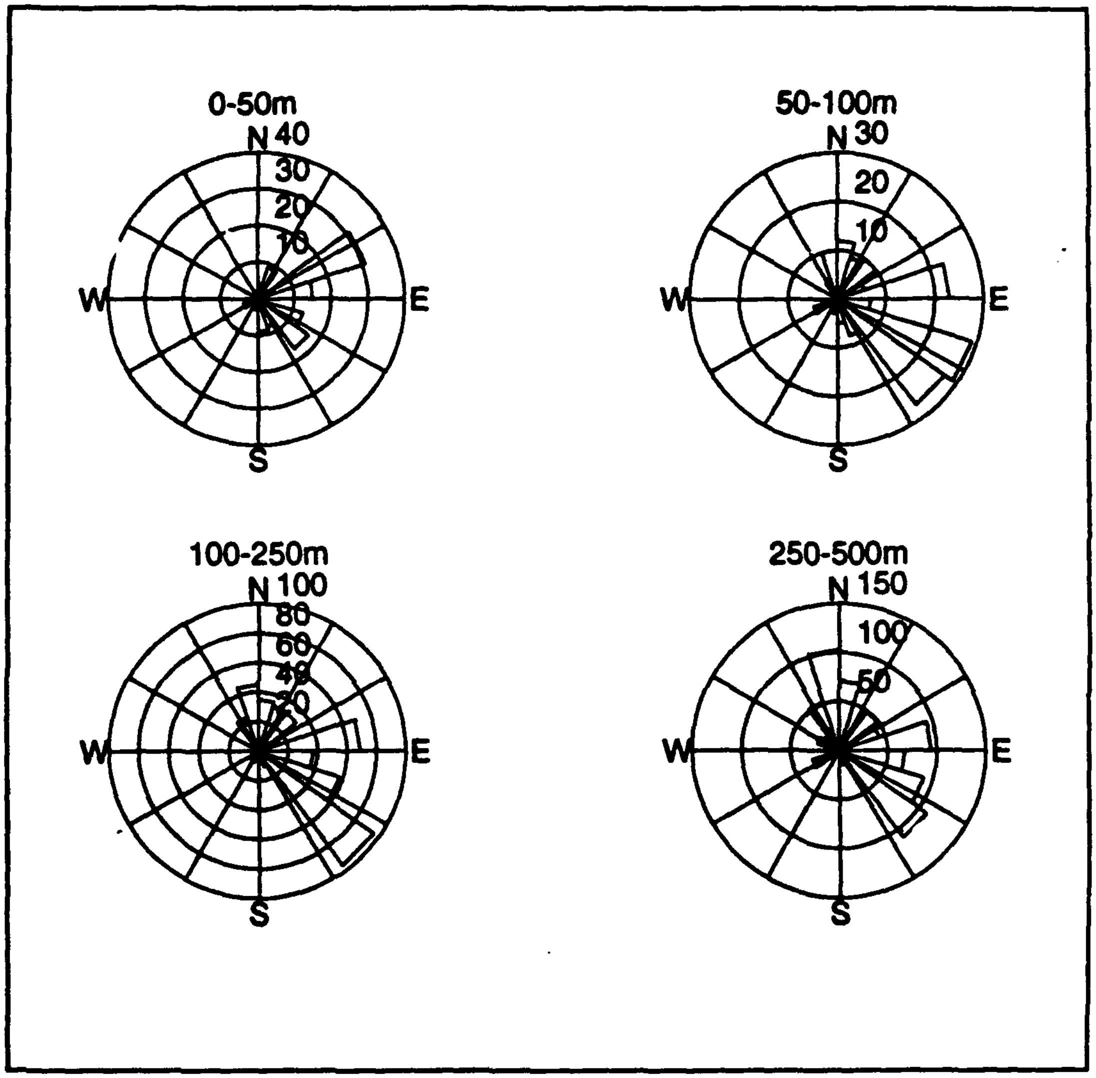

Figure 33. Current direction histograms for C9: Numbers represent observations.

IV DISCUSSION

This chapter focuses on the results of this study and compares and contrasts them to earlier studies of the CCS along central California. The first section contains a more detailed comparison with the results of Tisch et al (1992), since geostrophic velocities were determined along POST for six of the cruise periods analyzed in this study.

A. COMPARISON OF PEGASUS DATA WITH GEOSTROPHIC VELOCITIES

1. August 1988

Tisch et al. (1992) found equatorward surface flow along POST offshore from C2. The core of the CC was located near C7 with a maximum velocity in excess of 20 cm s^{-1}. Inshore of C3, the CUC was determined to have two cores, one at C2 with a speed greater than 20 cm s^{-1} at 190 m and the other 20 km inshore of C1, surfaced with a maximum surface speed in excess of 60 cm s^{-1}. PEGASUS data also show the core of the CC at C7, however the speed is greater than geostrophy indicates (25 cm s^{-1}). The surface equatorward flow found offshore from C2 is also evident from the PEGASUS data except that the absolute velocities show weak equatorward flow (< 5 cm s^{-1}) in contrast to the 20 cm s^{-1} equatorward flow estimated by geostrophy between C3 and C4. The PEGASUS data show the CUC to have a core depth and speed of 200 m and 25 cm s^{-1} respectively at C1.

2. November 1988

The geostrophic velocities indicated the presence of an anticyclonic eddy along POST. The maximum equatorward speeds inshore of C3 were greater than 30 cm s^{-1}, while the poleward speeds near C4 were in excess of 55 cm s^{-1}. PEGASUS data also reveal this anticyclonic feature. Maximum equatorward absolute velocities near C1 are 26 cm s^{-1}, while the maximum poleward velocity is 23 cm s^{-1} at C3. The only striking difference between geostrophy and absolute velocities is the depth of this eddy. Strong speeds (> 10 cm s^{-1}) were determined by geostrophy to 600m, whereas PEGASUS derived absolute velocities show speeds greater than 10 cm s^{-1} only to 300 m. The CUC was absent from the PEGASUS data which agreed favorably with geostrophy along the same portion of POST. The CUC determined from geostrophy was located 10 km inshore of C1 with a core depth of 460 m and a core speed greater than 30 cm s^{-1}.

3. February 1989

The geostrophic velocities for this cruise period agree favorably with PEGASUS data along POST. Strong poleward surface flow between C1 and C3 (25 cm s^{-1}), equatorward surface flow offshore from C3 (20 cm s^{-1}) and the CUC located 5 km inshore of C1 with a core depth and speed of 100 m and 30 cm s^{-1} respectively are all indicated by geostrophy. Absolute velocities show 28 cm s^{-1} poleward surface flow at C2, 12 cm s^{-1} equatorward surface flow near C5 and the CUC with a core speed of 27 cm s^{-1} at C1, 100 m below the surface. The geostrophic velocity field also indicates a second and stronger CUC core located 10 km inshore of C1 with a core depth and speed of 100 m and 35 cm s^{-1} respectively.

4. May 1989

The contrast between absolute velocities and geostrophically derived velocities is significant during this cruise. This is the only comparison of the two methods available during the peak in the upwelling season. The winds prior to and during this cruise were upwelling favorable. The geostrophic velocity field indicated poleward surface flow between C1 and C2 (10 cm s^{-1}), an equatorward jet (>40 cm s^{-1}) centered at C5, and equatorward flow offshore from C9 (15 cm s^{-1}). The CUC was located 25 km inshore of C1 with a speed in excess of 20 cm s^{-1} at 100 m in depth. PEGASUS data show poleward surface flow between C1 and C2 (8 cm s^{-1}) and weak equatorward flow (< 5 cm s^{-1}) at C8. The surface equatorward jet is absent near C5 and instead the flow is predominantly offshore west of C2. The CUC is located at C1 with maximum speeds greater than 20 cm s^{-1} . The subsurface poleward flow is unusually deep and strong during this cruise with velocities in excess of 10 cm s^{-1} to 850 m at C1. The CUC is clearly present offshore to C5. The geostrophically derived velocities fail to indicate this strong poleward subsurface flow. The contrast between geostrophic and absolute velocities is partially due to the choice of 1000 m as the level of no motion. Strong (to 10 cm s^{-1}) poleward flow is found to 2400 m at C4 and 1600 m at C3.

5. July 1989

The geostrophic velocity field indicated surface poleward flow (> 30 cm s^{-1}) along the entire transect with maximum speeds just inshore of C1. The poleward subsurface flow is weaker with velocities greater than 10 cm s^{-1} to 400 m. The absolute velocities also show poleward surface flow along POST except the observed speeds are not as strong. The maximum poleward speed is 20 cm s^{-1} at C4. Poleward subsurface flow is also indicated by PEGASUS with speeds in excess of 10 cm s^{-1} to 400 m. The core of the CUC was determined by geostrophy to be located 5 km inshore of C1 with a maximum speed of 15 cm s^{-1} at 400 m. The absolute velocities indicate that the CUC is located at C3, 80 m in depth. The difference in CUC positions is due to the meander present in the absolute velocity field. The CUC core has a significant onshore component (> 25 cm s^{-1}) that would not be determined with geostrophic velocities calculated normal to POST.

6. November 1989

A banded flow structure was revealed by geostrophy with poleward surface flow at C1 (> 25 cm s^{-1}), C2 (> 15 cm s^{-1}) and C7 (25 cm s^{-1}). Equatorward flow was present at C3 (5 cm s^{-1}), C6 (< 5 cm s^{-1}), C8 (> 10 cm s^{-1}) and C9 (> 15 cm s^{-1}). The absolute surface velocities also show this banding feature. The directions and magnitudes are almost identical except that the surface flow at C3 is poleward, the surface flow at C2 is stronger in the offshore direction giving it a poleward component of velocity of only 5 cm s^{-1} and the poleward surface speed at C7 is only 12 cm s^{-1}. The CUC was geostrophically determined to have a core depth and speed of 70 m and 35 cm s^{-1} respectively 5 km inshore of C1, whereas PEGASUS data indicate the CUC at 180 m in depth with a core speed of 30 cm s^{-1} at C1. The disparity in the two methods is again the result of a significant cross-shore component of subsurface flow evident in the absolute velocity field. It must be noted that strong (> 10 cm s^{-1}) subsurface flow is present at depths greater than 2000 m, negating the choice of 1000 m as the level of no motion.

B. COMPARISON OF PEGASUS DATA TO OTHER STUDIES OFF CENTRAL CALIFORNIA

Chelton (1984) studied 23 years of CalCOFI data off Point Sur and Point Conception. Mean geostrophic velocities for the data set indicated that the CUC has a seasonal variability off Point Sur. The CUC was found to be present from June through February with a peak velocity occurring in December (14 cm s^{-1}). Wickham et al. (1987) analyzed two years of current array measurements and hydrographic data near Cape San Martin. The variability of the CUC was also found to be seasonal, except that the flow was stronger and deeper between May and June. The maximum velocity of the CUC was 15 cm s^{-1} at a depth of 300 m, within 30 km of the coast. Lynn and Simpson (1987) noted seasonal variability of the CUC off central California in their harmonic analysis of the CalCOFI data set. It was determined that the CUC becomes weaker with a greater core depth from January to March and from March to May it was almost nonexistent. Peak velocities occurred in the fall (10 cm s^{-1}).

The results of this study, however, indicate that the variability of the CUC is interannual rather than seasonal. It must be remembered that data from 15 POST cruises are utilized for this study, whereas 23 years of data were available for the CalCOFI studies. In addition, earlier studies included velocity data from the upper slope and shelf region which are more strongly correlated to the seasonal wind cycle than currents over the continental slope. Another source of disparity is that the previous studies have focused on geostrophically derived velocities. It seems likely that the choice of 500 m as the level of no motion is in error, since strong flow at depths greater than 500 m is common along POST.

The CUC is a persistent feature along POST. It was found to be absent off Point Sur only twice during this study and on both occasions an anticyclonic eddy was found over the slope. The relationship between these two features is uncertain. The core of the CUC has speeds in excess of 20 cm s^{-1} during all seasons. It is likely that the CUC has greater speeds further upslope towards the shelf break. The depth of the CUC core varies between 50-500 m with extremely deep and strong signatures (> 10 cm s^{-1}) observed during February 1989 (600 m), March 1989 (1200 m), May 1989 (850 m) and November 1989 (2000 m). The cause of this anomalous poleward flow is uncertain. Hicks (1992) studied moored current meter data off central California during three periods extending from five to six months in length. The two moorings off Point Sur were located in the vicinity of C1 and C3, with instruments at 350 m and 500 m for each mooring. The sub-thermocline currents were predominantly poleward during the three time segments. Poleward maxima were found during February for segment 1 (December 1989 - April 1990) and segment 2 (August 1990 - March 1991), while the poleward maximum during segment 3 (May 1991 - November 1991) occurred in May. Mean poleward alongshore velocities were approximately 6 cm s^{-1} and 4 cm s^{-1} for the 350 m moorings 24 km and 50 km offshore, respectively. Maximum poleward alongshore speeds were in excess of 20 cm s^{-1} for all three time segments, 24 km offshore. During September 1991, Hicks observed the presence of an anticyclonic rotating feature off Monterey Bay. It is interesting to note that poleward flow was absent at both moorings while this feature persisted, suggesting further evidence of the relationship between the anticyclonic eddy off Monterey Bay and the disappearance of the CUC (or movement further inshore).

An important result that deserves further discussion is the unusually strong poleward subsurface flow observed during the upwelling season. Largier et al. (1993) hypothesized that during the upwelling season off Cape Mendocino, the alignment of predominantly equatorward winds has a significant effect on shelf and upper slope circulation. Equatorward winds on the north side of a cape have an onshore component which prevents upwelling and establishes a southward flowing shelf current. On the south side of a cape the wind has an offshore component so that upwelling is enhanced, resulting in reduced bottom pressure. An alongshore pressure gradient is established with shelf currents south of the cape acquiring a poleward component of flow. This localized pressure gradient may cause the poleward acceleration of surface and subsurface currents over the shelf and possibly the shelf break and upper slope as well. Chelton et al. (1988) observed strong poleward shelf currents south of Point Sur and equatorward shelf flow north of Point Sur from February to July 1984. Wickham et al. (1987) also found predominantly poleward shelf flow south of Point Sur between 1979 and 1980.

The core depth and speed of the CUC observed along POST varied considerably between individual cruises with no clear seasonal strengthening or deepening of flow. However, the water mass characteristics of the CUC seem to change seasonally. Two broad seasons occur in the waters off central California influenced heavily by the local wind field. The upwelling season from April through September is dominated by periods of strong equatorward wind stress. The relaxation season from October through March is characterized by weak equatorward winds with occasional poleward wind events related to the passage of winter storms. During most of the upwelling season, the CUC off Point Sur does not have a strong temperature or salinity signal. The CUC has water mass characteristics of a more southerly origin beginning in the end of the upwelling season and continuing into the relaxation season.

It is hypothesized that the CUC observed from the end of the upwelling season into the relaxation season is continuous along the west coast and results from the weakening of equatorward wind stress and relaxation of the poleward alongshore pressure gradient. The strong poleward subsurface flow observed during the upwelling season may be modulated by local upwelling related effects since the water mass characteristics indicate waters of a more local origin.

Chelton (1984) found the surface flow to be predominantly equatorward with poleward surface flow present from October through February. Chelton et al. (1988) utilized moored current meters off Point Sur and found the near surface (70 m) currents to be generally poleward from February through August 1984 (the length of the study). PEGASUS data show that equatorward flow inshore of C4 off Point Sur is the exception rather than the rule. Moderate Equatorward surface flow (> 5 cm s^{-1}) is observed only in conjunction with the presence of mesoscale features along POST.

Chelton (1984) determined that the core of the CC was positioned between 100 and 200 km offshore and restricted to the upper 200 m. Two equatorward maxima with speeds of 9 cm s^{-1} occurred from February through March and from July through August. Lynn and Simpson (1987) determined that the core of the CC was located 200 to 300 km offshore with maximum speeds of 8 cm s^{-1}. This study shows the core of the CC to be located between 100 and 200 km offshore with maximum speeds greater than 20 cm s^{-1} throughout the year. The highest speeds appear to be found in the upwelling season and may be the result of baroclinic enhancement of the equatorward flow. The CC transports cool, fresh Subarctic waters to the south, dividing relatively saline and cool upwelled waters near the coast from warmer and fresher waters offshore during the upwelling season. Huyer et al. (1991) and Bray and Greengrove (1993) both observed strong equatorward jets off the coast of northern California during the upwelling season. Data from surface drifters released in the vicinity of upwelled plumes off Point Arena and originally presented by Brink et al. (1991) show a persistent meander of the CC that intersects POST in the vicinity of C8 (Figure 34). The disparity between earlier measurements of the CC and those presented here is a result of coarse hydrographic station spacing which tends to miss fronts and narrow jets. The CC has a significant onshore component of flow off Point Sur. The data presented here are the first direct measurements of the CC.

During August 1990 and December 1990, low surface salinities (< 33) indicate the presence of CC water much farther inshore than usual. A possible meander or anticyclonic eddy consisting of Pacific Subarctic water is evident in August of 1990. Two distinct salinity minimums are found at C8 (32.7) and C4 (32.9). The flow at C8 is to the southeast while the flow at C4 is poleward. The salinity field for December 1990 shows a broad region of low surface salinity values (<33) inshore of C7. The surface flow inshore is poleward and surface velocity data are unavailable offshore from C6. It is unclear whether the strong poleward flow observed in December is an inshore meander of the CC that persisted from August 1990 since data are unavailable for the interim months.

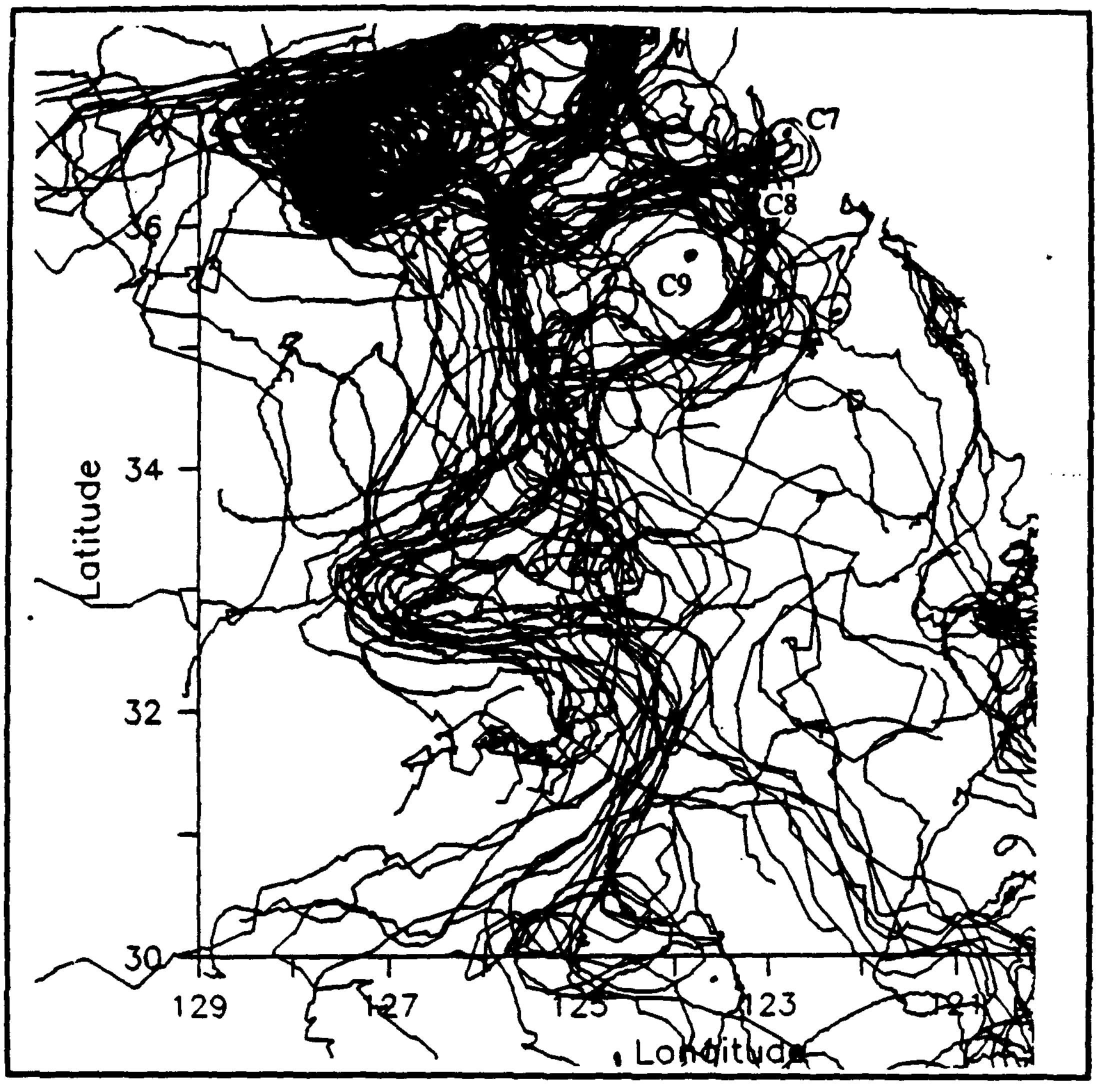

Figure 34. Surface drifter data collected from 1985-1988: Drifters were launched off Point Arena, California. Data originally presented by Brink et al. (1991)

V. CONCLUSIONS AND RECOMMENDATIONS

A. CONCLUSIONS

The variability of the CCS and more specifically the CUC off Point Sur was determined to be interannual rather than seasonal. The short duration of this data set when compared to earlier geostrophic studies and the absence of upper slope and shelf velocity data may account for the absence of a pronounced seasonal signal. Important findings of this study include;

- The temporal continuity and strength of the CUC. The CUC was observed with speeds in excess of 20 cm s^{-1} throughout the year. Mean speed and depth of the CUC was 10 cm s^{-1} and 100 m respectively at C1, 33 km offshore.

- The importance of mesoscale features in the coastal transition zone. Meanders of the CC and the CUC, anticyclonic eddies and cyclonic eddies were all present along POST during this study. The anticyclonic eddy often found in satellite sst imagery off Monterey Bay was present along the transect twice and on both occasions the CUC was entirely absent. The relationship between these two features is not evident.

- The persistent CC meander. The CC core was found to have an onshore meander located 150 km offshore with maximum speeds in excess of 20 cm s^{-1}.

- The occasional appearance of anomalously deep poleward flow. On four occasions the poleward subsurface flow was greater than 10 cm s^{-1} to depths of up to 2000 m. The cause of this deep flow is unclear.

- The agreement between geostrophically derived velocities along POST and PEGASUS velocities. There was favorable agreement between the two types of velocity measurements in regards to magnitude, direction and vertical extent. Differences between the two are a result of the selection of 1000 m as the level of no motion. Absolute velocities are often strong to 2000 m. Geostrophically derived surface velocities tend to show stronger poleward surface velocities, since wind stress is not accounted for with the geostrophic method. The only exception occurred during the peak of the upwelling season, in which PEGASUS data reveal strong poleward subsurface flow absent in the geostrophic velocity field. This may indicate a significant nongeostrophic component of poleward flow during the upwelling season.

B. RECOMMENDATIONS

This study raises some important questions which require further analysis. The cause of the strong poleward subsurface flow during the upwelling season is unclear. Other absolute velocity measurements along the west coast during the upwelling season may help determine the spatial continuity of this flow and a modeling study of an upwelling regime with variations in alongshore wind stress and topography may shed some light on the nongeostrophic nature of this flow. In addition, a thorough comparison of the PEGASUS data with geostrophically determined velocities for the months not compared in this study may help to determine if the disparity between geostrophic velocities and absolute velocities during the upwelling season is common or an isolated event. The relationship between the anticyclonic eddy and the CUC also requires further study to determine if the presence of the CUC further inshore allows the eddy to appear along POST or the eddy restricts the CUC to the upper slope and shelf. The cause of the anomalously deep poleward flow may be resolved with deep moored current meters off Point Sur. This would at least determine the persistence of such features, which was not adequately determined by this study.

APPENDIX A. EMPIRICAL ORTHOGONAL FUNCTION ANALYSIS

An Empirical Orthogonal Function (EOF) analysis was conducted on the PEGASUS derived absolute velocities in order to determine the temporal and spatial variability of the data set. The utility of an EOF analysis is that most of the variability of a data set can be explained with a few modes. Scalar EOF analysis is discussed by Priesendorfer et al. (1981) and can be expanded to include vector data so that directional information may be preserved. This expanded version is called complex or rotary Empirical Orthogonal Function analysis and has been described by Hardy (1977) and Denbo and Allen (1984). The velocity data set, where *u* and *v* represent the eastward and northward component of velocity respectively is as follows

$$D_{mn}= (u_{mn}-u_n)+ i(v_{mn}-v_n),$$

where u_n and v_n represent time averages and the subscripts m and n are time and space indices from 1 to T, where T is the number of temporal observations and 1 to S, where S is the number of spatial observations. The data set is a T X S matrix and a T X T covariance matrix can be determined with

$$COV= 1/T\, DD^T,$$

where the T superscript indicates the complex conjugate transpose.

The covariance matrix can be divided into a set of eigenfunctions which are mutually orthogonal and the eigenvalues corresponding to particular eigenvectors represent the percentage of the total variance explained by that eigenvector. In this particular case the eigenvectors represent a temporal pattern of variability, with the real component representing the amplitude and the imaginary component representing the phase.

For this data set there were 15 observations in time and 100 spatial points (only the upper 500 m of data were used in order to isolate the variability of surface currents and the CUC). The first mode accounted for at least 60 % of the total variance and up to 80 % at the inshore stations. The variability represented by the amplitude and phase for each PEGASUS station along the transect was clearly interannual with no seasonal signal present in the dominant modes. Plots of the first mode eigenvectors and spatial patterns are included for comparison. The values of the magnitudes and phases for both the eigenvectors and spatial patterns are arbitrary.

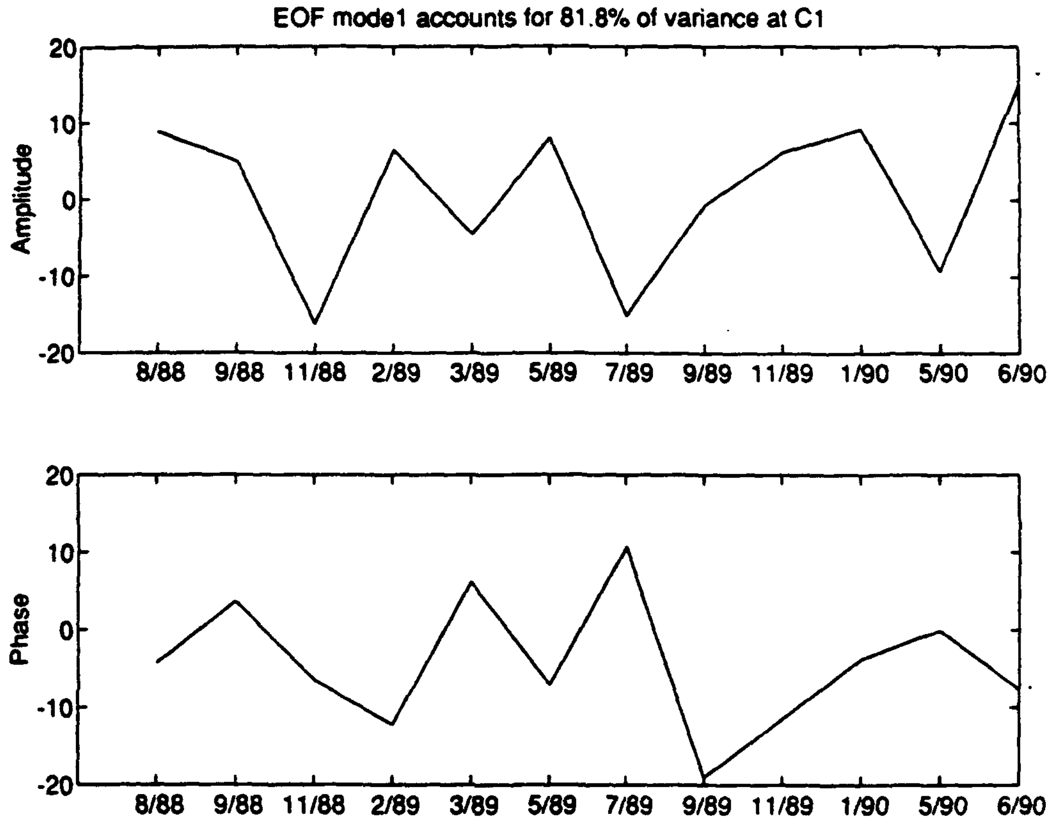

EOF mode1 accounts for 81.8% of variance at C1
Amplitude
Phase
20
10
0
-10
-20
8/88 9/88 11/88 2/89 3/89 5/89 7/89 9/89 11/89 1/90 5/90 6/90

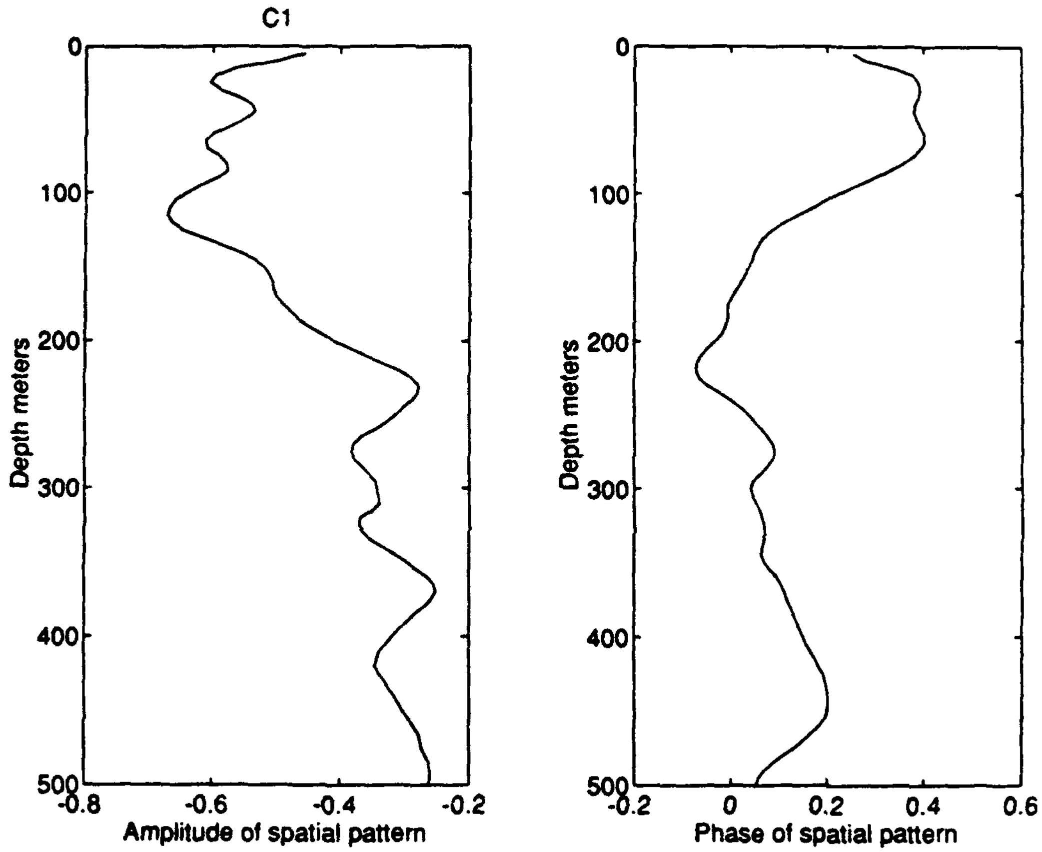
C1
0
100
200
300
400
500
Depth meters
-0.8
-0.6
-0.4
-0.2
Amplitude of spatial pattern
0
100
200
300
400
500
Depth meters
-0.2
0
0.2
0.4
0.6
Phase of spatial pattern

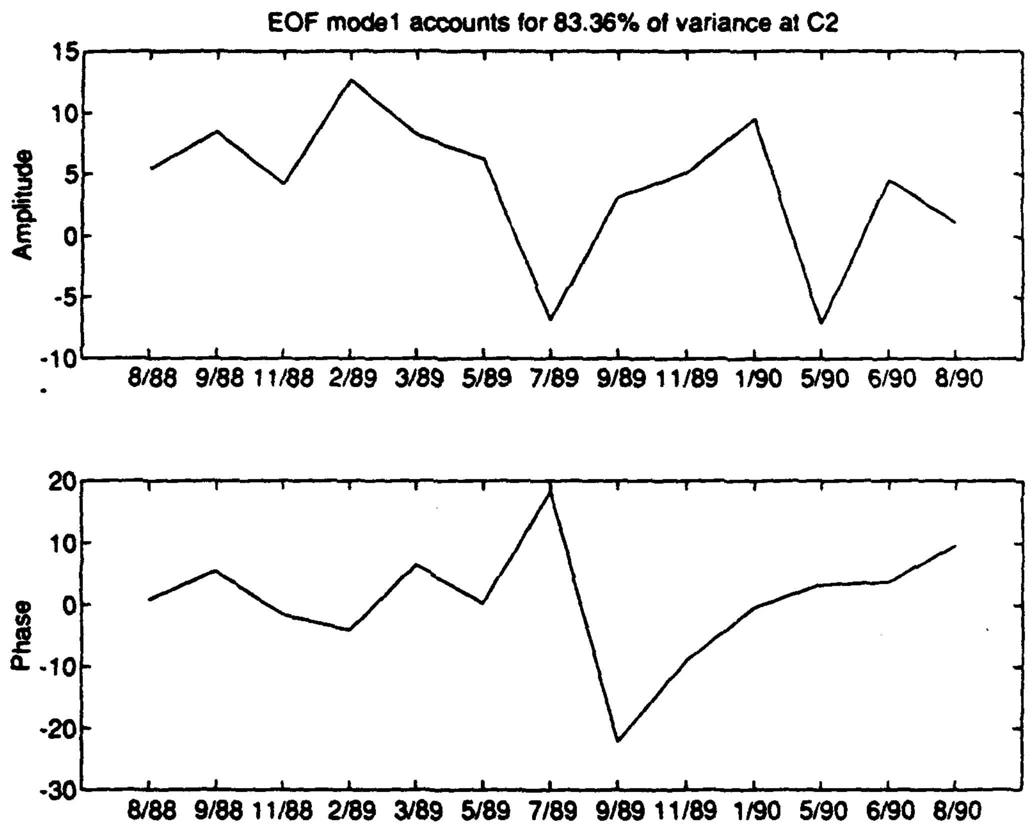
EOF mode1 accounts for 83.36% of variance at C2
Amplitude
15
10
5
0
-5
-10
8/88 9/88 11/88 2/89 3/89 5/89 7/89 9/89 11/89 1/90 5/90 6/90 8/90
Phase
20
10
0
-10
-20
-30
8/88 9/88 11/88 2/89 3/89 5/89 7/89 9/89 11/89 1/90 5/90 6/90 8/90

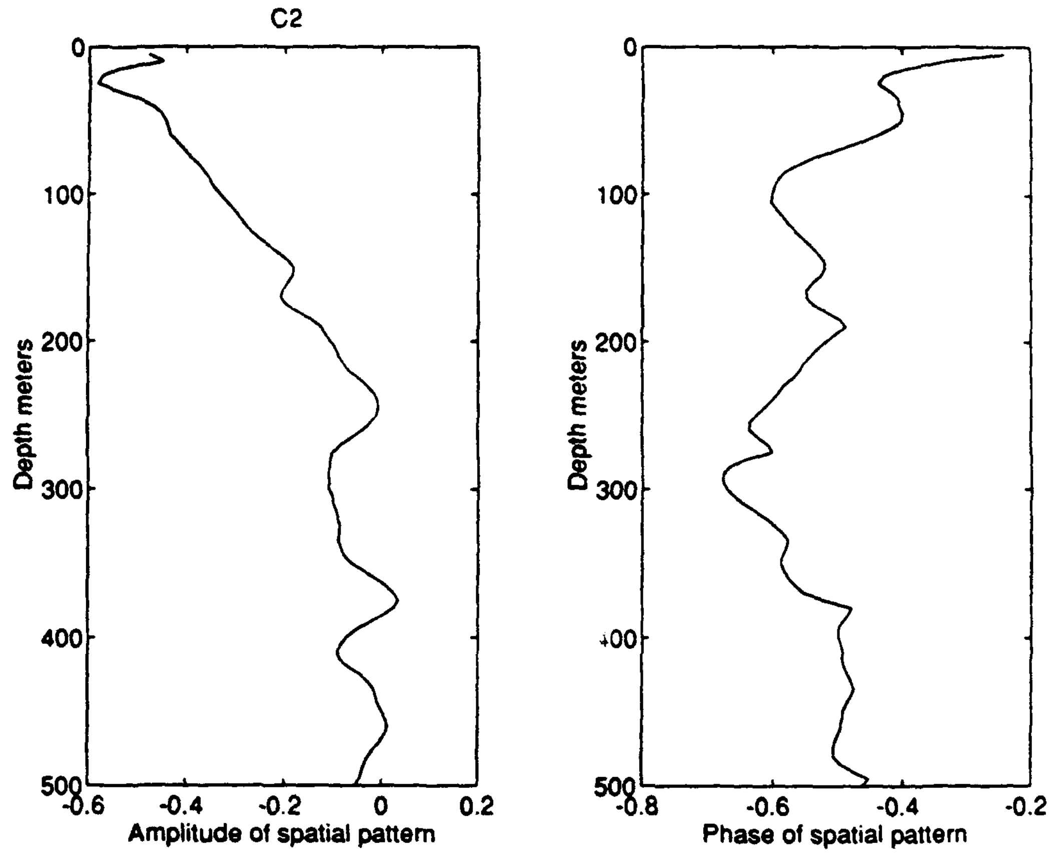

C2
0
100
200
300
400
500
Depth meters
-0.6
-0.4
-0.2
0
0.2
Amplitude of spatial pattern
0
100
200
300
400
500
Depth meters
-0.8
-0.6
-0.4
-0.2
Phase of spatial pattern

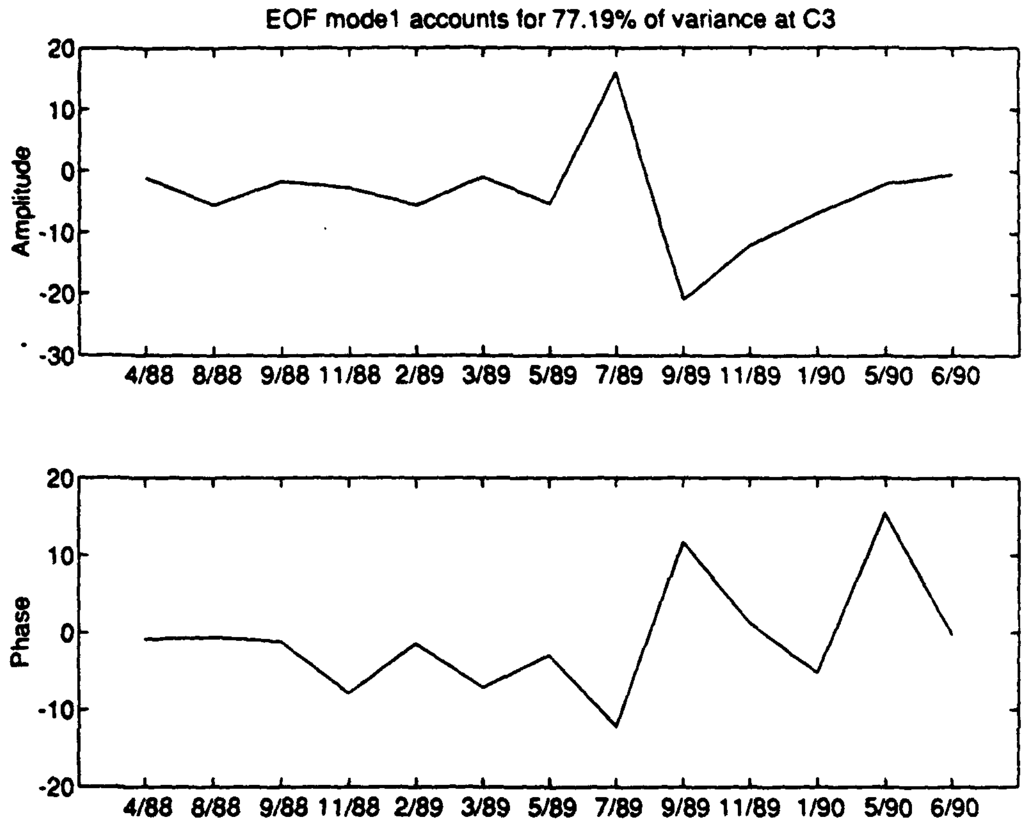
EOF mode1 accounts for 77.19% of variance at C3
Amplitude
20
10
0
-10
-20
-30
4/88 8/88 9/88 11/88 2/89 3/89 5/89 7/89 9/89 11/89 1/90 5/90 6/90
Phase
20
10
0
-10
-20
4/88 8/88 9/88 11/88 2/89 3/89 5/89 7/89 9/89 11/89 1/90 5/90 6/90

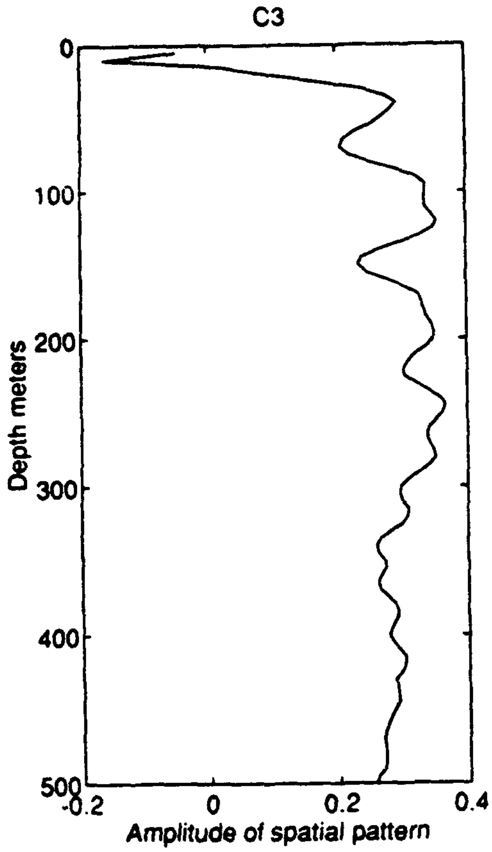
C3
Depth meters
0
100
200
300
400
500
-0.2
0
0.2
0.4
Amplitude of spatial pattern
Depth meters
0
100
200
300
400
500
0.3
0.4
0.5
0.6
0.7
Phase of spatial pattern

EOF mode1 accounts for 85.09% of variance at C4

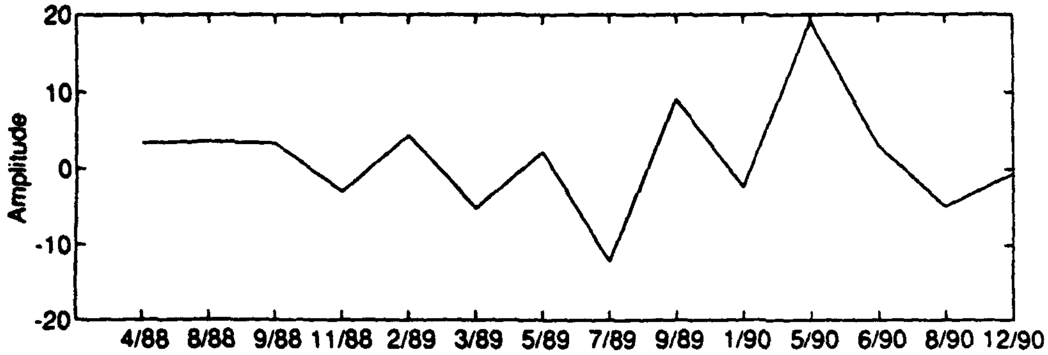

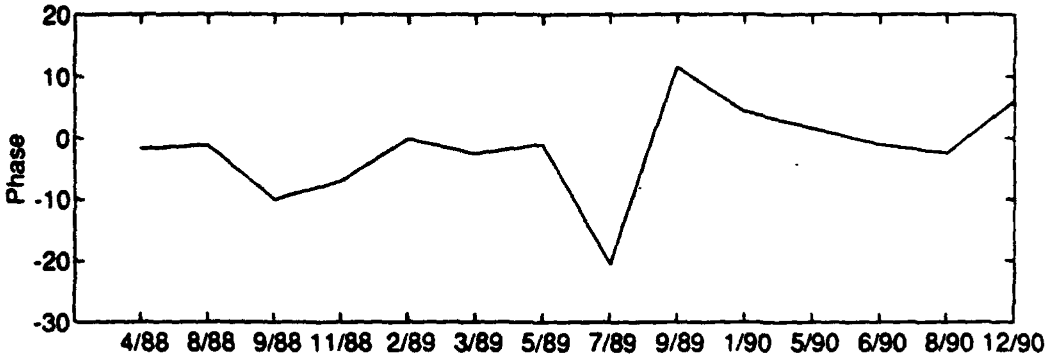

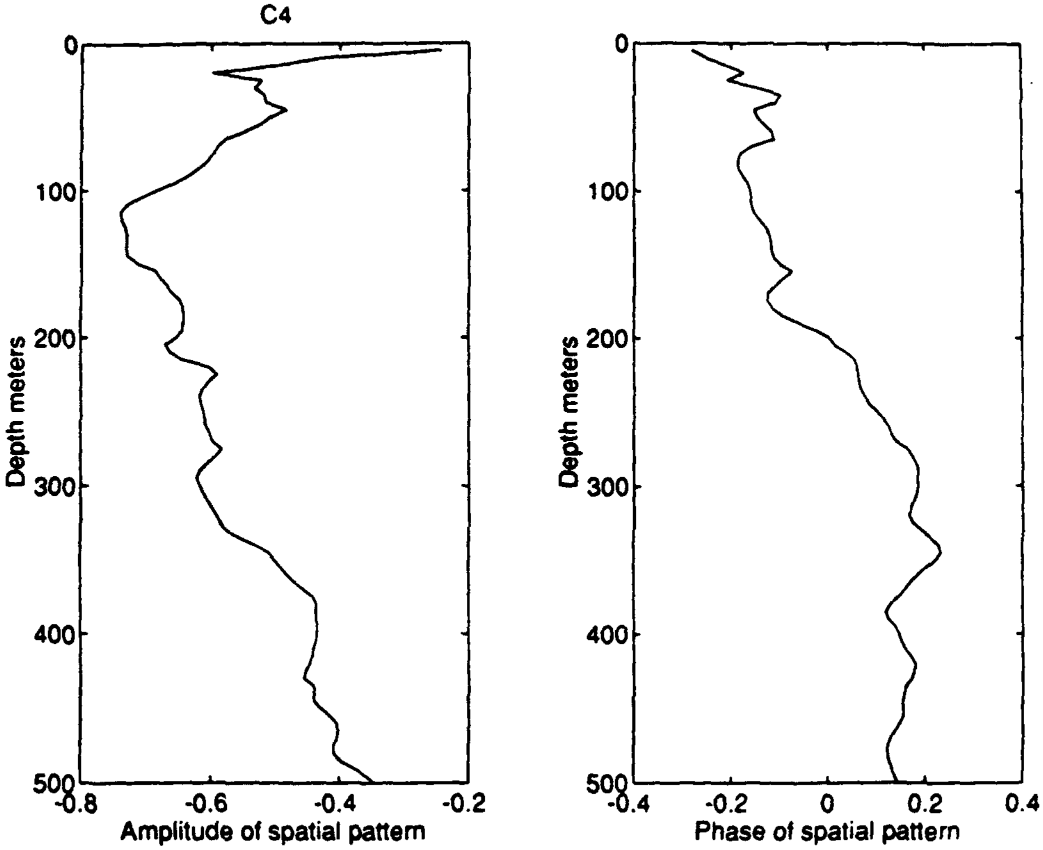
C4
Depth meters
0
100
200
300
400
500
-0.8
-0.6
-0.4
-0.2
Amplitude of spatial pattern
Depth meters
0
100
200
300
400
500
-0.4
-0.2
0
0.2
0.4
Phase of spatial pattern

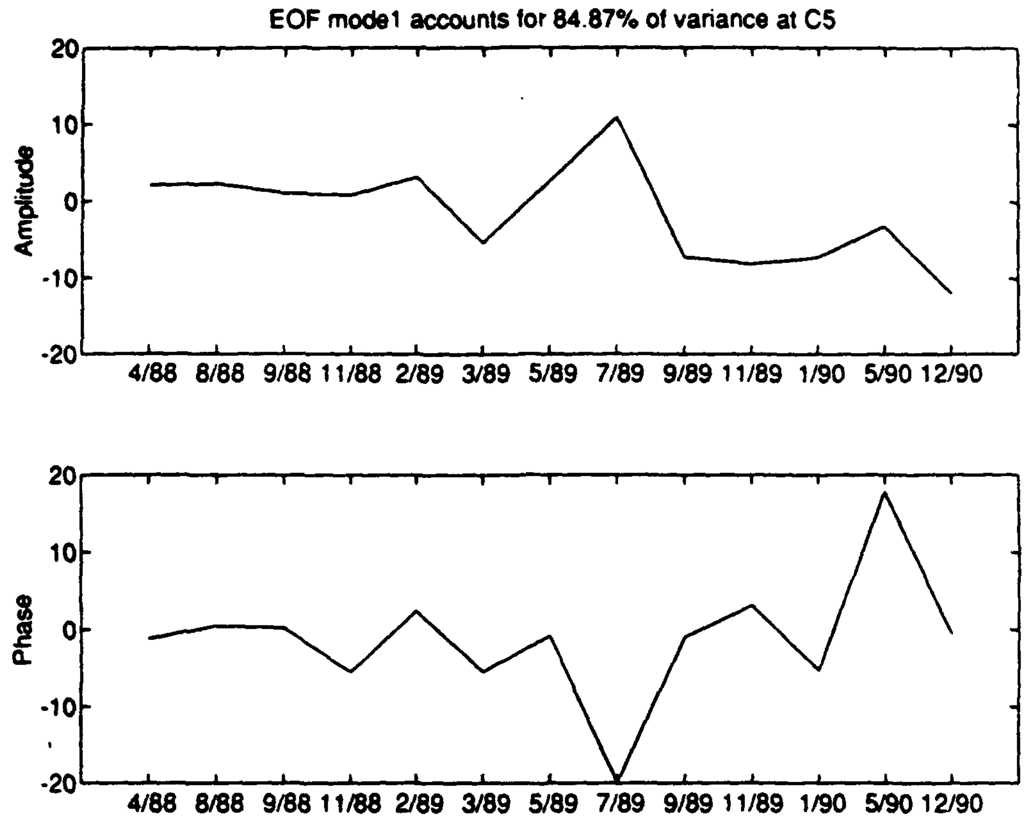
EOF mode1 accounts for 84.87% of variance at C5
Amplitude
Phase
20
10
0
-10
-20
4/88 8/88 9/88 11/88 2/89 3/89 5/89 7/89 9/89 11/89 1/90 5/90 12/90

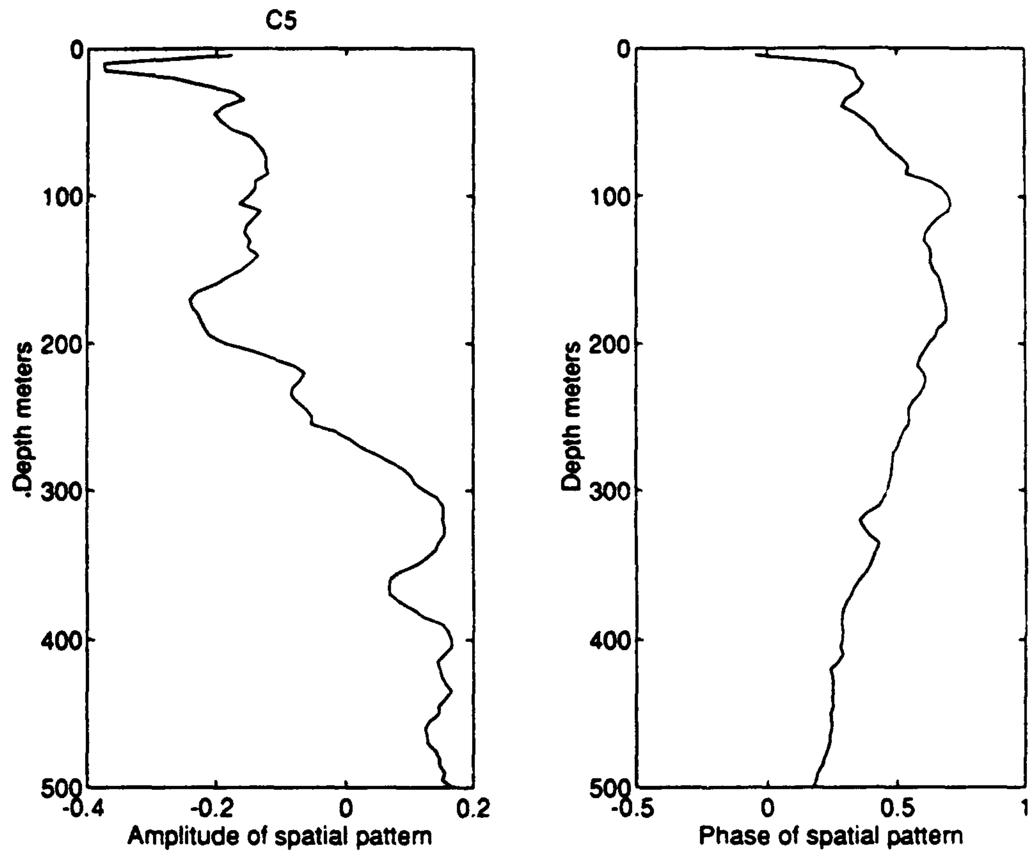
C5
0
100
200
300
400
500
Depth meters
-0.4
-0.2
0
0.2
Amplitude of spatial pattern
0
100
200
300
400
500
Depth meters
-0.5
0
0.5
1
Phase of spatial pattern

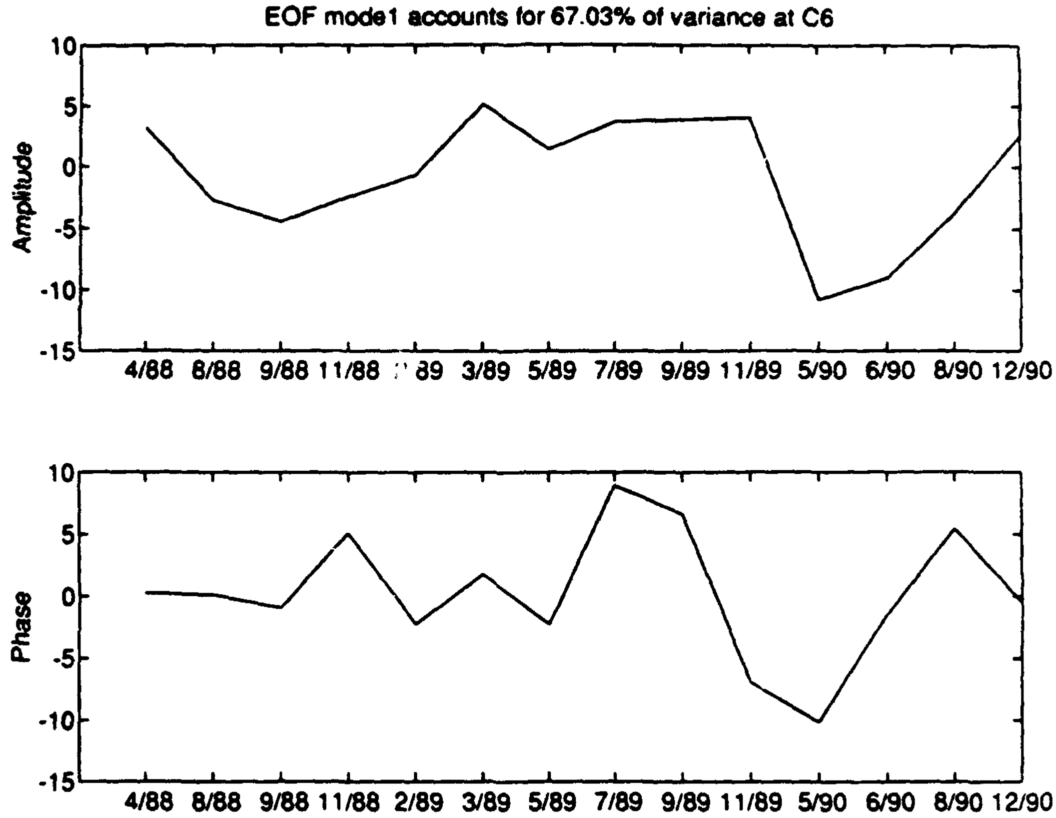
EOF mode1 accounts for 67.03% of variance at C6
Amplitude
10
5
0
-5
-10
-15
4/88 8/88 9/88 11/88 3/89 5/89 7/89 9/89 11/89 5/90 6/90 8/90 12/90
Phase
10
5
0
-5
-10
-15
4/88 8/88 9/88 11/88 2/89 3/89 5/89 7/89 9/89 11/89 5/90 6/90 8/90 12/90

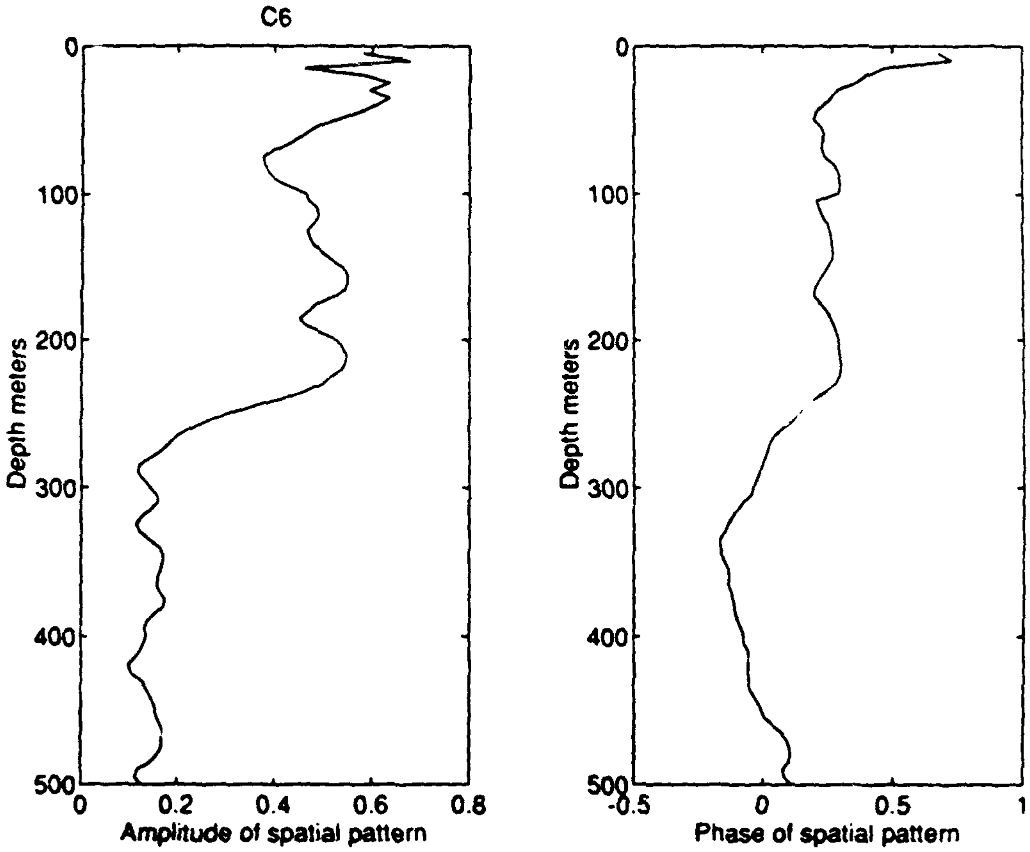
C6
0
100
200
300
400
500
Depth meters
0
0.2
0.4
0.6
0.8
Amplitude of spatial pattern
0
100
200
300
400
500
Depth meters
-0.5
0
0.5
1
Phase of spatial pattern

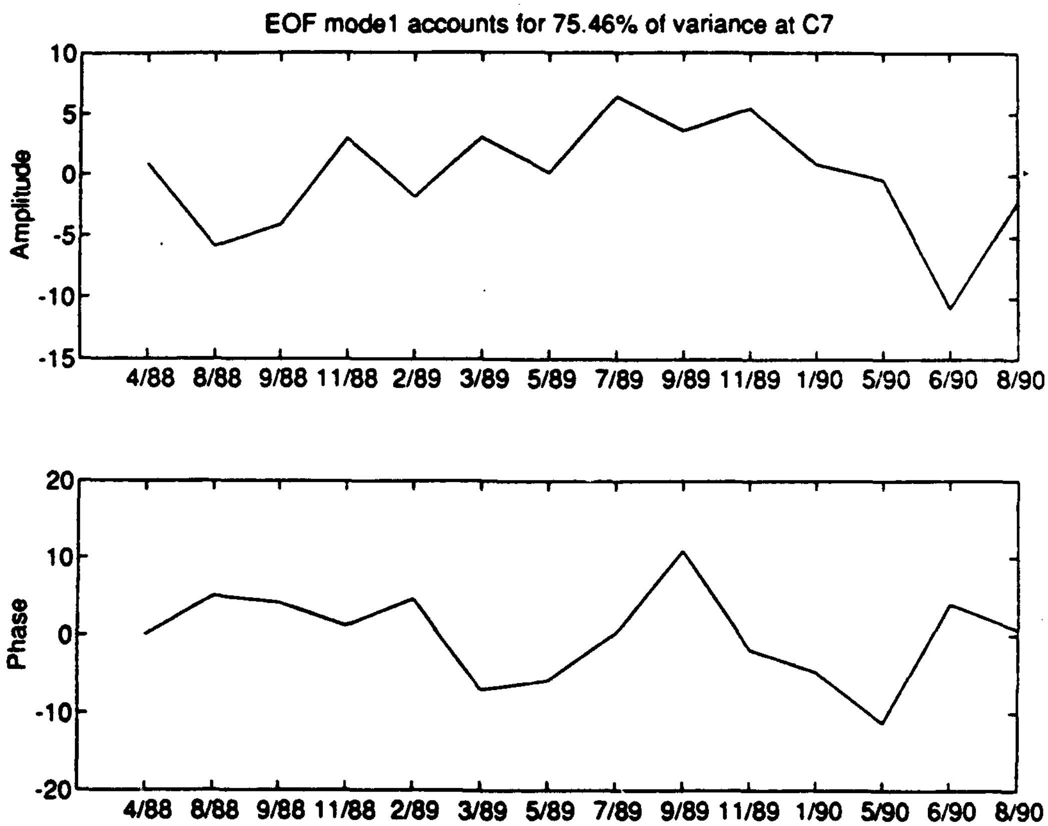

EOF mode1 accounts for 75.46% of variance at C7
Amplitude
10
5
0
-5
-10
-15
4/88 8/88 9/88 11/88 2/89 3/89 5/89 7/89 9/89 11/89 1/90 5/90 6/90 8/90
Phase
20
10
0
-10
-20
4/88 8/88 9/88 11/88 2/89 3/89 5/89 7/89 9/89 11/89 1/90 5/90 6/90 8/90

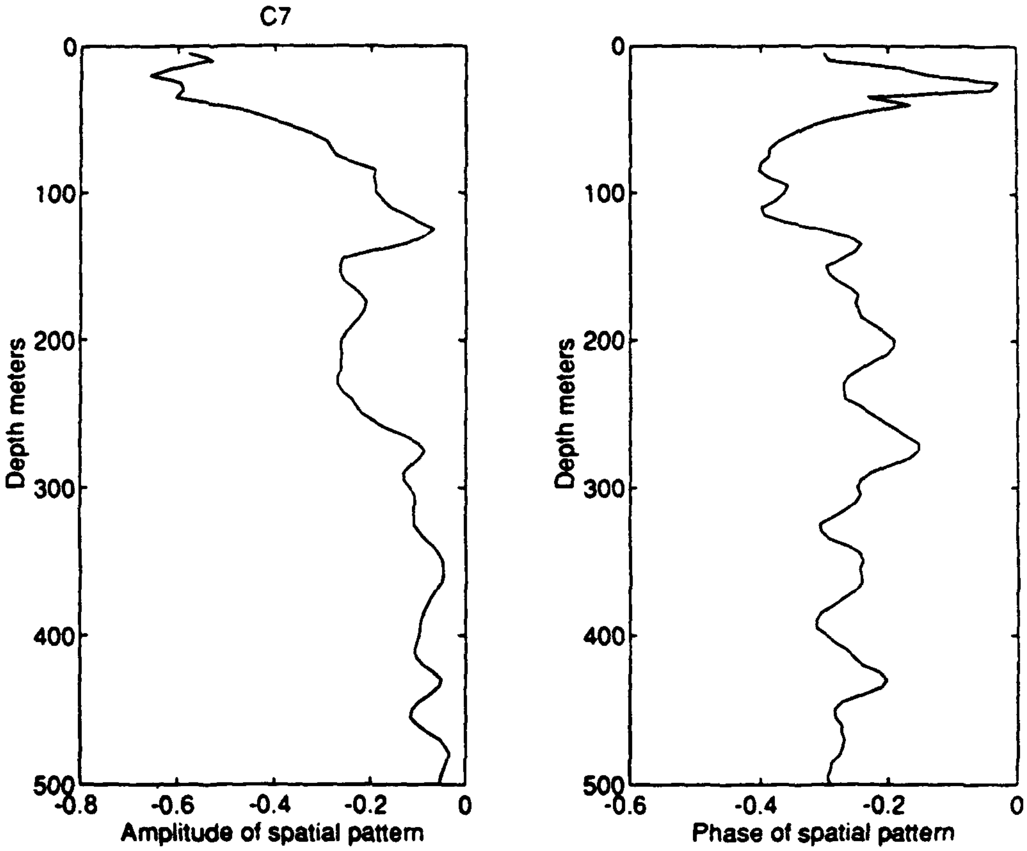
C7
Depth meters
0
100
200
300
400
500
-0.8
-0.6
-0.4
-0.2
0
Amplitude of spatial pattern
Depth meters
0
100
200
300
400
500
-0.6
-0.4
-0.2
0
Phase of spatial pattern

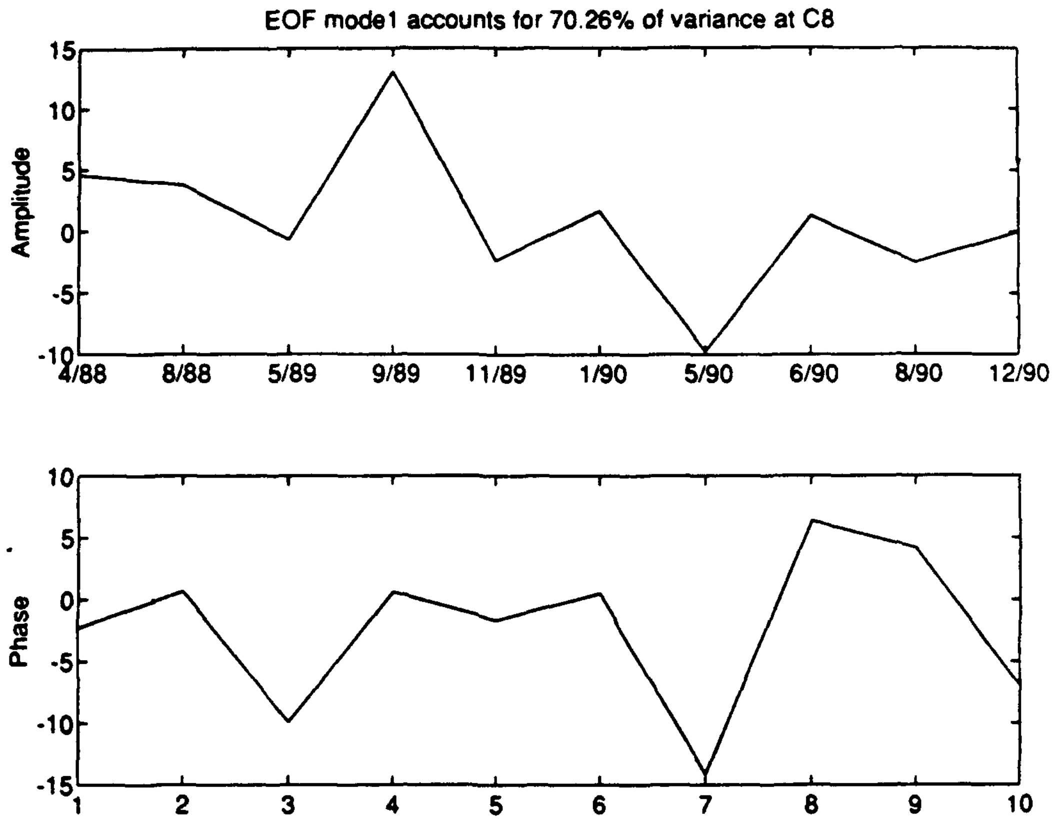
EOF mode1 accounts for 70.26% of variance at C8
Amplitude
15
10
5
0
-5
-10
4/88
8/88
5/89
9/89
11/89
1/90
5/90
6/90
8/90
12/90
Phase
10
5
0
-5
-10
-15
1
2
3
4
5
6
7
8
9
10

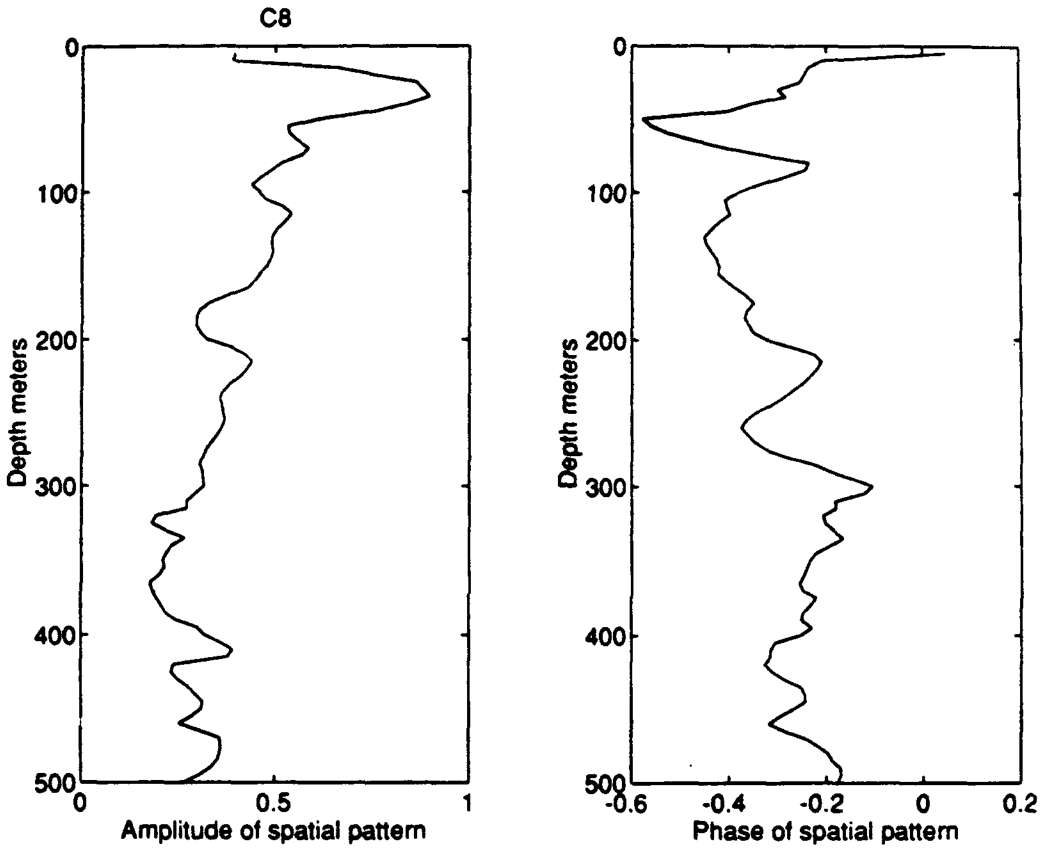
C8
Depth meters
Amplitude of spatial pattern
0
100
200
300
400
500
0
0.5
1
Depth meters
Phase of spatial pattern
-0.6
-0.4
-0.2
0
0.2

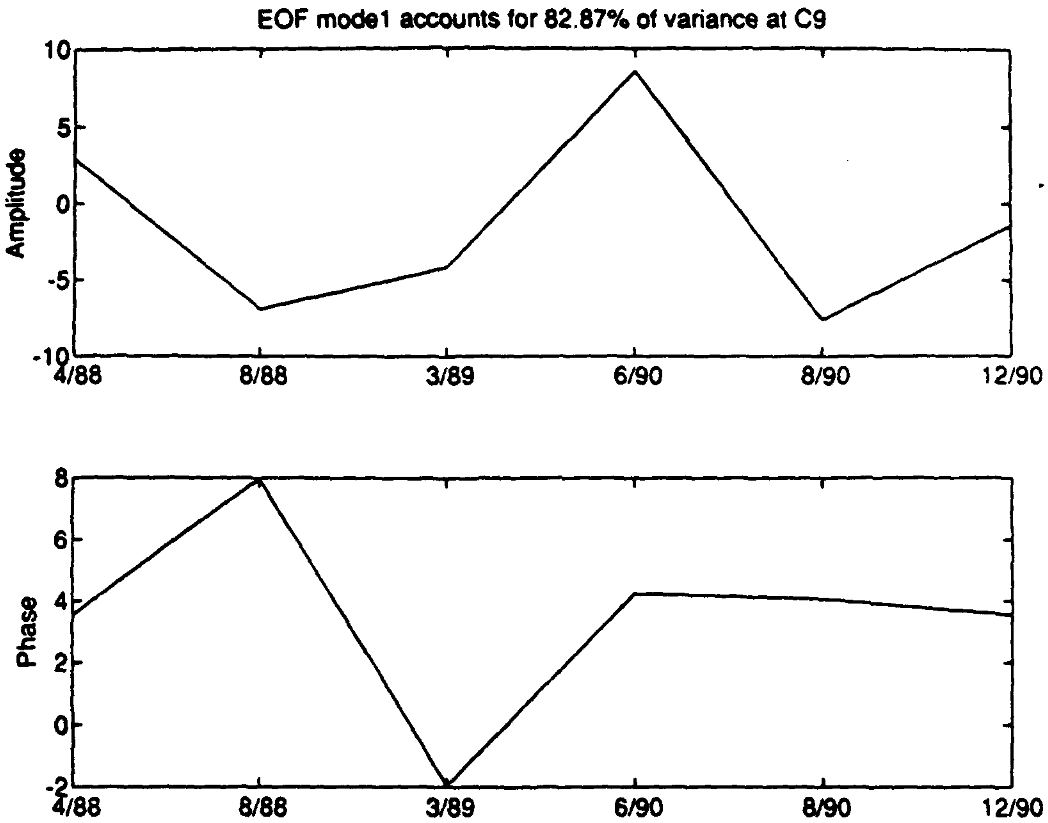

EOF mode1 accounts for 82.87% of variance at C9
10
5
0
-5
-10
Amplitude
4/88
8/88
3/89
6/90
8/90
12/90
8
6
4
2
0
-2
Phase
4/88
8/88
3/89
6/90
8/90
12/90

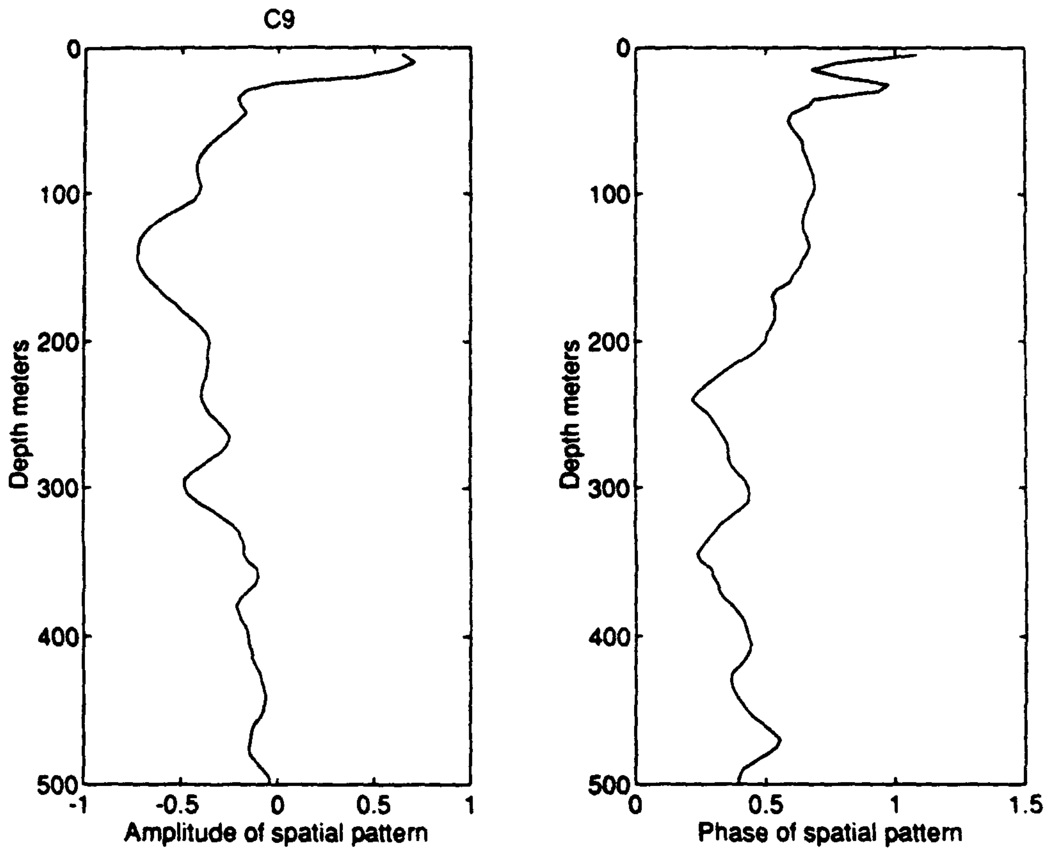
C9
Depth meters
Amplitude of spatial pattern
Phase of spatial pattern
0
100
200
300
400
500
-1
-0.5
0
0.5
1
1.5

APPENDIX B. WIND BUOY DATA

The following diagrams show the wind speed vectors in m s^{-1} for both the Cape San Martin buoy (BM28) and the Monterey buoy (BM42). Cruise periods are indicated with a horizontal line annotated with the cruise month.

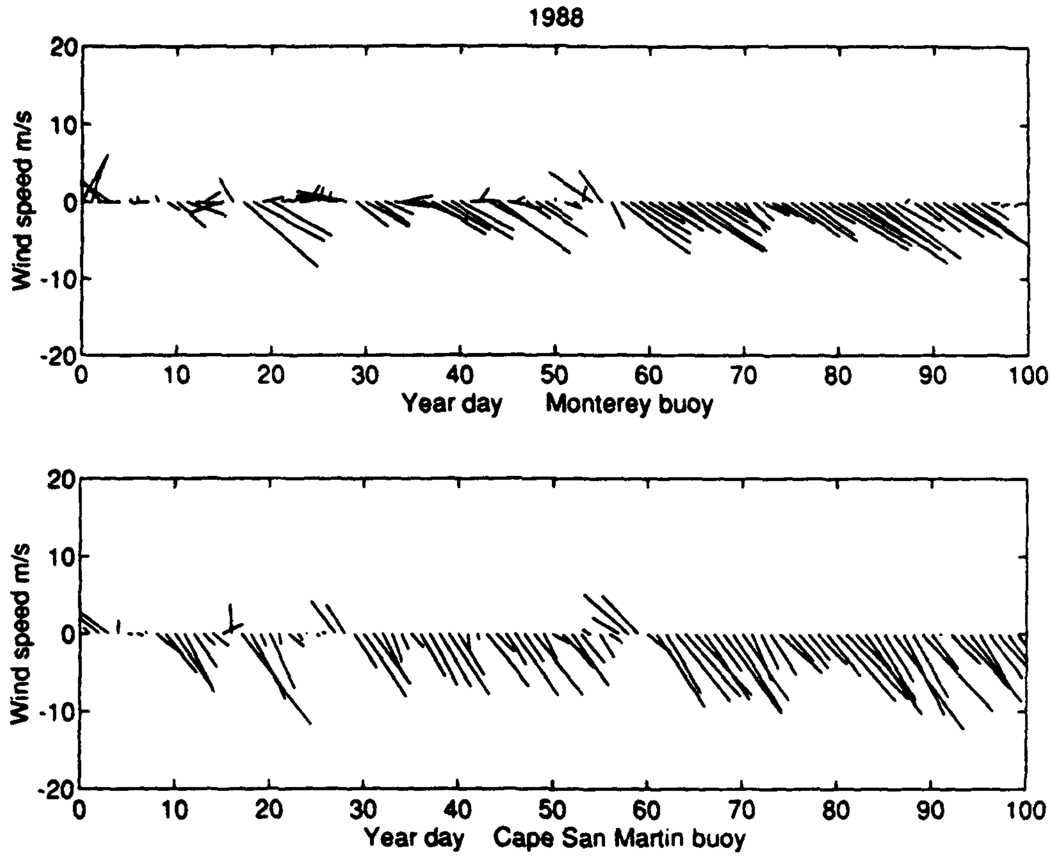
1988
20
10
0
-10
-20
Wind speed m/s
0
10
20
30
40
50
60
70
80
90
100
Year day Monterey buoy
20
10
0
-10
-20
Wind speed m/s
0
10
20
30
40
50
60
70
80
90
100
Year day Cape San Martin buoy

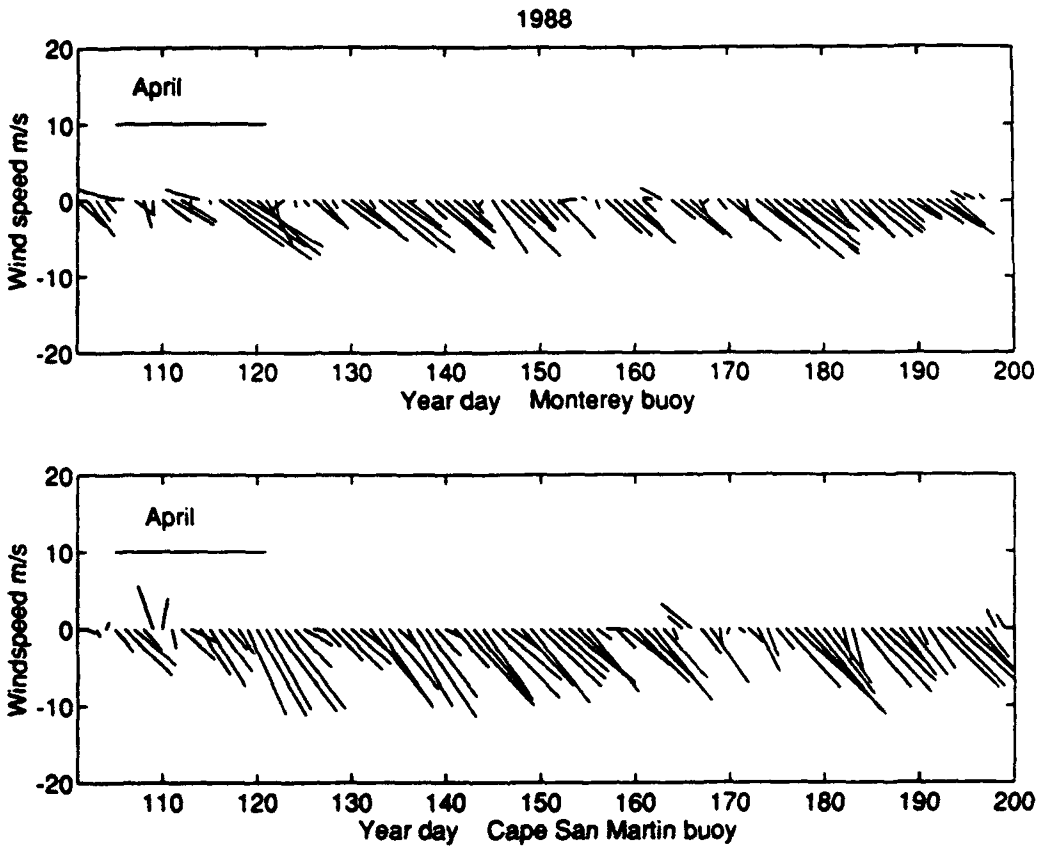
1988
20
April
10
0
-10
-20
Wind speed m/s
110
120
130
140
150
160
170
180
190
200
Year day Monterey buoy
20
April
10
0
-10
-20
Windspeed m/s
110
120
130
140
150
160
170
180
190
200
Year day Cape San Martin buoy

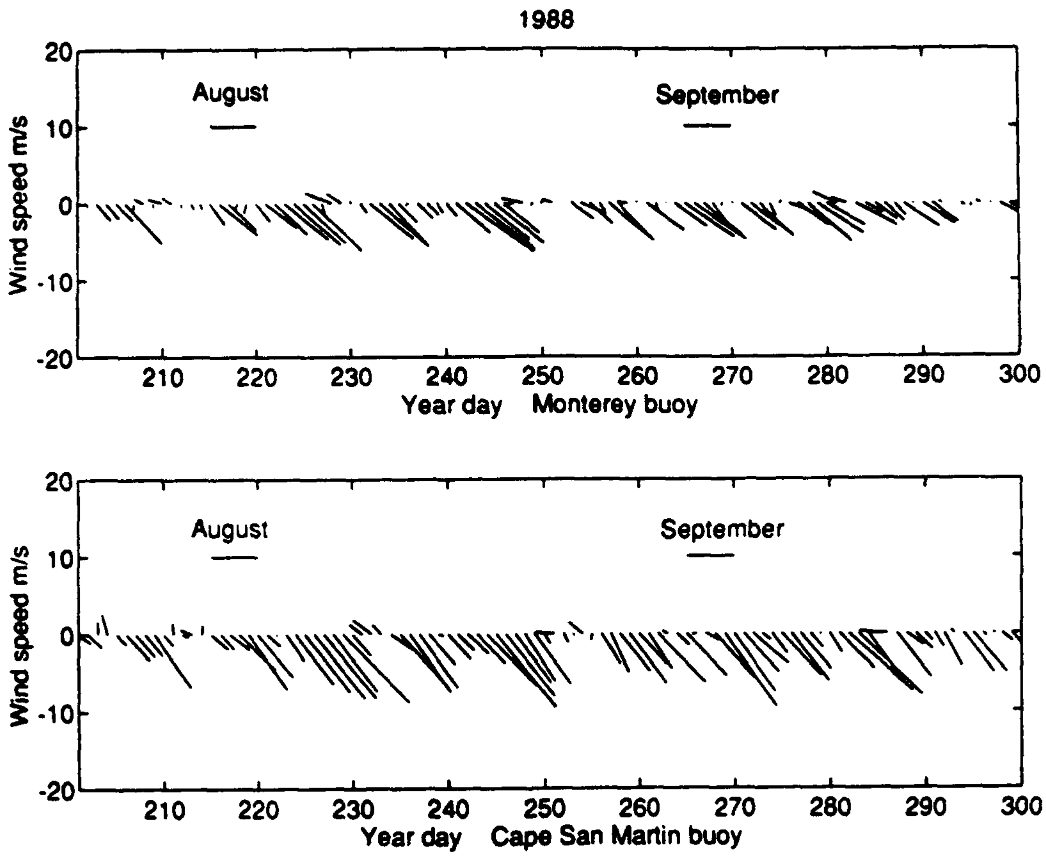
1988
20
10
0
-10
-20
Wind speed m/s
August
September
210
220
230
240
250
260
270
280
290
300
Year day Monterey buoy
20
10
0
-10
-20
Wind speed m/s
August
September
210
220
230
240
250
260
270
280
290
300
Year day Cape San Martin buoy

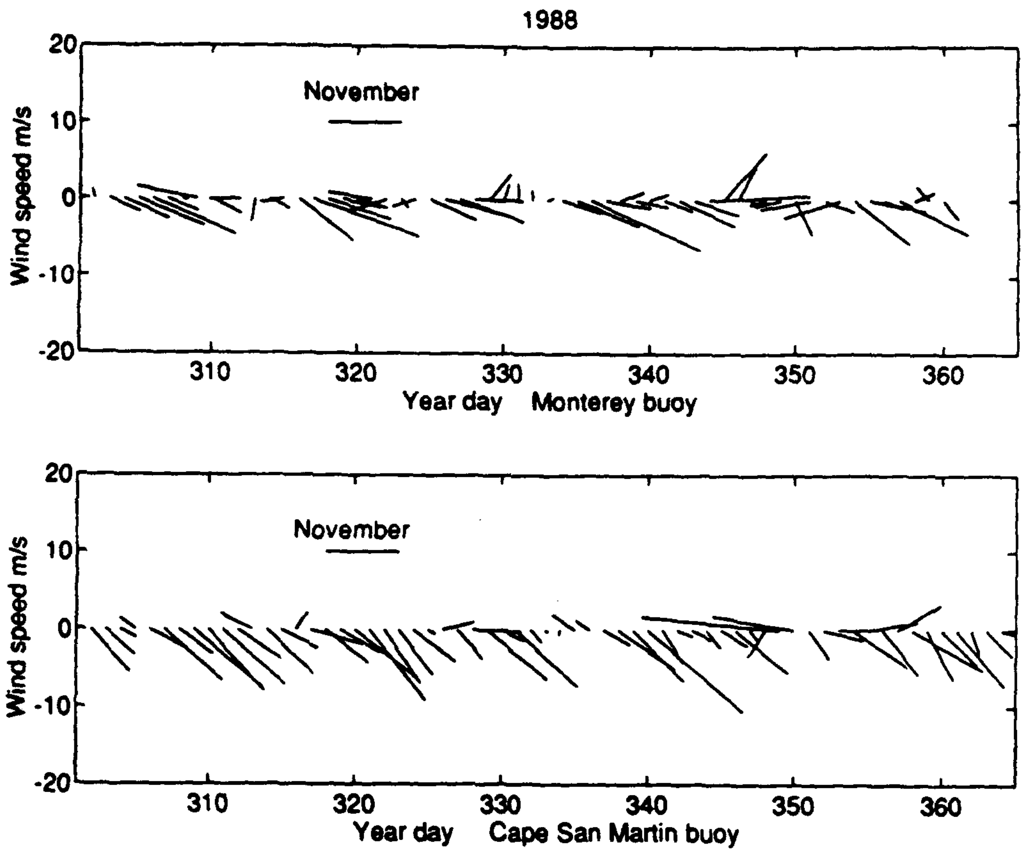
1988
November
Wind speed m/s
20
10
0
-10
-20
310
320
330
340
350
360
Year day Monterey buoy
November
Wind speed m/s
20
10
0
-10
-20
310
320
330
340
350
360
Year day Cape San Martin buoy

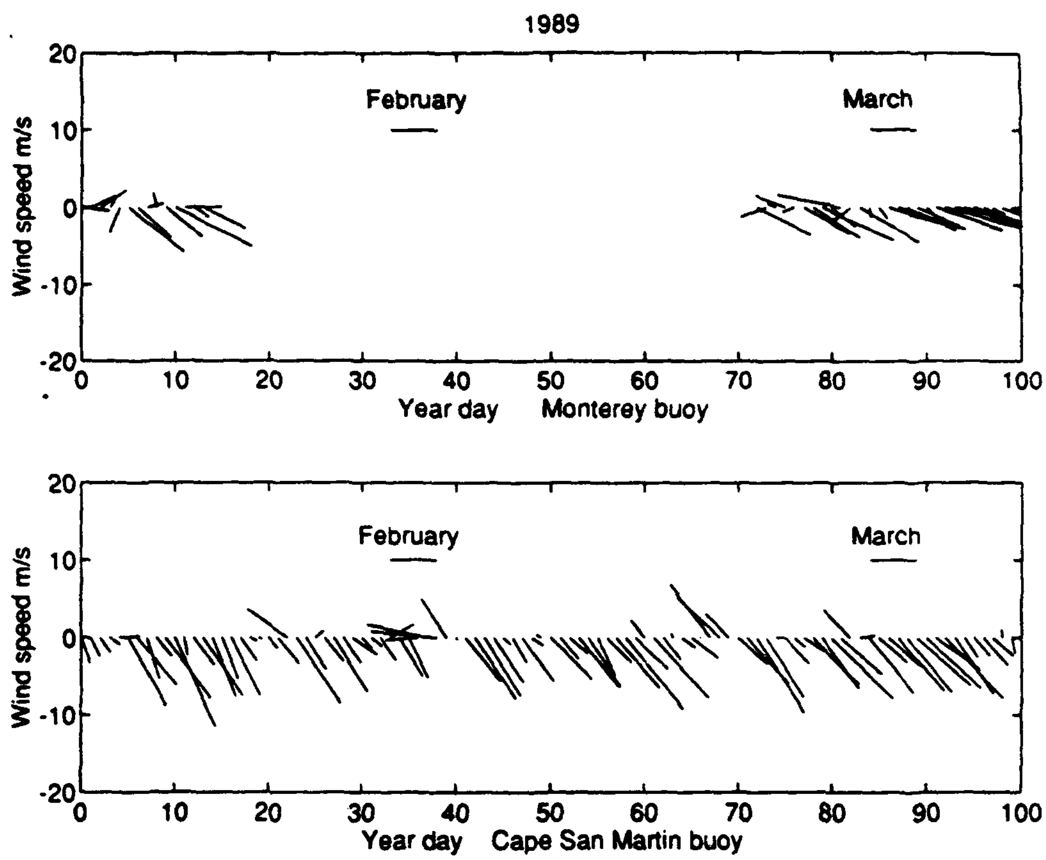
1989
February
March
Wind speed m/s
20
10
0
-10
-20
0
10
20
30
40
50
60
70
80
90
100
Year day
Monterey buoy
February
March
Wind speed m/s
Year day
Cape San Martin buoy

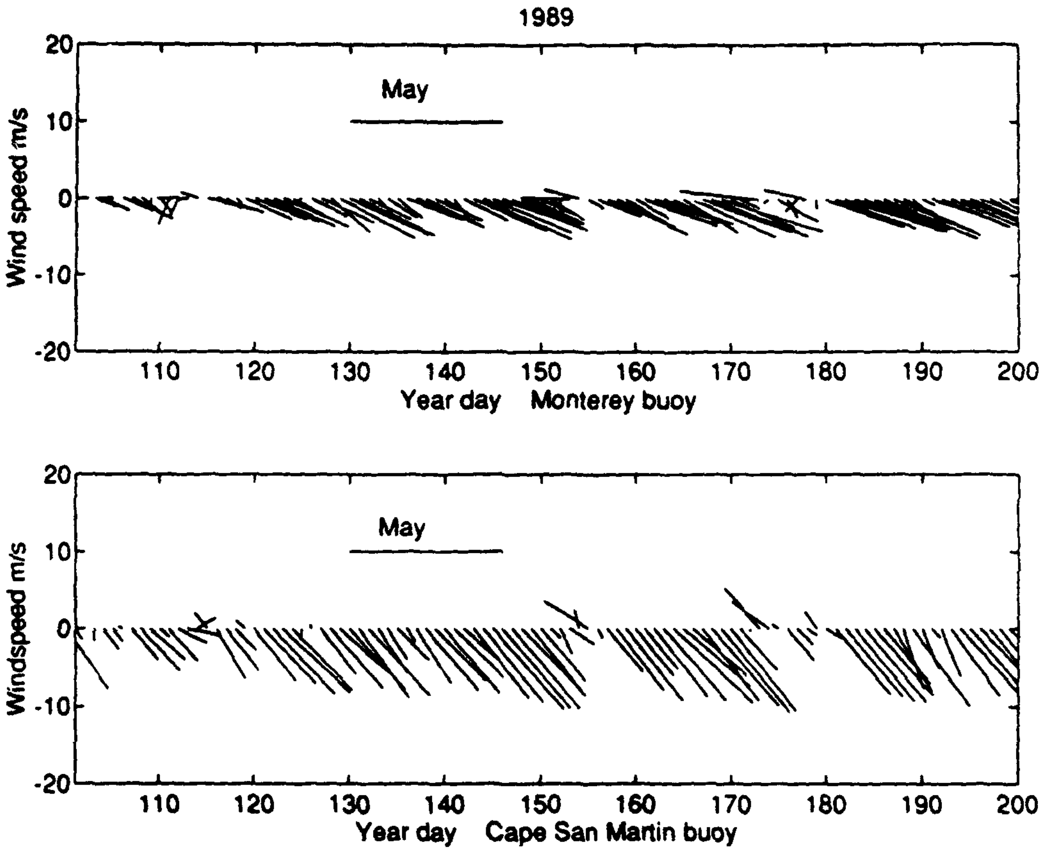
1989
May
Wind speed m/s
20
10
0
-10
-20
110
120
130
140
150
160
170
180
190
200
Year day Monterey buoy
May
Windspeed m/s
20
10
0
-10
-20
110
120
130
140
150
160
170
180
190
200
Year day Cape San Martin buoy

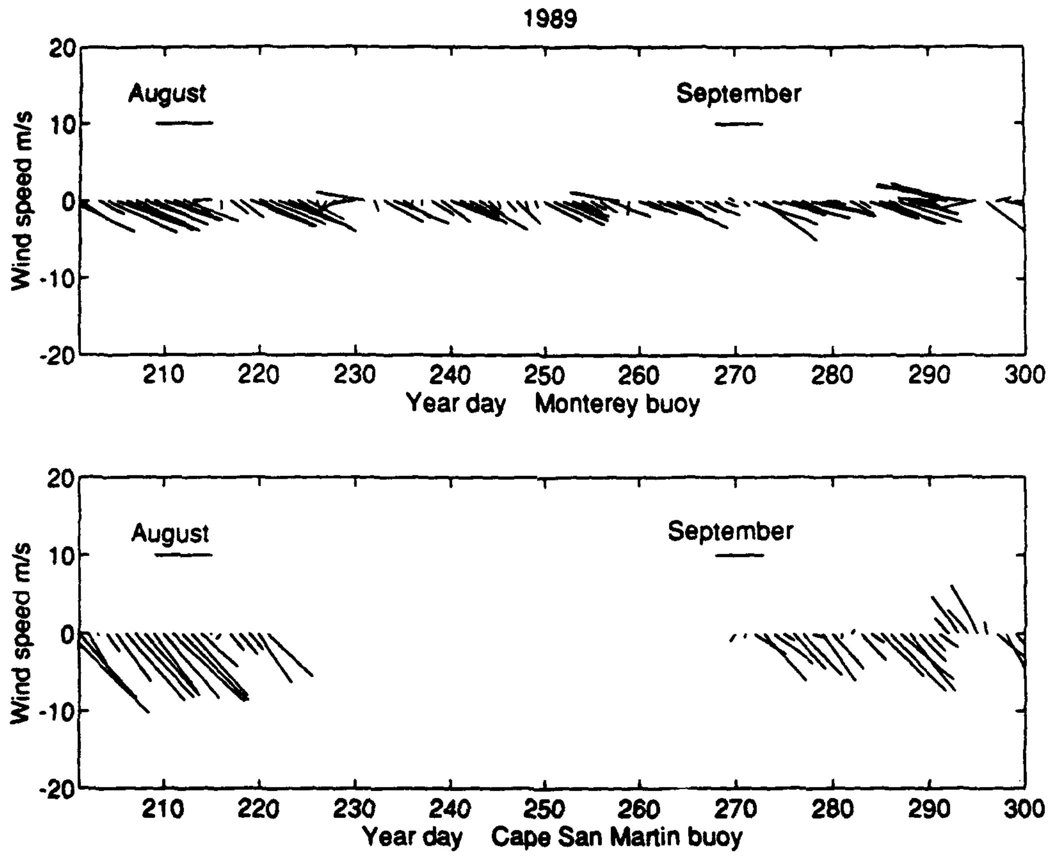
1989
20
10
0
-10
-20
Wind speed m/s
August
September
210
220
230
240
250
260
270
280
290
300
Year day Monterey buoy
20
10
0
-10
-20
Wind speed m/s
August
September
210
220
230
240
250
260
270
280
290
300
Year day Cape San Martin buoy

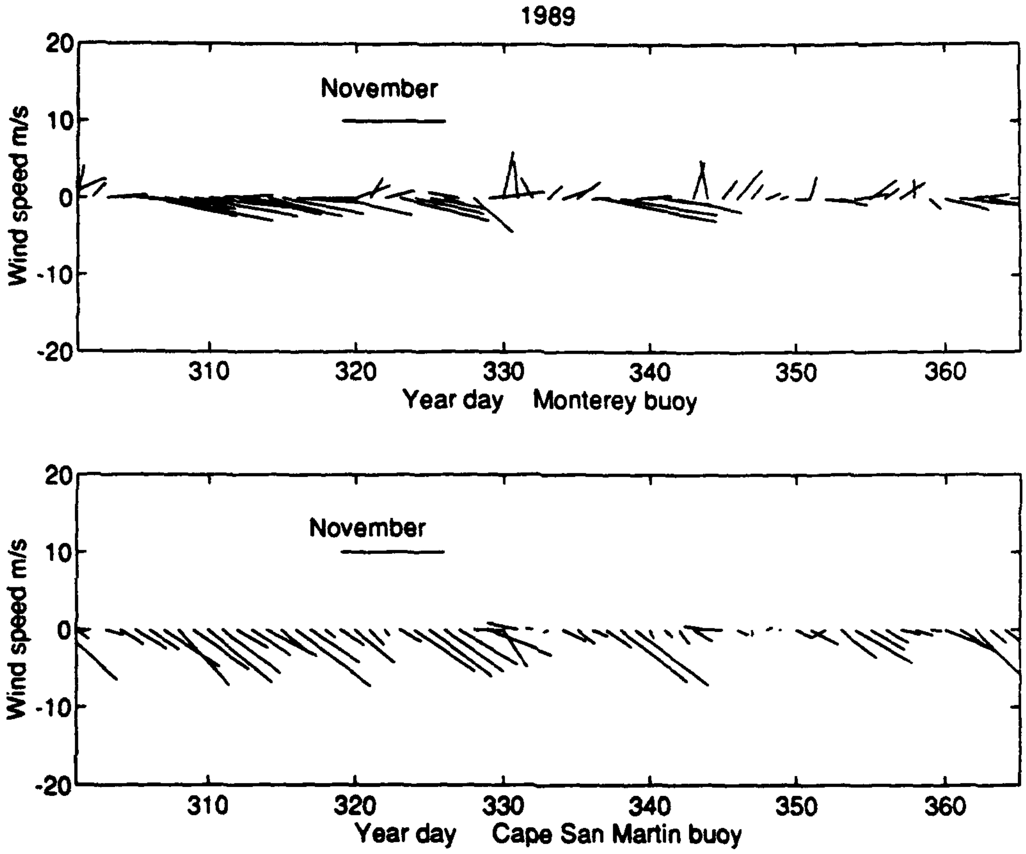
1989
November
Wind speed m/s
20
10
0
-10
-20
310
320
330
340
350
360
Year day Monterey buoy
November
Wind speed m/s
20
10
0
-10
-20
310
320
330
340
350
360
Year day Cape San Martin buoy

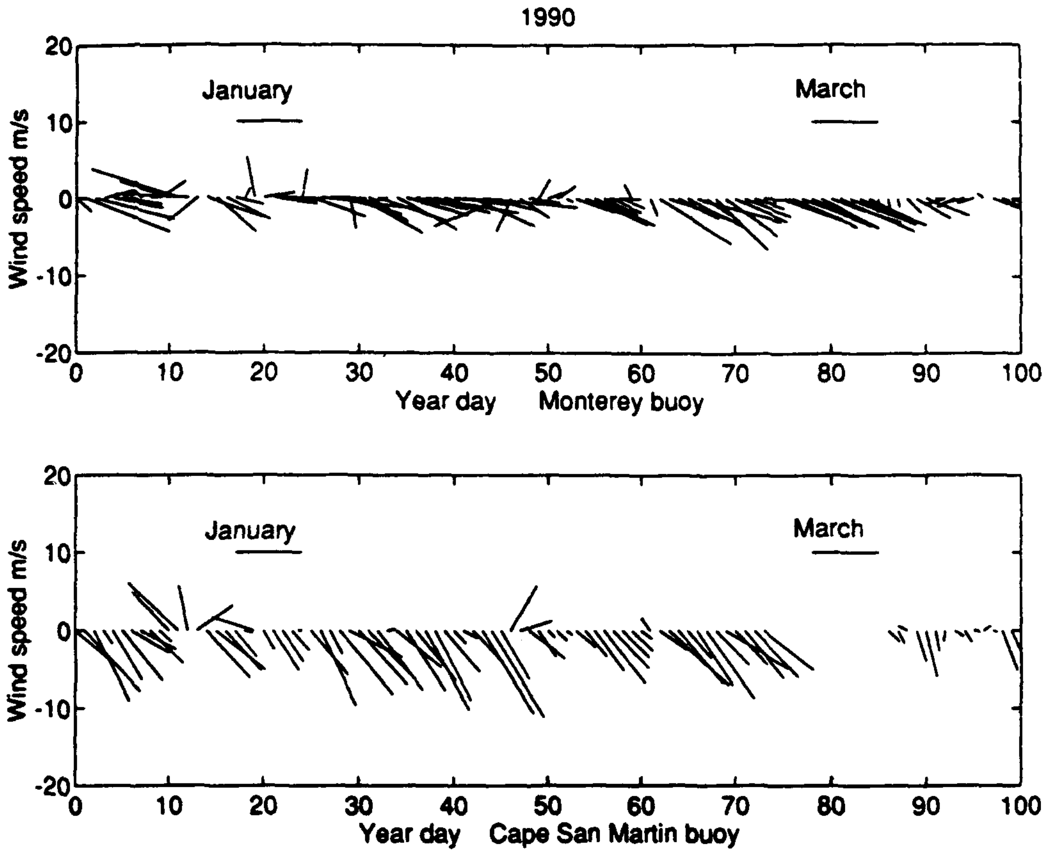
1990
January
March
Wind speed m/s
20
10
0
-10
-20
0 10 20 30 40 50 60 70 80 90 100
Year day Monterey buoy
January
March
Wind speed m/s
20
10
0
-10
-20
0 10 20 30 40 50 60 70 80 90 100
Year day Cape San Martin buoy

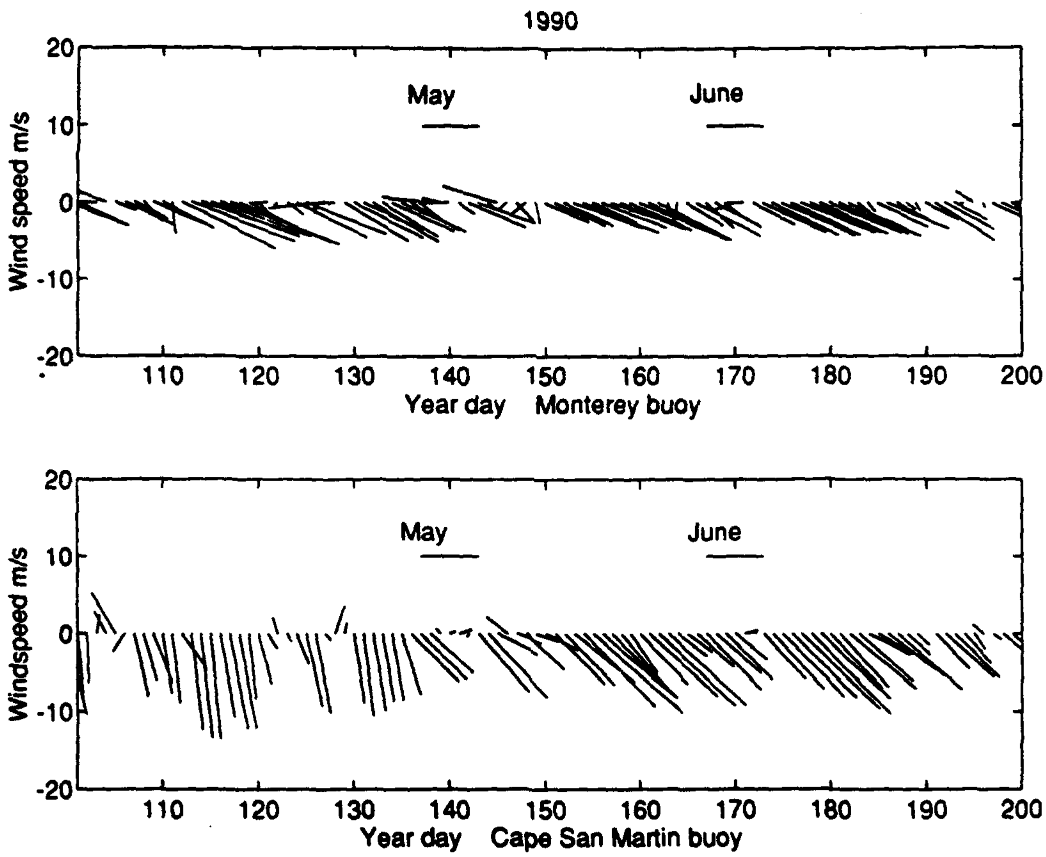
1990
20
10
0
-10
-20
Wind speed m/s
May
June
110
120
130
140
150
160
170
180
190
200
Year day Monterey buoy
20
10
0
-10
-20
Windspeed m/s
May
June
110
120
130
140
150
160
170
180
190
200
Year day Cape San Martin buoy

APPENDIX C. HYDROGRAPHIC DATA

CTD temperature and salinity contour plots are presented for each cruise period. Station numbers are indicated along the bottom of the plot. Hydrographic data were available in the vicinity of each PEGASUS station. A simple linear interpolation was utilized to fill in missing data when CTD data were not available for a particular station. MATLAB generated contouring errors were not corrected. The temperature plots were contoured in °C, while the salinity plots were contoured using PSS 78.

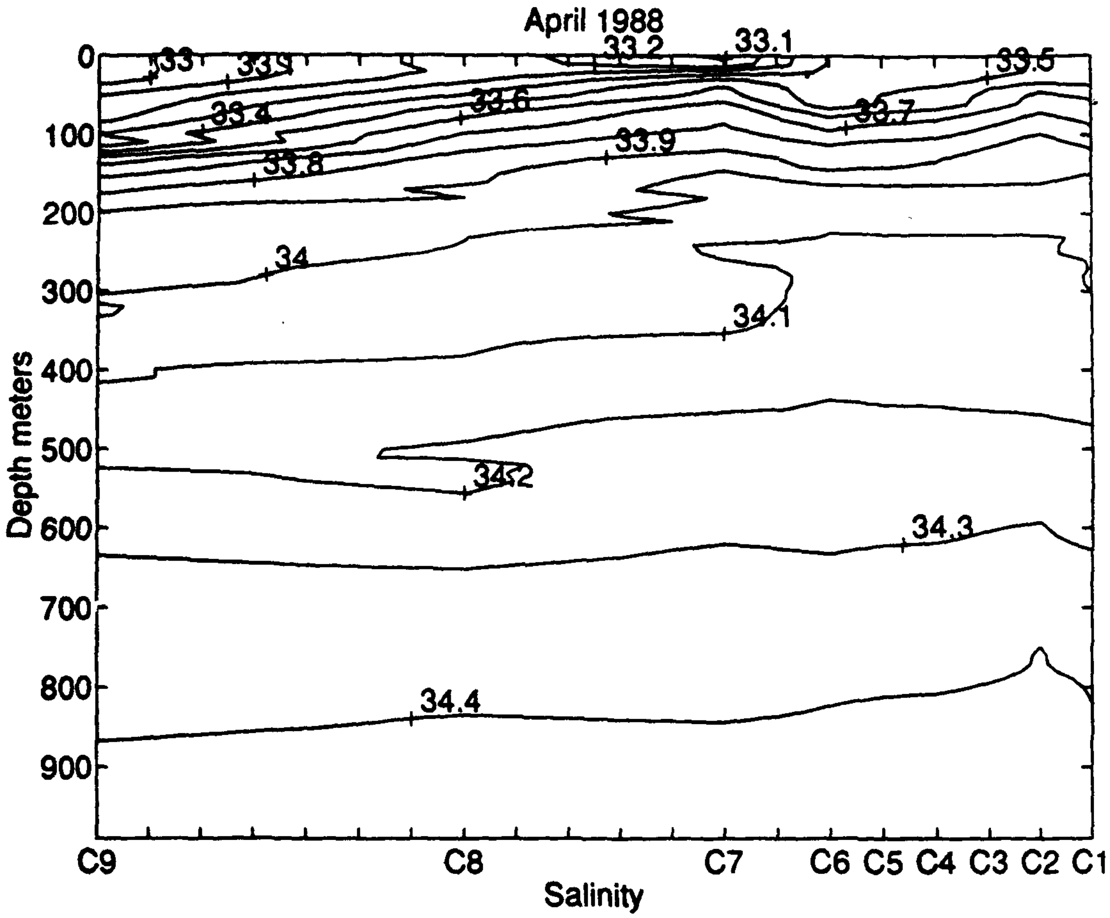
April 1988
Depth meters
Salinity
0
100
200
300
400
500
600
700
800
900
C9
C8
C7
C6
C5
C4
C3
C2
C1
33
33.3
33.4
33.6
33.8
33.9
33.2
33.1
33.5
33.7
34
34.1
34.2
34.3
34.4

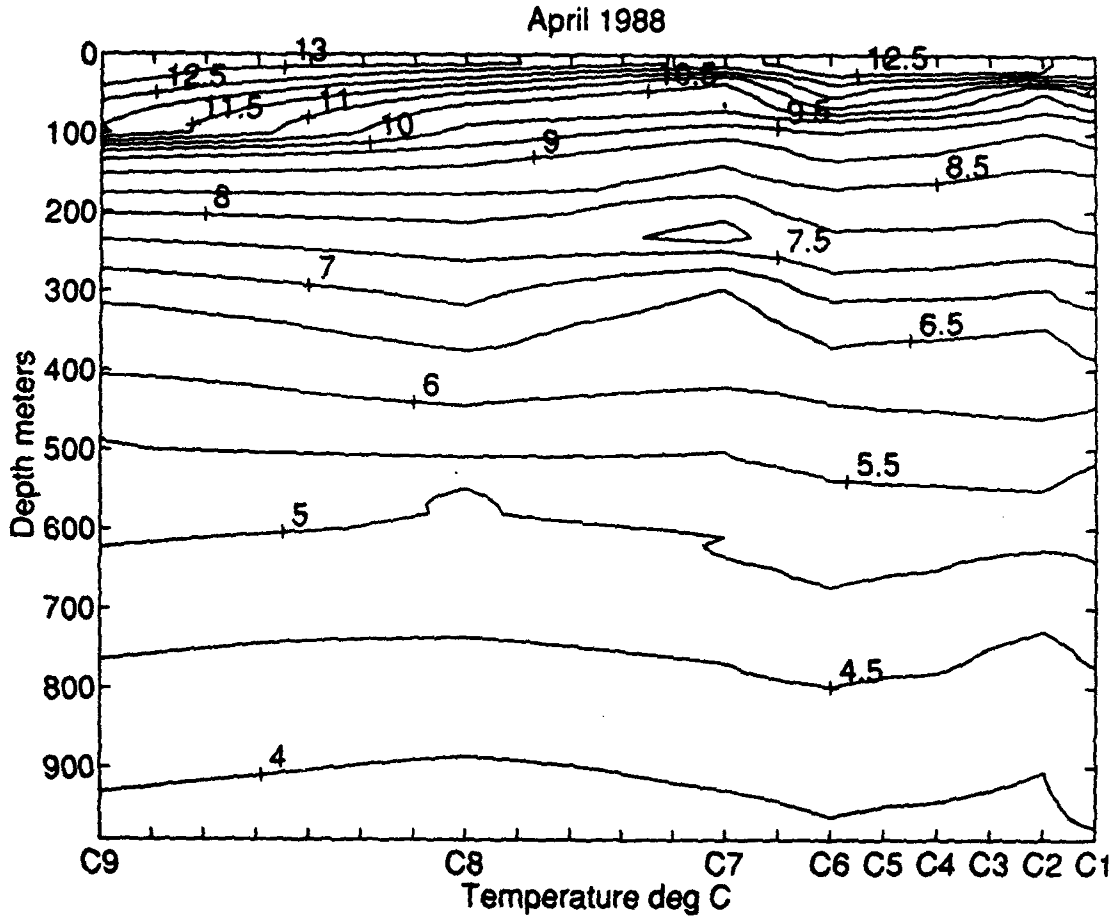
April 1988
Depth meters
0
100
200
300
400
500
600
700
800
900
13
12.5
11.5
11
10
10.5
9.5
9
8.5
8
7.5
7
6.5
6
5.5
5
4.5
4
C9
C8
C7
C6 C5 C4 C3 C2 C1
Temperature deg C

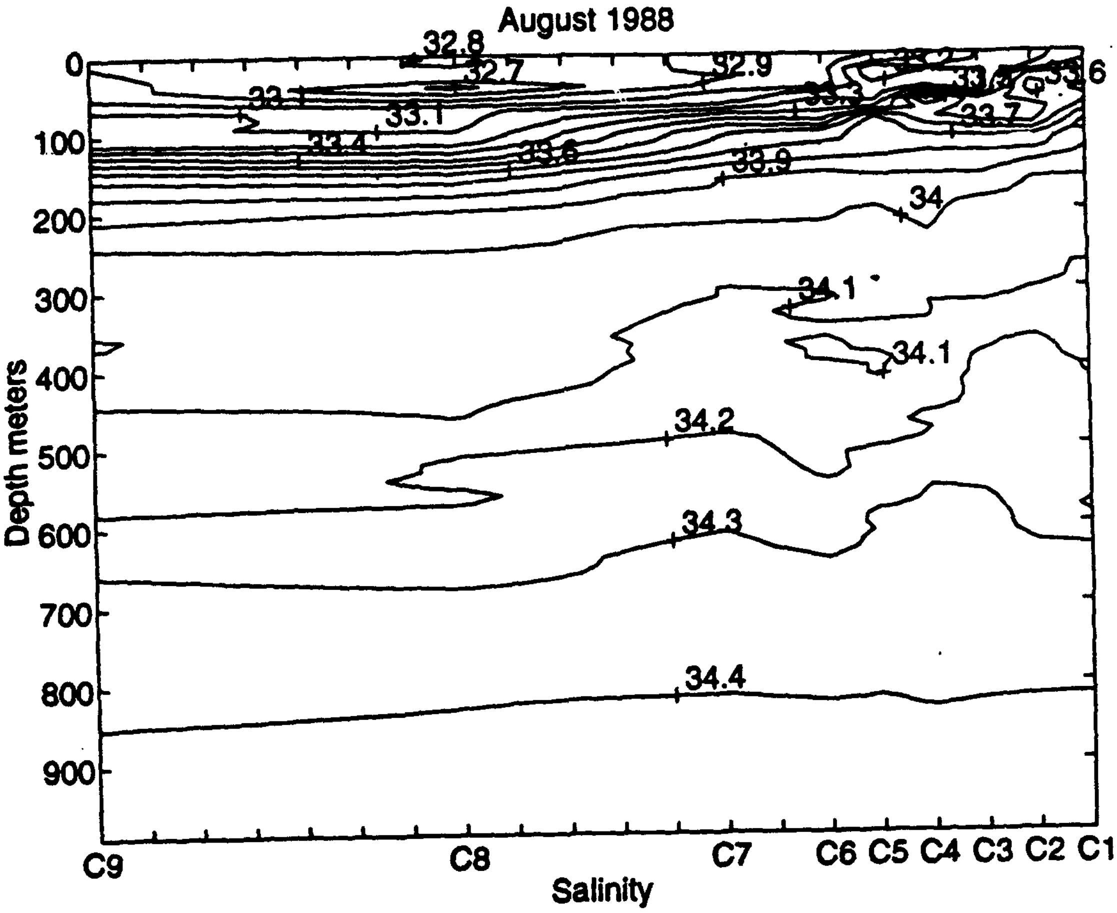

August 1988
Depth meters
Salinity
0
100
200
300
400
500
600
700
800
900
C9
C8
C7
C6 C5 C4 C3 C2 C1
32.8
32.7
32.9
33.1
33.1
33.3
33.4
33.6
33.7
33.9
34
34.1
34.1
34.2
34.3
34.4

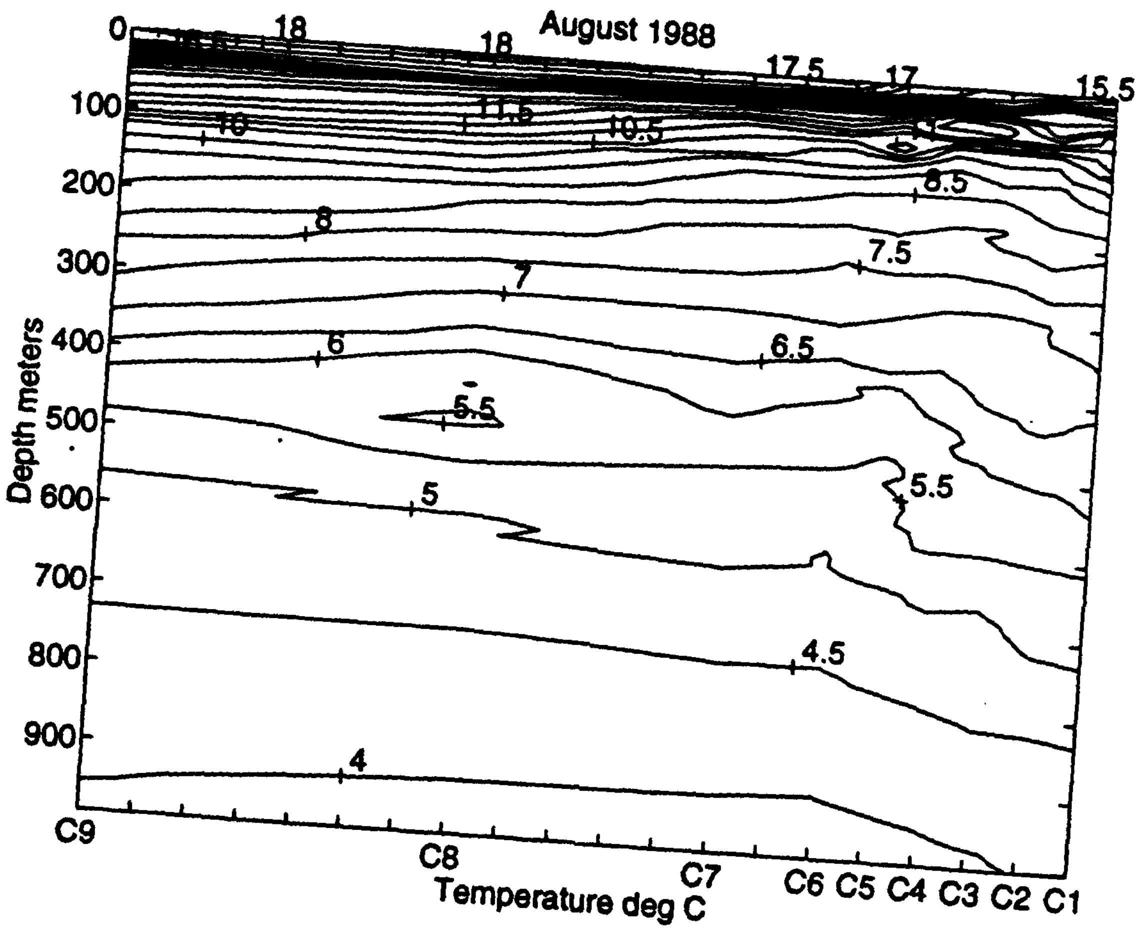
August 1988
Depth meters
Temperature deg C
0
100
200
300
400
500
600
700
800
900
C9
C8
C7
C6 C5 C4 C3 C2 C1
18
18
17.5
17
15.5
11.5
10.5
10
8.5
8
7.5
7
6.5
6
5.5
5.5
5
4.5
4

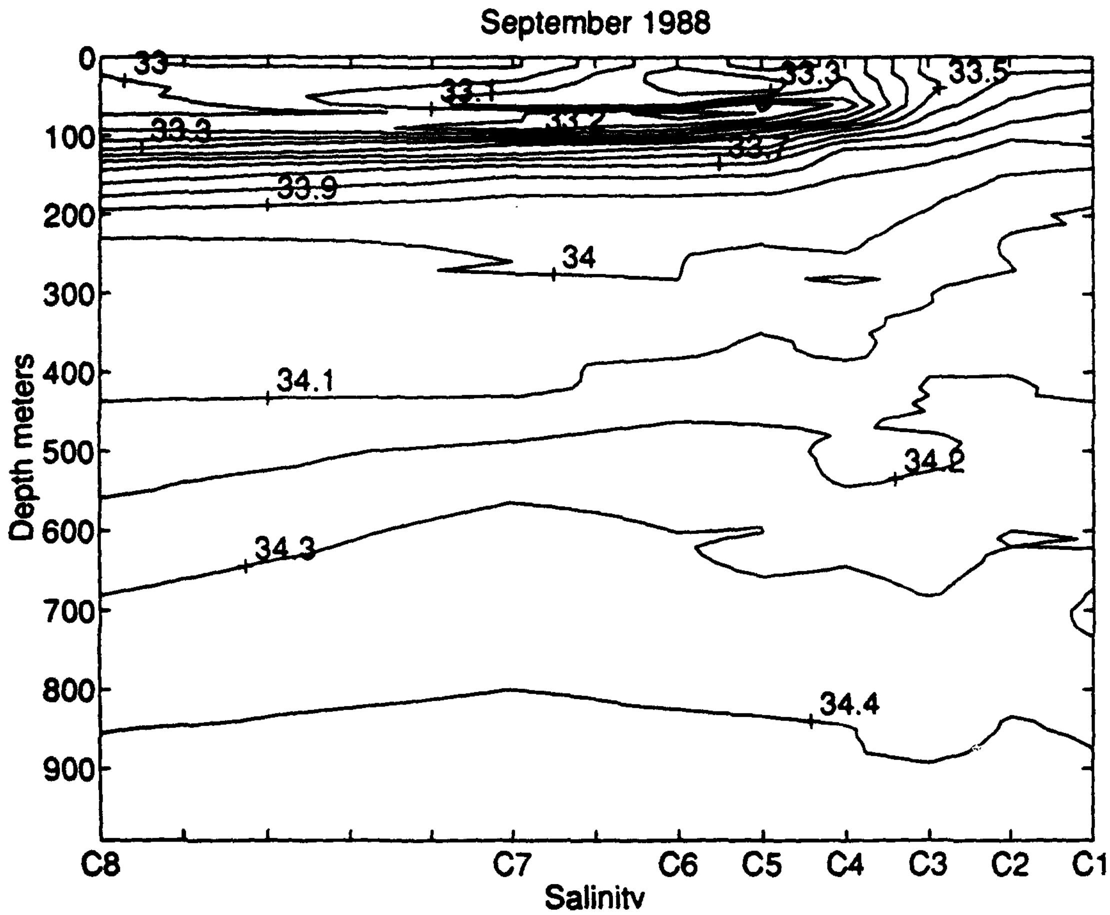
September 1988
Depth meters
Salinitv
0
100
200
300
400
500
600
700
800
900
C8
C7
C6
C5
C4
C3
C2
C1
33
33.1
33.2
33.3
33.3
33.5
33.7
33.9
34
34.1
34.2
34.3
34.4

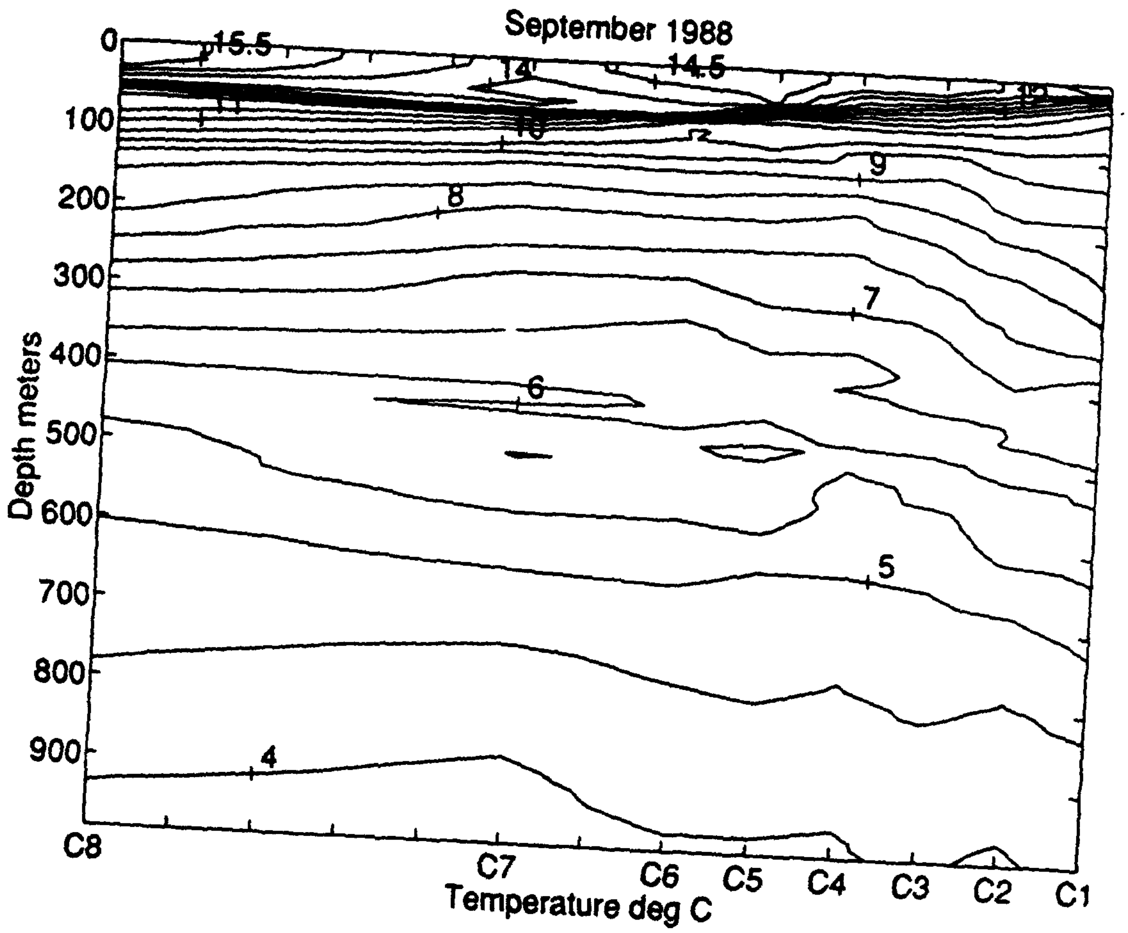

September 1988
Depth meters
0
100
200
300
400
500
600
700
800
900
15.5
14
14.5
11
10
12
9
8
7
6
5
4
C8
C7
C6
C5
C4
C3
C2
C1
Temperature deg C

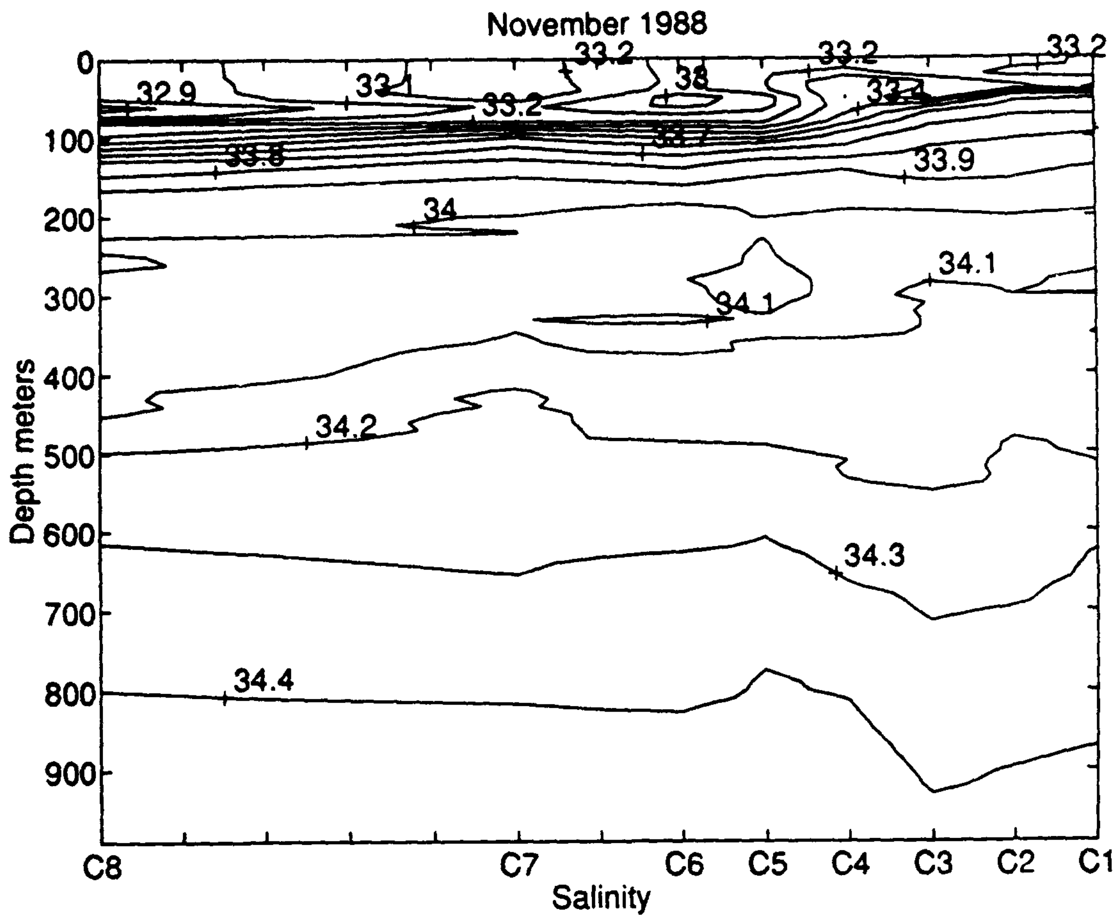

November 1988
32.9
33.1
33.2
33.2
38
33.2
33.4
33.2
33.7
33.8
33.9
34
34.1
34.1
34.2
34.3
34.4
Depth meters
0
100
200
300
400
500
600
700
800
900
C8
C7
C6
C5
C4
C3
C2
C1
Salinity

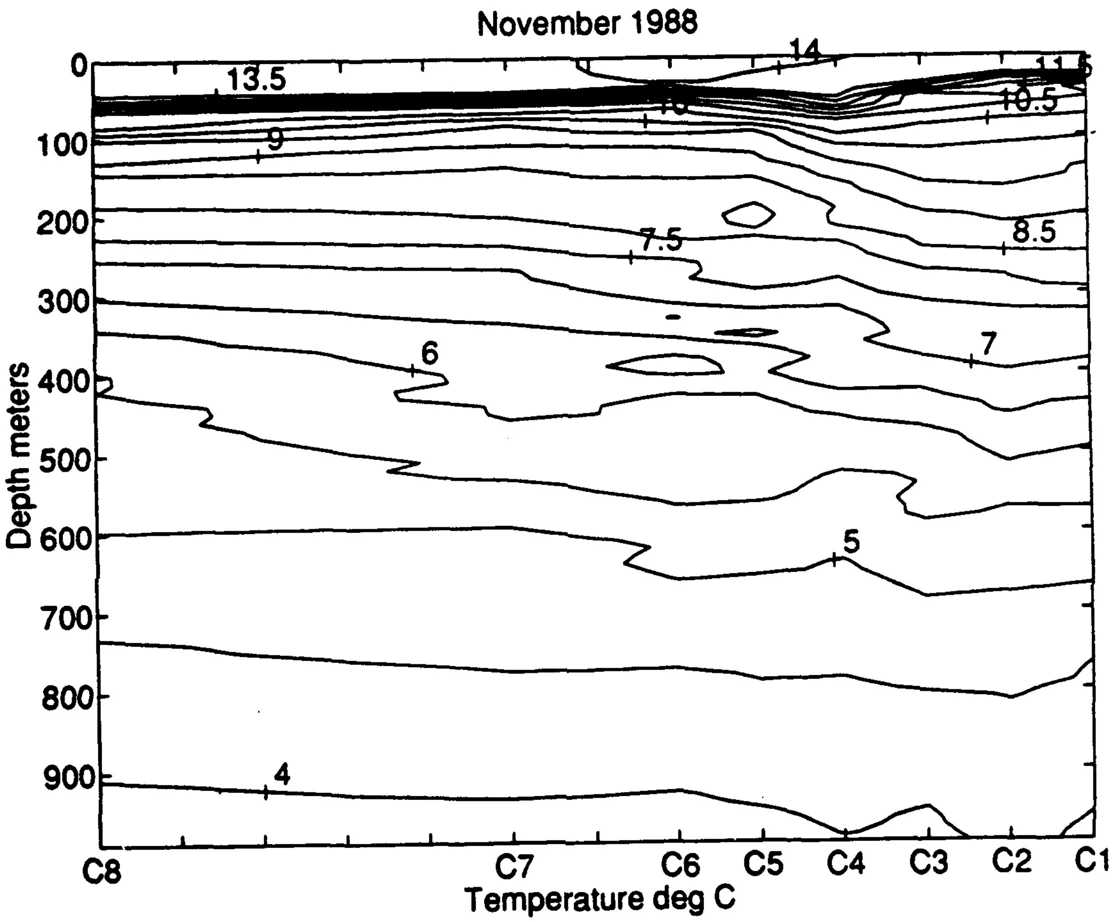

November 1988
Depth meters
0
100
200
300
400
500
600
700
800
900
13.5
14
11.5
10.5
10
9
8.5
7.5
7
6
5
4
C8
C7
C6
C5
C4
C3
C2
C1
Temperature deg C

February 1989

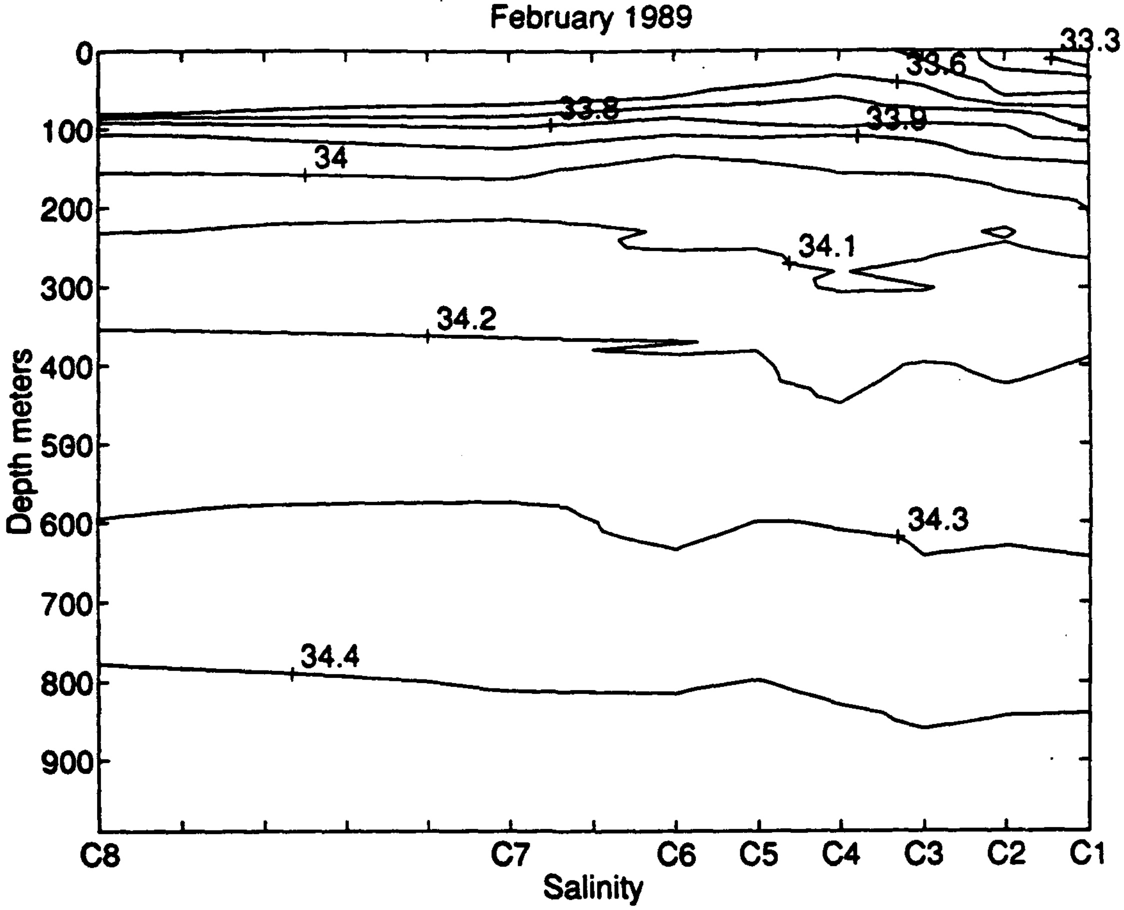

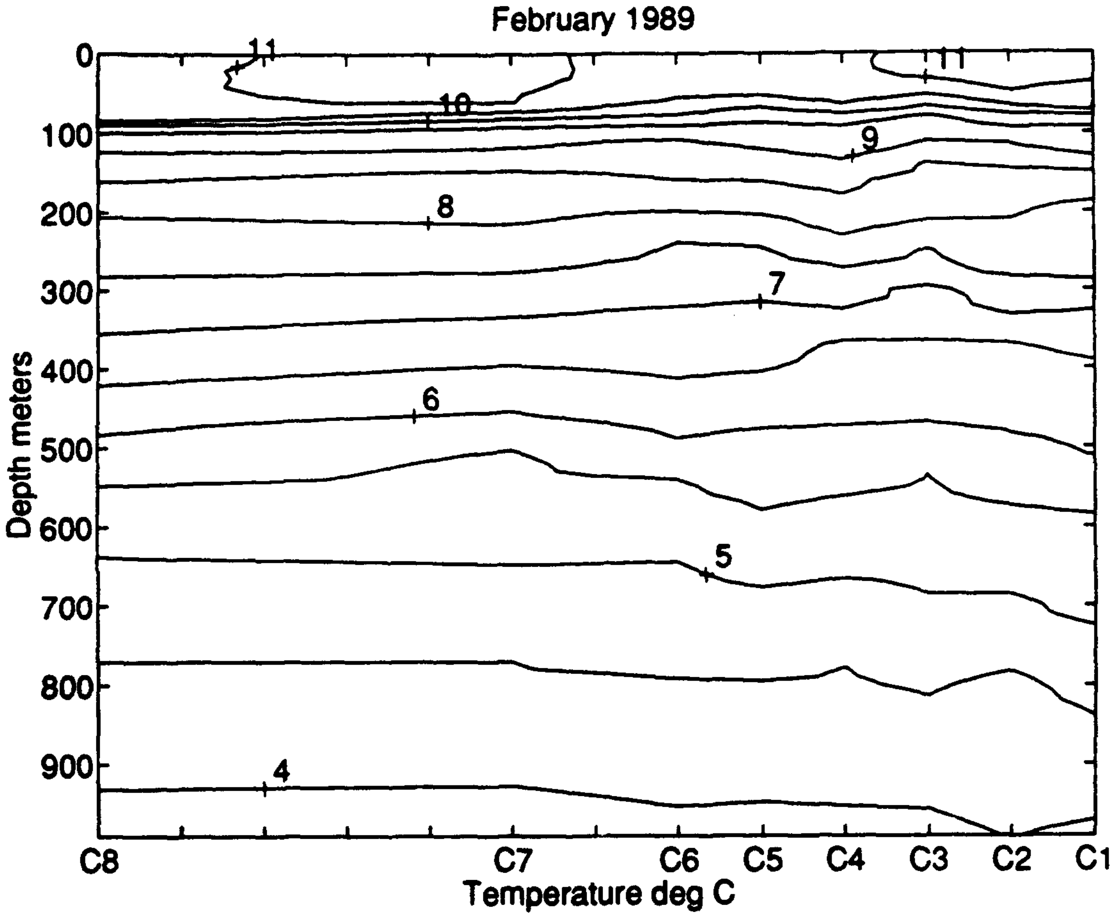

February 1989
0
100
200
300
400
500
600
700
800
900
Depth meters
11
10
9
8
7
6
5
4
11
C8
C7
C6
C5
C4
C3
C2
C1
Temperature deg C

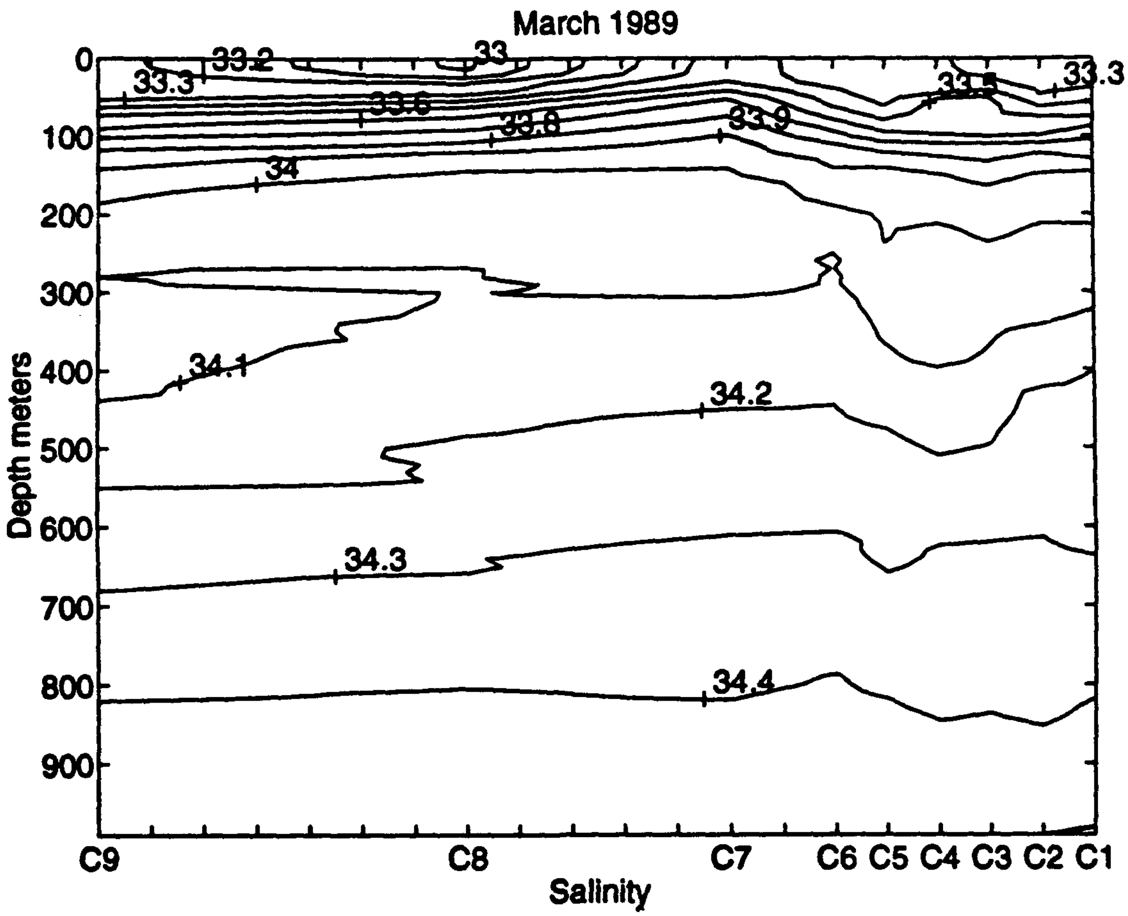
March 1989
Depth meters
Salinity
0
100
200
300
400
500
600
700
800
900
C9
C8
C7
C6 C5 C4 C3 C2 C1
33.2
33
33.3
33.6
33.8
33.9
34
34.1
34.2
34.3
34.4
33.3

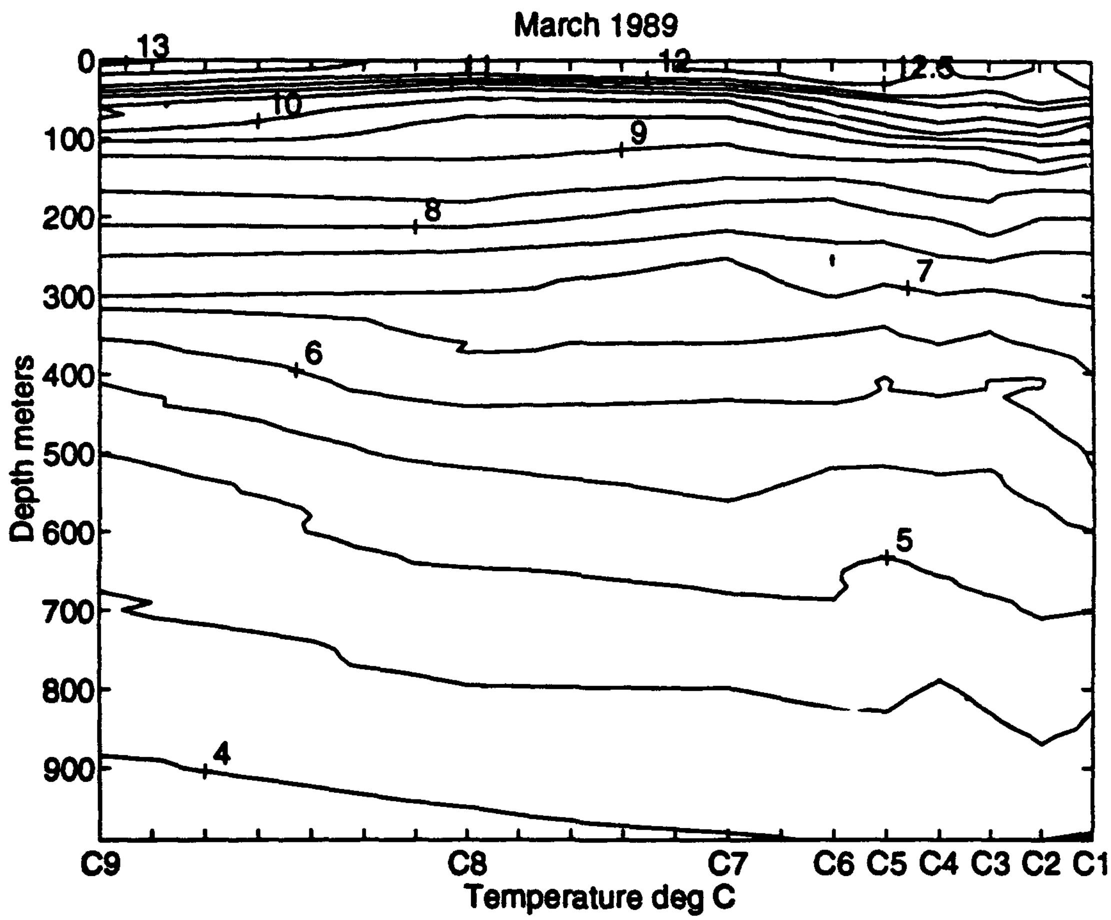

March 1989
13
11
12
12.5
10
9
8
7
6
5
4
0
100
200
300
400
500
600
700
800
900
Depth meters
C9
C8
C7
C6
C5
C4
C3
C2
C1
Temperature deg C

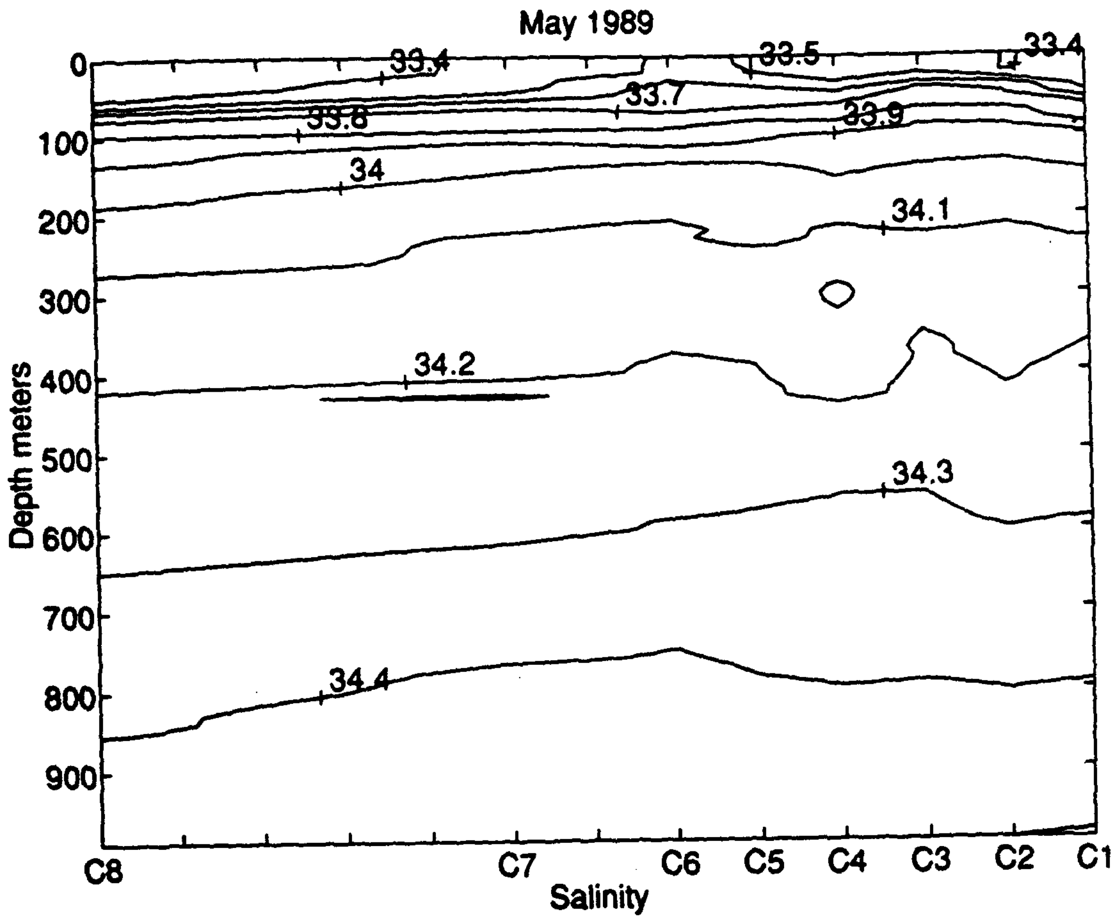

May 1989
33.4
33.5
33.4
33.7
33.8
33.9
34
34.1
34.2
34.3
34.4
0
100
200
300
400
500
600
700
800
900
Depth meters
C8
C7
C6
C5
C4
C3
C2
C1
Salinity

May 1989

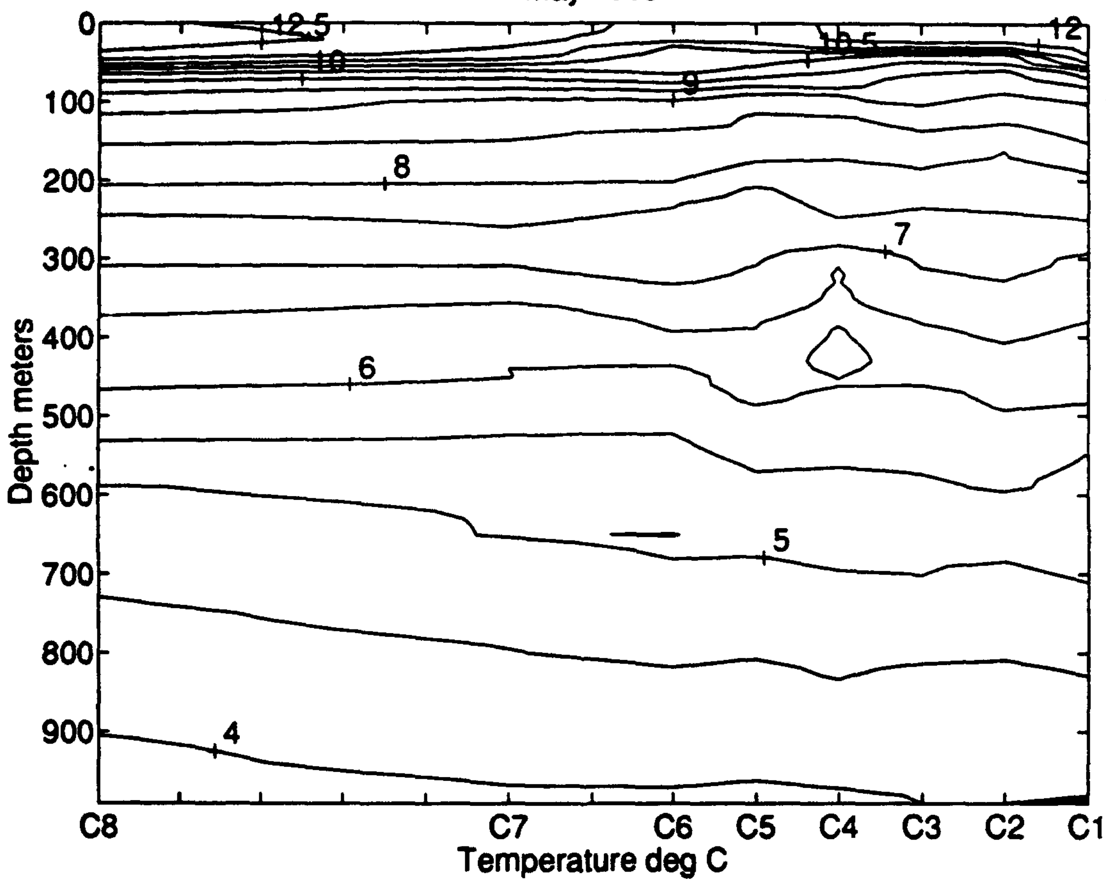

12.5
10
10.5
12
9
8
7
6
5
4
0
100
200
300
400
500
600
700
800
900
Depth meters
C8
C7
C6
C5
C4
C3
C2
C1
Temperature deg C

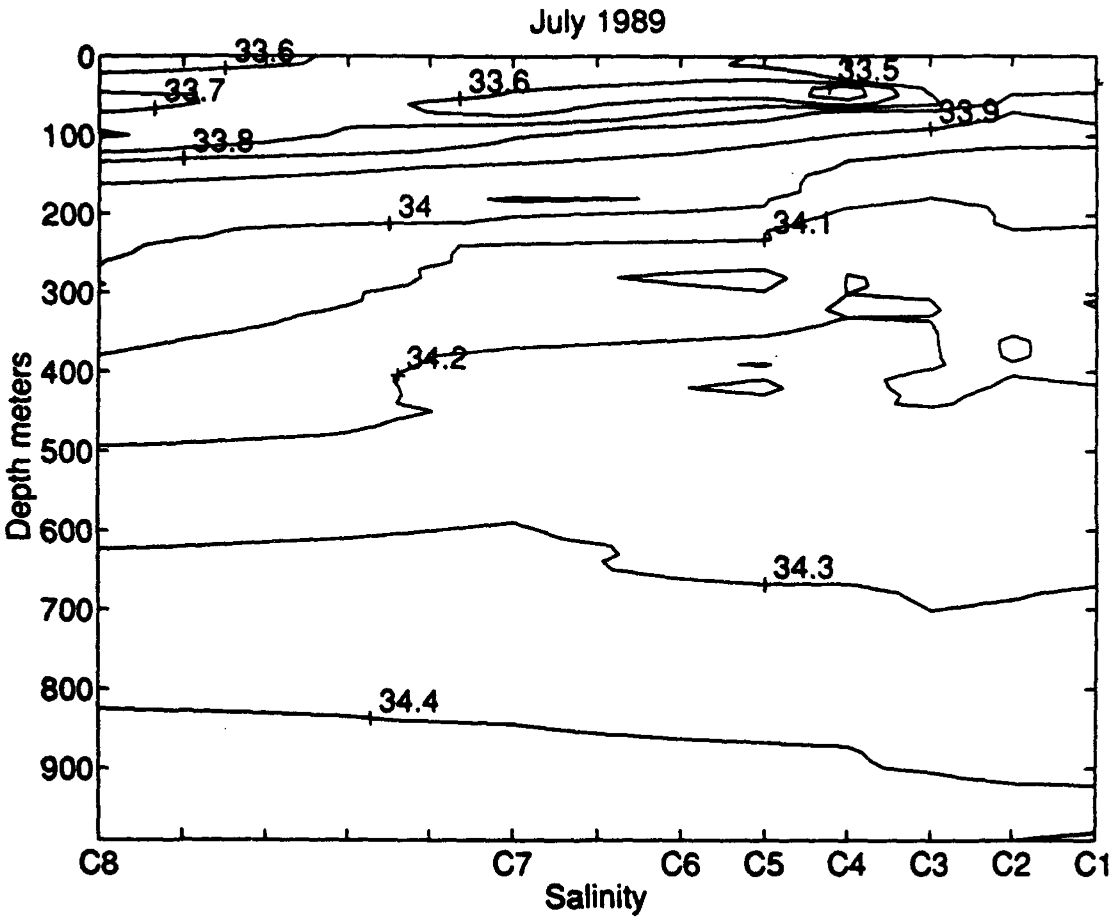

July 1989
33.6
33.7
33.6
33.5
33.8
33.9
34
34.1
34.2
34.3
34.4
0
100
200
300
400
500
600
700
800
900
Depth meters
C8
C7
C6
C5
C4
C3
C2
C1
Salinity

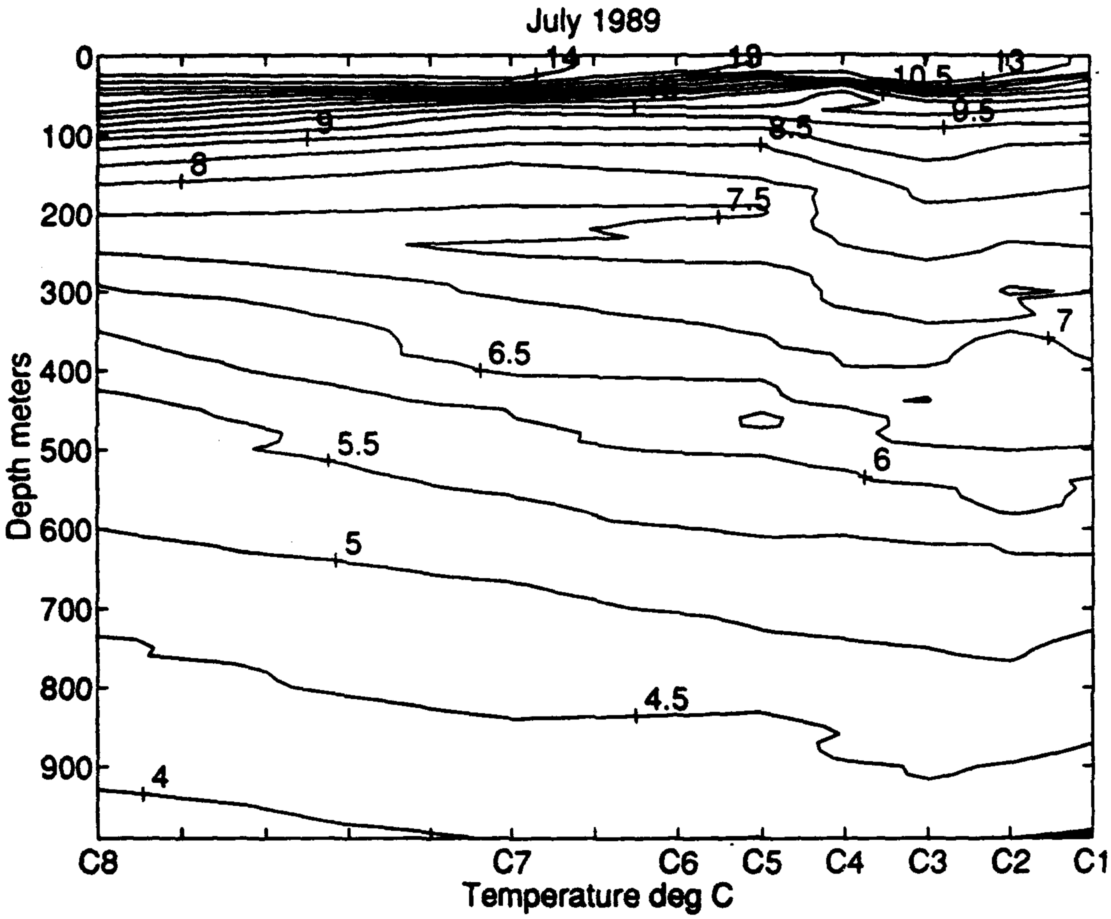
July 1989
Depth meters
Temperature deg C
0
100
200
300
400
500
600
700
800
900
C8
C7
C6
C5
C4
C3
C2
C1
14
13
10.5
13
9
9.5
8.5
8
7.5
7
6.5
5.5
6
5
4.5
4

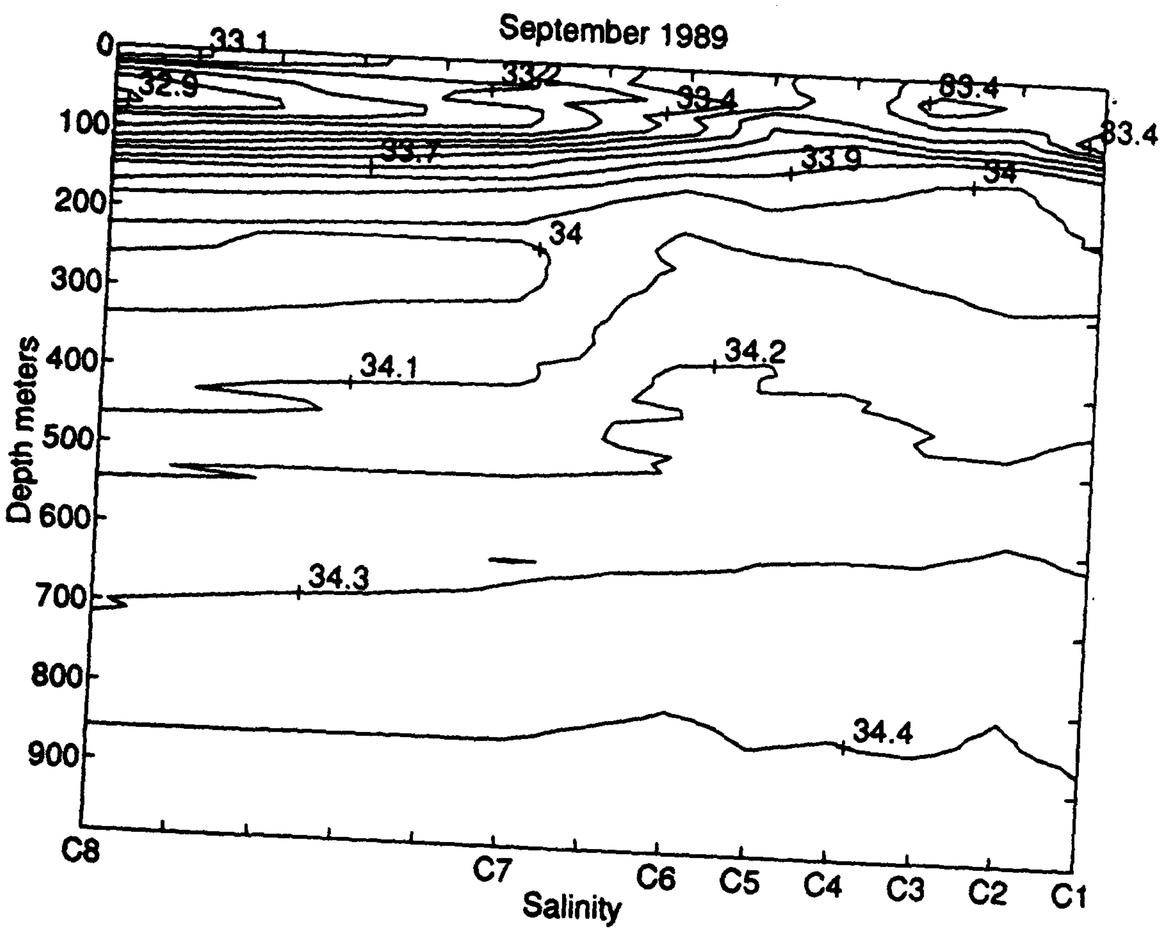

September 1989
Depth meters
Salinity
0
100
200
300
400
500
600
700
800
900
C8
C7
C6
C5
C4
C3
C2
C1
33.1
32.9
33.2
33.4
33.4
33.4
33.7
33.9
34
34
34.1
34.2
34.3
34.4

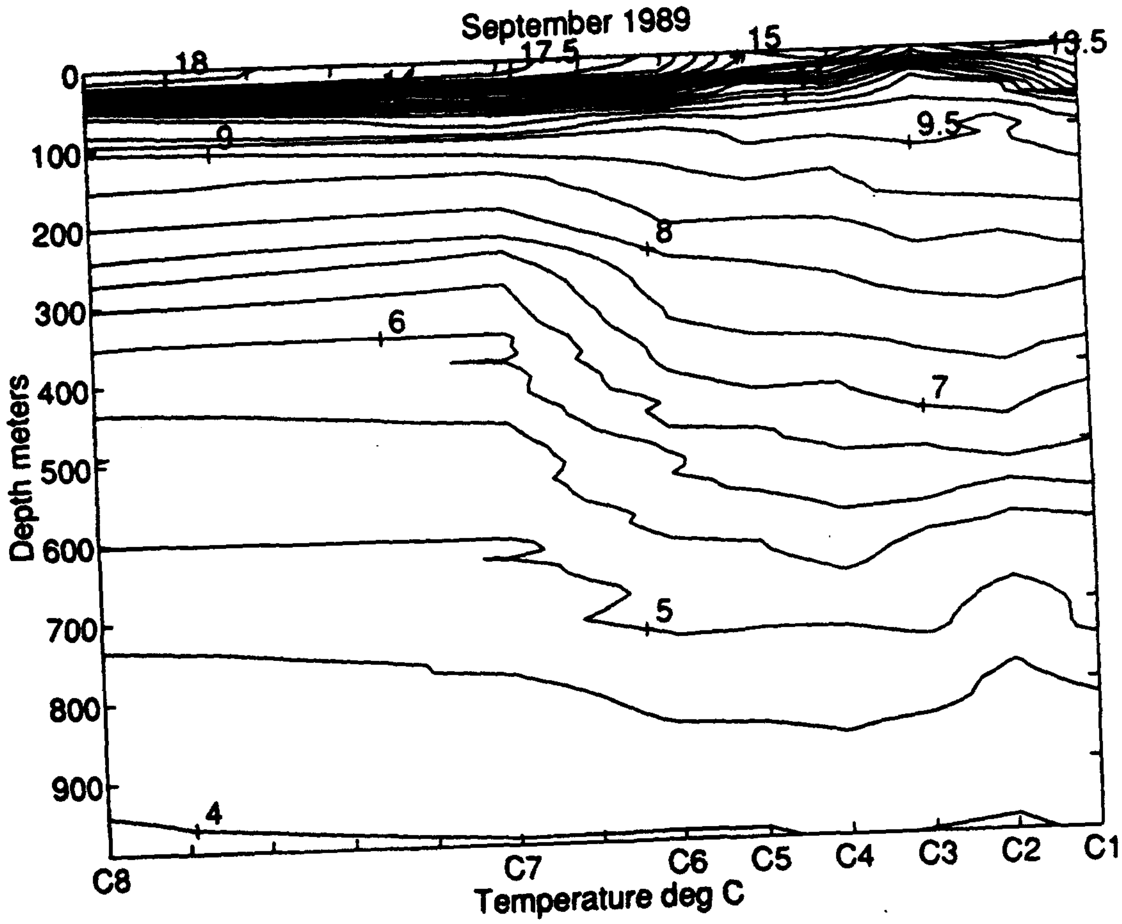
September 1989
18
17.5
15
13.5
9.5
9
8
6
7
5
4
0
100
200
300
400
500
600
700
800
900
Depth meters
C8
C7
C6
C5
C4
C3
C2
C1
Temperature deg C

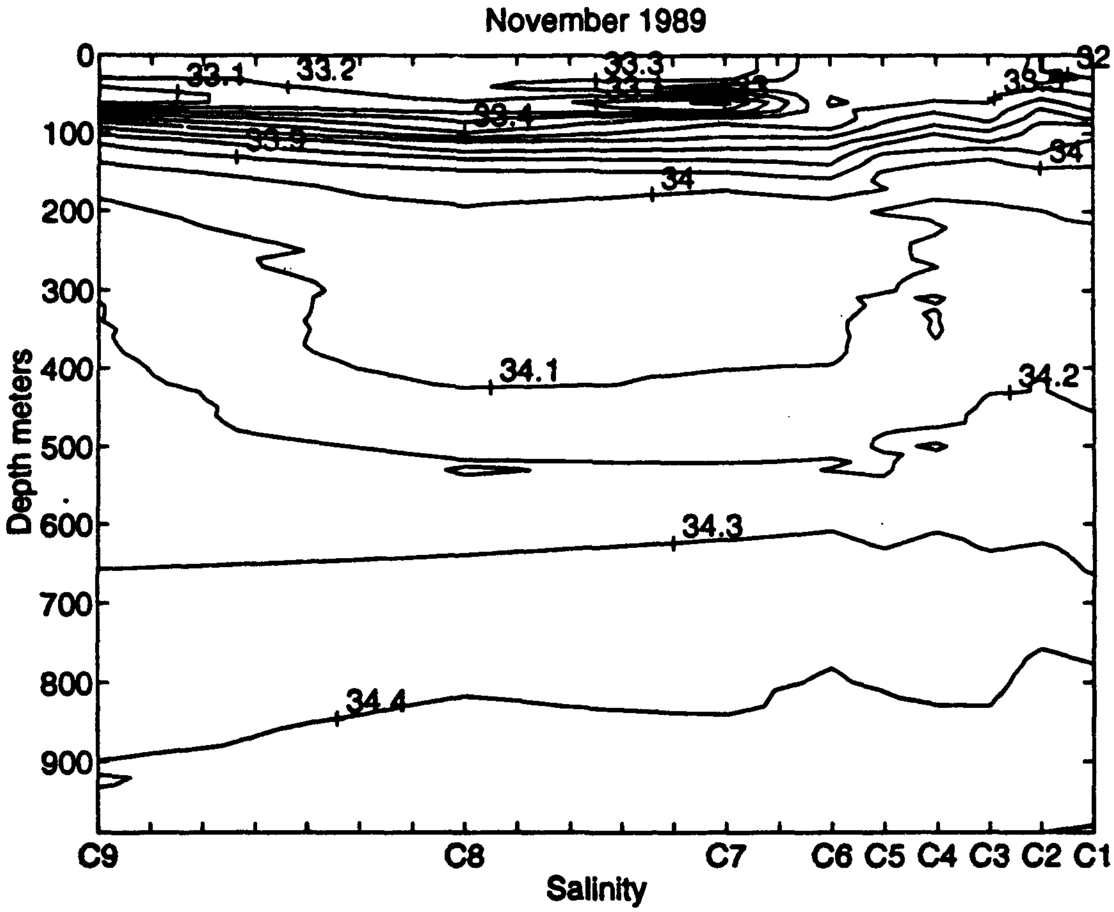
November 1989
Depth meters
Salinity
0
100
200
300
400
500
600
700
800
900
C9
C8
C7
C6
C5
C4
C3
C2
C1
33.1
33.2
33.3
33.4
33.9
34
34.1
34.2
34.3
34.4
32

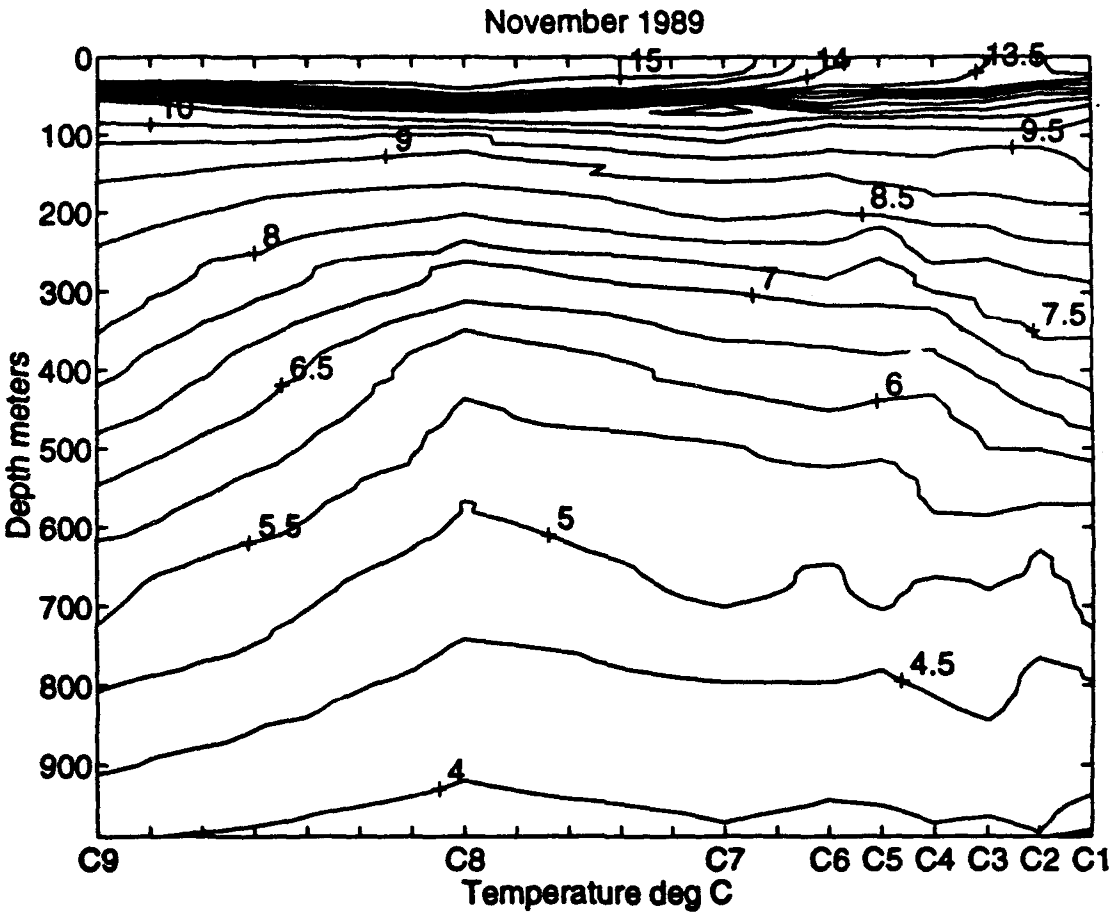

November 1989
Depth meters
0
100
200
300
400
500
600
700
800
900
15
14
13.5
10
9
9.5
8.5
8
7
7.5
6.5
6
5.5
5
4.5
4
C9
C8
C7
C6
C5
C4
C3
C2
C1
Temperature deg C

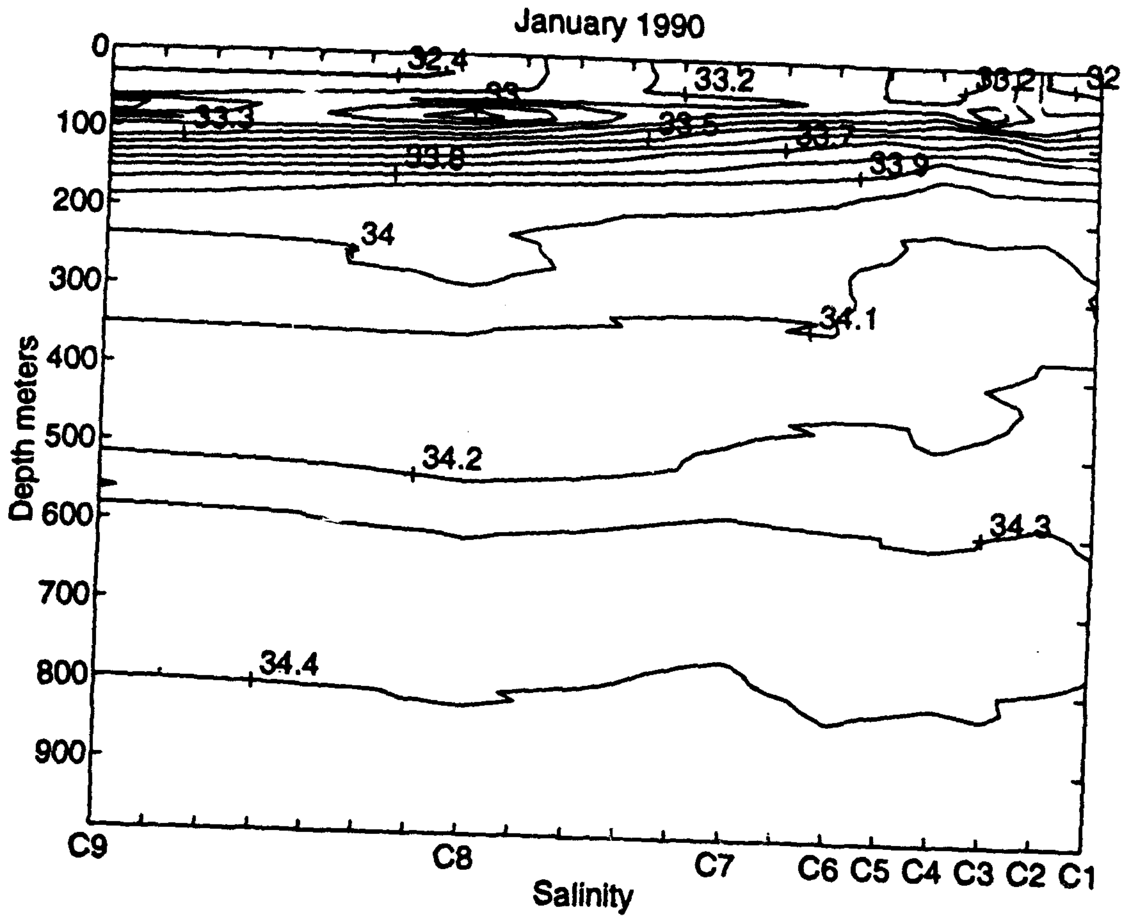
January 1990
Depth meters
Salinity
0
100
200
300
400
500
600
700
800
900
C9
C8
C7
C6
C5
C4
C3
C2
C1
32.4
33.2
32
33.3
33.5
33.7
33.8
33.9
34
34.1
34.2
34.3
34.4

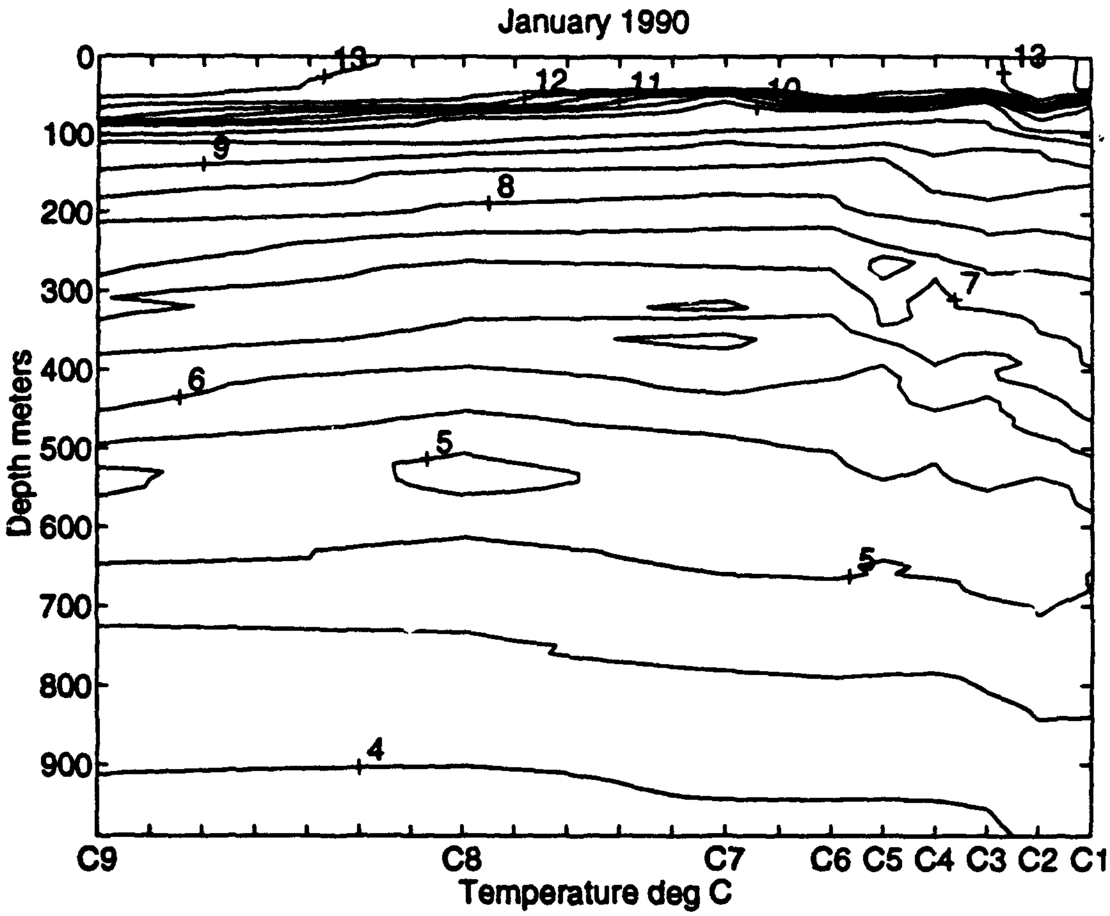
January 1990
Depth meters
Temperature deg C
0
100
200
300
400
500
600
700
800
900
C9
C8
C7
C6
C5
C4
C3
C2
C1
13
12
11
10
9
8
7
6
5
5
4

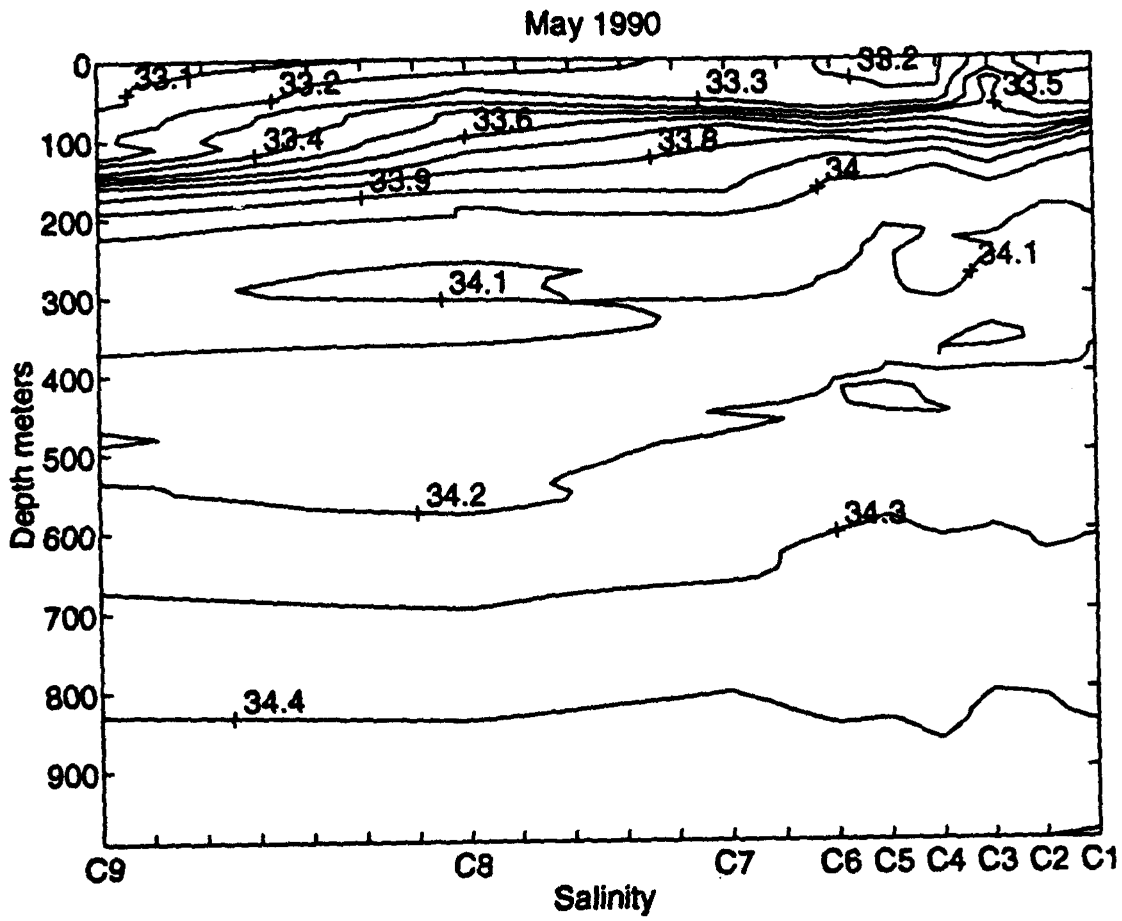
May 1990
33.1
33.2
33.3
33.2
33.5
33.4
33.6
33.8
33.9
34
34.1
34.1
34.2
34.3
34.4
0
100
200
300
400
500
600
700
800
900
Depth meters
C9
C8
C7
C6 C5 C4 C3 C2 C1
Salinity

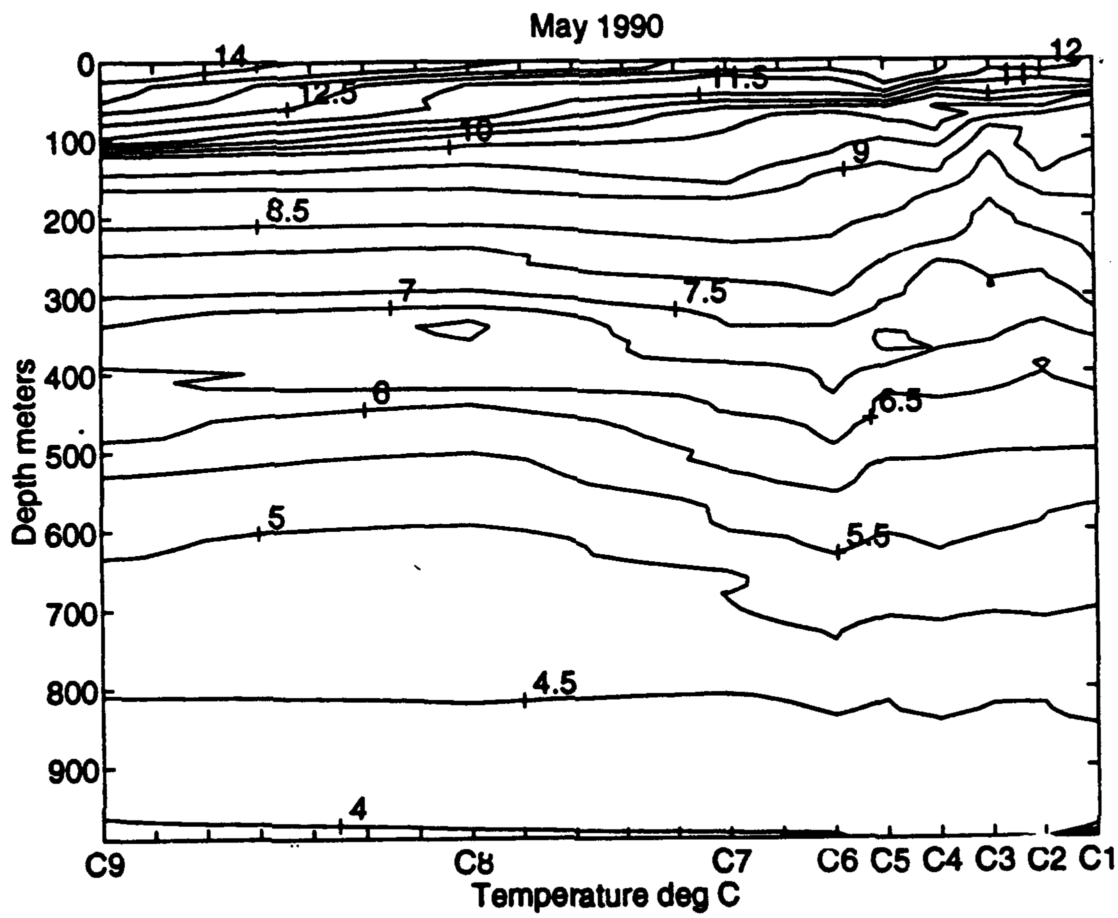
May 1990
Depth meters
Temperature deg C
0
100
200
300
400
500
600
700
800
900
C9
C8
C7
C6 C5 C4 C3 C2 C1
14
12.5
10
11.5
11
12
9
8.5
7
7.5
6
6.5
5
5.5
4.5
4

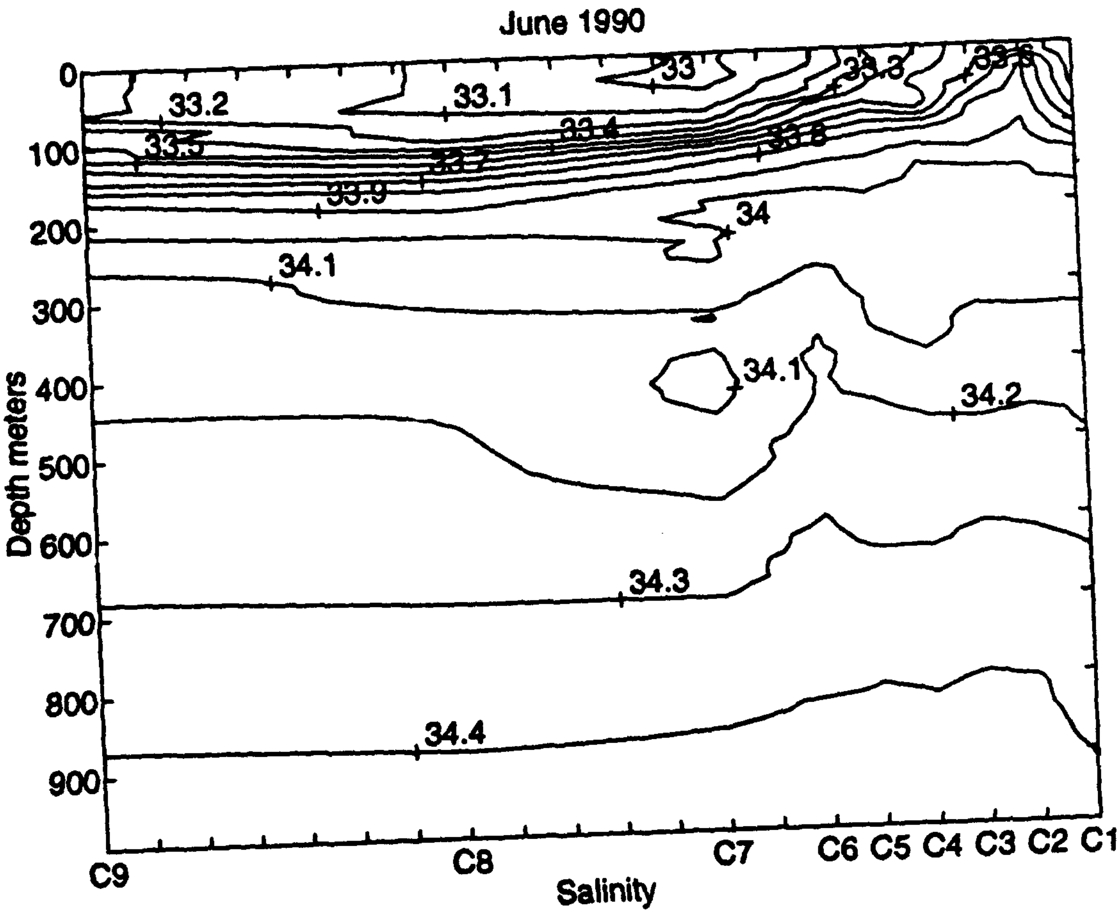
June 1990
33.2
33.1
33
33.3
33.6
33.5
33.4
33.8
33.7
33.9
34
34.1
34.1
34.2
34.3
34.4
Depth meters
0
100
200
300
400
500
600
700
800
900
C9
C8
C7
C6 C5 C4 C3 C2 C1
Salinity

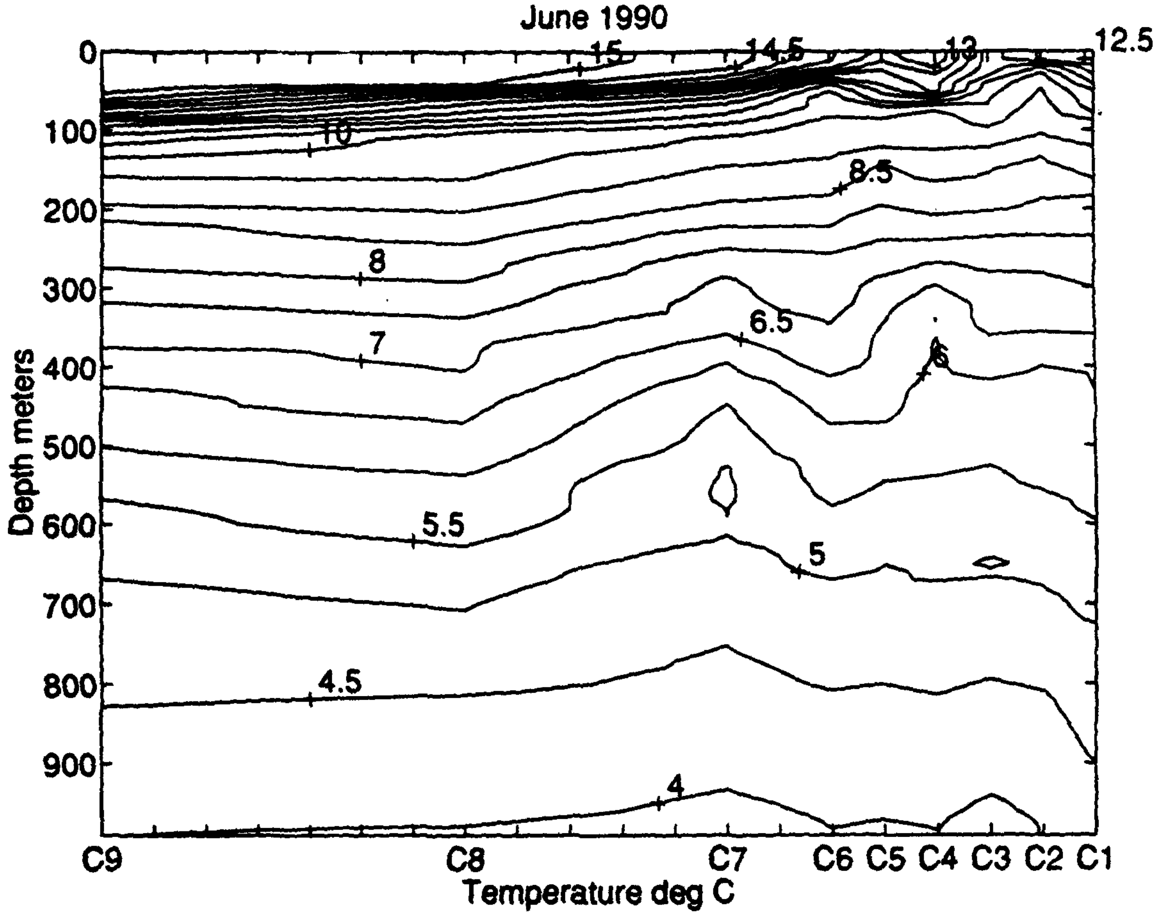
June 1990
Depth meters
Temperature deg C
0
100
200
300
400
500
600
700
800
900
C9
C8
C7
C6 C5 C4 C3 C2 C1
15
14.5
13
12.5
10
8.5
8
7
6.5
6
5.5
5
4.5
4

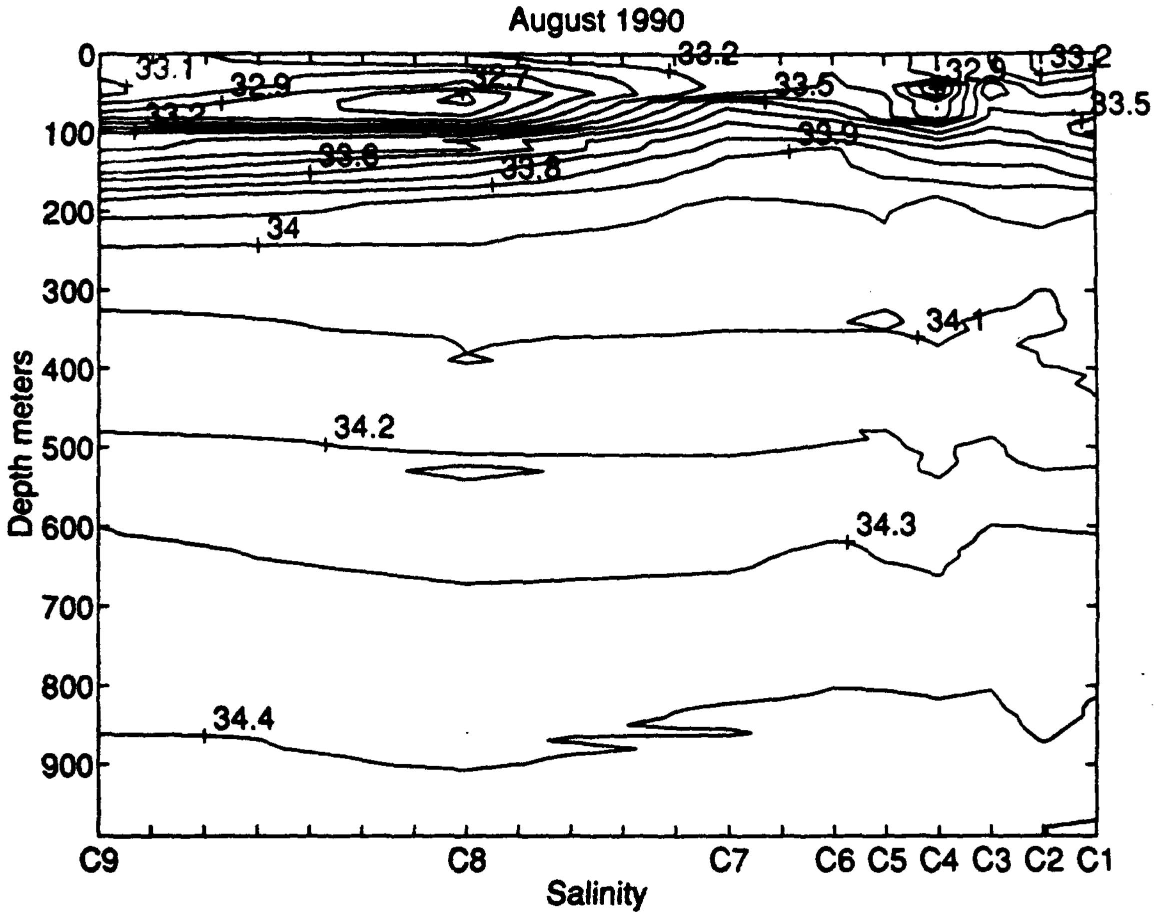
August 1990
Depth meters
0
100
200
300
400
500
600
700
800
900
33.1
32.9
32.7
33.2
33.5
32.9
33.2
33.5
33.9
33.8
34
34.1
34.2
34.3
34.4
C9
C8
C7
C6 C5 C4 C3 C2 C1
Salinity

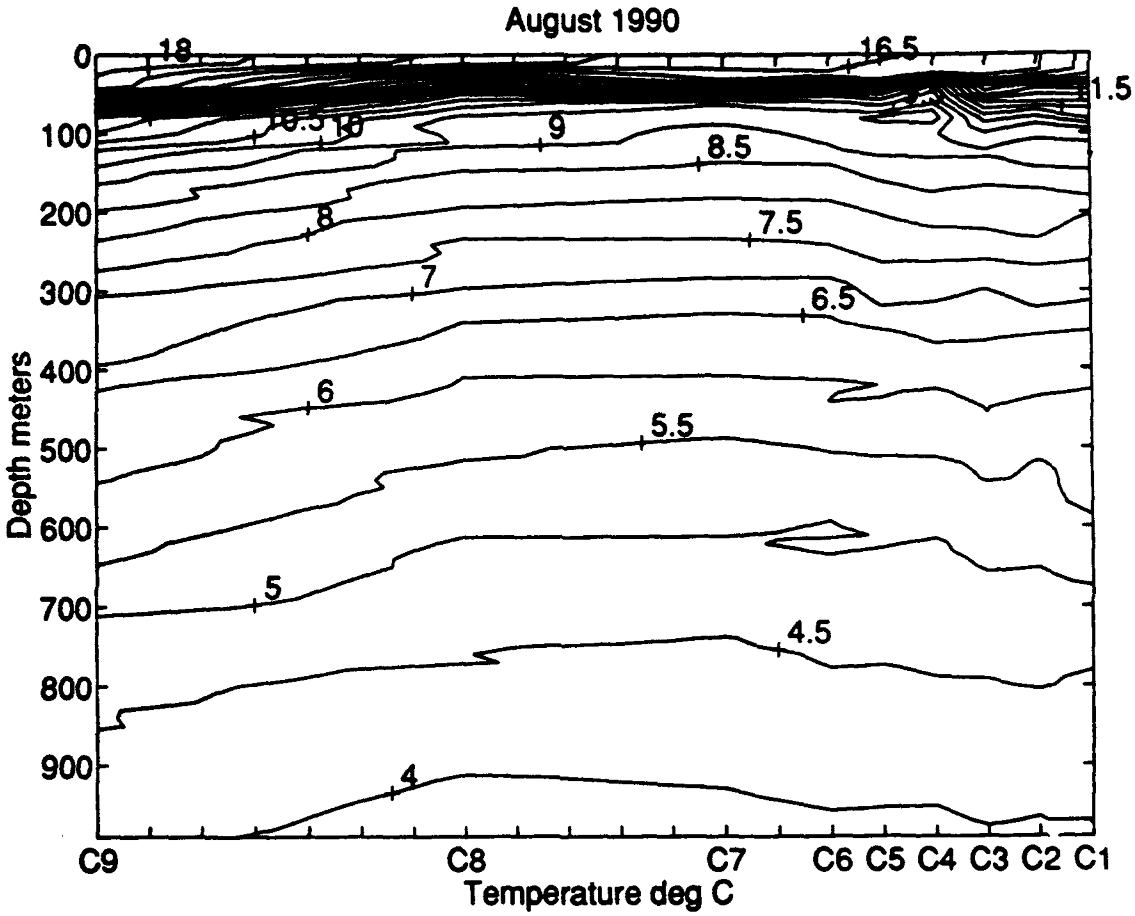

August 1990
18
16.5
11.5
10.5
10
9
8.5
8
7.5
7
6.5
6
5.5
5
4.5
4
0
100
200
300
400
500
600
700
800
900
Depth meters
C9
C8
C7
C6
C5
C4
C3
C2
C1
Temperature deg C

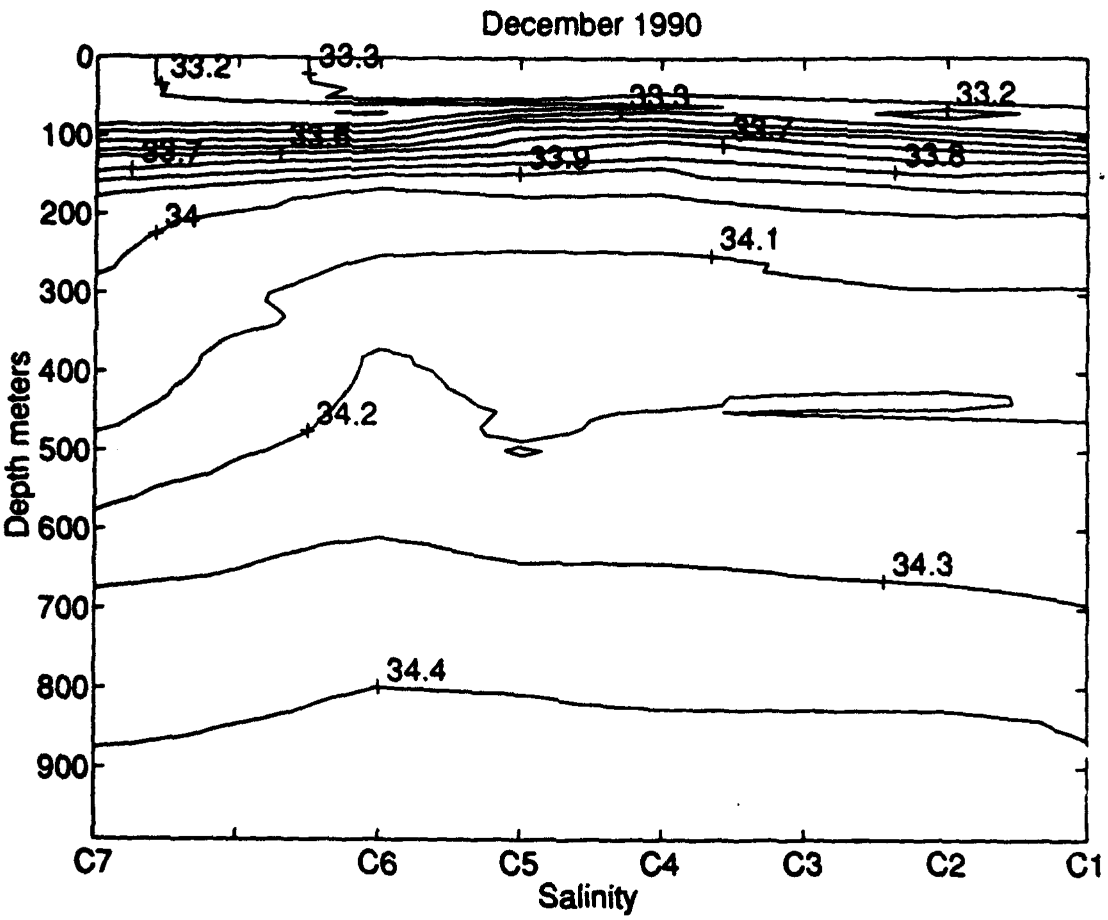
December 1990
Depth meters
Salinity
0
100
200
300
400
500
600
700
800
900
C7
C6
C5
C4
C3
C2
C1
33.2
33.3
33.3
33.2
33.7
33.8
33.9
33.7
33.8
34
34.1
34.2
34.3
34.4

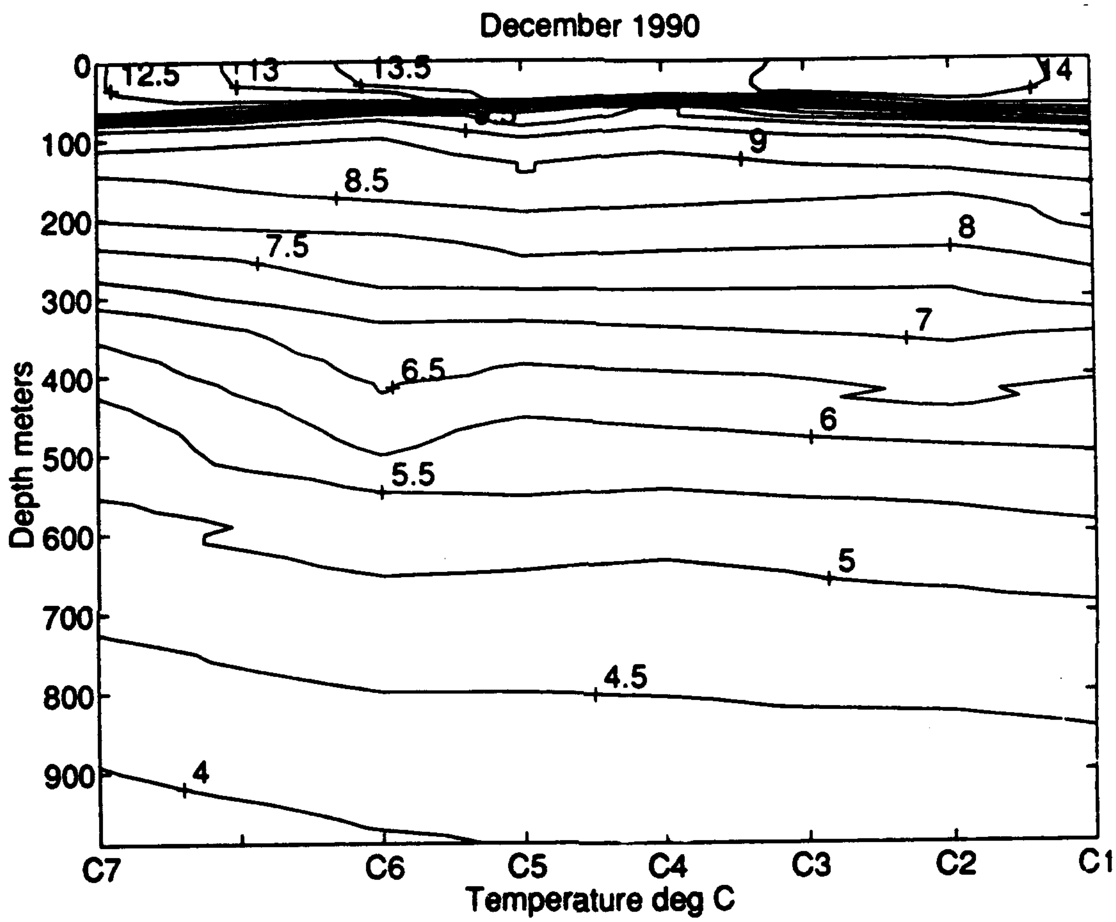

December 1990
Depth meters
Temperature deg C
0
100
200
300
400
500
600
700
800
900
C7
C6
C5
C4
C3
C2
C1
12.5
13
13.5
14
9
8.5
8
7.5
7
6.5
6
5.5
5
4.5
4

APPENDIX D. PEGASUS DATA

PEGASUS data are presented for each cruise period. The current stick vector plots show velocity data averaged in bins from 0-50 m, 50-100 m, 100-250 m, and 250-500 m. When currents along POST are extremely deep, a 500-1000 m interval is also included. PEGASUS stations are not labeled with a plus sign if data is not available during a particular cruise period.

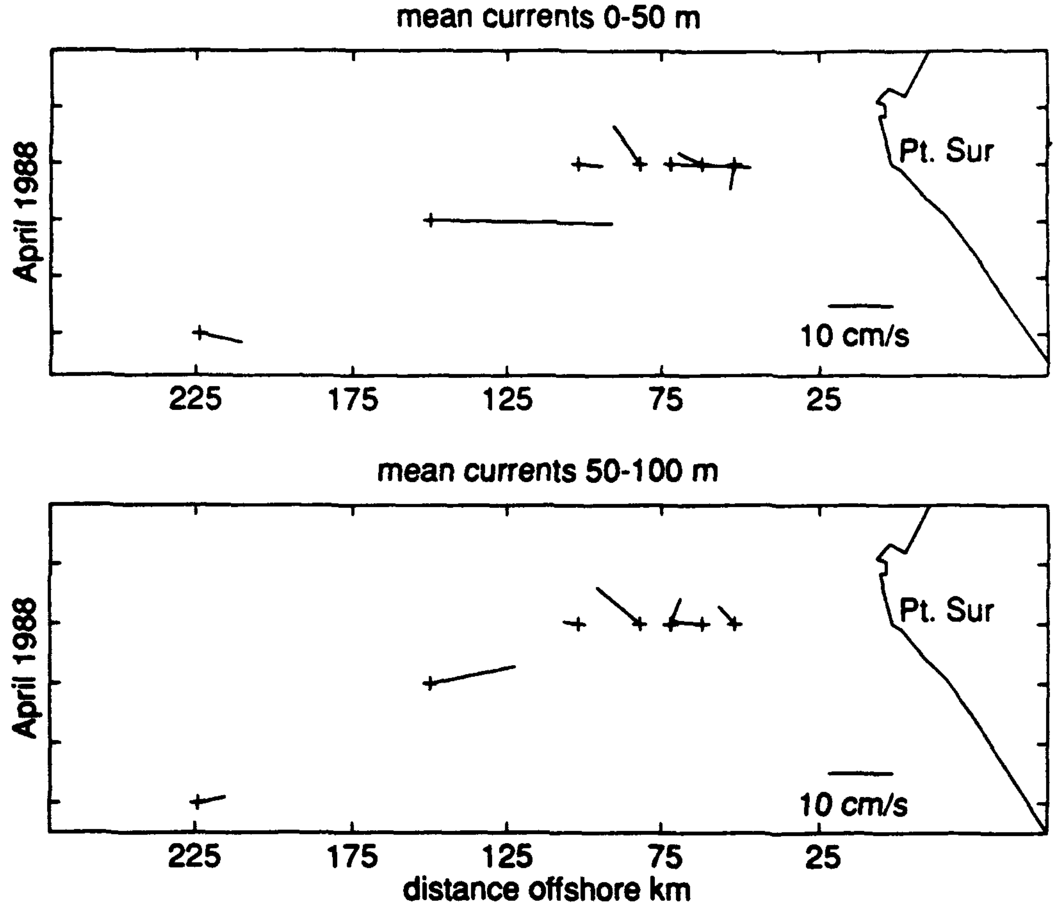

mean currents 0-50 m
April 1988
Pt. Sur
10 cm/s
225
175
125
75
25
mean currents 50-100 m
April 1988
Pt. Sur
10 cm/s
225
175
125
75
25
distance offshore km

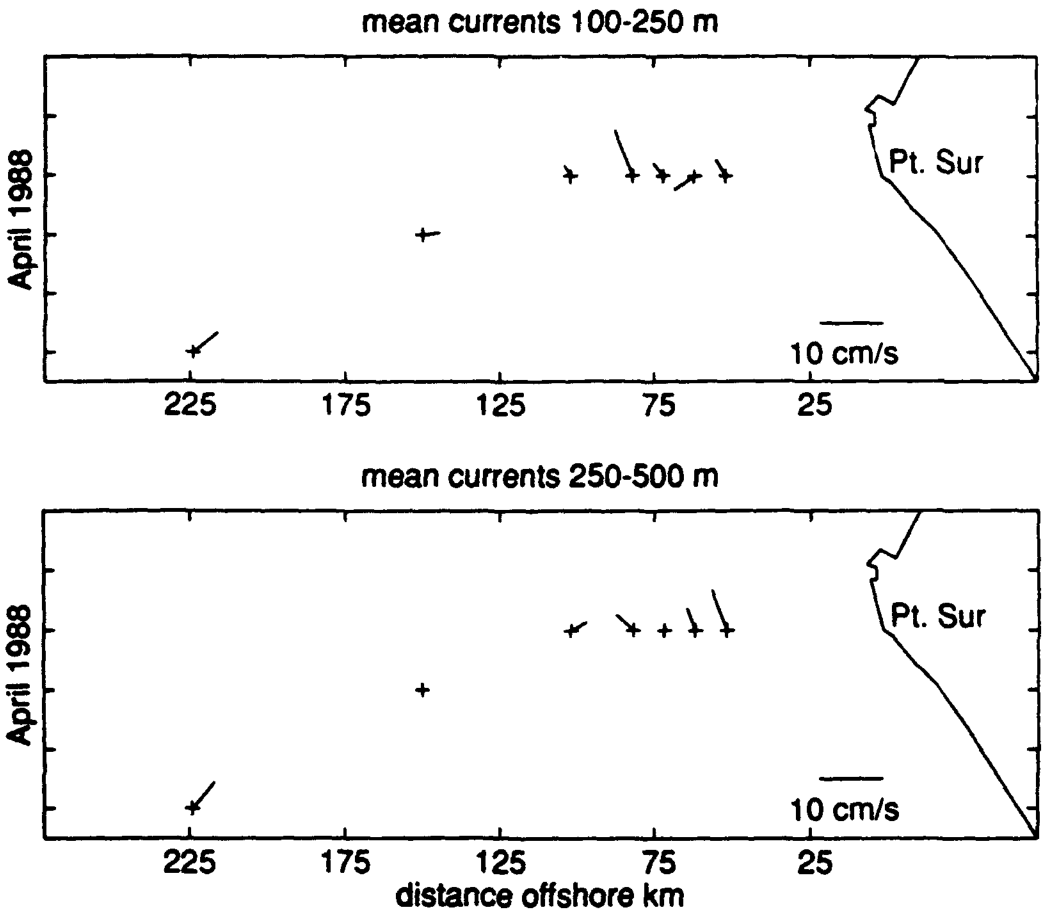
mean currents 100-250 m
April 1988
Pt. Sur
10 cm/s
225
175
125
75
25
mean currents 250-500 m
April 1988
Pt. Sur
10 cm/s
225
175
125
75
25
distance offshore km

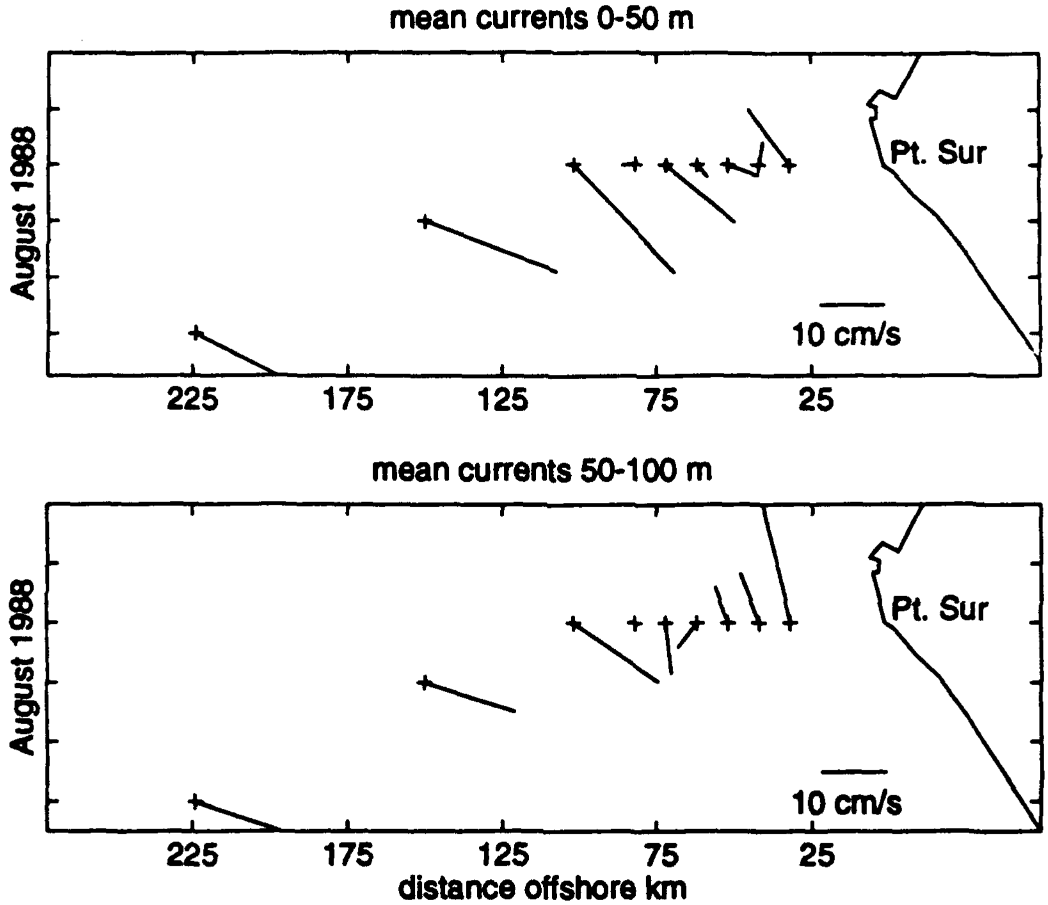
mean currents 0-50 m
August 1988
Pt. Sur
10 cm/s
225
175
125
75
25
mean currents 50-100 m
August 1988
Pt. Sur
10 cm/s
225
175
125
75
25
distance offshore km

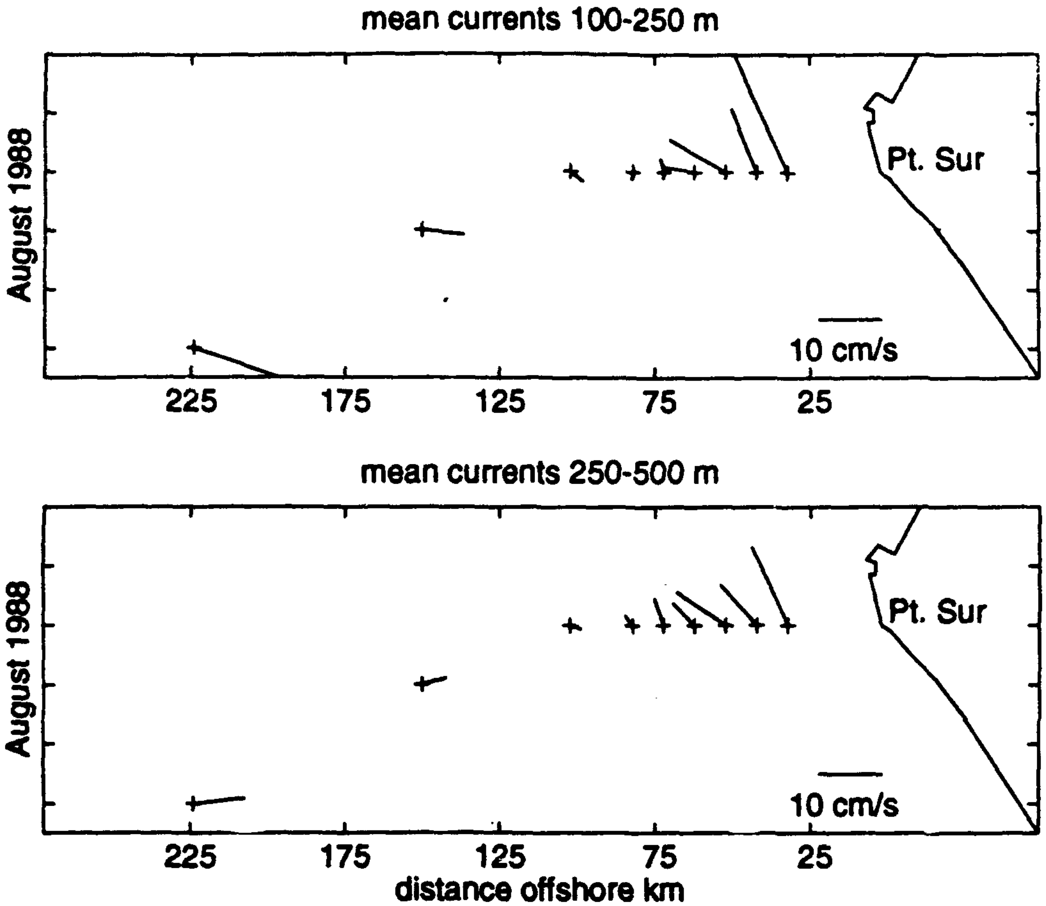
mean currents 100-250 m
August 1988
Pt. Sur
10 cm/s
225
175
125
75
25
mean currents 250-500 m
August 1988
Pt. Sur
10 cm/s
225
175
125
75
25
distance offshore km

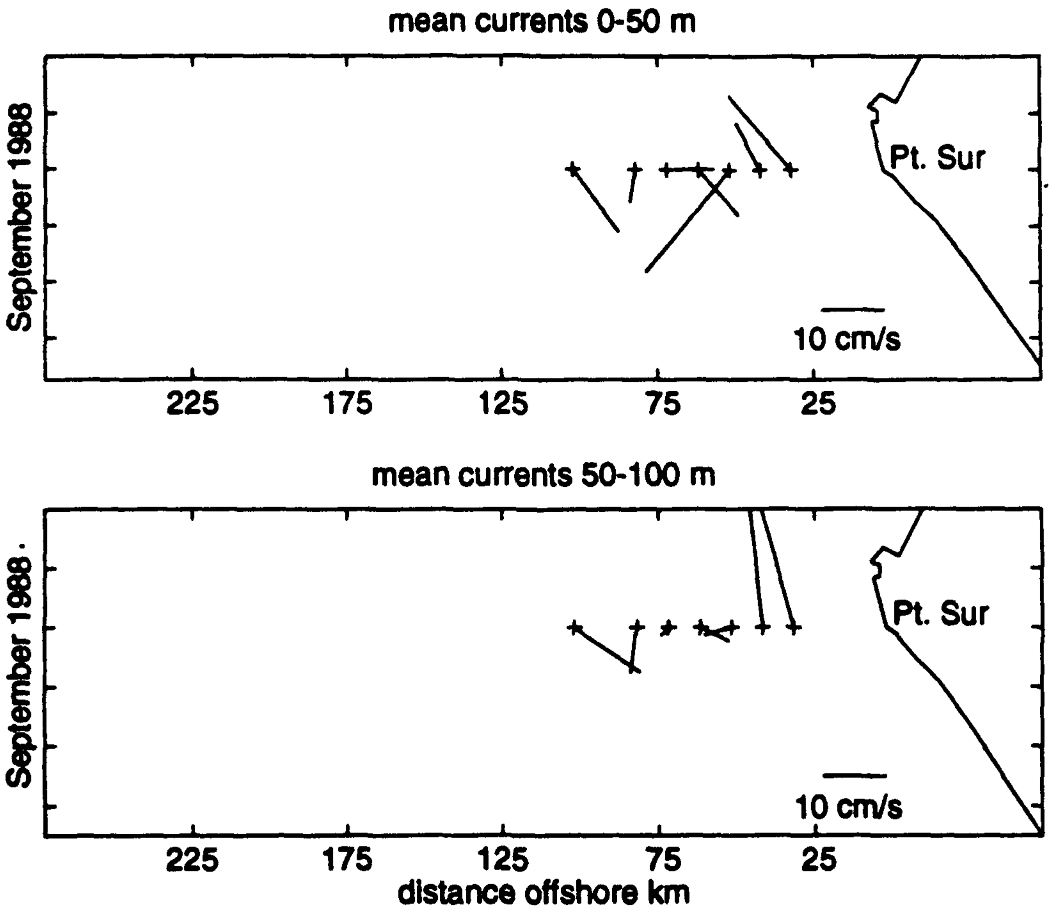
mean currents 0-50 m
September 1988
Pt. Sur
10 cm/s
225
175
125
75
25
mean currents 50-100 m
September 1988
Pt. Sur
10 cm/s
225
175
125
75
25
distance offshore km

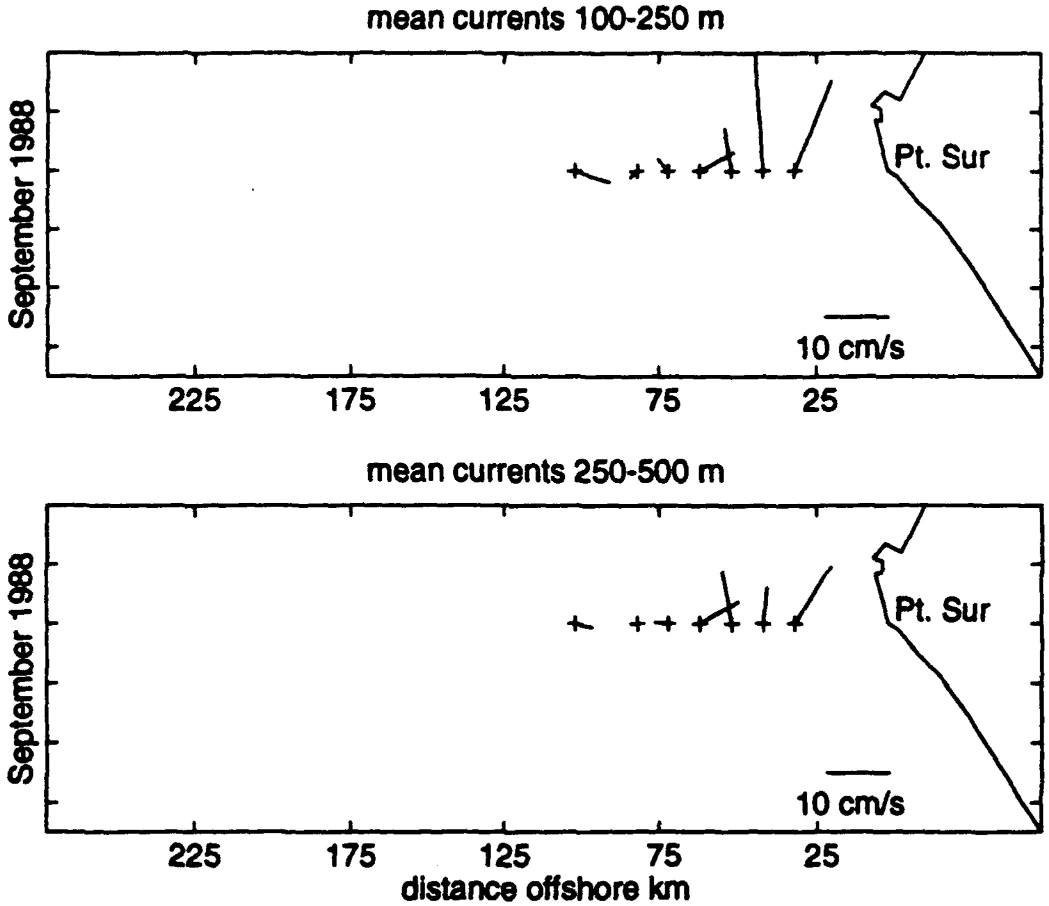
mean currents 100-250 m
September 1988
Pt. Sur
10 cm/s
225
175
125
75
25
mean currents 250-500 m
September 1988
Pt. Sur
10 cm/s
225
175
125
75
25
distance offshore km

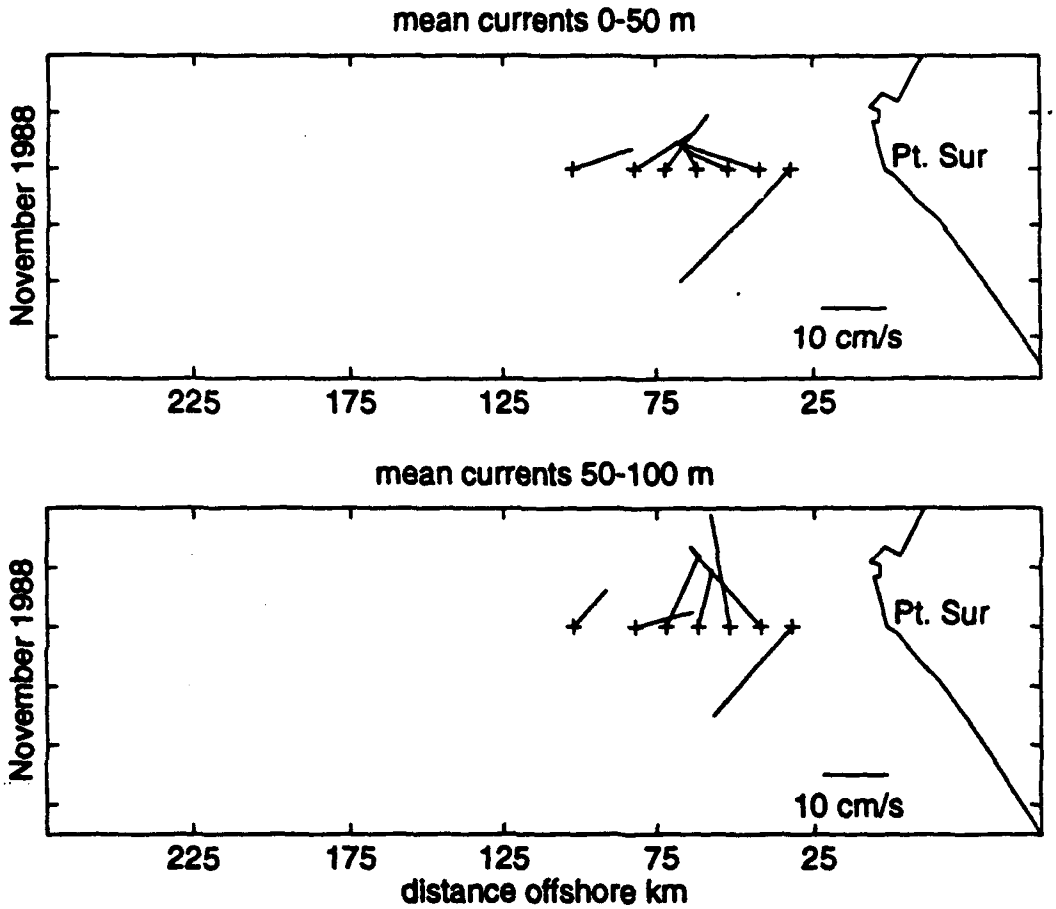
mean currents 0-50 m
November 1988
Pt. Sur
10 cm/s
225
175
125
75
25
mean currents 50-100 m
November 1988
Pt. Sur
10 cm/s
225
175
125
75
25
distance offshore km

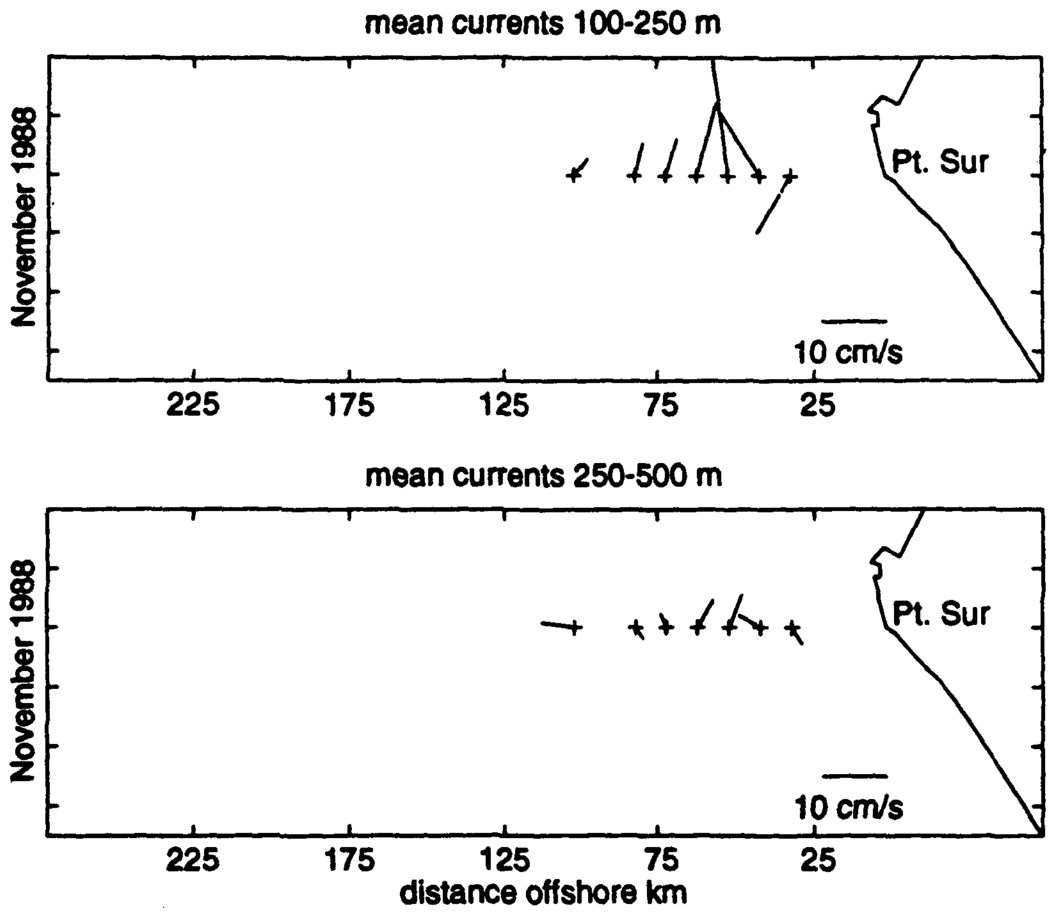
mean currents 100-250 m
November 1988
Pt. Sur
10 cm/s
225
175
125
75
25
mean currents 250-500 m
November 1988
Pt. Sur
10 cm/s
225
175
125
75
25
distance offshore km

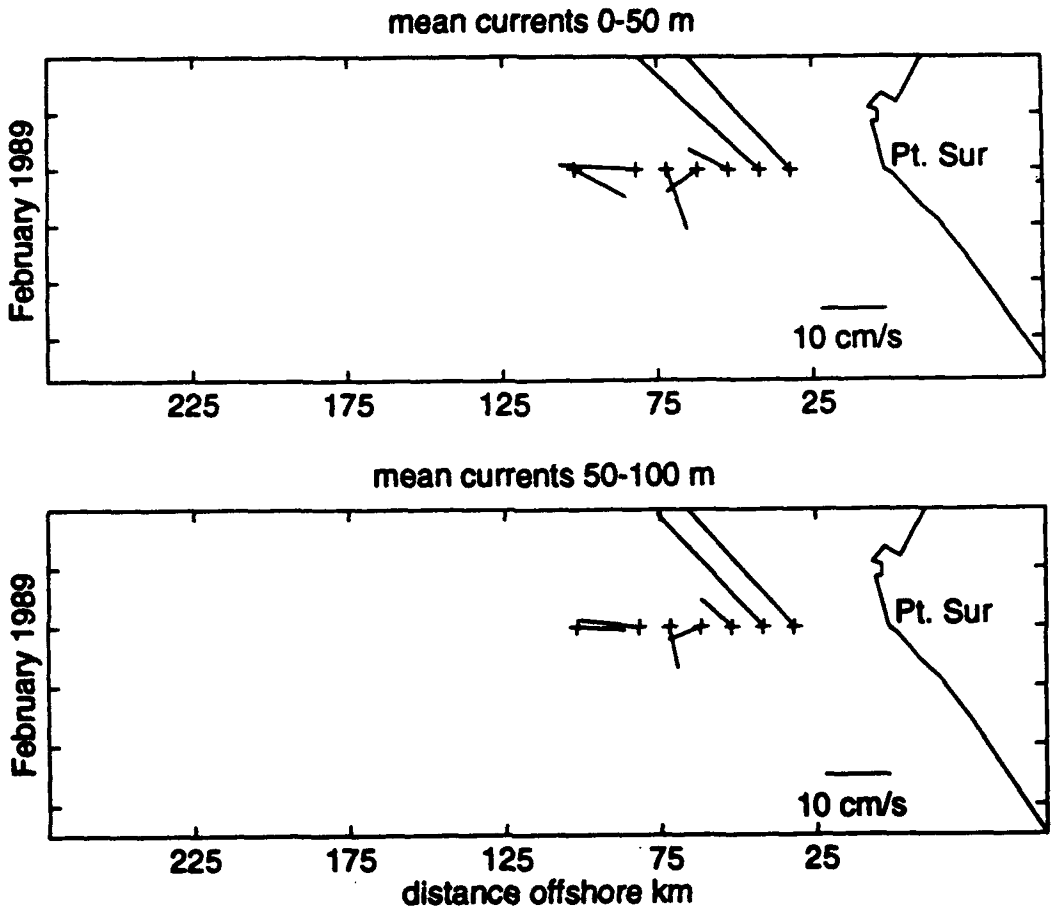
mean currents 0-50 m
February 1989
Pt. Sur
10 cm/s
225
175
125
75
25
mean currents 50-100 m
February 1989
Pt. Sur
10 cm/s
225
175
125
75
25
distance offshore km

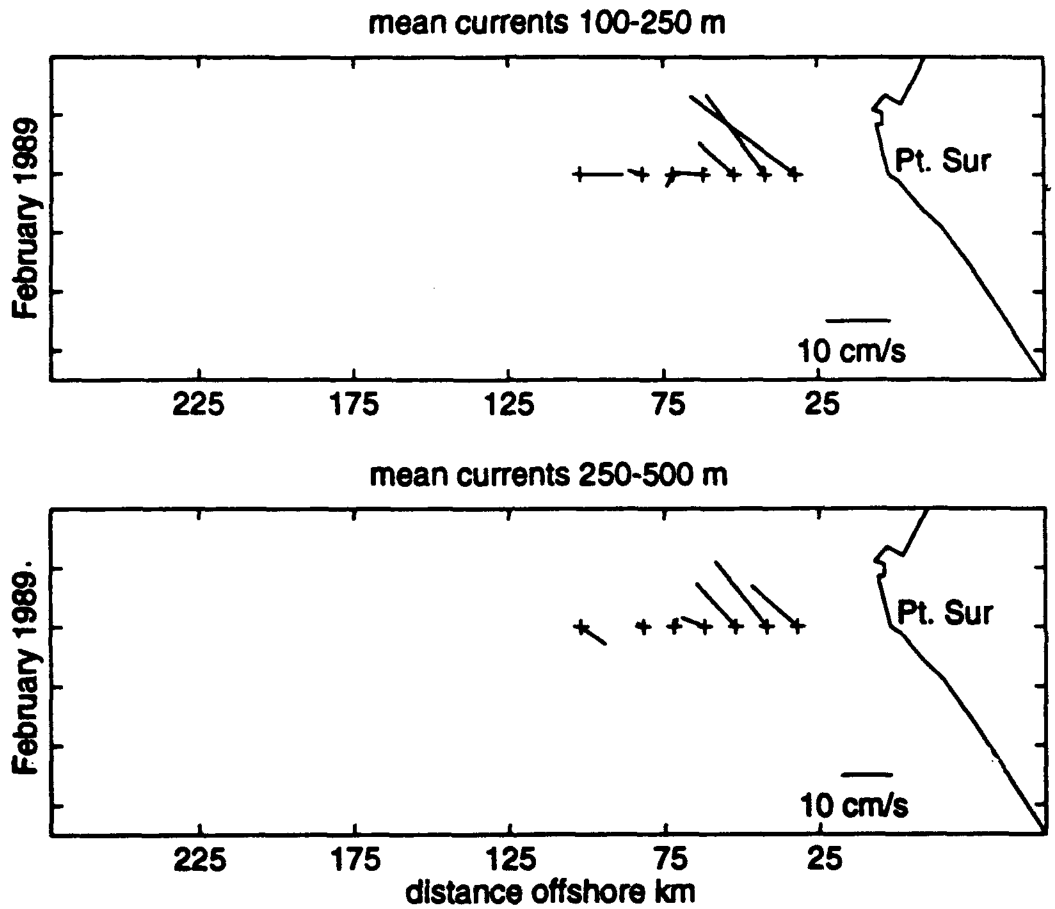

mean currents 100-250 m
February 1989
Pt. Sur
10 cm/s
225
175
125
75
25
mean currents 250-500 m
February 1989
Pt. Sur
10 cm/s
225
175
125
75
25
distance offshore km

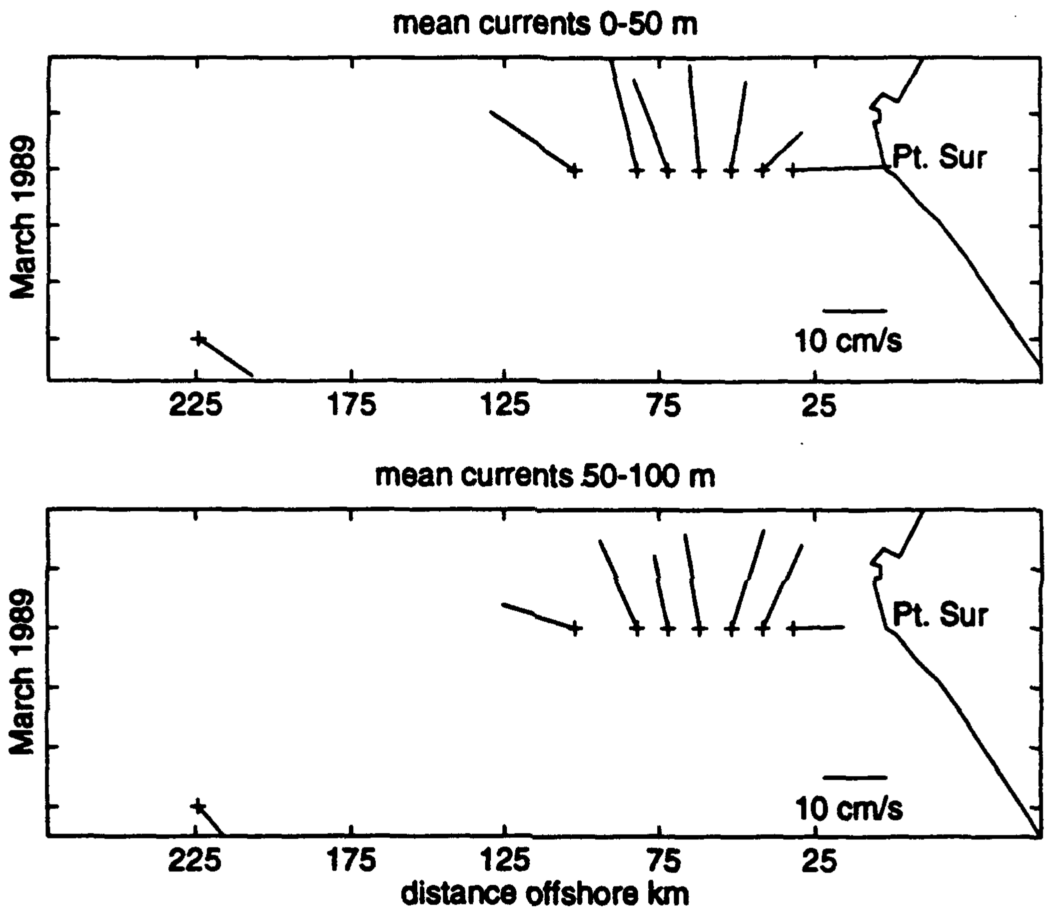
mean currents 0-50 m
March 1989
Pt. Sur
10 cm/s
225
175
125
75
25
mean currents 50-100 m
March 1989
Pt. Sur
10 cm/s
225
175
125
75
25
distance offshore km

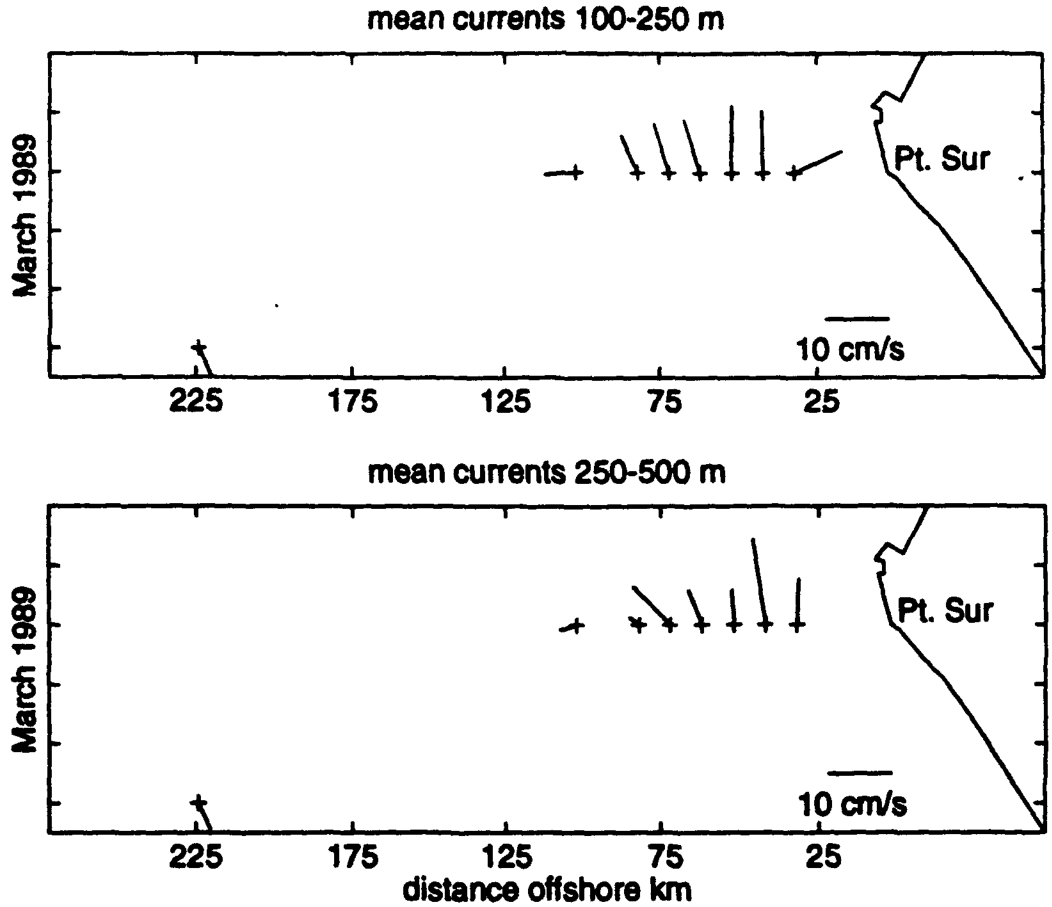
mean currents 100-250 m
March 1989
Pt. Sur
10 cm/s
225
175
125
75
25
mean currents 250-500 m
March 1989
Pt. Sur
10 cm/s
225
175
125
75
25
distance offshore km

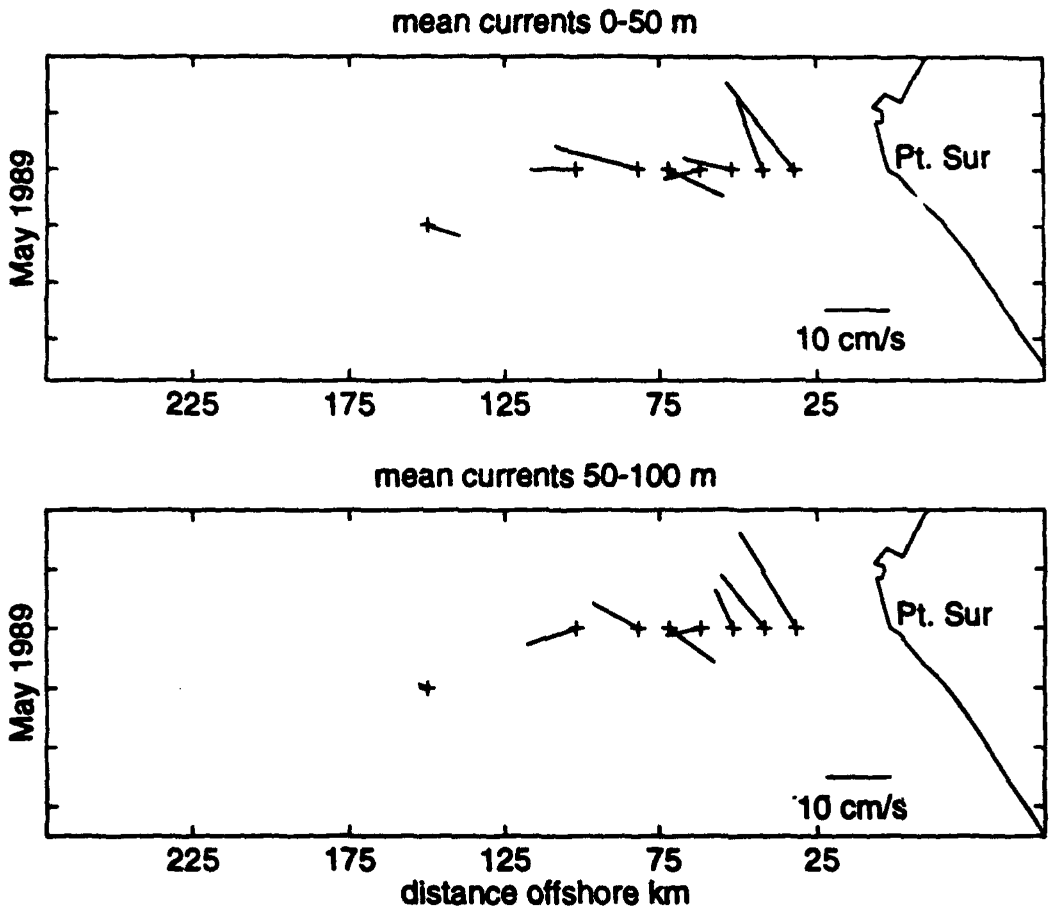
mean currents 0-50 m
May 1989
Pt. Sur
10 cm/s
225
175
125
75
25
mean currents 50-100 m
May 1989
Pt. Sur
10 cm/s
225
175
125
75
25
distance offshore km

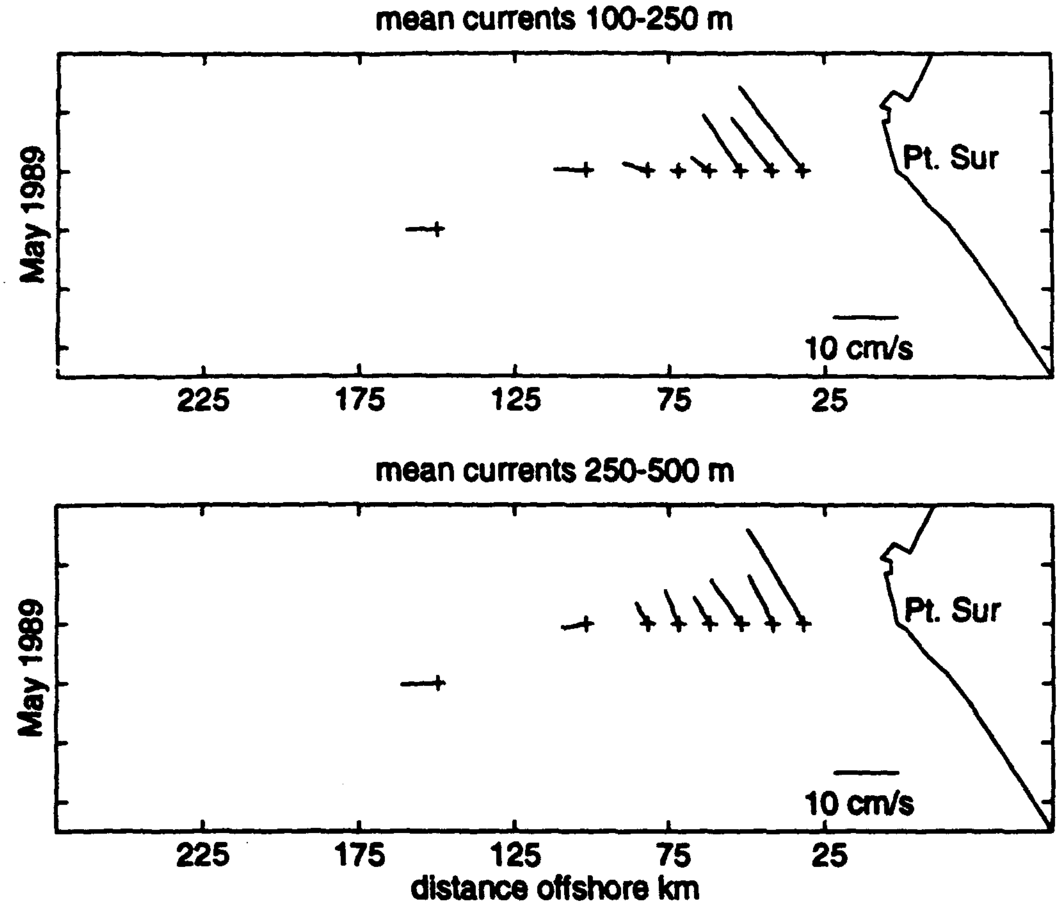
mean currents 100-250 m
May 1989
Pt. Sur
10 cm/s
225
175
125
75
25
mean currents 250-500 m
May 1989
Pt. Sur
10 cm/s
225
175
125
75
25
distance offshore km

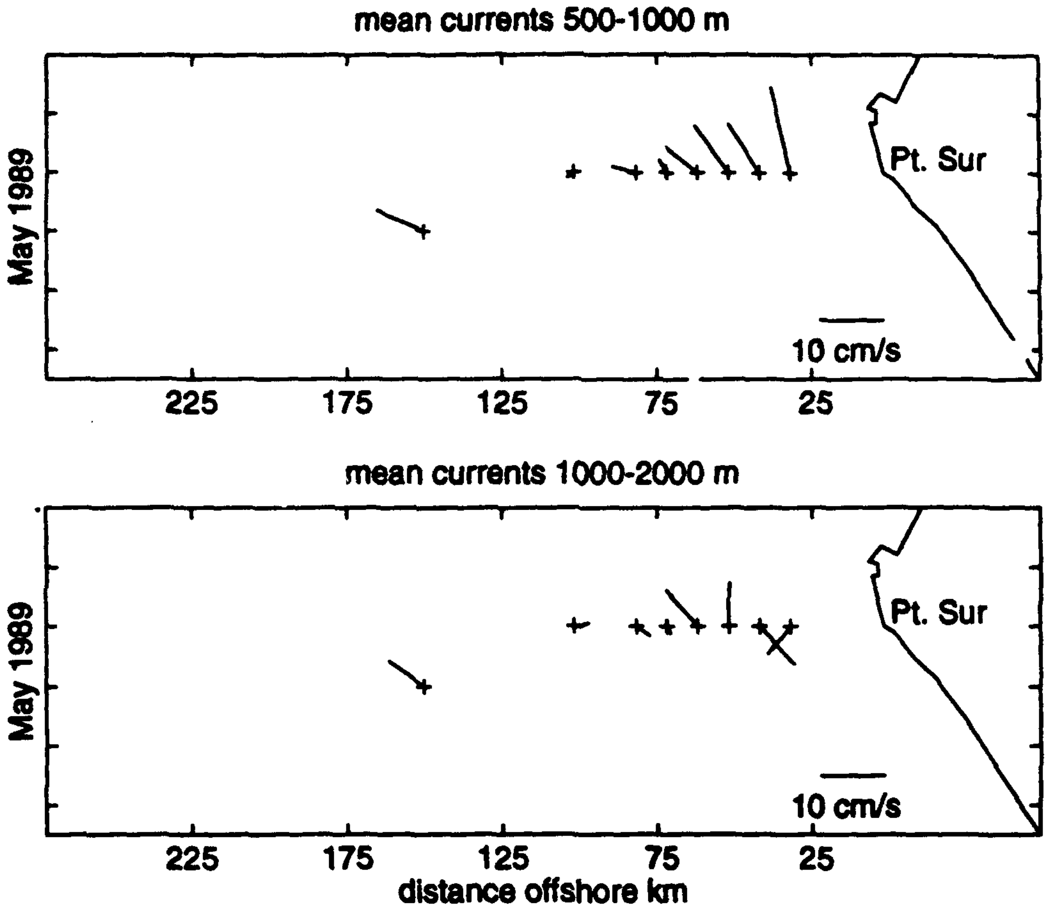

mean currents 500-1000 m
May 1989
Pt. Sur
10 cm/s
225
175
125
75
25
mean currents 1000-2000 m
May 1989
Pt. Sur
10 cm/s
225
175
125
75
25
distance offshore km

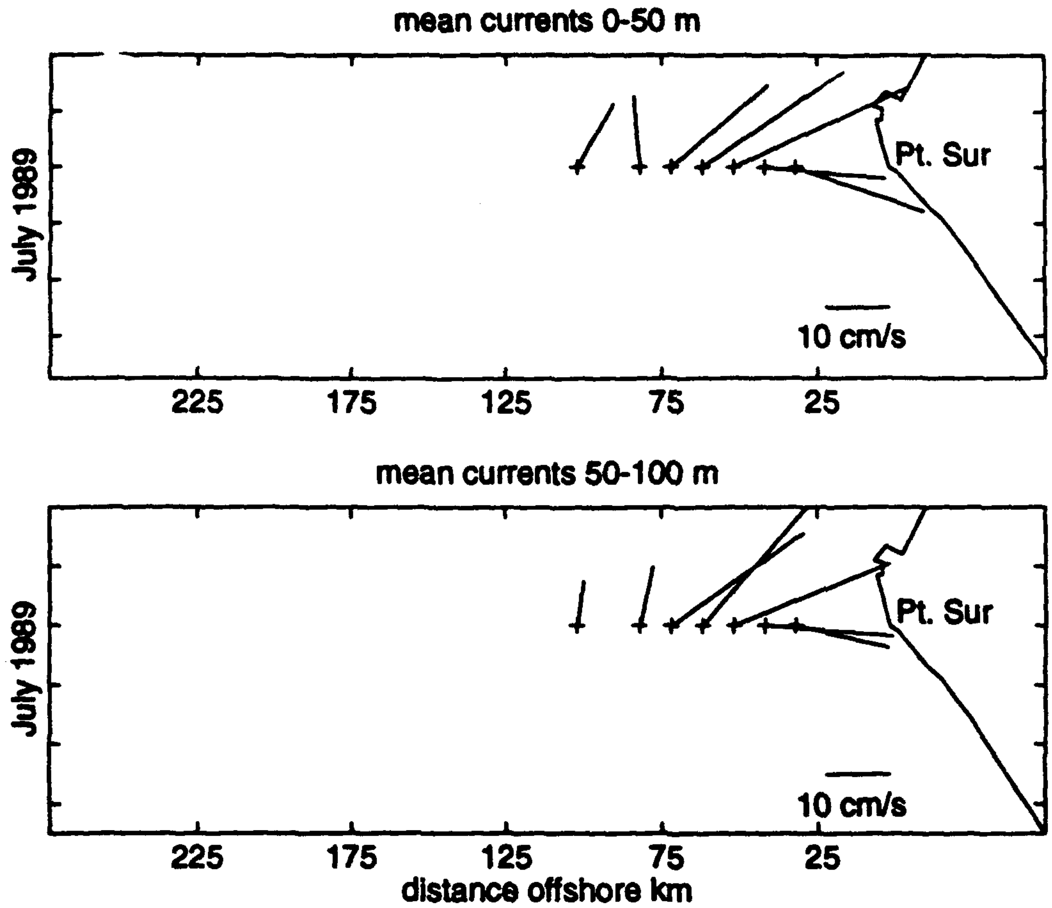
mean currents 0-50 m
July 1989
Pt. Sur
10 cm/s
225
175
125
75
25
mean currents 50-100 m
July 1989
Pt. Sur
10 cm/s
225
175
125
75
25
distance offshore km

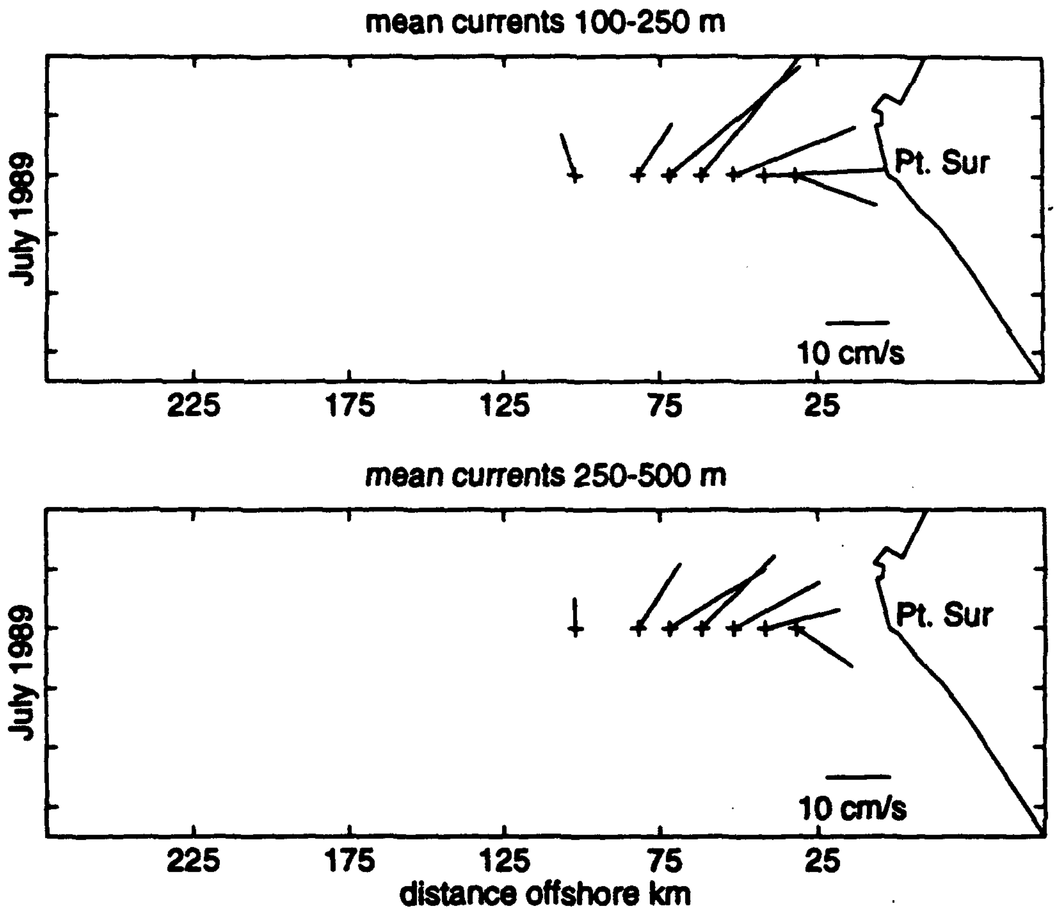

mean currents 100-250 m
July 1989
Pt. Sur
10 cm/s
225
175
125
75
25
mean currents 250-500 m
July 1989
Pt. Sur
10 cm/s
225
175
125
75
25
distance offshore km

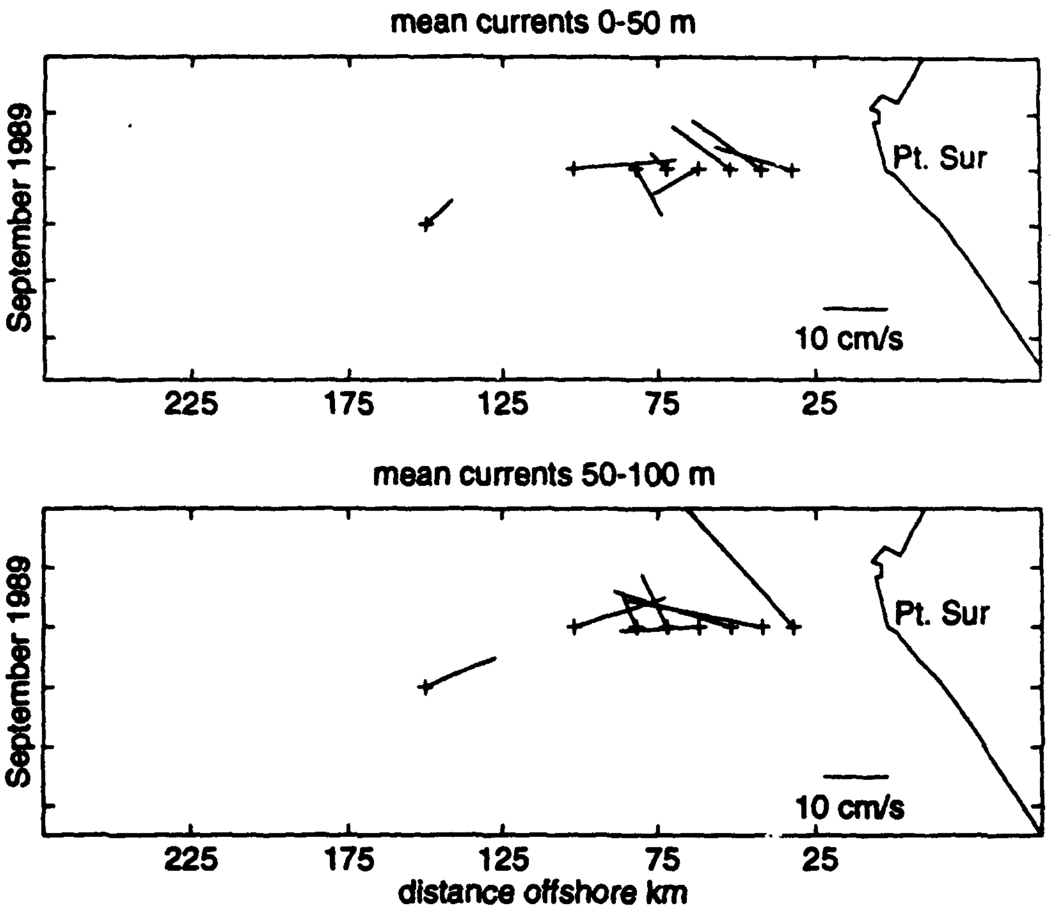
mean currents 0-50 m
September 1989
Pt. Sur
10 cm/s
225
175
125
75
25
mean currents 50-100 m
September 1989
Pt. Sur
10 cm/s
225
175
125
75
25
distance offshore km

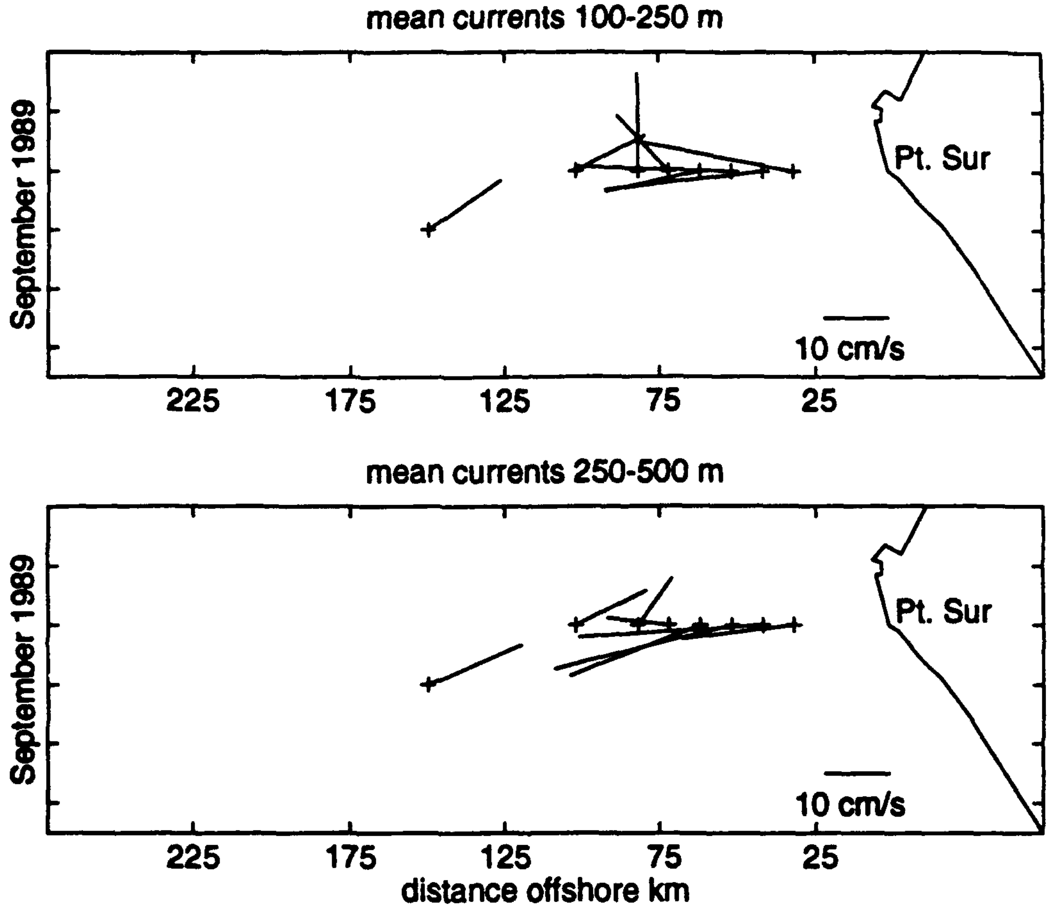

mean currents 100-250 m
September 1989
Pt. Sur
10 cm/s
225
175
125
75
25
mean currents 250-500 m
September 1989
Pt. Sur
10 cm/s
225
175
125
75
25
distance offshore km

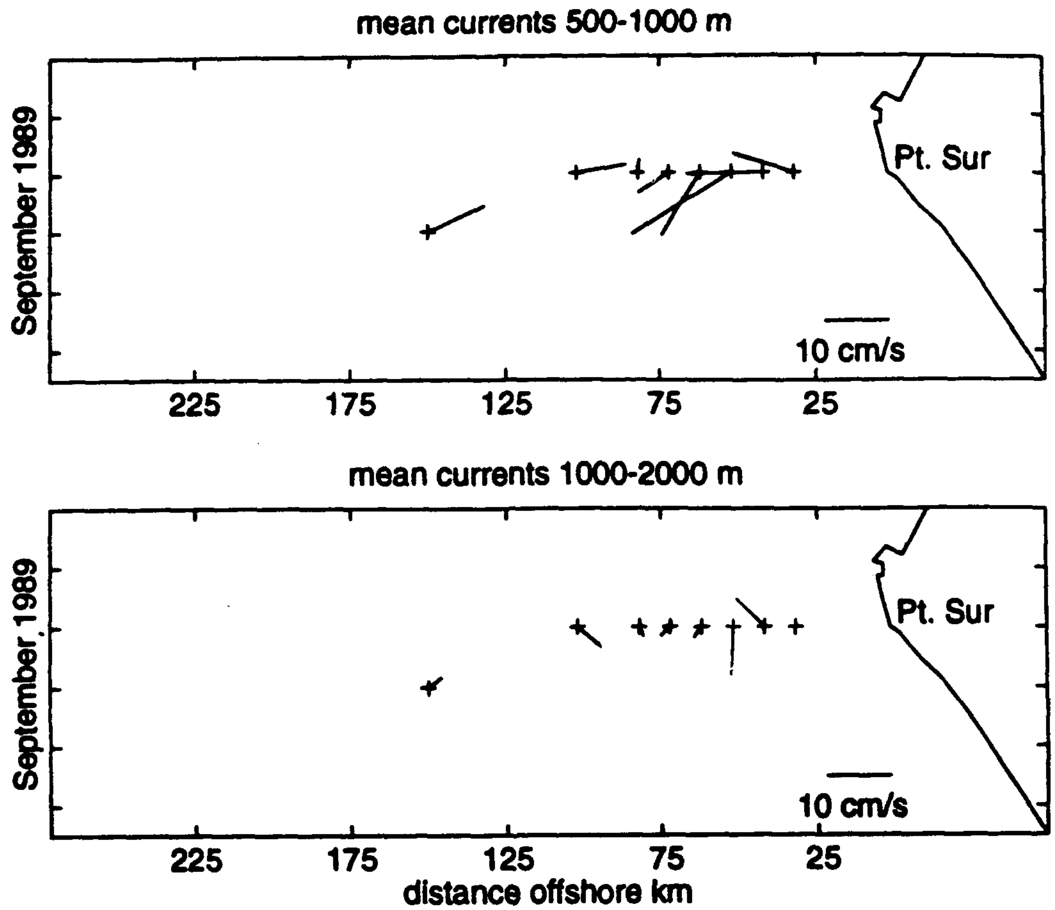
mean currents 500-1000 m
September 1989
Pt. Sur
10 cm/s
225
175
125
75
25
mean currents 1000-2000 m
September 1989
Pt. Sur
10 cm/s
225
175
125
75
25
distance offshore km

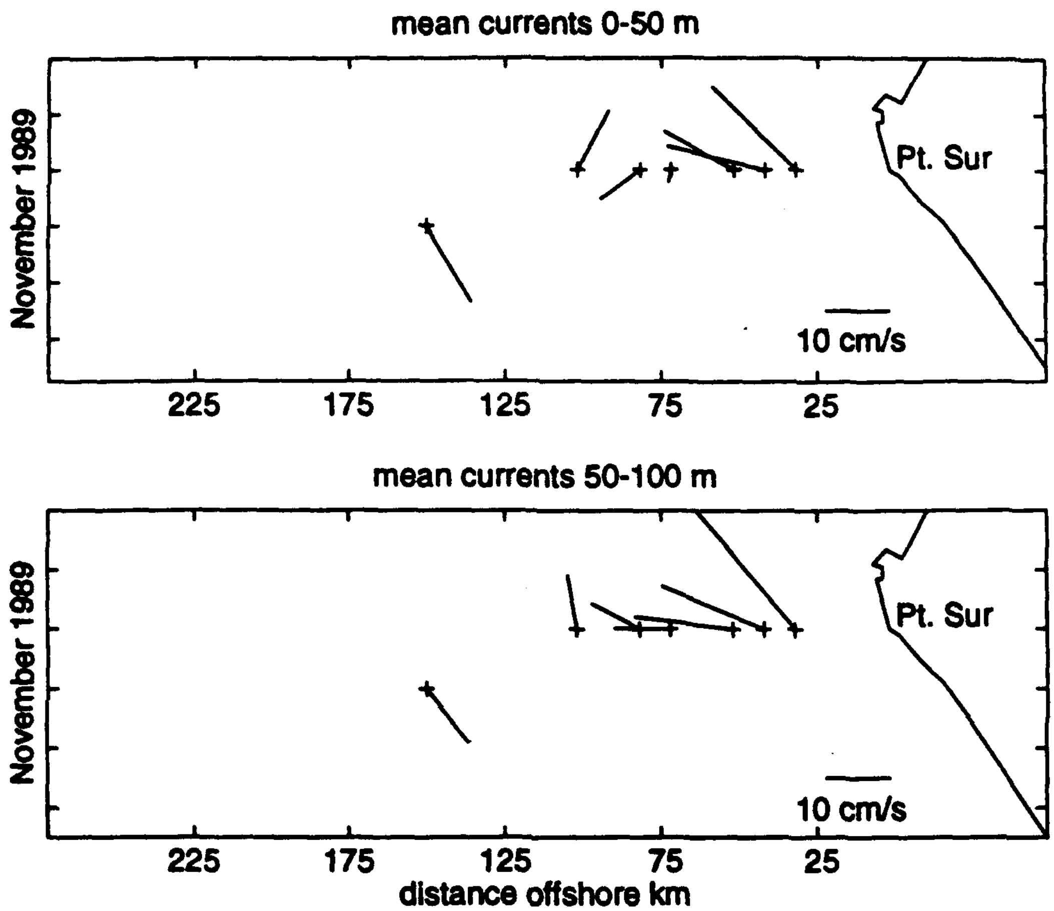
mean currents 0-50 m
November 1989
Pt. Sur
10 cm/s
225
175
125
75
25
mean currents 50-100 m
November 1989
Pt. Sur
10 cm/s
225
175
125
75
25
distance offshore km

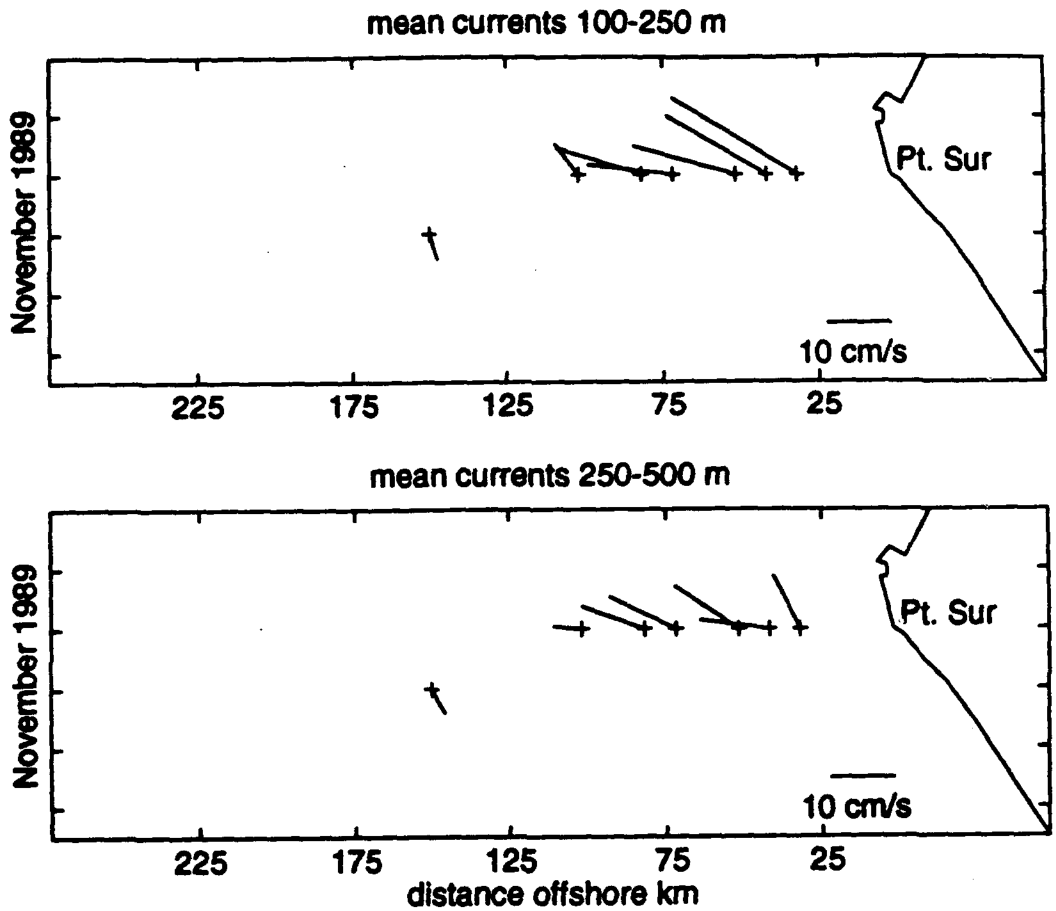
mean currents 100-250 m
November 1989
Pt. Sur
10 cm/s
225
175
125
75
25
mean currents 250-500 m
November 1989
Pt. Sur
10 cm/s
225
175
125
75
25
distance offshore km

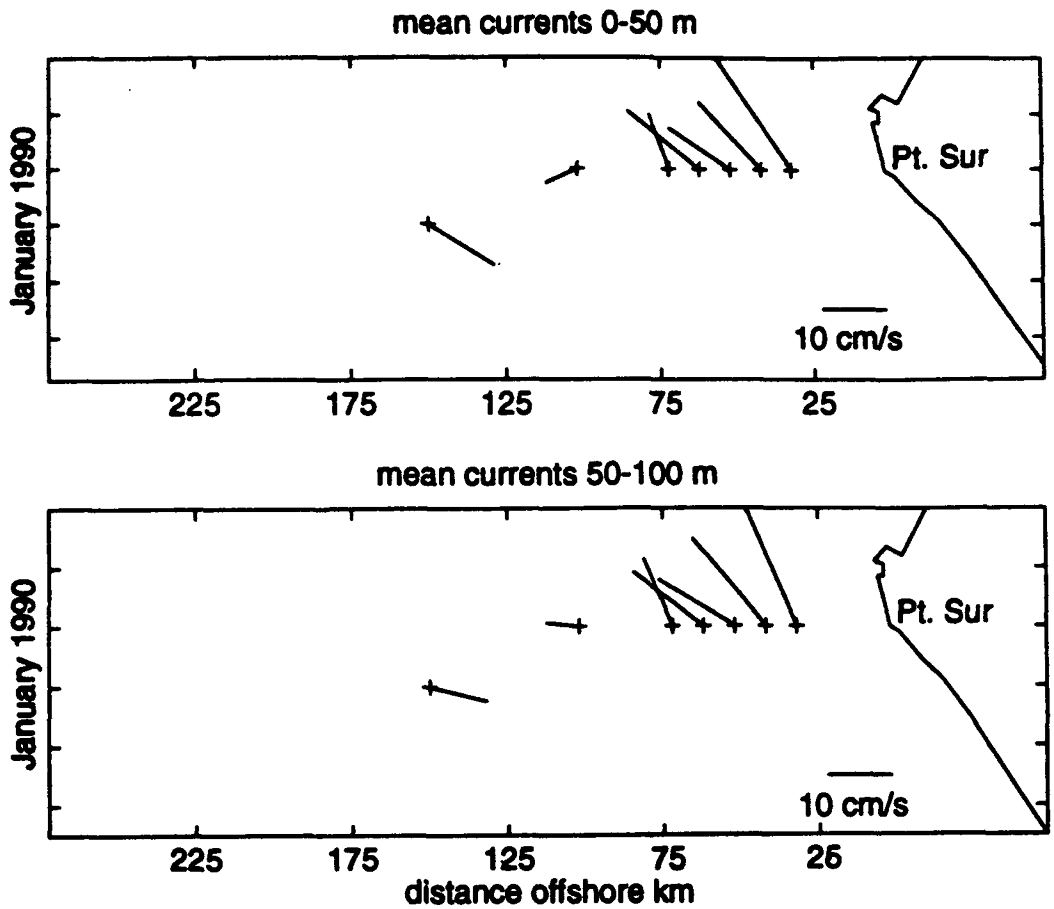

mean currents 0-50 m
January 1990
Pt. Sur
10 cm/s
225
175
125
75
25
mean currents 50-100 m
January 1990
Pt. Sur
10 cm/s
225
175
125
75
25
distance offshore km

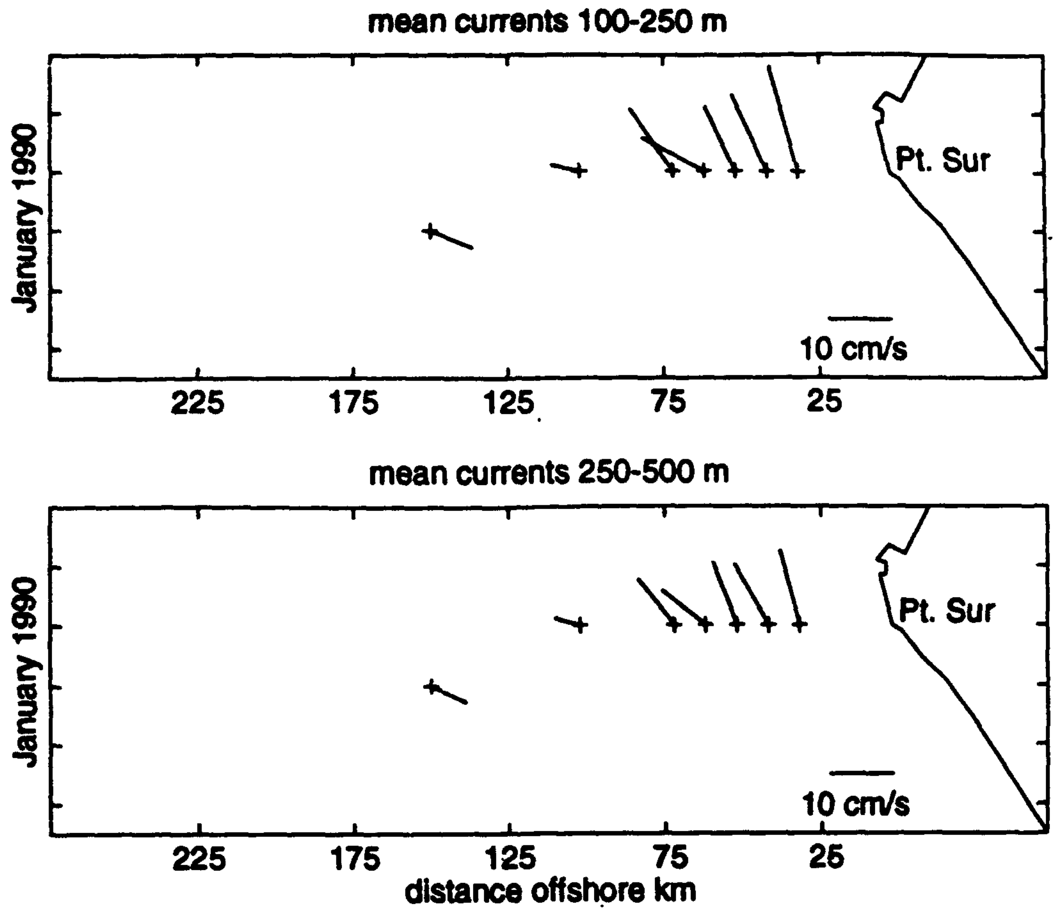
mean currents 100-250 m
January 1990
Pt. Sur
10 cm/s
225
175
125
75
25
mean currents 250-500 m
January 1990
Pt. Sur
10 cm/s
225
175
125
75
25
distance offshore km

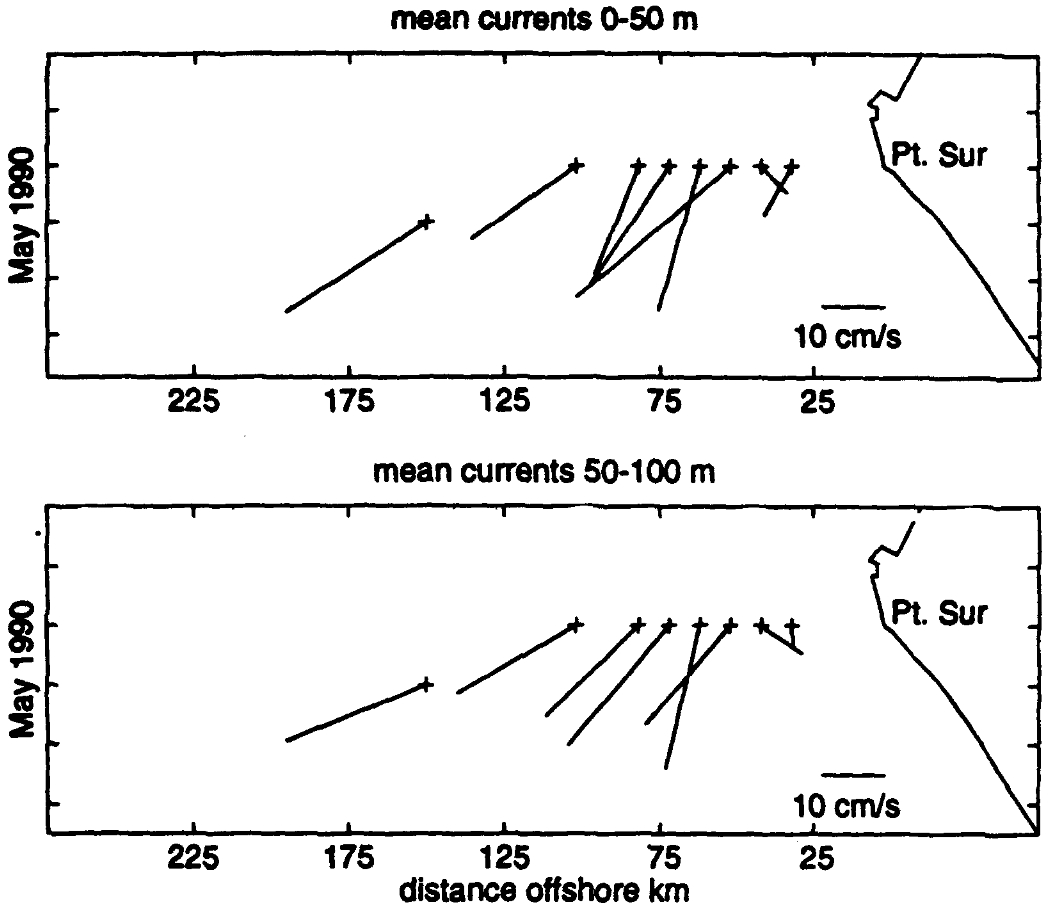
mean currents 0-50 m
May 1990
Pt. Sur
10 cm/s
225
175
125
75
25
mean currents 50-100 m
May 1990
Pt. Sur
10 cm/s
225
175
125
75
25
distance offshore km

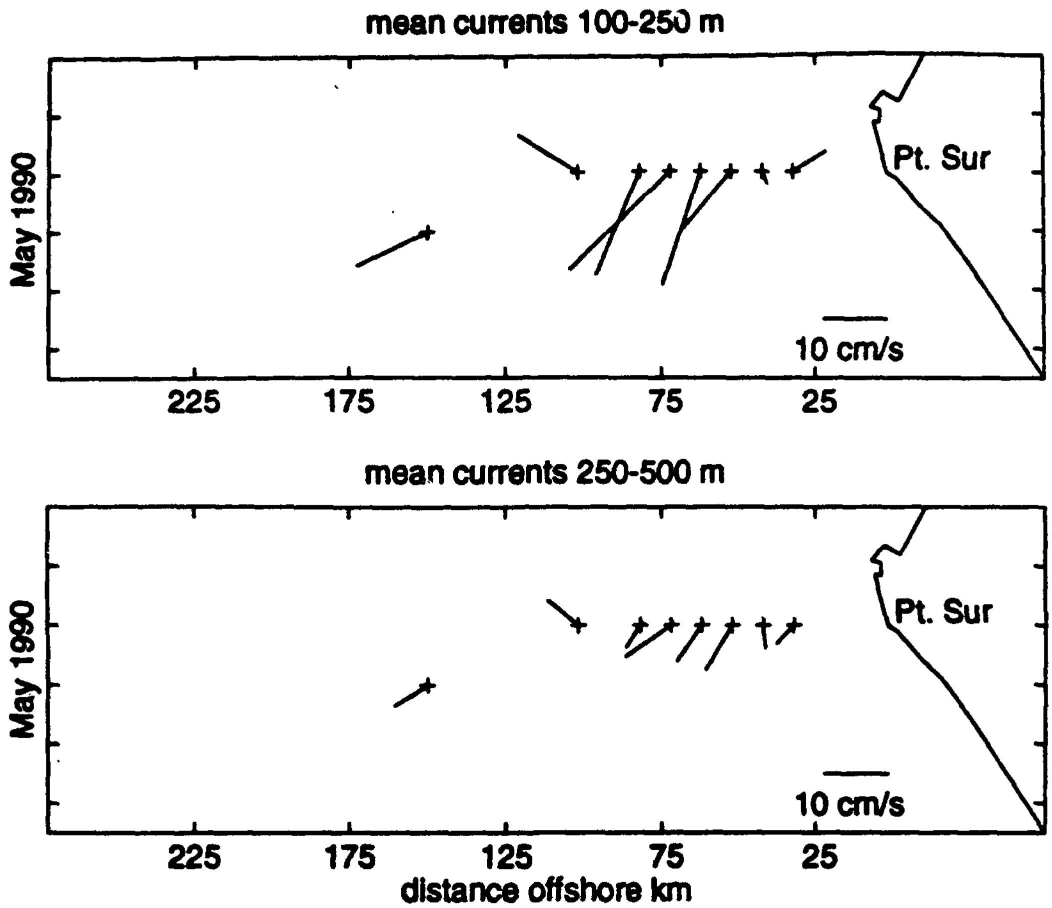
mean currents 100-250 m
Pt. Sur
10 cm/s
May 1990
225
175
125
75
25
mean currents 250-500 m
Pt. Sur
10 cm/s
May 1990
225
175
125
75
25
distance offshore km

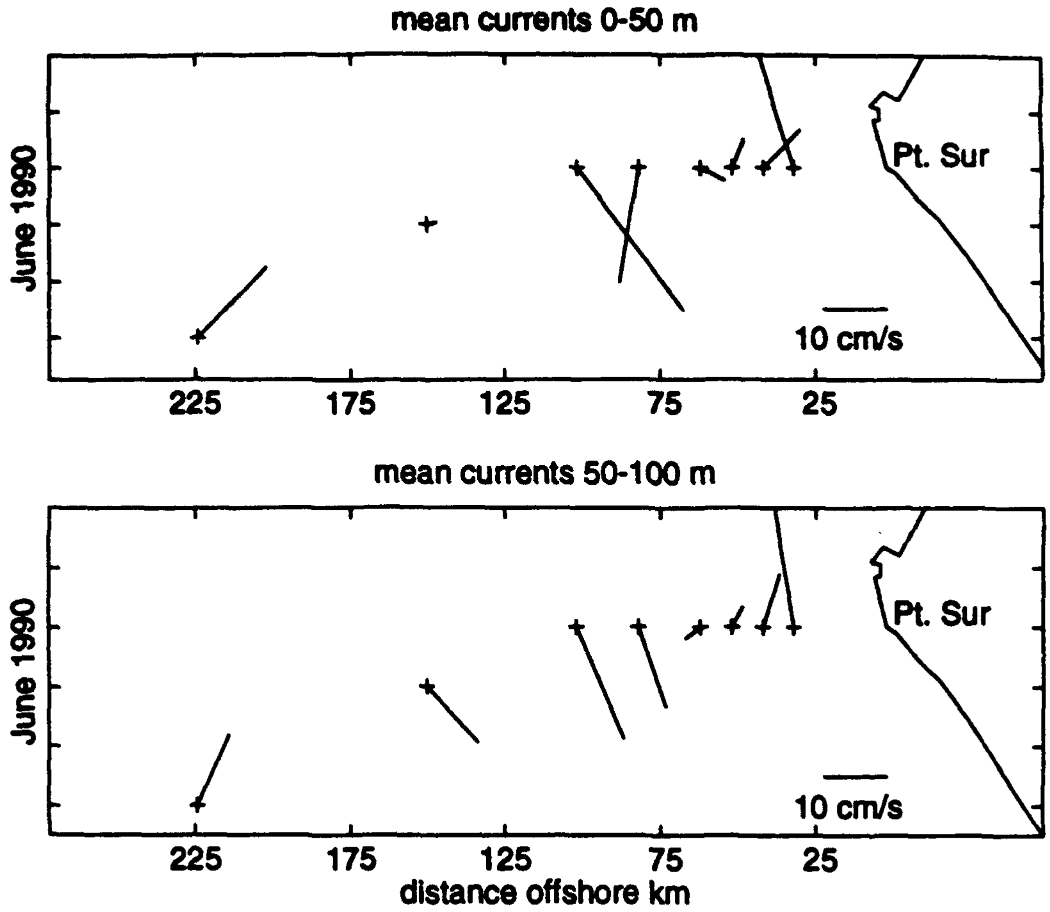

mean currents 0-50 m
June 1990
Pt. Sur
10 cm/s
225
175
125
75
25
mean currents 50-100 m
June 1990
Pt. Sur
10 cm/s
225
175
125
75
25
distance offshore km

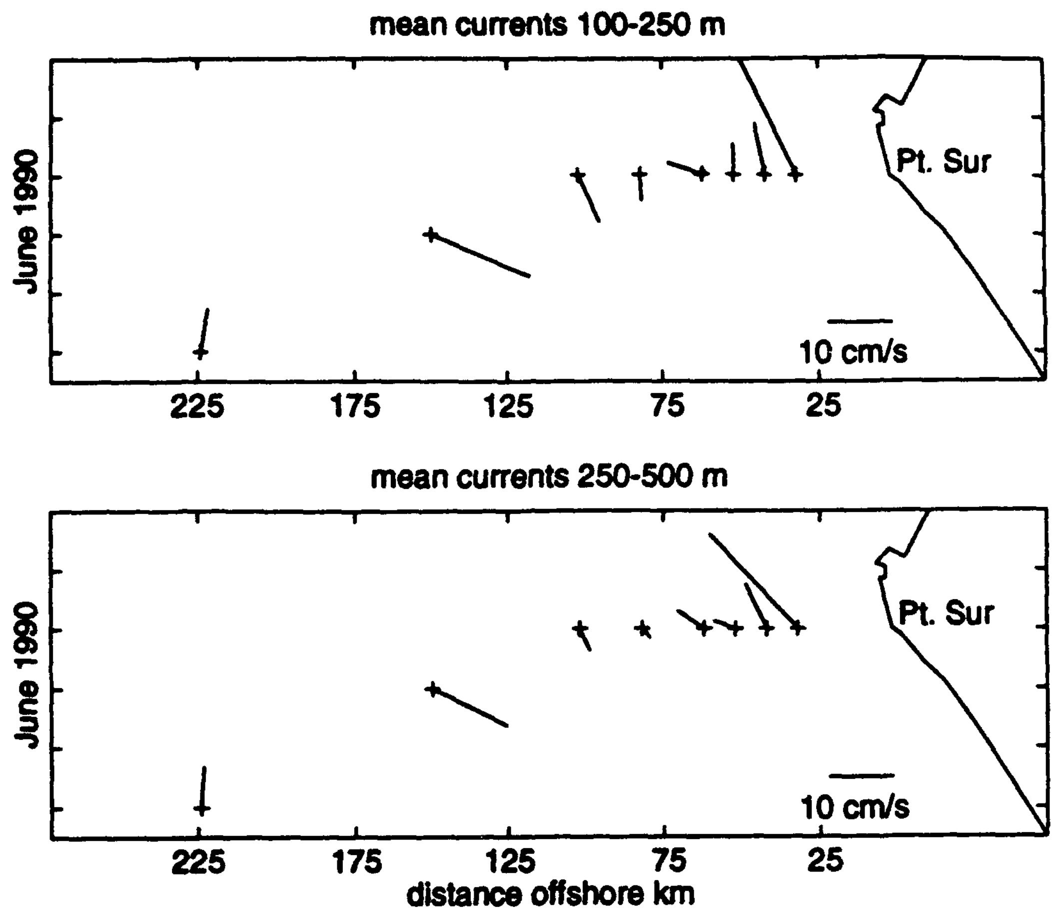

mean currents 100-250 m
June 1990
Pt. Sur
10 cm/s
225
175
125
75
25
mean currents 250-500 m
June 1990
Pt. Sur
10 cm/s
225
175
125
75
25
distance offshore km

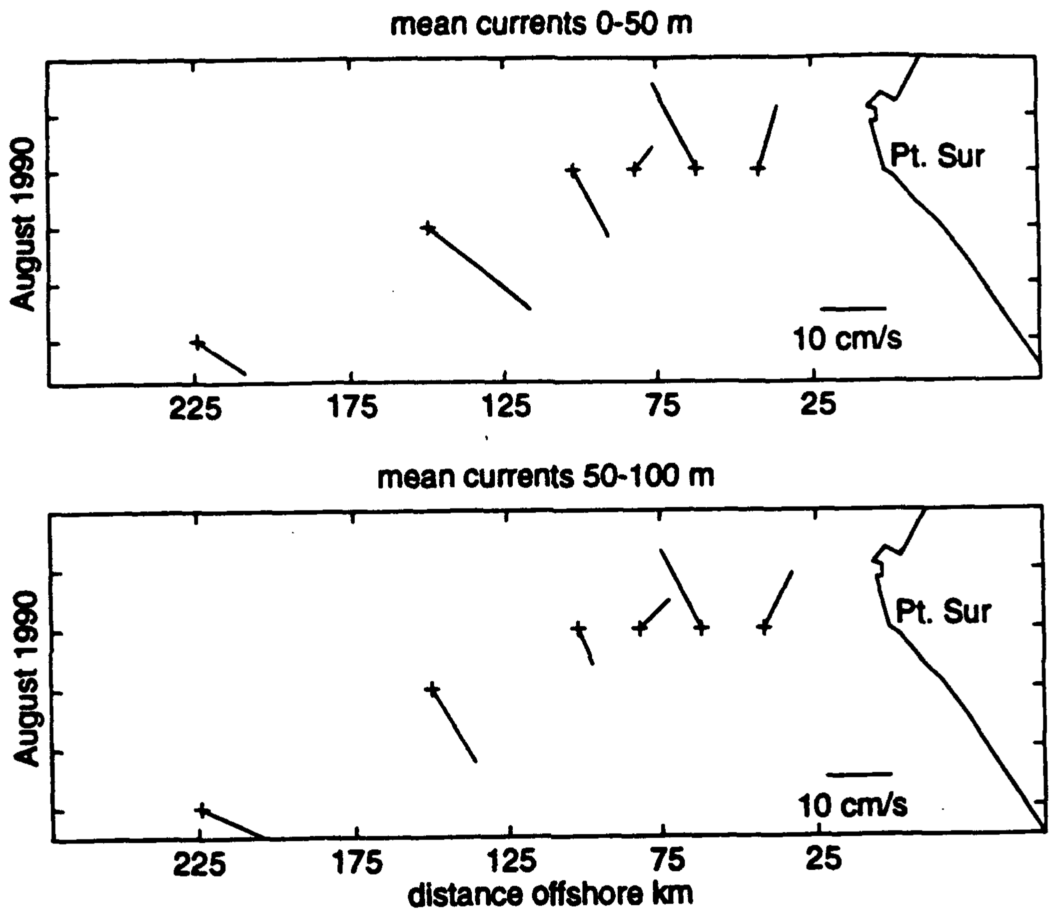
mean currents 0-50 m
August 1990
Pt. Sur
10 cm/s
225
175
125
75
25
mean currents 50-100 m
August 1990
Pt. Sur
10 cm/s
225
175
125
75
25
distance offshore km

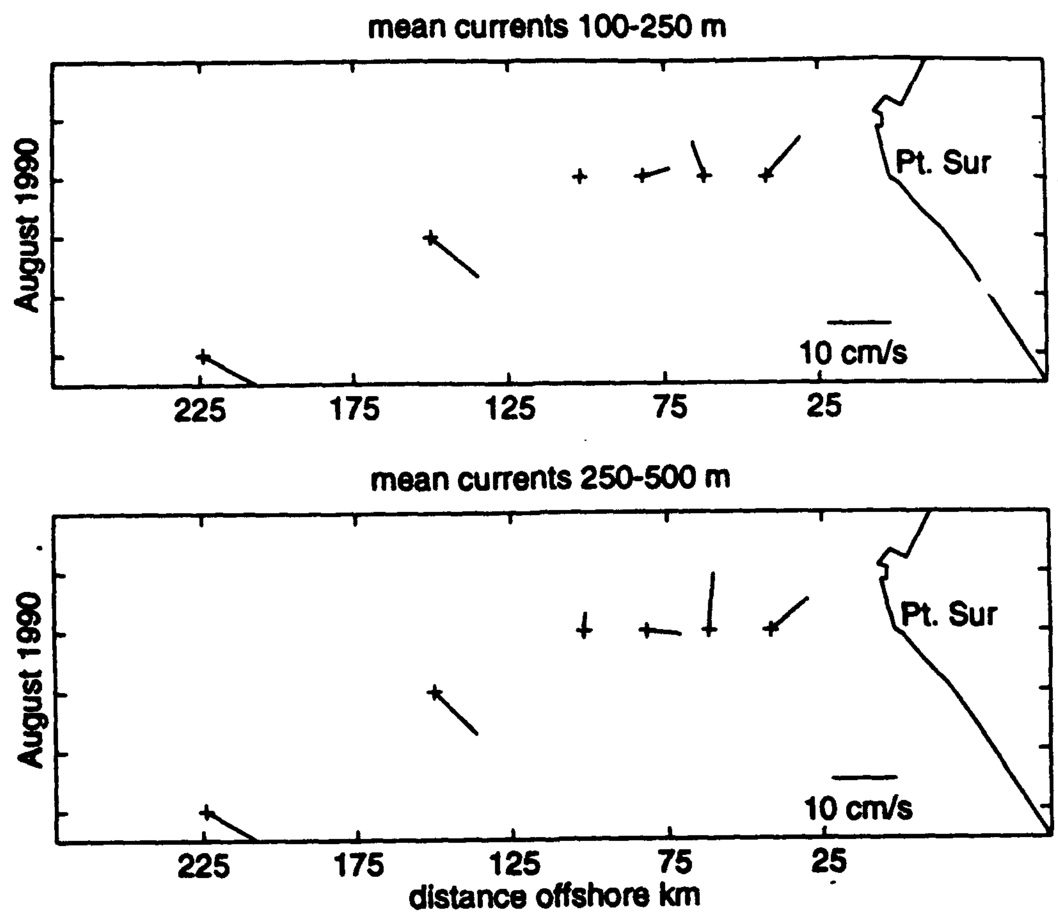
mean currents 100-250 m
August 1990
Pt. Sur
10 cm/s
225
175
125
75
25
mean currents 250-500 m
August 1990
Pt. Sur
10 cm/s
225
175
125
75
25
distance offshore km

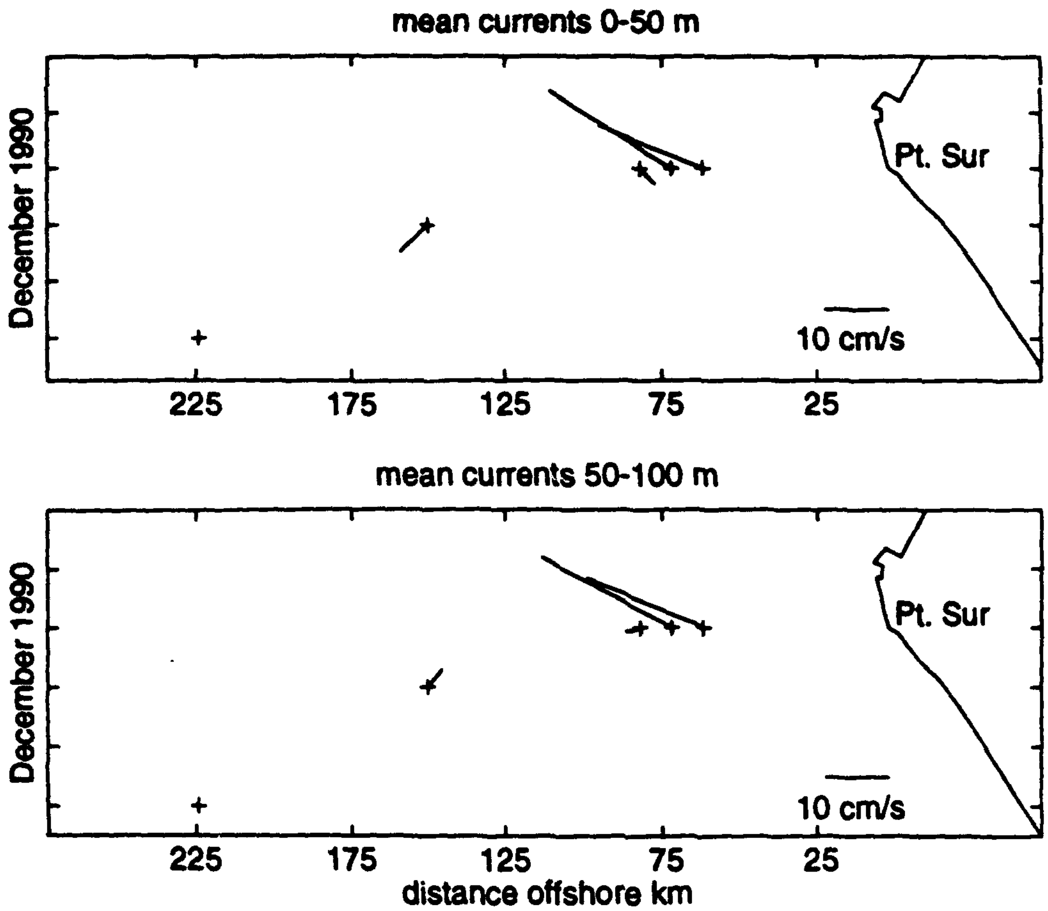
mean currents 0-50 m
December 1990
Pt. Sur
10 cm/s
225
175
125
75
25
mean currents 50-100 m
December 1990
Pt. Sur
10 cm/s
225
175
125
75
25
distance offshore km

REFERENCES

Berryman, P., 1989: Study of Currents along the Pt. Sur Transect in February 1989, Master's Thesis, Naval Postgraduate School, Monterey, California, 51pp.

Bray, N.A. and C.L. Greengrove, 1993: Circulation over the Shelf and Slope off Northern California, *J. Geophys. Res.*, **98**, 18119-18145.

Brink, K.H. and T.J. Cowles, 1991: The Coastal Transition Zone Program, *J. Geophys. Res.*, **96**, 14637-14647.

Brink, K.H., R.C. Beardsley, P.P. Niiler, M. Abbott, A. Huyer, S. Ramp, T. Stanton, and D. Stuart, 1991: Statistical Properties of Near-Surface Flow in the California Coastal Transition Zone, *J. Geophys. Res.*, **96**, 14693-14706.

Buckley, K.A., 1990: Measurements of Ocean Currents across the Continental Margin off Pt. Sur, California, during January, 1990, Master's Thesis, Naval Postgraduate school, Monterey, California, 78 pp.

Chelton, D.B., 1984: Seasonal Variability of Alongshore Geostrophic Velocity off Central California, *J. Geophys. Res.*, **89**, 3473-3486.

Chelton, D.B., A.W. Bratkovich, R.L. Bernstein, and P.M. Kosro, 1988: Poleward Flow off Central California during the Spring and Summer of 1981 and 1984, *J. Geophys. Res.*, **93**, 10604-10620.

Denbo, D.W. and J.S. Allen, 1984: Rotary Empirical Orthogonal Analysis of Currents near the Oregon Coast, *J. Phys. Oceanogr.*, **14**, 35-46.

Garfield, T. and Rago T., 1993: The Naval Postgraduate School PEGASUS Processing Routines, unpublished manuscript.

Hardy, D.M., 1977: Empirical Eigenvector Analysis of Vector Observations, *Geophys. Res. Lett.*, **4**, 319-320.

Hickey, B.M., 1979: The California Current System - Hypotheses and Facts, *Prog. Oceanog.*, **8**, 191-279.

Hicks, M.R., 1992: Alongshore Sub-Thermocline Current Variability in the Central California Current System, Master's Thesis, Naval Postgraduate School, Monterey, California, 111 pp.

Hunt, M.M., W.M. Marquet, D.A. Moller, K.R. Peal, W.K. Smith, and R.C. Spindel, 1974: An Acoustic Navigation System, Woods Hole Oceanographic Institution Technical Report 74-6, Woods Hole Oceanographic Institution, Woods Hole, Ma.

Huyer, A., P.M. Kosro, J. Fleischbein, S.R. Ramp, T. Stanton, L. Washburn, F.P. Chavez, T.J. Cowles, S.D. Pierce, and R.L. Smith, 1991: Currents and Water Masses of the Coastal Transition Zone off Northern California, June to August 1988, *J. Geophys. Res.*, **96**, 14809-14831.

Ikeda M., W.J. Emery, L.A. Mysak, 1984: Seasonal Variability in Meanders of the California Current System off Vancouver Island, *J. Geophys. Res.*, **89**, 3487-3505.

King, C.H., 1989: A Comparison of Pegasus and Combined CTD ADCP Current Profiles off the California Coast, Master's Thesis, Naval Postgraduate School, Monterey, California, 44 pp.

Large, W.G. and S. Pond, 1981: Open Ocean Momentum Flux Measurements in Moderate to Strong Winds, *J. Phys. Oceanogr.*, **11**, 324-336.

Largier, J.L., B.A. Magnell, C.D. Winant, 1993: Subtidal Circulation over the Northern California Shelf, *J. Geophys. Res.*, **98**, 18147-18179.

Lynn, R.J., 1986: The Subarctic and Northern Subtropical Fronts in the Eastern North Pacific in Spring, *J. Geophys. Res.*, **16**, 209-222.

Lynn, R.J. and J.J. Simpson, 1987: The California Current System: the Seasonal Variability of its Physical Characteristics, *J. Geophys. Res.*, **92**, 12947-12966.

Luyten, J.R., G. Needell, and J. Thomson, 1982: An Acoustic Dropsonde-Design, Performance and Evaluation, *Deep-sea Res.*, **4**, 499-524.

Negron, A.J., 1993: Measurements of Ocean Currents Across the Continental Margin off Point Sur, California, during March 1989, Master's Thesis, Naval Postgraduate School, Monterey, California, 78 pp.

Priesendorfer, R.W., F.W. Zwiers and T.P. Barnett, 1981: Foundations of Principal Component Selection Rules. SIO Ref. Ser. 81-4, Scripps Institution of Oceanography, La Jolla, Ca. 192 pp.

Reece, R.H., 1989: An Analysis of Hydrographic Data Collected off Point Sur, California in November 1988, Master's Thesis, Naval Postgraduate School, Monterey, California, 75 pp.

Reid, J.L., G.I. Roden, and J.G. Wyllie, 1958: Studies of the California Current System, CalCOFI Progress Reports 1 July 1956 to 1 January 1958, Calif. Coop. Oceanic Fish. Invest., La Jolla, Ca. 27-56.

Reid, J.L., 1962: Measurements of the California Countercurrent at a Depth of 250 m, *J. Mar. Res.*, **20**, 134-137.

Reid, J.L. and R.A. Schwartzlose, 1962: Direct Measurements of the Davidson Current off Central California, *J. Geophys. Res.*, **67**, 2491-2497.

Robson, A.J., 1990: Circulation of the California Undercurrent Near Monterey in May 1989, Master's Thesis, Naval Postgraduate School, Monterey, California, 74 pp.

Simpson, J.J., C.J. Koblinsky, J. Pelaez, L.R. Haury, and D. Wiesenhahn, 1986: Temperature-Plant Pigment-Optical Relations in a Recurrent Offshore Mesoscale Eddy near Pt. Conception, California, *J. Geophys. Res.*, **91**, 12919-12936.

Spain, P.F. , D.L. Dorson, and H.T. Rossby, 1981: PEGASUS: a Simple, Acoustically Tracked, Velocity Profiler, *Deep-sea Res.*, **28**, 1553-1567.

Sverdrup, H.U., R.H. Johnson, and M.W. Fleming, 1942: *The Oceans*, Prentice-Hall, Inc. Englewood Cliffs, N.J. 1066 pp.

Tibby, R.B., 1941: The Water Masses off the West Coast of North America, *J. Mar. Res.*, **4**, 112-121.

Tisch, T.D., S.R. Ramp, and C.A. Collins, 1992: Observations of the Geostrophic Current and Water Mass Characteristics off Point Sur, California, from May 1988 through November 1989, *J. Geophys. Res.*, **97**, 12535-12555.

Tziagidis, G.Th., 1991: An Analysis of Hydrographic Data Collected off Point Sur, California in June 1990, Master's Thesis, Naval Postgraduate School, Monterey, California, 62 pp.

Wickham J.B., 1975: Observations of the California Countercurrent, *J. Mar. Res.*, **33**, 325-340.

Wickham J.B., A.A. Bird, and C.N.K. Mooers, 1987: Mean and Variable Flow over the Central California Continental Margin, 1978-1980, *Continental Shelf Res.*, **7**, 827-849.

Wooster, W.S. and J.H. Jones, 1970: California Undercurrent off Northern Baja California, *J. Mar. Res.*, **28**, 253-260.

Wooster, W.S. and J.L. Reid, 1963: Eastern Boundary Currents, *The Sea*, **2**, 253-280.

INITIAL DISTRIBUTION LIST

		No. Copies
1.	DEFENSE TECHNICAL INFORMATION CENTER CAMERON STATION ALEXANDRIA, VA 22304-6145	2
2.	LIBRARIAN CODE 52 NAVAL POSTGRADUATE SCHOOL 411 DYER RD RM 104 MONTEREY, CA 93943-5101	2
3.	OCEANOGRAPHY DEPARTMENT CODE OC/CO NAVAL POSTGRADUATE SCHOOL 833 DYER RD RM 350 MONTEREY, CA 93943-5122	2
4.	PROFESSOR HANEY (MR/HY) NAVAL POSTGRADUATE SCHOOL 589 DYER RD RM 252 MONTEREY, CA 93943-5114	1
5.	PROFESSOR NEWELL GARFIELD (OC/GF) NAVAL POSTGRADUATE SCHOOL 833 DYER RD RM 342D MONTEREY, CA 93943-5114	1
6.	LT. FREDERICK RISCHMILLER DEPARTMENT HEAD CLASS 132 SURFACE WARFARE OFFICERS SCHOOL COMMAND 446 CUSHING ROAD, NEWPORT, RI 02841-1209	1
7.	LIBRARY NAVAL OCEANOGRAPHIC OFFICE STENNIS SPACE CENTER MS 39529-5001	1

8. PROFESSOR J.L. REID, JR. 1
SCRIPPS INSTITUTION OF OCEANOGRAPHY
P.O. BOX 2367
LA JOLLA, CA 92037

9. PROFESSOR JAMES SIMPSON 1
SCRIPPS INSTITUTION OF OCEANOGRAPHY
P.O. BOX 2367
LA JOLLA, CA 92037

10. LIBRARY 2
MOSS LANDING MARINE LAB
CALIFORNIA STATE COLLEGES
SANDHOLT ROAD
MOSS LANDING, CA 95039

11. DR. THOMAS KINDER 1
ENVIRONMENTAL SCIENCES DIVISION
OFFICE OF NAVAL RESEARCH
ARLINGTON, VA 22217